



**HAL**  
open science

# Better understanding of the ON-bipolar cell signaling cascade and development of therapies for congenital stationary night blindness

Juliette Varin

► **To cite this version:**

Juliette Varin. Better understanding of the ON-bipolar cell signaling cascade and development of therapies for congenital stationary night blindness. Sensory Organs. Sorbonne Université, 2020. English. NNT: 2020SORUS361 . tel-03406098

**HAL Id: tel-03406098**

**<https://theses.hal.science/tel-03406098v1>**

Submitted on 27 Oct 2021

**HAL** is a multi-disciplinary open access archive for the deposit and dissemination of scientific research documents, whether they are published or not. The documents may come from teaching and research institutions in France or abroad, or from public or private research centers.

L'archive ouverte pluridisciplinaire **HAL**, est destinée au dépôt et à la diffusion de documents scientifiques de niveau recherche, publiés ou non, émanant des établissements d'enseignement et de recherche français ou étrangers, des laboratoires publics ou privés.

Sorbonne Université

Ecole doctorale 394 : Physiologie, physiopathologie et thérapeutique

Institut de la Vision – Département de Génétique - Identification des défauts génétiques  
conduisant à des pathologies oculaires progressives et non-progressives

# Better understanding of the ON-bipolar cell signaling cascade and development of therapies for Congenital Stationary Night Blindness

Par Juliette Varin

Thèse de doctorat en Neurosciences

Sous la direction du Dr. Christina Zeitz

Présentée et soutenue publiquement le 07 octobre 2020

Devant un jury composé de :

Dr Nathalie Cartier, DR2, Présidente du jury

Pr Bart Leroy, PU-PH, Rapporteur

Dr Jean-Michel Rozet, DR2, Rapporteur

Dr Therese Cronin, Examinatrice

Dr Christina Zeitz, DR2, Directrice de thèse



Except where otherwise noted, this work is licensed under  
<http://creativecommons.org/licenses/by-nc-nd/3.0/>

*A ceux que j'aime*

# Acknowledgments- Remerciements

---

Tout d'abord j'aimerais remercier les membres du jury, le Dr. Nathalie Cartier, le Dr. Therese Cronin ainsi que les deux rapporteurs le Pr. Bart Leroy et le Dr. Jean-Michel Rozet d'avoir accepté d'évaluer mon travail. Vous m'avez tous apporté scientifiquement à travers nos rencontres ou vos présentations lors de congrès. Pour Bart, merci de m'avoir accompagnée pendant ces 4 années aux travers de mes comités de suivi de thèse. Vos commentaires ont toujours été bienveillants et éclairés.

Merci Christina d'avoir eu confiance en moi et de m'avoir accompagnée pendant toute ma thèse. Tu as su me rassurer quand il le fallait et tu m'as permis de présenter mon travail à de nombreuses reprises. Même si cela a toujours été source de stress, je te remercie pour ces opportunités. Merci aussi de m'avoir sensibilisée à la CSNB et de m'avoir laissée rencontrer des patients. C'est pour eux que je fais ce métier.

J'aimerais aussi remercier Isabelle. Merci pour tes conseils, pour ton œil aiguisé sur mes ERG et pour tes commentaires tout au long de ma thèse. Merci également à toi Deniz pour cette belle collaboration et d'avoir été ma tutrice de thèse. Tes conseils, tes suggestions m'ont toujours aidée à améliorer ce projet ! J'espère que l'on pourra continuer à collaborer dans le futur.

Merci mille fois à ma Boubou, merci de m'avoir accompagnée dans ce projet. Merci d'être toi, aussi drôle, tête en l'air, investie et bordélique. Merci d'avoir pleuré avec moi pour les ondes b, pour les fous rires au labo, merci de m'avoir consolée aussi quand il le fallait ... Cette thèse elle est là aussi grâce à toi فريق قوي إلى الأبد

Juliette, ma partner in crime, on en aura vécu des choses ensemble ! Merci d'avoir été là, de m'avoir soutenue, de m'avoir encouragée et d'avoir rendu cette période un peu plus douce. J'espère t'avoir rendu la pareille. Je sais, depuis le début, que tu es une excellente scientifique et j'espère que tu t'épanouiras complètement à Seattle. Pour finir ... "Together we're unlimited, Together we'll be the greatest team there's ever been, Dreams the way we planned'em, If we work in tandem, there's no fight we cannot win, Just you and I, defying gravity"

Cécile, mon petit bout de femme. C'était un plaisir de te soutenir pendant ta thèse, ton moment, alors merci mille fois de l'avoir fait en retour ! Merci pour nos « derniers verres » après nos appels Skype pendant le confinement, merci pour ta douceur et ta compréhension. Merci de m'avoir écoutée râler et me plaindre mais aussi et surtout d'avoir ri avec moi ! Love you baby

Marco, I don't even know where to begin ... You are a wonderful man, kind & funny, an excellent doctor and a scientist, you're such a good listener and hell of a cheerleader. Thank you for always pushing me further! I will value our friendship forever, truly. Ti amo Marcolino

J'aimerai aussi remercier l'équipe S6 pour son soutien pendant ces 4 années et d'avoir été pour certains, les cobayes de mes tests en pâtisserie : Marine, Nuria, Maria, Camille, Christel, Christelle, Aline, Vasily, Baptiste et Armel.

I would also like to thank the members of the office who were there to laugh with me and share some thoughts about life (and sometimes science): Takuma, Yosra, Tristan, Dragos, Martijn and last but not least Oriol (again, sorry for letting you down at the restaurant that one time :p)

Un immense merci, aussi et surtout, à notre super animalerie ! Mille mercis Quenol, Julie, Manu, Elena, Mylène pour votre patience, vos conseils et encouragements. Merci bonus pour Julie et Manu qui ont trimbalé la poubelle tournante entre l'IDV et l'ICM plusieurs fois pour que je puisse faire mes opto ! Natalia, Marion, Andrei, Alexis, Christian, Mehdi, Vanessa merci d'avoir pris soin de mes petites souris.

Un grand merci à toi Corentin ! Merci pour toutes ces sessions de MEA, c'était chouette d'apprendre à te connaître ! Vive l'ASM et Mister Ketchup ;) Merci aussi Guillaume de m'avoir briefée pour les mosaïques à 2 semaines de rendre mon manuscrit ! Merci à toi Grégory pour ton implication dans le projet LRIT3 et ces belles figures !

J'aimerai également remercier Yvrick, Manuela et Stéphane pour leurs conseils, de carrière ou scientifiques. Et plus généralement, tout le 4<sup>ème</sup> étage de l'IDV, vous ferez toujours partie de cette période de ma vie.

J'aimerai aussi remercier mon « Beauty R+4 » crew : Gégé & Alex. C'était tellement chouette de vous avoir avec moi ! Merci pour nos calendriers de l'avant, nos soirées karaoké chez Gégé et votre soutien infailible ! Un merci aussi à Emma, Marie, Mariangela, Emmanuele, Fred, Seiki pour m'avoir aidée ou simplement écoutée raconter mes bêtises ...

Un petit mot aussi pour mes copains thésards ! Merci Sergi pour ta bienveillance et tes coups de mains quand j'en ai eu besoin, merci Robin pour ta bonne humeur et les réglages du confocal :p Merci Oriane, Alice, Frank vous êtes des gens formidables et j'espère de tout cœur que le futur vous apportera plein de bonheur ! Merci Yoan pour ta folie, ta bonne humeur communicative et tes accents improbables ! Et puis merci Sarah, c'était un plaisir d'apprendre à te connaître au fil des déjeuners, soirées et pots de thèse !

On dit souvent qu'on se passionne pour quelque chose grâce à un professeur. Pour moi ça aura été vous M. Burnel ! Grâce à votre pédagogie je me suis réellement découvert une passion pour la biologie et j'en fais aujourd'hui mon métier. Merci !

Un immense merci à tous mes amis ! Ma Mathilde, merci d'avoir pris de mes nouvelles et de m'avoir appelée quand je ne le faisais pas, de m'avoir soutenue. Les rôles s'inversent maintenant ! Merci ma Chachou, beaucoup de mes meilleurs souvenirs d'amitié sont avec toi, merci pour tous tes encouragements et merci de m'avoir soutenue tout du long, tu m'es très

chère ma belle. Merci Chloé ! Tu es un arc-en-ciel sur pattes, toujours de bonne humeur, drôle et merci d'avoir pris de mes nouvelles pendant cette (dure) période et de m'avoir reboostée à chaque fois. Merci Mathieu ! Je suis heureuse de te compter parmi mes amis et vivement notre prochain « double date ». Merci Julia ! Pour ton humour, pour tes bonnes adresses, pour ta bonne humeur. Les copains, vivement la 2<sup>ème</sup> édition de l'Île aux Moines, merci pour votre soutien à tous, je vous aime !

Gabrielle, ma Gaby, mon petit soleil. Tu as été un de mes rocs ! Merci de m'avoir appris à compter les jours de la semaine, pour tous tes inépuisables encouragements, pour les heures qu'on a passées au téléphone (je crois qu'à ce jour tu détiens le record !). Tous ces moments ont été des bouffées d'oxygène, tu es une amie exceptionnelle et je suis heureuse que tu te sois retrouvée sur ma route ... Merci merci merci, kiss et love (avec des paillettes !)

Maman, Papa, merci pour tout. Vous m'avez donné les clés pour réussir et vous avez toujours fais en sorte que je puisse faire mes études sereinement. Un immense merci de m'avoir soutenue tout du long, pendant ces 27 années mais surtout pendant les 4 dernières, d'avoir été attentifs quand je vous racontais mes bons résultats ou mes déboires avec mes souris et de m'avoir bichonnée quand il le fallait. Je crois que vous aviez presque aussi hâte que moi que ça se termine ;) J'espère vous rendre fiers. Mimi, ma grande sœur d'amour, merci d'avoir été toujours là. Malgré ta vie déjà très prenante je savais que je pouvais me tourner vers toi si j'en avais le besoin. Merci pour nos quelques déjeuners quand tu étais de passage à Paris ou quand j'étais à Caen, j'aime vraiment partager ces moments avec toi. Je suis fière de toi et de la femme que tu es. Merci à toi aussi Camille tu es comme un grand frère pour moi ! Jules et Joséphine, vous ne vous en rendez pas compte mais vous faites partie de mes petites bulles de bonheur. Merci à toi aussi Mamie, quand on s'appelle tu prends autant de mes nouvelles que moi des tiennes, alors qu'on a 70 ans d'écart... Je vous aime tous énormément.

A ton tour Augustin ... Merci mon amour de m'avoir portée et supportée pendant cette thèse ! Tu as souvent eu confiance en moi à ma place et tu as toujours eu les bons mots pour me redonner de l'élan dans les moments difficiles. Te savoir à mes côtés m'a rendue plus sereine. Merci aussi de m'avoir inlassablement répété que tu étais fier de moi, d'avoir toujours été prêt à fêter chaque résultat, et surtout, surtout, de m'avoir toujours fais rire même quand je n'en avais pas envie. Comme tu aimes à le dire, merci d'avoir « parié sur l'avenir » avec moi. Je t'aime

# Table of Contents

---

Acknowledgments - Remerciements .....	1
List of figures .....	5
List of abbreviations .....	7
Introduction.....	11
I.    THE VISUAL PROCESS .....	11
A.    PRIMARY ELEMENTS OF VISION .....	11
B.    VISUAL PROCESSING IN THE RETINA.....	14
C.    INVESTIGATION OF THE RETINAL STRUCTURE AND FUNCTION .....	21
II.   BIPOLAR CELL SIGNALING DEFECT: CSNB AND MAR .....	27
A.    CONGENITAL STATIONARY NIGHT BLINDNESS (CSNB) .....	27
B.    FURTHER INSIGHT IN TWO CCSNB PROTEINS: MGLUR6 AND LRIT3.....	36
C.    PARANEOPLASTIC BIPOLAR CELL DYSFUNCTION .....	41
III.  GENE THERAPY FOR INHERITED RETINAL DISORDERS (IRDs) .....	44
A.    PRINCIPLE OF GENE THERAPY .....	44
B.    MAJOR GENE THERAPY AUGMENTATION TRIALS FOR IRDs.....	49
C.    CSNB GENE THERAPY .....	53
D.    OTHER INNOVATIVE THERAPIES FOR IRDs .....	54
Aim of this study.....	57
Results .....	58
I.    IDENTIFICATION AND CHARACTERIZATION OF NOVEL TRPM1 AUTOANTIBODIES FROM SERUM OF PATIENTS WITH MELANOMA-ASSOCIATED RETINOPATHY .....	58
Results .....	77
II.   RESTORATION OF MGLUR6 LOCALIZATION FOLLOWING AAV-MEDIATED DELIVERY IN A MOUSE MODEL OF CONGENITAL STATIONARY NIGHT BLINDNESS.....	77
Results .....	104
III.  RESTORATION OF NIGHT VISION IN ADULT MICE WITH CONGENITAL STATIONARY NIGHT BLINDNESS	104
Discussion & Perspectives .....	138
I.    IDENTIFICATION OF AUTOANTIBODIES INVOLVED IN PARANEOPLASTIC RETINOPATHY ASSOCIATED WITH ON-BCs DYSFUNCTION: FUNDAMENTAL AND THERAPEUTIC INTEREST.....	138
II.   TREATING CSNB THROUGH GENE THERAPY .....	140
III.  WHAT IS LEFT TO DECIPHER.....	138
References.....	140

# List of figures

---

Figure 1: Comparative structure of human and mouse ocular globe.....	11
Figure 2: Basic retinal structure .....	13
Figure 3: Representation of the retinal cell development over time .....	14
Figure 4: Simple anatomy and repartition of photoreceptors.....	15
Figure 5: Schematic representation of the rod phototransduction.....	16
Figure 6: Schematic drawing of the synapse of photoreceptor.....	17
Figure 7: Signaling cascade at the synapse between photoreceptors and ON-BCs .....	18
Figure 8: Illustration of the thirteen types of BCs in the retina .....	19
Figure 9: Simple outline of the ON- & OFF-pathways in the mammalian retina.....	20
Figure 10: Normal fundus of human and mouse .....	21
Figure 11: SD-OCT from an unaffected patient.....	22
Figure 12: Schema schematic of the optomotor test performed on mice seen from above..	23
Figure 13: Representation of the cellular origin of the a- and b-wave of the ERG.....	25
Figure 14: Multi-electrode array set-up and results .....	26
Figure 15: Congenital Stationary Night Blindness phenotype. ....	27
Figure 16: Schematic representation of the ERG phenotypes of Riggs-type CSNB, incomplete CSNB, complete CSNB and unaffected individual .....	29
Figure 17: Prevalence of the gene defects underlying cCSNB .....	31
Figure 18: Schematic representation of ERG recordings of five different species known displaying a cCSNB phenotype .....	33
Figure 19: Schematic drawing of the mGluR6 protein along with the localization of the different mutations causing cCSNB.....	38
Figure 20: Mutations in <i>LRIT3</i> causing cCSNB .....	40
Figure 21: Usual retinal phenotype of patients affected by paraneoplastic retinopathy associated with ON-bipolar cell dysfunction .....	43
Figure 22: Gene therapy milestones .....	44
Figure 23: Schema of the gene augmentation strategy using an AAV vector .....	45
Figure 24: CRISPR-Cas9 system mechanism.....	46

Figure 25: Proportion of types of viral vectors and the ratio of the various AAV serotypes used in ocular gene therapy.....	48
Figure 26: Schematic representation of the two modes of administration for ocular gene therapy .....	49
Figure 27: Schematic representation of the optogenetic principle.....	56
Table 1: Cellular origins of the two major components of the ERG .....	24
Table 2: Mouse models of cCSNB. *: proteins which are only missing in CBCs.....	34
Table 3: Gene therapy clinical trials for retinal diseases using recombinant viruses.....	51
Table 4: Patients harboring mutations in TRPM1 leading to cCSNB and which presented unusual skin features .....	139
Table 5: AAV serotypes and promoters used to target ON-BCs in the retina .....	136

# List of abbreviations

---

AAV: adeno-associated virus

ACs: amacrine cells

AMPA:  $\alpha$ -amino-3-hydroxy-5-methyl-4-isoxazolepropionic acid

AON: anti-sense oligonucleotide

BCs: bipolar cells

CABP4: calcium binding protein 4

CAR: carcinoma-associated retinopathy

CACNA1F: calcium channel, voltage-dependent, alpha 1F subunit

CACNA2D4: calcium channel, voltage-dependent, alpha 2/delta subunit 4

CBCs: cone bipolar cells

cd: candela

*CEP290*: central protein of 290 kDa

CNTF: ciliary neurotrophic factor

CRISPR-Cas9: clustered regularly interspaced short palindromic repeats-associated protein 9

CSNB: congenital stationary night blindness

cCSNB: complete CSNB

cGMP: cyclic guanosine monophosphate

DA: dark-adaptation

DLT: Dawson Trick Litzkow

DNA: deoxyribonucleic acid

EDTRS: early treatment diabetic retinopathy study

ERG: electroretinogram

FDA: USA food and drug administration

ff-ERG: full-field ERG

GCL: ganglion cell layer

*GNAT1*: guanine nucleotide binding protein, alpha transducin 1

*GPR179*/*GPR179*: G protein-coupled receptor 179

*GRK1*: g protein-coupled receptor kinase 1

*GRM6*/*Grm6*/*mGluR6*: metabotropic glutamate receptor 6

G $\beta$ 5: G protein subunit beta 5

HCs: horizontal cells

HDR: homology-directed repair

icCSNB: incomplete CSNB

ILM: inner limiting membrane

INL: inner nuclear layer

IPL: inner plexiform layer

iPS: induced pluripotent stem (cells)

IRDs: inherited retinal disorders

IS: inner segment

ISCEV: International Society for Clinical Electrophysiology of Vision

IVT: intravitreal

LA: light-adaptation

LCA: Leber congenital amaurosis

LHON: Leber hereditary optic neuropathy

*LRIT3*/*LRIT3*: Leucine rich-repeat, immunoglobulin-like and transmembrane domains 3

LSC: leopard-spotting complex

MAR: melanoma-associated retinopathy

MEA: multi-electrode array

MO: morpholino

NFL: nerve fiber layer

NGS: next generation sequencing

NHEJ: non-homologous end-joining

NMD: non-sense mediated mRNA decay

*nob*: no b-wave

*NYX/NYX*: nyctalopin

OKN: optokinetic nystagmus

OLM: outer limiting membrane

ONL: outer nuclear layer

OPL: outer plexiform layer

OPS: oscillatory potentials

OS: outer segment

P: post-natal day

PDE: phosphodiesterase

*PDE6B*: phosphodiesterase 6B

RCS: royal college of surgeon

RdCVF: rod-derived cone viability factor

*RDH5*: retinol dehydrogenase 5

RGCs: retinal ganglion cells

RGS7: regulator of G-protein signaling 7

RGS11: regulator of G-protein signaling 11

*RHO*: rhodopsin

RP: retinitis pigmentosa

RPE: retinal pigment epithelium

*RPE65*: retinal pigment epithelium specific protein 65

R9AP: regulator of G-protein signaling 9 binding protein

*SAG*: s-antigen

SD-OCT: spectral domain optical coherence tomography

*SLC24A1*: solute carrier family 24, member 1

TALEN: transcription activator-like effector nuclease

TRPM1/TRPM1: transient receptor potential cation channel, subfamily M, member 1

USH1B: Usher syndrome type 1B

VEP: visually-evoked potentials

WES: whole exome sequencing

WGS: whole genome sequencing

ZFN: zinc-finger nuclease

# Introduction

---

## I. THE VISUAL PROCESS

### A. PRIMARY ELEMENTS OF VISION

#### 1. OCULAR GLOBE STRUCTURE

The processing of an image by the brain starts by the entry of light in the ocular globe. The light first goes through the cornea and the aqueous humor to reach the pupil. The size of the pupil varies; it gets wider in the dark and narrower in the light. These changes of the size of the pupil are controlled by the iris, which is the colored part of the eye that is unique to each individual. After passing through the pupil, the light is focused by the lens, through the vitreous, on the retina, which is located at the back of the eye. Subsequently, the light crosses the retina to reach the photoreceptors that transform this light signal into a biochemical one which converges in the optic nerve. The latter, which is composed of the axons of retinal ganglion cells (RGCs), guides the visual signal towards the brain to be processed in the visual cortex [1]. The mouse eye is mainly structured the same way but smaller with a relatively much larger lens and the global shape of the cornea is less protruding [2](Fig.1).

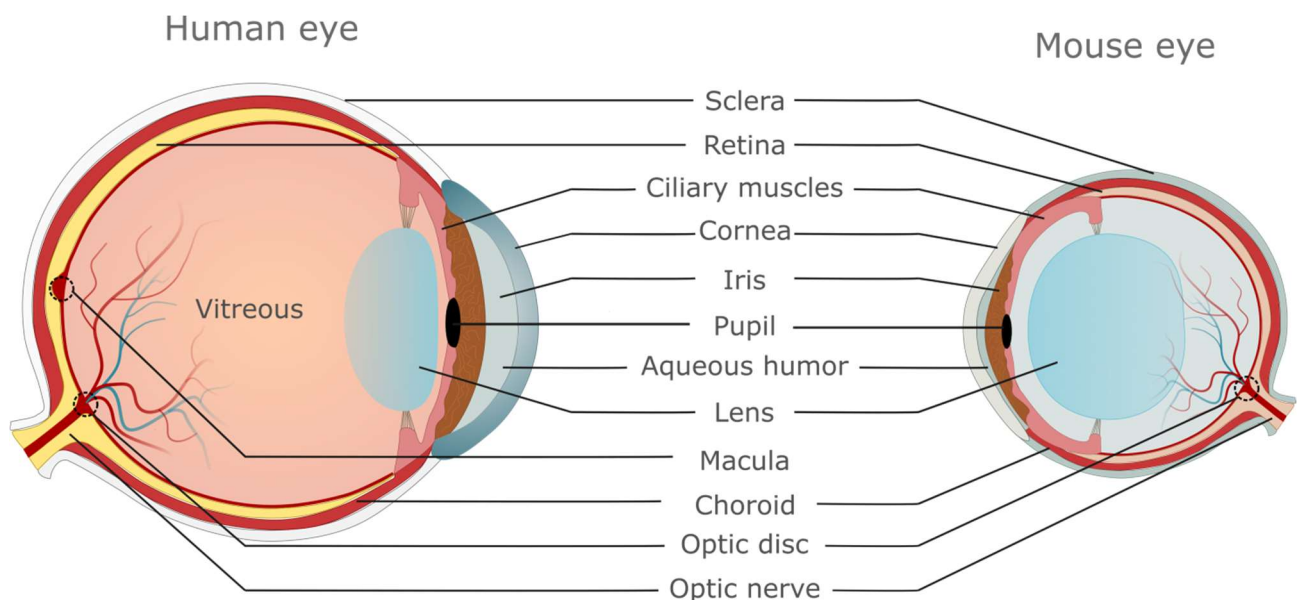


Figure 1: Comparative structure of human and mouse ocular globe

## 2. THE RETINA, KEY ORGAN OF VISION

### **Retinal structure**

The retina, the visual organ located at the posterior part of the ocular globe, is multi-stratified. These layers are enumerated as follows, from the choroidal side to the vitreous side (Fig.2):

- The retinal pigmented epithelium (RPE) plays a role in the phagocytosis of photoreceptor outer segments and the recycling of retinoid acid, which are essential to ensure a proper function of the retina.
- The photoreceptor layer comprises the outer (OS) and inner segments (IS) of photoreceptors
- The outer limiting membrane (OLM) separates the inner segments of photoreceptors from their nuclei through gap junctions between the IS of the photoreceptors and Müller cells
- The outer nuclear layer (ONL) contains nuclei of rod and cone photoreceptors,
- The outer plexiform layer (OPL), is the region where the synapses of photoreceptors connect with bipolar (BCs) and horizontal cells (HCs),
- The inner nuclear layer (INL) includes the nuclei of amacrine (ACs), BCs, HCs and Müller glial cells,
- The inner plexiform layer (IPL) is the region, where the synapses of ACs and BCs connect with RGCs
- The ganglion cell layer (GCL) comprises the nuclei of RGCs
- The nerve fiber layer (NFL) contains the axons of the RGCs that form the optic nerve
- The inner limiting membrane (ILM) separates the retina from the vitreous

Finally, Müller cells expanse from the OLM to the ILM where they act as support structures of the retina. They also protect retinal cells from potential overflows of neurotransmitters [1] (Fig.2).

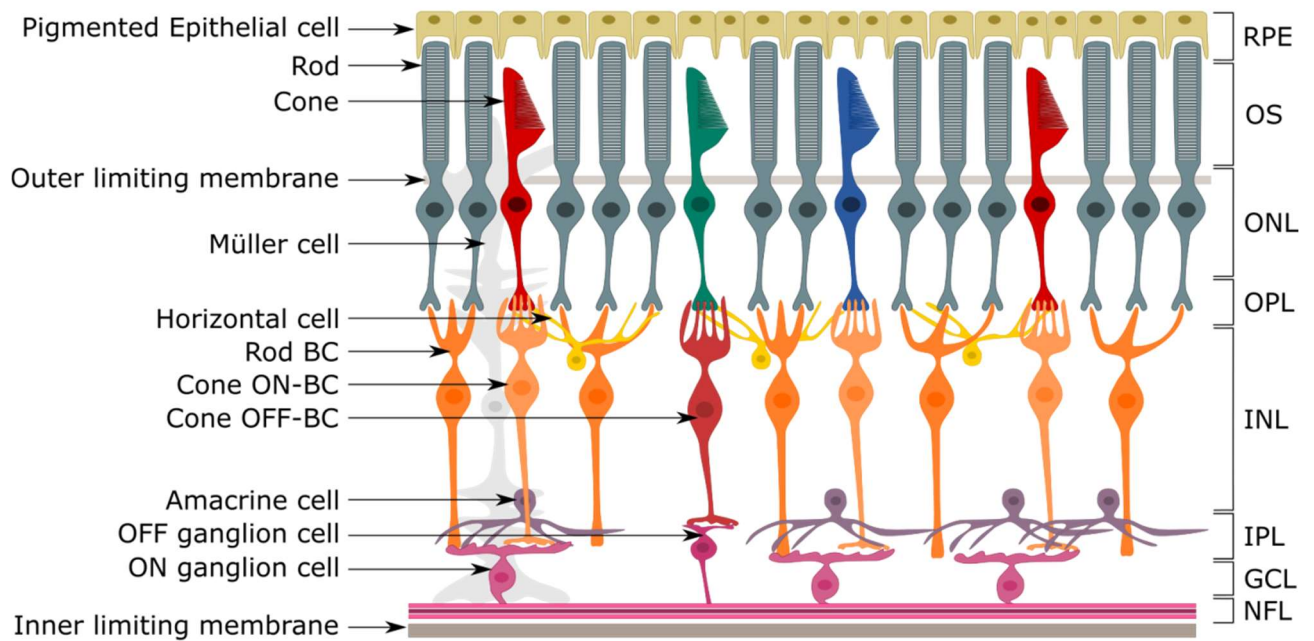


Figure 2: Basic retinal structure

## Retinal development

Studies in mouse showed that retinal cells start to differentiate from progenitors at different gestation times. Horizontal cells and cones only mature *in utero* while RGCs, BCs, ACs, Müller cells and rods start to differentiate *in utero* but complete their maturation at different post-natal days. In particular, differentiation and maturation of the BCs extends from embryonic day 14.5 to post-natal day 11 [3] (Fig.3A).

In humans, the retina is fully developed prior to birth [4]. Interestingly, the development of the human retinal cells is quite similar to the one observed in the mouse as RGCs, horizontal cells and cones are the first cells to differentiate, followed by amacrine cells, rods, bipolar cells and finally Müller cells [5] (Fig. 3B).

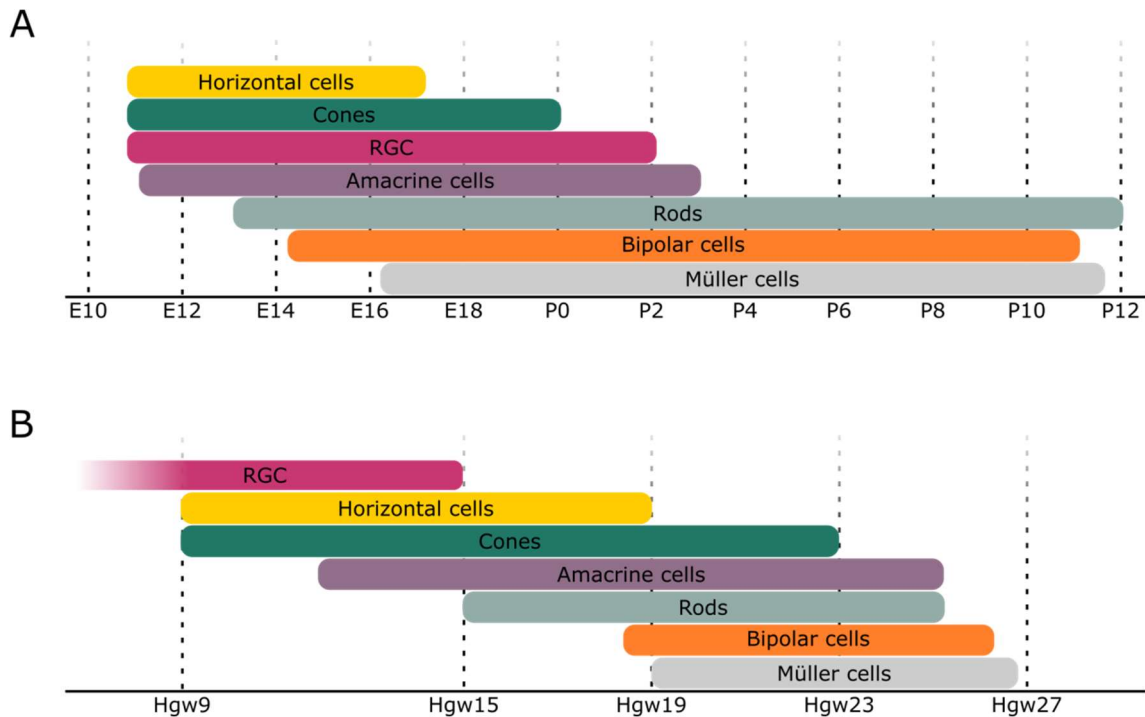
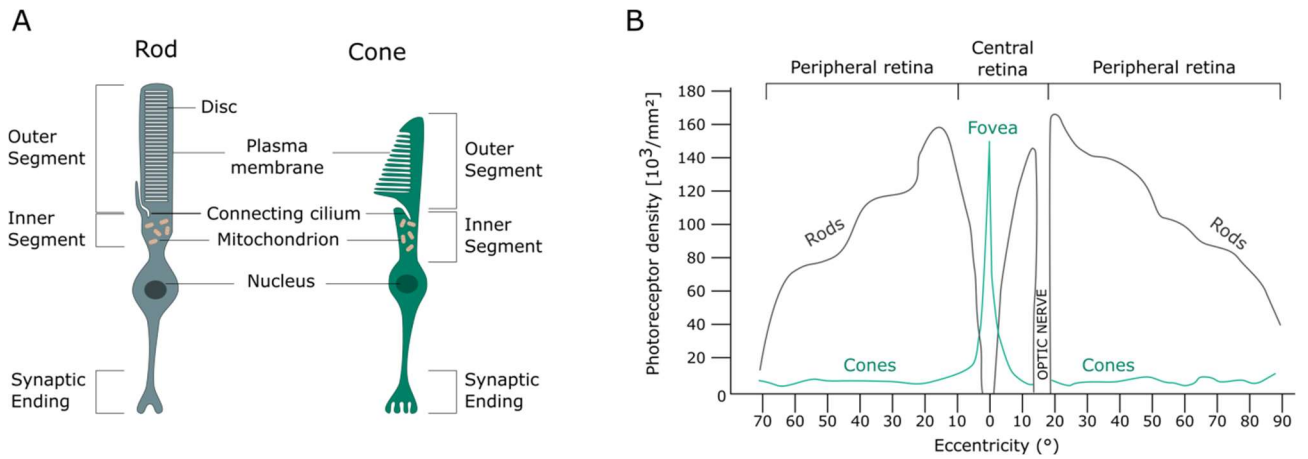


Figure 3: Representation of the retinal cell development over time. (A) Retinal cell development in the mouse; E: Embryonic day; P: Post-natal day. (B) Retinal cell development in humans; Hgw: Human gestation week

## B. VISUAL PROCESSING IN THE RETINA

### 1. GENESIS OF THE VISUAL PROCESS

As light reaches the retina, photoreceptors, which are the main photosensitive cells of the retina, initiate the visual signaling. Two types of photoreceptors have been described based on the shape of their outer segments: rods and cones (Fig.4A). Rods are involved in vision in dim-light, while cones are involved in day light vision, color vision and visual acuity. Three subtypes of cones are present in the retina, which defer in their respective photopigment, called opsins, and their respective distinct spectral sensitivities: S-cones have a maximal sensitivity to short wavelengths (also called blue cones), M-cones have a maximal sensitivity to medium wavelengths (also referred as green cones) and L-cones have a maximal sensitivity to long wavelengths (also called red cones) [6]. In mice, only two types of cones (M-cones and S-cones) have been described, expressing two distinct opsins sensitive to various wavelengths [7].



**Figure 4: Simple anatomy and repartition of photoreceptors. (A) Schematic drawing of the structure of photoreceptors. (B) Representation of the organization of the photoreceptors in the human retina, modified from Osterberg *et al.*, 1935**

Photoreceptors are organized in a specific manner. Both rods and cones are present at the entire surface of the retina. However, rods outnumber cones in the peripheral retina while the density of cones is at its maximum at the fovea, which is solely composed of cones [8] (Fig.4B). Mice do not have a fovea but the organization of photoreceptors in the mouse retina is comparable to the one of humans with an area enriched in cones (area centralis) [9]. In the human retina, rods are the most represented type of photoreceptors as they are about 120 million (95%) while there are 6 million cones (5%) [8]. This proportion is approximately the same in the mouse retina where rods represent 97% of the photoreceptors and cones 3% [10].

### Rod phototransduction cascade

Photoreceptors transform light into a biochemical signal through a G-protein signaling pathway. Under dark conditions, all proteins involved in phototransduction are at a resting state. cGMP-gated channels are opened, photoreceptors are depolarized, leading to the release of the neurotransmitter glutamate at the synaptic cleft.

In rods at light, the light-sensitive G-protein coupled receptor rhodopsin absorbs a photon driving the activation of the G-protein transducin. The  $\alpha$ -subunit of transducin activates the phosphodiesterase (PDE) provoking the hydrolyzation of cGMP. This light-induced drop of cGMP triggers the closure of the cGMP-gated channels. Subsequently, photoreceptors hyperpolarize and the outflow of glutamate decreases [11] (Fig.5).

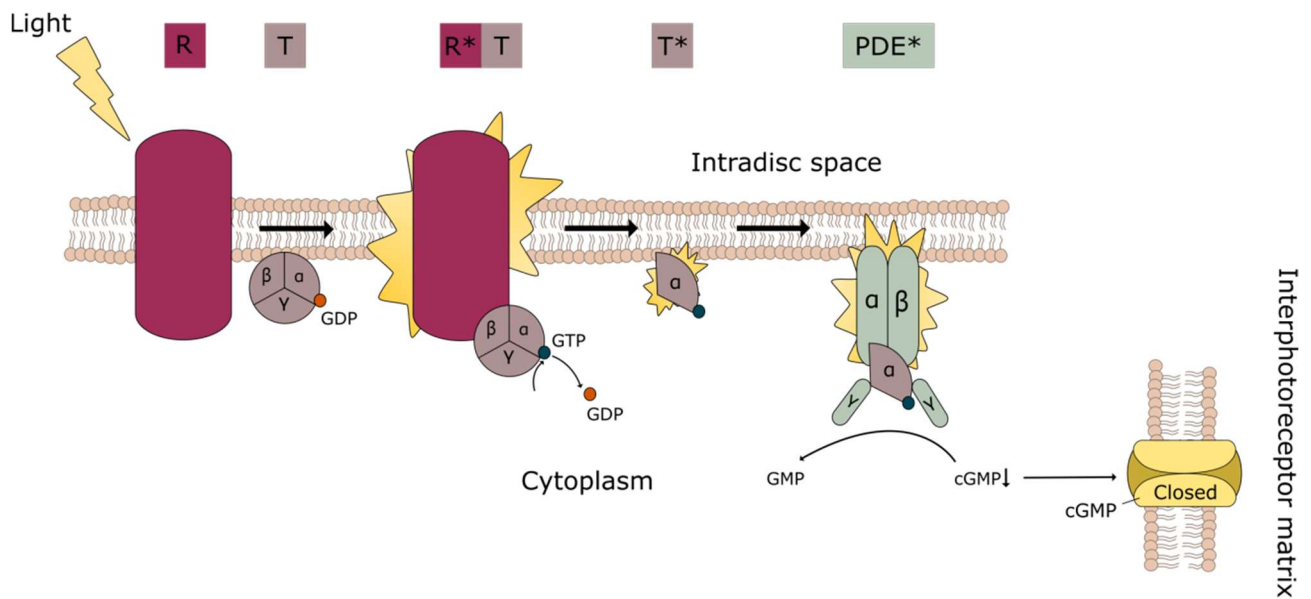


Figure 5: Schematic representation of the rod phototransduction. \* means activated

## 2. TRANSMISSION OF THE SIGNAL: GLUTAMATE RELEASE

At the synaptic terminals of rods and cones, the biochemical signals are transmitted to HCs and BCs through glutamate release.

### Photoreceptor to bipolar cell synapses

The synaptic terminal of cones is referred as the cone pedicle (Fig. 6A). It displays dense structures called synaptic ribbons and is filled with synaptic vesicles containing glutamate, the neurotransmitter essential for the propagation of the visual signal from the photoreceptors to the BCs. In one cone pedicle, approximately 30 ribbons are found which are associated with the same number of triads [12]. These triads are the combination of three elements: the dendritic terminal of an invaginating BC at the center and two flanking dendritic terminals of HCs [13]. Most cone bipolar cells (CBCs) contact several cones, they are referred as diffuse BCs; while some contact a single cone pedicle and are cited as midget BCs.

The synaptic terminals of rods are quite similar to the ones of cones. They are called rod spherule and are also composed of presynaptic ribbon flanked by synaptic vesicles (Fig.6B). In apposition, invaginating processes of HCs and BCs are found. While the cone pedicle contains multiple ribbons, which deliver the information to more than a hundred BCs, the rod spherule includes a ribbon contacting rod BCs (RBCs) and two HCs [14].

Rod spherules contact with only one type of bipolar cell, the RBCs, while the cone pedicle can connect to different types of CBCs, ON- and OFF-CBCs. These diverse connections discriminate two pathways of light processing in the retina: the ON- and OFF-pathway.

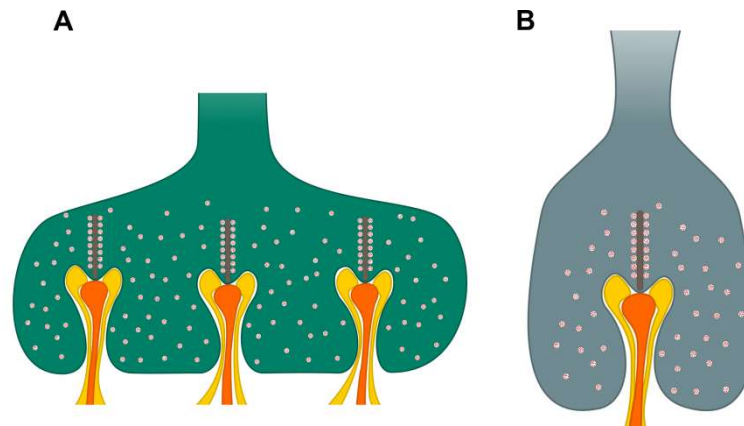


Figure 6: Schematic drawing of the synapse of photoreceptor. (A) Representation of the cone pedicle, the base of the cone is represented in green, invaginating HCs are depicted in yellow, invaginating dendrites of BCs are represented in orange forming the triad. The ribbon is apposed to the invaginating HCs and BCs- Synaptic vesicles are drawn in red. (B) Representation of the rod spherule, the base of the rod is showed in grey; the other components are represented by the same color code as for the cone pedicle.

### Glutamate release by photoreceptors

Glutamate release at the photoreceptor synapse is controlled by  $\text{Ca}^{2+}$  currents and requires an L-type voltage-dependent  $\text{Ca}^{2+}$  channel composed of a heteromultimeric protein complex [11]. *CACNA1F* codes for the  $\alpha_1$  subunit (*CACNA1F*, Cav1.4) of this channel. This subunit is the pore through which calcium influxes across the synaptic membrane. The  $\beta$ ,  $\gamma$  and  $\alpha_2$  subunits, modulate calcium currents and are involved in the correct structure and localization of the complex at the synaptic membrane [15, 16]. The  $\alpha_2$  subunit is encoded by *CACNA2D4*. *CACNA1F* is also associated to *CABP4*, which is a  $\text{Ca}^{2+}$  binding protein that contributes to *CACNA1F* modulation. In darkness, *CACNA1F* is in an open conformation and calcium influx triggers a continuous release of glutamate in the synaptic cleft. Conversely, when the phototransduction cascade is initiated by light, photoreceptors hyperpolarize and glutamate release is reduced [17] (Fig.7).

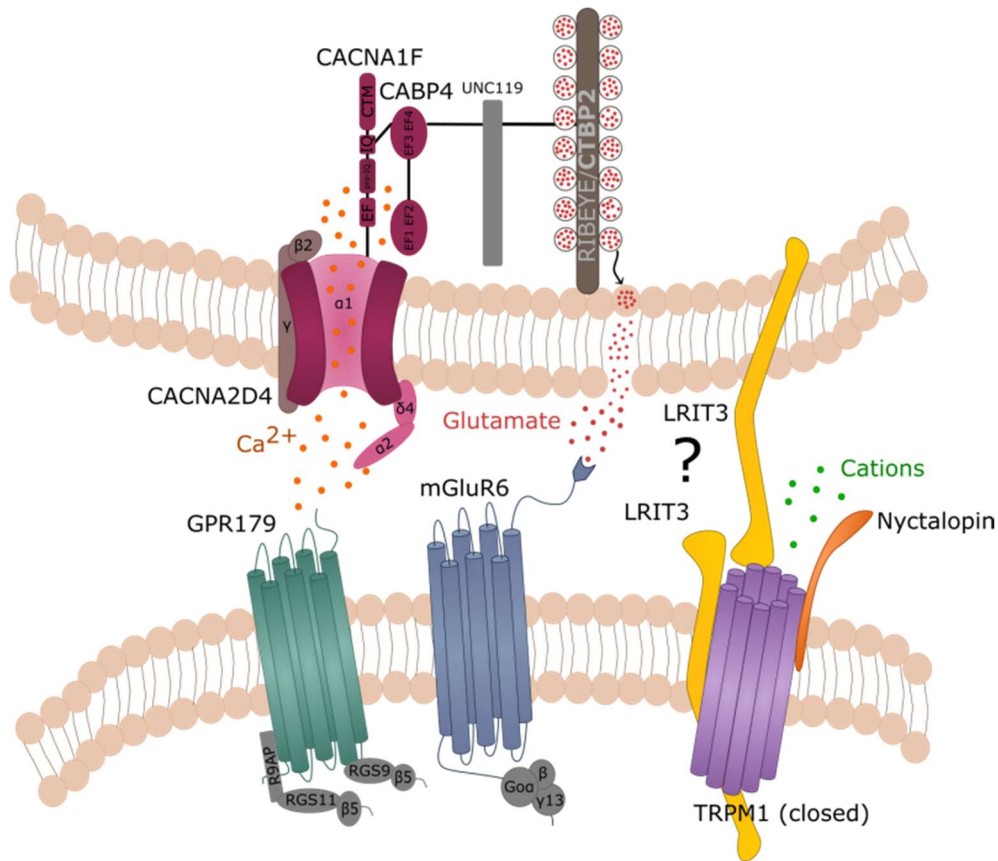


Figure 7: Signaling cascade at the synapse between photoreceptors (top) and ON-bipolar cells (bottom). The exact localization of LRIT3 is not elucidated between pre- and post-synaptic.

### 3. BIPOLAR CELL PROCESSING: ON- & OFF-PATHWAYS

#### Bipolar cells

As mentioned before, BCs can be subdivided in two groups: RBCs and CBCs. So far, one type of RBC has been described versus twelve for the CBCs depending on morphology and connections. They are also classified as follows:

- Diffuse BCs that can contact 5 to 10 M- or L-cone pedicles
- Midget BCs which contact a single M- or L-cone pedicle; they can also be subdivided in flat (OFF) or invaginating (ON) midget BCs
- S-cone BCs only connect to S-cones (1-5) and carry an ON-pathway
- RBC which contact 20-80 rod spherules [14]

RBCs are only transmitting the visual signal through the ON-pathway while CBCs can follow either the ON-pathway or the OFF-pathway (Fig.8).

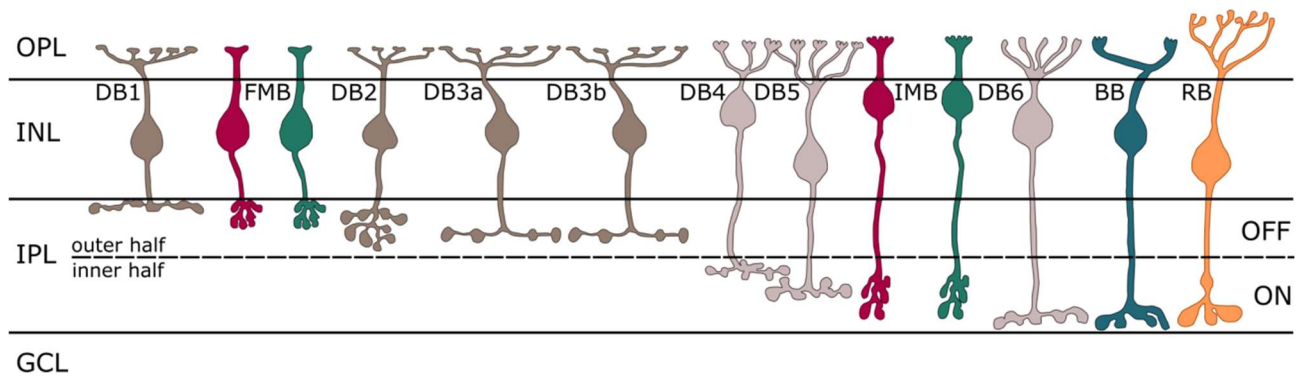


Figure 8: Illustration of the thirteen types of BCs in the retina. DB: diffuse bipolar cell; FMB: flat midget bipolar cell; IMB: invaginating midget bipolar cell; BB: S-cone bipolar cell and RB: rod bipolar cell. Green FMB and IMB are connecting to M-cones and red FMB and IMB are related to L-cones.

## ON-pathway

When released in the synaptic cleft, glutamate binds the metabotropic glutamate receptor 6 (mGluR6), localized at the membrane of ON-BCs [18, 19]. mGluR6 activates the  $\alpha$ -subunit of a G-protein,  $G\alpha_o$  [20]. The dissociation of the G-protein subunits causes the closure of a non-selective ion channel TRPM1 for Transient Receptor Potential cation channel subfamily Member 1. In the light, the amount of glutamate released by photoreceptors decreases, leading to the opening of the TRPM1 channel at the end of the cascade. This phenomenon is consistent with ON-BC depolarization, therefore these cells are also called depolarizing BCs [21]. Since photoreceptors hyperpolarize in response to light while ON-BCs depolarize, the synapse between photoreceptors and ON-BCs is called a sign-inverting synapse. Other regulatory proteins play a role in this cascade: GPR179 is an orphan seven transmembrane G-protein coupled receptor, which is required for the depolarization of bipolar cells, plays a role in mGluR6 sensitivity and interacts directly with TRPM1 [22]. Specific intracellular motifs present in LRIT3 and *in vivo/in vitro* studies of nyctalopin and TRPM1 suggest that nyctalopin and LRIT3 are important for the correct localization of TRPM1 to the dendritic tips of ON-BCs (Fig.7) [23, 24].

Two ON-pathways have been described depending on the type of photoreceptor implicated: either the rod ON-pathway (ON1, Fig.9) or the cone ON-pathway (ON2, Fig.9). Rods deliver the signal to RBCs which communicate it to a type II AC that then transmit it to ON-CBC which convey it to ON-RGC. Cones transmit the signal directly to ON-CBC to finally pass it to ON-RGC (Fig.9).

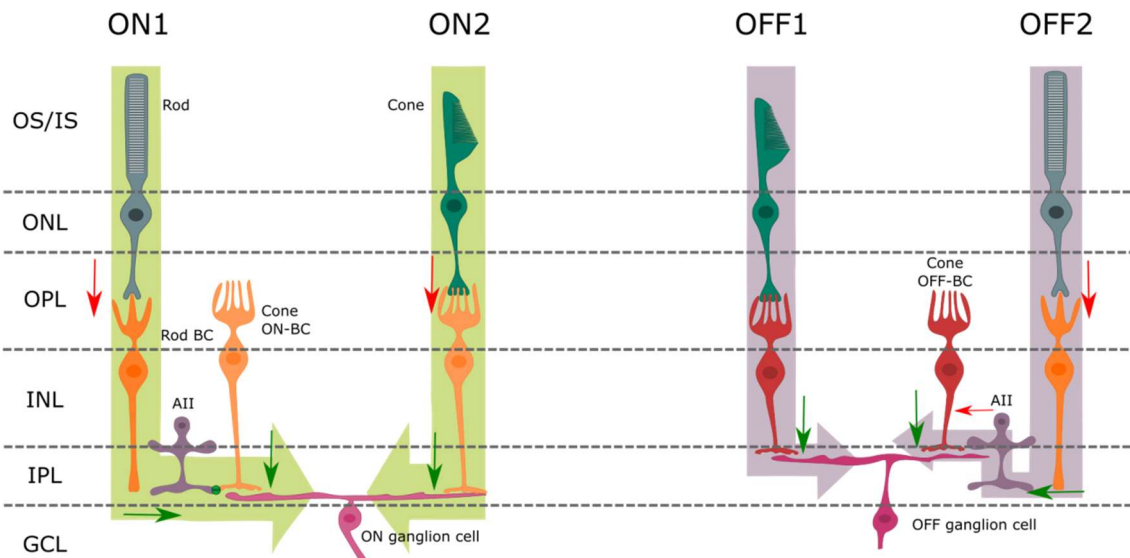


Figure 9: Simple outline of the ON- & OFF-pathways in the mammalian retina.

### OFF-pathway

In contrast to ON-CBCs, OFF-CBCs express ionotropic glutamate receptors at their dendrites. These receptors are formed by a complex of receptor and channel subunits. It is not a sign-inverting synapse and OFF-CBCs hyperpolarize in response to light, as photoreceptors. Therefore, these BCs are also called hyperpolarizing BCs. Two types of ionotropic receptors are expressed by OFF-CBCs depending on the neurotransmitter to which they bound. The first type is the ionotropic receptor sensitive to  $\alpha$ -amino-3-hydroxy-5-methyl-4-isoxazolepropionic acid (AMPA) and the second one to kainate. The major OFF-pathway originates in cones which transmit this signal to OFF-CBCs that convey the signal towards OFF-RGCs [14] (fig 9, OFF1).

#### 4. BIPOLAR TO GANGLION CELL SYNAPSE

ON- and OFF-BCs are not only expressing different glutamate receptors, they also display distinct morphological features.

### OFF-pathway

OFF-CBC axons are shorter than the ones from ON-BCs and end in the OFF sublamina (outer half) of the IPL (Fig.8). They directly transfer the signal through their excitatory synapses onto OFF-RGC.

## ON-pathway

Conversely, ON-cone and axons of the RBCs terminate in the ON sublamina (inner half) of the IPL (Fig.8). ON-CBCs can convey the signal straight to the ON-RGCs while RBCs first pass on the signal to type II ACs, which are depolarizing in response to light. These type II ACs are forming electrical synapses into the axon terminals of ON-CBCs that finally synapse onto ON-RGCs [25]. This pathway is actually the most sensitive one as it can be triggered by the absorption of only one photon. Ultimately, OFF- and ON-RGCs dendrites transmit the signals towards the brain.

### C. INVESTIGATION OF THE RETINAL STRUCTURE AND FUNCTION

#### 1. STRUCTURAL STUDY OF THE RETINA

To control the retinal integrity, two ophthalmological exams can be performed:

- A Fundoscopy

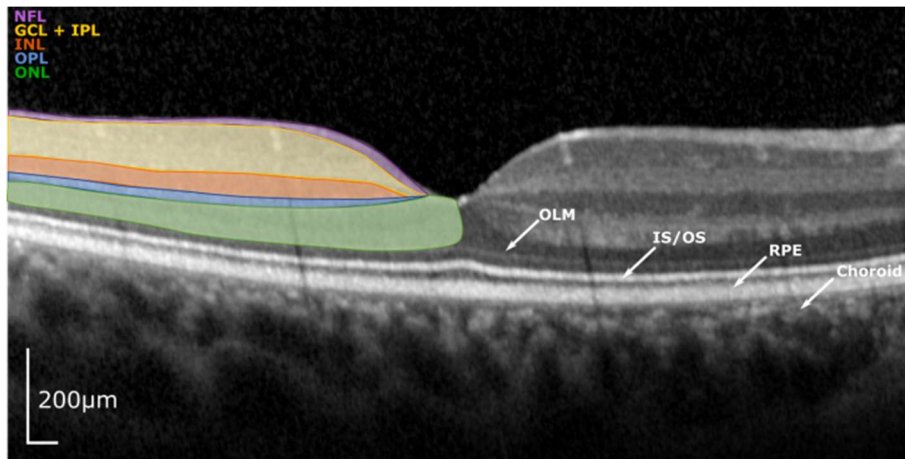
As a result of the transparency of the cornea and the vitreous humor, the retina is easily observable. The funduscopy consists of the observation of the inner face of the retina through a magnifying lens using a light beam that illuminates the retina through the pupil [26]. Retinal vessels and the optic disc (head of the optic nerve) can also be observed. In a normal fundus, the background retina appears of a light orange color, the optic disc is orange-pink and the blood vessels light red. Several retinal disorders present characteristic fundus abnormalities such as fundus albipunctatus [27] or choroideremia [28]. The physiologic fundus appearance of the mouse retina resembles the one of humans even though a difference in color is notable (Fig. 10).



Figure 10: Normal fundus of human (left) [29] and mouse (right).

- A Spectral-Domain Optical-Coherence-Tomography (SD-OCT)

The SD-OCT allows the observation of the retinal structure through cross-sections. Multiple retinal layers are documented such as the nerve fiber layer, a combination of the RGC layer and the IPL, the INL, the OPL, the ONL and the outer segments of the photoreceptors. The thickness of these layers can be measured or the reflectivity of the different layers studied in order to evaluate a retinal disorder [30]. The SD-OCT can be performed as well in rodents [31].



**Figure 11: SD-OCT from an unaffected patient. NFL: nerve fiber layer; GCL: ganglion cell layer; IPL: inner plexiform layer; INL: inner nuclear layer; OPL: outer plexiform layer; ONL: outer nuclear layer; OLM: outer limiting membrane; IS: inner segments; OS: outer segments; RPE: retinal pigment epithelium. Courtesy of Dr. Marco Nassisi**

## 2. VISUAL ACUITY

The visual acuity is the spatial resolving capacity of the visual system and is often described as the ability to see fine details [32]. It depends on the sharpness of the light focus on the retina, the proper health and function of the fovea and finally the treatment of the visual information by the brain [33]. To measure the visual acuity of patients, subjective or objective measurement can be performed.

As a subjective test, the measure of visual acuity by presenting optotype after optimal optical correction is the most common method. Different optotype charts are used and the standardized method of the Early Treatment Diabetic Retinopathy Study (ETDRS) is probably the most commonly used [34, 35]. The ETDRS charts represent letters, numbers or drawings, depending on the age and the educational level of the patient, of decreasing sizes. Patients are placed in front of the chart and the visual acuity is determined by the smallest symbol correctly read [36].

In order to estimate the visual acuity in an objective way, the recording of Visually-Evoked Potentials (VEP) and the stimulation of the optokinetic nystagmus (OKN, mostly used in infants) are suitable. To record VEP, electrodes are placed on the scalp at the level of the right and left occipital lobes and the retina is stimulated through pattern stimulus. Recordings are then made directly at the level of the visual occipital areas. Finally, to elicit the OKN a rotating stripe drum is shown to the patient. First, the eye will follow the direction of the stimulus then it will go back to the primary position to finally start again to follow the stimulus. If there is an abnormal visual acuity, the nasal-to-temporal stimulus will not be effective to elicit OKN [37].

In mice, several tests can be used to investigate the visual response. Similarly to the OKN in human patients, optomotor test can be performed on mice [38]. To elicit head movements, mice are placed on a platform at the center of a striped drum that turns at a speed of two revolutions per minute, clockwise or anti-clockwise (Fig.12). The visual perception of the mice is then measured by the number of head movements in a specific frame of time with a given optomotor frequency.

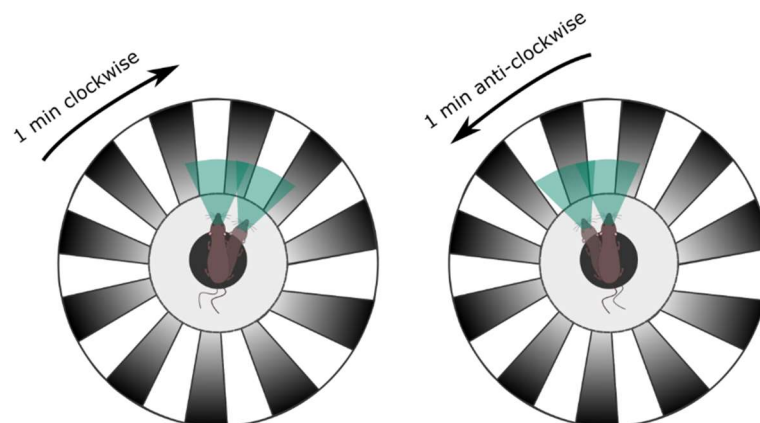


**Figure 12: Schema schematic of the optomotor test performed on mice seen from above. When spun clockwise, a mouse with normal vision follows the movement of the stripes, towards the right. Conversely, it follows the movement towards the left when the spinning observes an anti-clockwise sense.**

### 3. FULL-FIELD ELECTRORETINOGRAM (FF-ERG)

The Full-field electroretinogram (ff-ERG) is an ophthalmological exam which assesses the retinal function by recording the response of the retina to light flashes. Using different types of electrodes such as Dawson Trick Litzkow (DLT) fibers [39] or contact lenses at the surface of the cornea, the ERG records the variation of retinal potentials upon stimulation which is then transferred to the cornea. The International Society for Clinical Electrophysiology of

Vision (ISCEV) established standardized protocols which are minimum testing to precisely document retinal function upon specific light stimulation which are suited to diagnosed most generalized retinal disorders [40]. This exam can also be performed in mice even though there is no standardized protocol. Dark-adapted ERG can also be referred as ERG in scotopic condition and light-adapted ERG as ERG in photopic condition. After a dark-adaptation of at least 20 minutes in human and usually overnight in mice, eyes are submitted to low intensity flashes ( $0.01 \text{ cd.s/m}^2$ ) to elicit rod-driven responses. Increasing intensities, 3.0 then  $10.0 \text{ cd.s/m}^2$ , allow the recording of mixed rod and cone responses, even though dominated by rods which outnumber the cones. These recordings are referred as dark-adapted or scotopic ERG. A light-adaptation of at least 10 minutes is usually done to ensure the saturation of rods and therefore elicit responses initiated by cones (light-adapted or photopic ERG). Two types of recordings are performed in this condition: a single flash of  $3.0 \text{ cd.s/m}^2$  intensity and about 2 Hz frequency and a  $3.0 \text{ cd.s/m}^2$  30Hz flicker to induce responses of L- and M-cone-driven ON- and OFF-pathways (Table1). This kind of protocol can be used in mice with some adjustments in flash intensities or time of dark/light adaptation.

**Table 1: Cellular origins of the two major components of the ERG relying on the ISCEV protocol [39]**

ERG test ISCEV protocol	a-wave	b-wave
DA 0.01 ERG	No	RBCs
DA 3.0 ERG	Combined rod-cone response dominated by rods with neglectable contribution of OFF-CBC	ON-BCs with neglectable contribution of OFF-CBCs
DA 10.0 ERG	Driven by rods and cones	ON-BCs with some OFF-CBCs
LA 3.0 ERG	Cone response along with OFF-CBCs	ON-CBCs then OFF-CBCs
LA 30Hz flicker	L- and S-cone driven ON- and OFF-CBCs	

Two major features prevail in the ERG: the a-wave, transposing the hyperpolarization of the membrane of photoreceptors in response to the flash (see Rod phototransduction cascade); and the b-wave due to the depolarization of ON-BCs once photoreceptors decreased their

glutamate release (See ON-pathway) (Fig.13). In addition, small wavelets can be seen at the ascending limb of the b-wave, under both scotopic and photopic conditions, called oscillatory potentials. They can be isolated in modifying the recording bandwidth and are thought to be at least partially generated at the level of the amacrine cells [41, 42]. Several other ERG waves initiated from different cell types are distinguishable on the ERG but very rarely used due to their high variability such as the c-wave initiated by RPE cells [43, 44], the d-wave corresponding to the response of OFF-BCs [45].

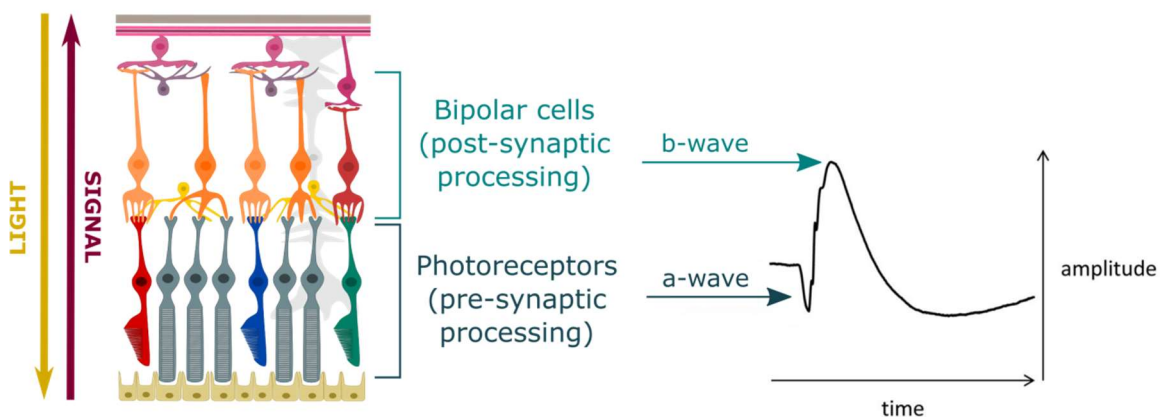


Figure 13: Representation of the cellular origin of the a- and b-wave of the ERG. On the left, schematic representation of the retinal structure, on the right representative trace of the mixed rod-cone responses under dark-adapted conditions.

#### 4. MULTI-ELECTRODE ARRAY (MEA) RECORDINGS

To assess the transmission of the visual signal through ON- and OFF-pathways directly at the level of RGCs, multi-electrode array (MEA) recordings can be performed on *ex vivo* retina [46]. The retina is flat-mounted pressed on the MEA which is composed of a chip containing 256 electrodes while being perfused with heated oxygenated medium to keep it alive (Fig.14A&B). As for the ERG, light stimulus elicits the response of RGCs that is recorded as spikes (Fig.14C). At light onset, ON-RGCs will spike while OFF-RGCs will be activated at light off-set. The full-field light stimuli can be modulated; multiple wavelengths and intensities can be used along with different frequencies.

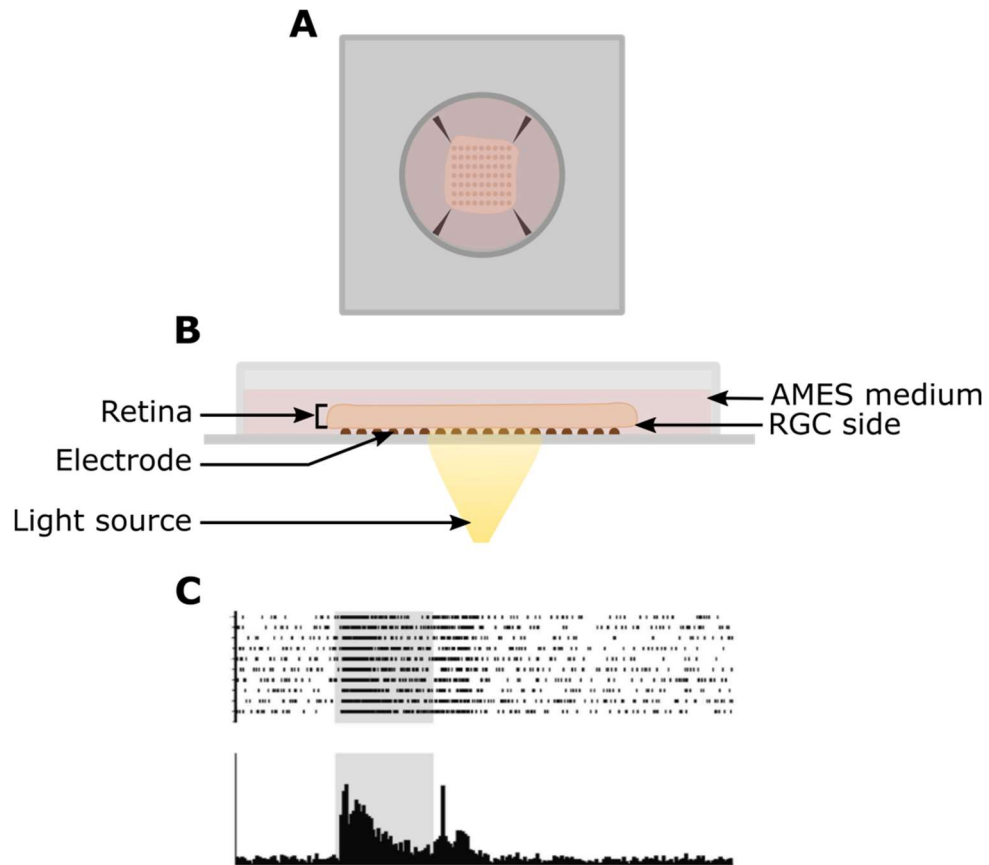


Figure 14: Multi-electrode array set-up and results. (A) MEA set-up seen from above, the retina is maintained in a heated and oxygenated medium while pressed on the electrodes. (B) MEA set-up laterally, RGCs are in direct contact with the electrodes and the stimulating light passes through the retinal layers as physiologically. (C) Spiking activity of RGCs, the grey rectangle represents the duration of the light stimulus. ON-RGCs are spiking at light onset while OFF-RGCs are spiking at light offset; modified from [47].

## II. BIPOLAR CELL SIGNALING DEFECT: CSNB AND MAR

Revealed by the ERG examination, some patients display a “no b-wave” phenotype, outlining a probable transmission defect between photoreceptors and BCs. Among others, two major causes can explain such a phenotype. The first one is an inherited retinal disorder named congenital stationary night blindness (CSNB). The second is a paraneoplastic syndrome associated with ON-BC dysfunction and often called melanoma-associated retinopathy (MAR).

### A. CONGENITAL STATIONARY NIGHT BLINDNESS (CSNB)

Congenital Stationary Night Blindness (CSNB) is a non-degenerative inherited retinal disorder. CSNB can be associated with fundus abnormalities or relatively preserved fundi [17]. Furthermore, it can be separated in two classes: the Riggs-type and the Schubert-Bornschein type of CSNB [48, 49]. Most people suffering from this disease present impairment of night vision in early childhood, preserved retina structure and normal fundi (Fig. 15A, B and C).

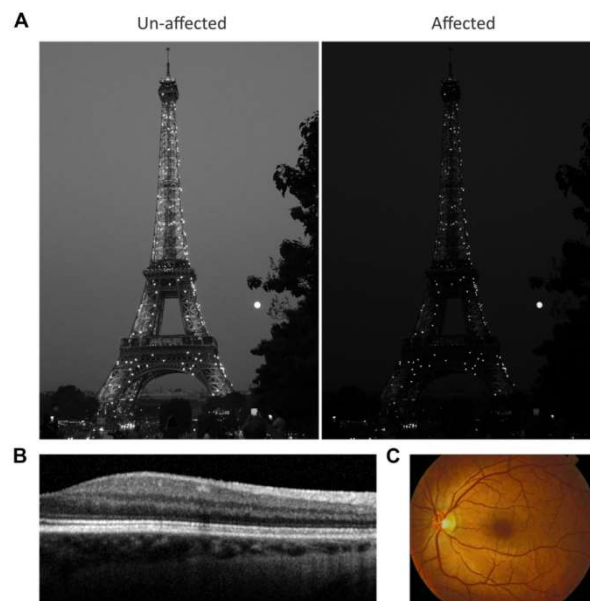


**Figure 15: Congenital Stationary Night Blindness phenotype. (A) Representation of the vision of CSNB patients. Contrasts are not well perceived. (B) Normal SD-OCT. (C) Normal fundus. Both (B) and (C) were modified from [29]**

#### **Riggs type of CNSB**

The Riggs type of CSNB is very rare and most likely overlooked. At low light intensities under dark adaptation (DA 0.01) the b-wave is severely reduced near absent, both a-wave and b-

wave are reduced to a bright flash (DA 3.0 and DA 10.0 ERG) while the light-adapted responses seem to be normal (LA 3.0) confirming normal cone function. These results are consistent with isolated rod photoreceptor dysfunction [48]. Riggs patients present normal visual acuity and visual fields but have problems to orientate during dim light conditions. This particular type of CSNB is found in patients with preserved fundi and mutations in *RHO* [50], *PDE6B* [51, 52], *GNAT1* [53] and *SLC24A1* [54, 55] (Fig.15). In addition, this particular type of CSNB is also found in patients with Fundus Albipunctatus and Oguchi disease due to mutations in *RDH5* [56, 57], and either *SAG* or *GRK1* [58-60], respectively (Fig. 17).

### **Schubert and Bornschein type of CSNB**

Patients with the most frequent form of CSNB, the so-called Schubert-Bornschein type of CSNB, have an electronegative ERG, which means that, in dark-adapted conditions the a-wave is preserved and the b-wave is extremely reduced (DA 3.0 and DA 10.0 ERG) in keeping with post-photoreceptor dysfunction. This class of CSNB can be further subdivided in two forms: complete CSNB (cCSNB) and incomplete CSNB (icCSNB) [61].

#### **1. INCOMPLETE CSNB (icCSNB)**

Patients with the incomplete type of CSNB (icCSNB) do not always report night blindness, even though they might be suffering from it, but most commonly complain of light sensitivity, have nystagmus, and may show strabismus variable degrees of myopia and/or hyperopia [17, 62, 63]. Under dark-adapted conditions (DA 0.01 ERG) the ERG b-wave is detectable but delayed and of subnormal amplitude thus, the term incomplete. With a bright-flash (DA 3.0 and 10.0 ERG) only the b-wave is reduced. In light-adapted conditions (LA 3.0 ERG) the b/a ratio is reduced [17]. Both ON- and OFF responses are affected, as shown by long-duration stimulation [64], in this particular sub-form of Schubert-Bornschein CSNB. icCSNB is caused by mutations in genes localized at the photoreceptor synapse: mainly in *CACNA1F* [65, 66] and very rarely in *CABP4* [67] and in *CACNA2D4* [68], with the latter showing finally a distinct phenotype, closer to a cone dystrophy [68, 69](Fig.17).

#### **2. COMPLETE CSNB (cCSNB)**

Herein, due to the topic of my thesis, I will concentrate on cCSNB describing the phenotype, genetics, animal models and pathogenic mechanisms in more details.

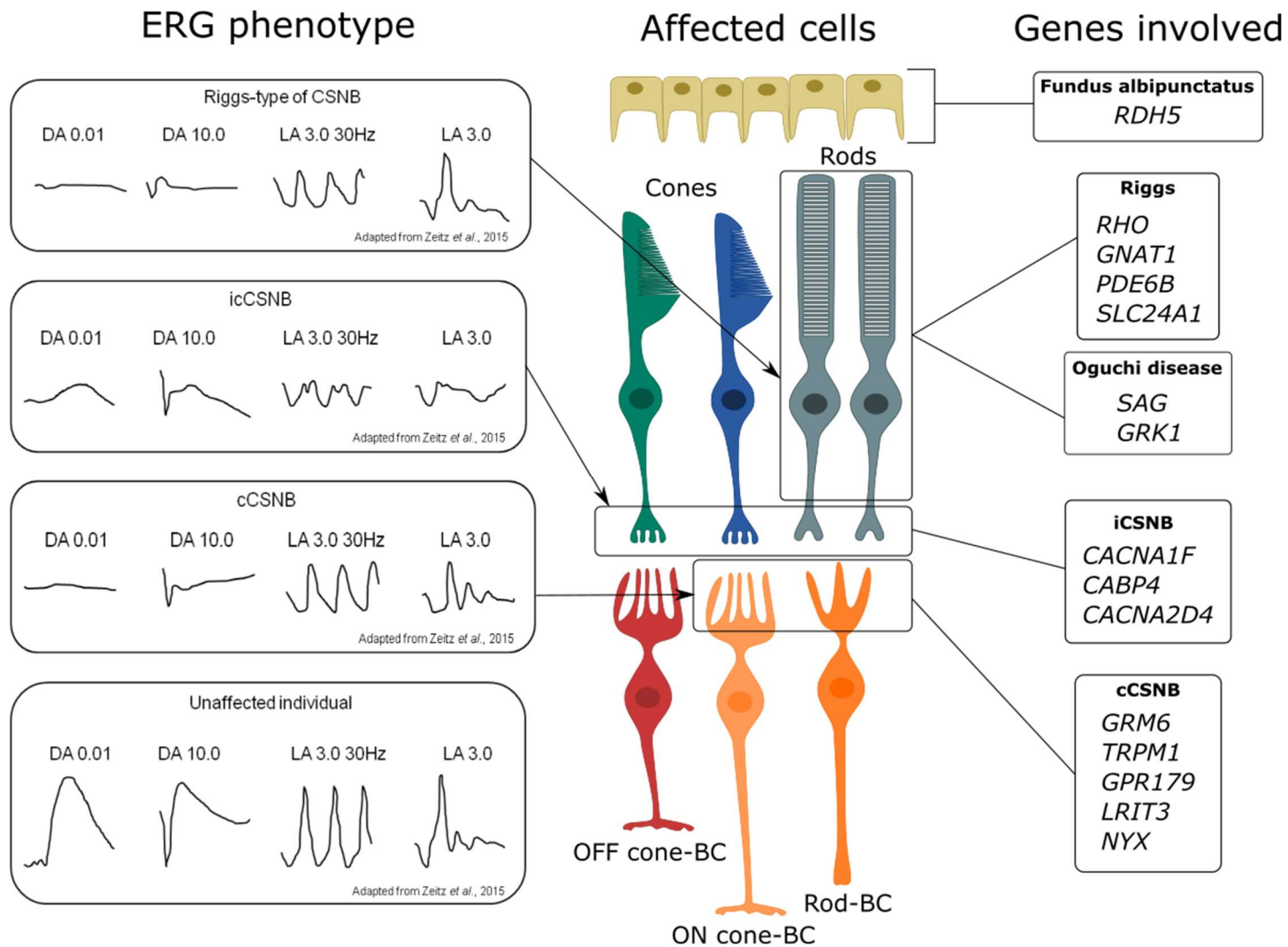


Figure 16: Schematic representation of the ERG phenotypes of Riggs-type CSNB, incomplete CSNB, complete CSNB and unaffected individual. These ERG defects are due to a cellular dysfunction, which is explained by mutations in the corresponding genes. The expression and localization of LRIT3 is not certain yet; here it is depicted as having solely an effect on ON-BCs.

## **cCSNB phenotype**

Patients affected with the complete type of CSNB (cCSNB) report night blindness more consistently than patients with icCSNB, frequently have a nystagmus, severe myopia and may show strabismus [17, 62, 63]. In dark-adapted conditions, there is no detectable b-wave to dim flash on the ERG (DA 0.01 ERG): thus, the term complete. The a-wave is normal presuming a normal rod photoreceptor function but the b-wave is severely absent leading to an electronegative waveform in keeping with post-photoreceptor dysfunction (DA 3.0 and 10.0 ERG). At light adapted conditions (LA 30 Hz ERG), the ERG response is usually of normal amplitude, but has a pathognomonic flattened trough and an implicit time shift. The single-flash cone ERG (LA 3.0) displays normal amplitude of the a-wave with a broadened trough; the waveform has a sharply rising b-wave with no oscillatory potentials and a reduced b/a ratio. Unlike icCSNB, only ON-responses are affected in the complete form as shown by long duration stimuli [64, 70] (Fig. 16).

## **Genes involved in cCSNB**

cCSNB is a genetically heterogenous inherited retinal disorder. The five genes affected in cCSNB code for proteins involved in the signaling cascade between photoreceptors and ON-BCs triggered by glutamate release (Fig.7 & Fig.16). These genes were identified through classical linkage [71, 72], candidate gene approach using existing animal models [73-77] or whole exome sequencing (WES) [78, 79]. The most prevalent gene affected in cCSNB is *NYX* coding for nyctalopin [17, 71, 72]. Mutations in *NYX* are the only ones leading to X-linked cCSNB [71, 72], all other genes lie on autosomes and mutations in these are inherited as a recessive trait [17, 73-80]. The second most prevalent gene mutated in cCSNB is *TRPM1* which codes for the Transient Receptor Potential channel subfamily M member 1 (TRPM1) [73-75]. Thirdly, *GRM6* codes for the metabotropic glutamate receptor 6 (mGluR6) [76, 77]. Fourthly, *GPR179* codes for an orphan seven transmembrane G-protein coupled receptor [78]. *LRIT3*, finally, is the less prevalent gene with to date six mutations described leading to cCSNB [17, 79, 81] (Fig.17).

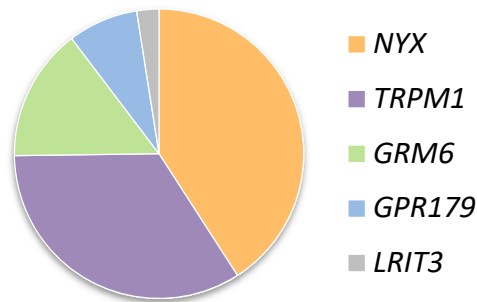


Figure 17: Prevalence of the gene defects underlying cCSNB, modified from [17]

### Animal models for cCSNB

Several animal models, either spontaneous or genetically modified, have been described as displaying the CSNB phenotype, showing an electronegative ERG-phenotype. These models served my host laboratory as candidate genes to identify the gene defect for the human pathology [67, 68, 73, 77], help to better understand the pathophysiology and develop therapies [17]. Especially, in cCSNB ERG findings under scotopic conditions pinpoint to similarities between the animal model and the human phenotype. Under photopic conditions, a higher variability can be noted (Fig. 18). Other differences may be due to physiological species differences or different ERG protocols used. Four species have been used as models: horses, dogs, zebrafishes and mice, and their ERG-phenotypes are described below.

#### Horses with cCSNB

Previously, Appaloosa horses showing a specific skin pattern (leopard-spotting complex LSC) and a Tennessee walking horse were diagnosed by electroretinography with CSNB [82-84]. Linkage and expression analyses for the Appaloosa horses or whole genome sequencing for the Tennessee walking horse, revealed a homozygous endogenous retroviral long-terminal repeat insertion in *TRPM1* [85, 86] and a missense mutation in *GRM6* [84] respectively, as disease causing. As in patients, strabismus was identified in a few *TRPM1*<sup>-/-</sup> horses [87], while the retinal structure was well preserved [82]. The Tennessee walking horse had navigation difficulties in dim-light condition. Under scotopic conditions to both dim- and bright flash, these CSNB horses displayed an electronegative ERG. Under photopic conditions for the Appaloosa horse, the a-wave has a greater amplitude than unaffected horses and there is a reduced b/a ratio [87](Fig. 18).

### Beagle dogs with cCSNB

Recently, a cCSNB phenotype was also observed in beagle dogs [88, 89]. One of the studies revealed a 1-bp-deletion in *LRIT3* found by whole genome sequencing, confirming the cCSNB phenotype of these animals [90]. As CSNB patients, the retinal structure is preserved in the affected dogs. On the ERG, under scotopic condition to dim flashes, the b-wave was absent in affected dogs with a preserved a-wave. With a brighter flash, e.g. when responses are driven by both rods and cones, a very small inflection is noticed in affected dogs while the b-wave is recordable in wild-type animals [88]. Under photopic conditions at low light intensities, the a- and b-waves were quite similar between unaffected and affected dogs while the b-wave is severely reduced at brighter intensities along with an absence of oscillatory potentials in the cCSNB dogs [88] (Fig. 18). The time-course of the disease seems to be also stationary because the ERG did not change in a four-year course [88].

### Zebrafish models of cCSNB

Three zebrafish models of CSNB were described using morpholinos for *Nyx*, *Grm6* or *Gpr179*. All models presented a reduction of the b-wave upon ERG measurements [80, 91, 92] (Fig. 18).

### Mouse models of cCSNB

Several mouse models for all genes involved in cCSNB have been described. The global retinal morphology of these mouse models is well preserved. Under scotopic conditions, no b-wave is detectable in mutant mice and the a-wave is preserved. Under photopic conditions, most mouse models reveal a lack of the b-wave while it is always present in cCSNB patients. Together, these clinical characteristics of the mouse models for cCSNB highlight the similarities in respect to the retinal structure and ERG-findings under scotopic conditions, but depict also the limitations of these models to mimic the human phenotype under photopic conditions [17, 93] (Fig. 18, Table 2).

Almost all mouse models do not produce the corresponding protein and most of the time other proteins of the cascade or lead to a mislocalization of these partners [17] (Table 2). The acute characterization of these models is primary; in order to further investigate the signaling cascade of ON-BCs and the pathogenic mechanisms underlying cCSNB.

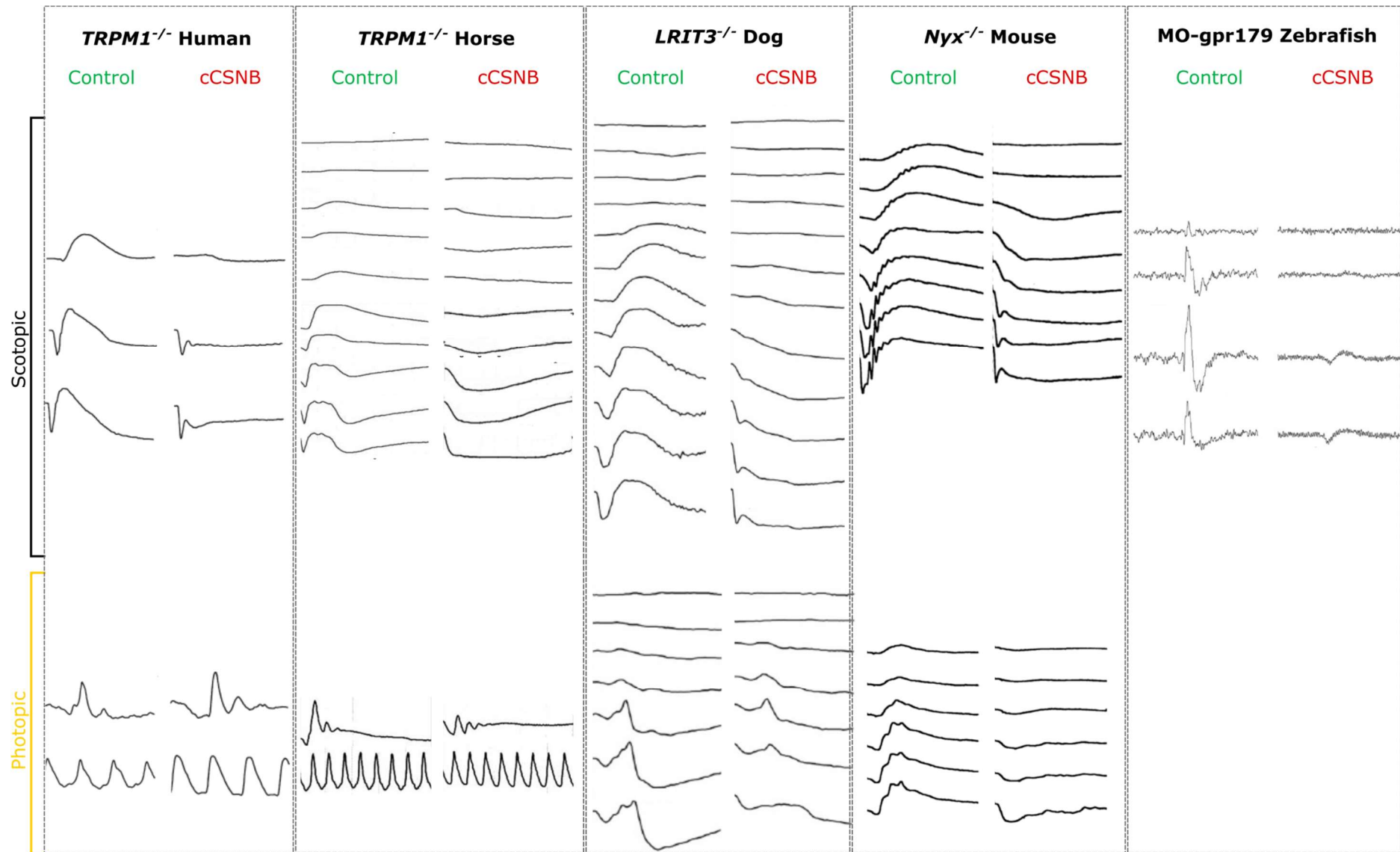


Figure 18: Schematic representation of ERG recordings of five different species known displaying a cCSNB phenotype. Figures were adapted from Audo *et al.*, 2009 (for human CSNB, patient with mutations in *TRPM1*) from Sandmeyer *et al.*, 2007 (for the *TRPM1<sup>-/-</sup>* Appaloosa horse ERG), from Kondo *et al.*, 2015 (for the *LRIT3<sup>-/-</sup>* Beagle dog ERG), from Pardue *et al.*, 1998 (for the *Nyx<sup>-/-</sup>* mouse ERG) and from Peachey *et al.*, 2012 (for the MO-gpr179 zebrafish ERG).

Table 2: Mouse models of cCSNB. \*: proteins which are only missing in CBCs

Gene	Name	Mutation	Designed/Spontaneous	ERG Phenotype	Missing or mislocalized proteins	First publication
<b>Nyx</b>	<i>nob</i>	Deletion in exon 4	Spontaneous	Both scotopic and photopic ERG: no b-wave	Nyctalopin, TRPM1[23, 94]	Pardue 1998[93] Gregg 2003 [95]
<b>Trpm1</b>	<i>Trpm1<sup>tm1Lex/tm1Lex</sup></i>	Deletion of exons 4 to 6	Designed	Both scotopic and photopic ERG: no b-wave	TRPM1[21-23, 94, 96, 97]	Koike 2009[96], Morgans 2009[21], Shen 2009[98]
	<i>Trpm1<sup>tvrm27</sup></i>	ENU induced missense mutation in exon 23	Designed	Both scotopic and photopic ERG: no b-wave		Peachey 2012a[99]
<b>Grm6</b>	<i>Grm6<sup>tm1Nak</sup></i>	Insertion of neomycin cassette in exon 8	Designed	Both scotopic and photopic ERG: no b-wave	mGluR6[23, 94, 100-102], reduced TRPM1[101], RGS7[94], RGS11[94, 101], reduced Gβ5[101], R9AP[94], GPR179 (this study)	Masu 1995[100]
	<i>nob3</i>	Mutation in exon 2	Spontaneous	Both scotopic and photopic ERG: no b-wave	mGluR6[103], GPR179[104], TRPM1[104, 105]	Maddox 2008[103]
	<i>nob4</i>	ENU induced missense mutation in exon 3	Designed	Both scotopic and photopic ERG: no b-wave	mGluR6[106, 107], TRPM1[105], reduced RGS7[108], RGS11[106, 108], Gβ5[108], R9AP[108]	Pinto 2007[107]
	<i>nob7</i>	Missense mutation in exon 8	Spontaneous	Both scotopic and photopic ERG: no b-wave	mGluR6	Qian 2015[109]

Gene	Name	Mutation	Designed/Spontaneous	ERG Phenotype	Missing or mislocalized proteins	First publication
<b>Grm6</b>	<i>nob8</i>	Missense mutation	Spontaneous	Reduced b-wave	Reduced mGluR6	Peachey 2017 [110]
<b>Gpr179</b>	<i>nob5</i>	Transposon insertion in exon 1	Spontaneous	Scotopic ERG: no b-wave and photopic ERG: severely reduced nay missing	GPR179[22, 80, 94, 111-113], RGS7[94, 111], RGS11[94, 112], Gβ5[112], R9AP[94, 112]	Peachey 2012b[80]
<b>Lrit3</b>	<i>nob6 (Lrit3<sup>-/-</sup>)</i>	Insertion cassette between exon 3 and 4	Designed	Scotopic ERG: no b-wave and photopic ERG: severely reduced nay missing	LRIT3, TRPM1, mGluR6*, GPR179*, RGS7*, RGS11*, Gβ5*	Neuillé 2014[114]
	<i>Lrit3<sup>tvrm257</sup></i>	ENU induced missense mutation in exon 2	Designed	Both scotopic and photopic ERG: no b-wave		Charette 2016[115]
	<i>Lrit3<sup>emrgg1</sup></i>	ZFN targeting of exon 2 leading to 40bp deletion	Designed	Both scotopic and photopic ERG: no b-wave	LRIT3, Nyctalopin, GPR179*, mGluR6*, RGS7*, RGS11*, Gβ5*, R9AP*, TRPM1	Hasan 2020[116]

## Pathogenic mechanism underlying cCSNB

*In vitro* and *in vivo* studies of gene defect causing cCSNB showed that most likely all of them lead to a loss of function of the protein. These similarities are in accordance with the comparable complete lack of b-wave phenotypes under scotopic conditions in patients with cCSNB [17].

*In vitro* and *in vivo* studies revealed that NYX (nyctalopin) is crucial for the correct localization of TRPM1, along with LRIT3 [23, 24]. Therefore, it is most likely that the cCSNB phenotype in cases of NYX mutations is due to the mislocalization of TRPM1 [23]. *TRPM1* intronic mutations seem to lead to the absence of the protein or an abnormal protein production while missense mutations cause a mislocalization explaining a loss of function of TRPM1 [117]. Nonsense and frameshift mutations of *GRM6* are probably leading to nonsense mediated mRNA decay (NMD) or a non-functional truncated receptor. *In vitro* studies revealed that missense mutations in different domains of the protein lead to a trafficking defect [118]. As mentioned before, mGluR6 plays a major role at the initiation of the ON-BCs cascade and is central for the regulation and correct localization of other partners of the cascade such as regulatory proteins [94]. *GPR179* nonsense and frameshift mutations most likely lead to a loss of function of the protein or the elimination of the mutated mRNA through NMD. GPR179 is important for the correct localization of regulatory proteins but not directly for the proper localization of TRPM1 [104]. Mutations in *LRIT3* seem to abolish the production of the LRIT3 protein which interacts with nyctalopin with the latter probably holding TRPM1 in place at the dendritic tips of ON-BCs [24].

### B. FURTHER INSIGHT IN TWO CCSNB PROTEINS: MGLUR6 AND LRIT3

In this thesis project we decided to concentrate on two genes/proteins leading to cCSNB when mutated: mGluR6 and *LRIT3*/LRIT3. Several reasons guided this choice: albeit mutations in NYX represent a major cause of cCSNB and the size of the gene accommodates with the packaging capacity of adeno-associated virus (AAV) vector (4.7 kb [119]), the respective mouse model, *nob*, is not freely accessible. In addition, an antibody directed against the respective mouse nyctalopin protein is not available. The second most prevalent gene defect underlying cCSNB are mutations in *TRPM1*. However, as mentioned above, the maximum size of a gene to be

encapsidated in an AAV vector is 4.7 kb and TRPM1 is 5.4 kb in size, which makes gene replacement therapy impossible with AAV vectors. Therefore, we chose to focus on *GRM6* (2.6 kb RefSeq NM\_000843.4), which is the third most prevalent mutated gene in cCSNB, small enough to fit in an AAV vector, with the mouse model available in our laboratory. In addition, *LRIT3* has been chosen because of its small size (approximately 2 kb RefSeq NM\_198506.3), because of previous interest of our lab to elucidate the function of this particular protein and the availability of a mouse model in our laboratory.

### 1. [GRM6/MGLUR6](#)

*GRM6* is a gene located on chromosome 5 (5q35). It is composed of 10 exons and codes for a protein of 877 amino acids [120]. Its structure is divided in an extracellular region with ligand-binding domains and cysteine-rich domains, seven transmembrane regions and a cytoplasmic region (Fig.19).

#### ***GRM6* mutations lead to cCSNB**

Different mutations have been identified including frameshift, nonsense and missense mutations. All frameshift and nonsense mutations are predicted to lead to the absence of a functional protein [76, 77]. Interestingly, all investigated missense mutations in *GRM6* lead to a trafficking defect of the mGluR6 proteins to the membrane [118]. Together, these mutations may lead to an absence of the protein or a misfolding of mGluR6 and subsequently to the incorrect uptake of glutamate, leading to the absent b-wave in the ERG.

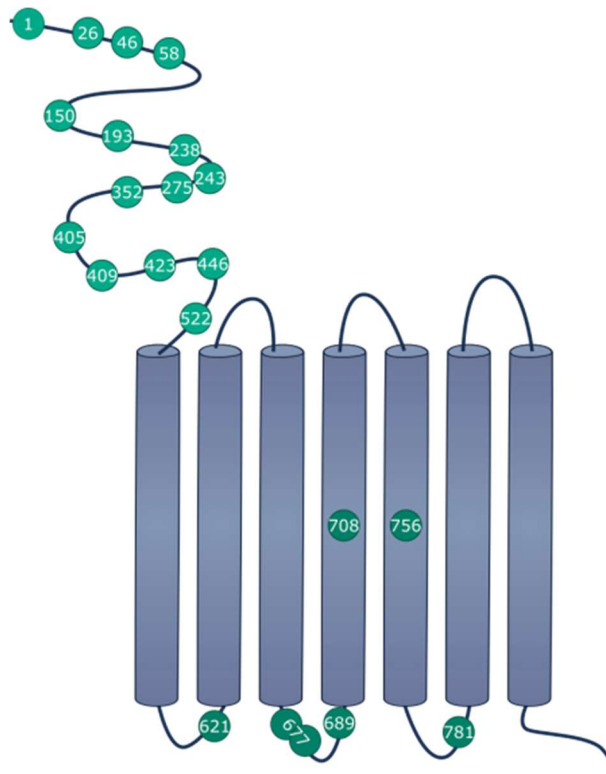


Figure 19: Schematic drawing of the mGluR6 protein (UniProtKB/Swiss-Prot protein O15303) along with the localization of the different mutations causing cCSNB, modified from [17]

### **mGluR6 is the key component of the ON-bipolar cell pathway**

mGluR6 is a metabotropic G-coupled receptor composed of 7 transmembrane domains [18, 19, 100]. The mGluR6 protein is the sensor of the glutamate released by photoreceptors in the synaptic cleft and triggers the signaling cascade at the dendritic tips of ON-BCs [18]. It is essential for the proper localization of other proteins of the cascade such as TRPM1 and regulatory proteins (RGS7, RGS11, Gβ5 and R9AP). It has been demonstrated that deletion of mGluR6 inactivates the cation channel TRPM1 [101].

### **The synaptic organization between photoreceptors and bipolar cells involves mGluR6**

It has been shown that ON-BCs are normally distributed in the mouse retina in absence of mGluR6 [102]. However, it seems that mGluR6 plays a role at the photoreceptor to bipolar cell synapse. Indeed, invaginating dendrites of RBCs are larger and often contain ectopic ribbons while the number of invaginating dendrites of cone ON-BCs and ribbons decrease at the cone pedicles in the *Grm6<sup>tm1Nak</sup>* mouse model [121, 122]. Finally, Tummala and colleagues showed that mGluR6 had also a role pre-synaptically as several presynaptic matrix-associated proteins

such as pikachurin, dystrophin and dystroglycan are reduced at the rod-to-RBC synapse in the same mouse model [123].

## 2. LRIT3

*LRIT3* is a gene located on chromosome 4 (4q25). It is composed of four exons and codes for a protein of 679 amino acids. *LRIT3* codes for the Leucine rich-repeat, immunoglobulin-like, transmembrane domain 3 (Fig. 20). Previously it was reported that LRIT3 can influence the maturation and signaling of FGFR1 [124]. However, its role in the retina is not entirely understood.

### **cCSNB can be caused by mutations in *LRIT3***

More recently it was shown by our group that LRIT3 mutations lead to cCSNB [79]. To date, seven mutations in *LRIT3* leading to cCSNB have been described: four mutations in the fourth exon (c.983G>A p.Cys328Tyr, c.1151C>G p.Ser384\*, c.1318C>T p.Arg440\*, c.1538\_1539del p.Ser513Cysfs\*59 [79], one in the second exon ((c.345T>A p.Asn115Lys) [17], one on the start codon (c.1A>G p.0?) [81] and a seventh mutation was found in the third exon (c.608G>T p.Trp203Leu) [81]. To date, the seven reported *LRIT3* pathogenic mutations are localized in different domains of the protein: in the leucine-rich domains, a disulfide bond or the serine-rich domain for example (Fig.20). Together, these mutations may lead to absence of the protein, misfolding or disrupted interaction with a putative scaffolding protein and therefore to the lack of TRPM1 channel at the membrane leading to the absent b-wave in the ERG.

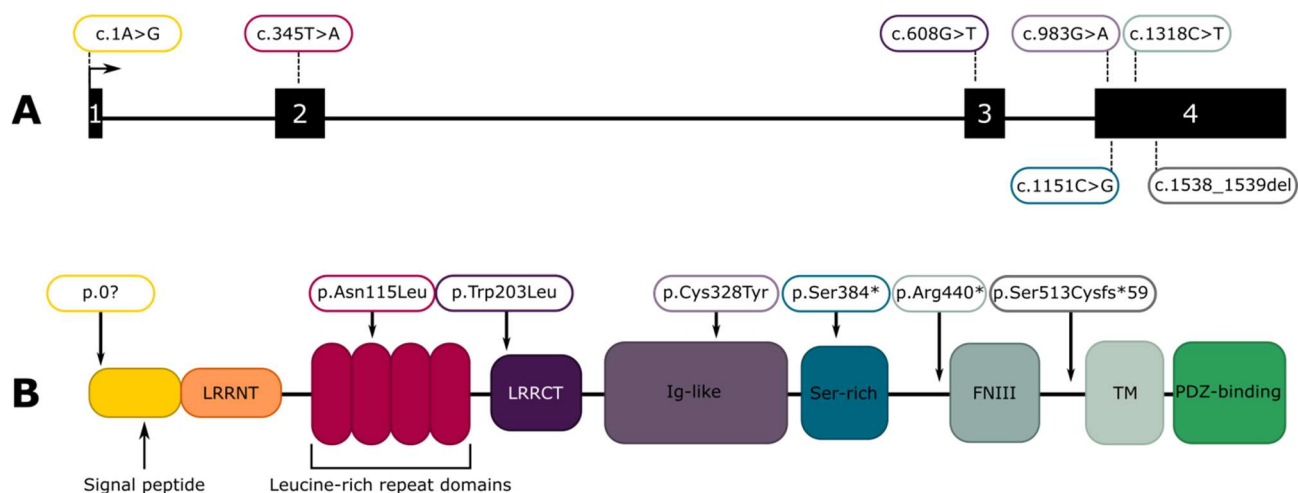


**Figure 20: Mutations in *LRIT3* causing cCSNB. (A) Exonic localization of the *LRIT3* mutations. (B) Proteic localization of the *LRIT3* mutations. LRRNT: Leucine-Rich Repeat N-terminal; LRRCT: LRR C-terminal; Ig-like: Immunoglobulin-like domain; Ser-rich: Serine-rich domain; FNIII: Fibronectin type 3 domain; TM: trans-membrane domain.**

### **LRIT3 is involved in the localization of TRPM1**

Immunolocalization studies in the human retina identified LRIT3 in the OPL [79]. As mentioned before, the phenotype of patients with mutations in *LRIT3* resemble the one of patients with mutations in other genes coding for proteins of the ON-BC signaling cascade [79]. These observations suggested that LRIT3 might as well be present at the dendritic tips of RBCs and CBCs [79]. In the *Lrit3*<sup>-/-</sup> mouse, an abolishment of TRPM1 cation channel was observed at the dendritic tips of both, rod and cone ON-BCs. In contrast immunolocalization of TRPM1 in the cell bodies of ON-BCs was not affected [125]. When quantified, the total amount of TRPM1 in the *Lrit3*<sup>-/-</sup> retina was the same as in *Lrit3*<sup>+/+</sup> mice [125], as observed in the *LRIT3*-CSNB canine model [90], consistent with a trafficking defect of TRPM1. Therefore, these results suggest a role of LRIT3 in the trafficking of TRPM1 and its maintenance at the membrane of the dendritic tips of ON-BCs. Similarly, nyctalopin was shown to be essential for the proper localization of TRPM1 [23]. However, it was suggested that nyctalopin alone might not be sufficient to bring TRPM1 to the membrane as nyctalopin is mainly an extracellular protein [23]. Since LRIT3 harbors a PDZ-binding motif, it was suggested that it corresponds to the molecule which interacts with intracellular scaffolding complexes to bring the TRPM1 channel to the dendritic tips of ON-BCs. Subsequently, together, nyctalopin and LRIT3 may hold the channel in this form. Recently, it was shown that LRIT3 is also required for nyctalopin localization at the dendritic tips of ON-BCs [116]. Thus the authors concluded that the loss of TRPM1 at the dendrites of ON-BCs is due to the absence of nyctalopin induced by the abolishment of LRIT3,

leading to the no b-wave phenotype, as studied in the *Lrit3<sup>emrgg1</sup>* mouse [116]. In addition, the localization of LRIT3 in ON-BCs was lately questioned since its expression in rods led to a restoration of the cCSNB phenotype [126] and a single-cell transcriptomic analysis showed a strong expression of LRIT3 in photoreceptors and a mild expression in BCs [127].

### **LRIT3 plays a role at the cone synapse**

Another major role for LRIT3 has been identified through the *Lrit3<sup>-/-</sup>* mouse and confirmed by the *LRIT3*-CSNB canine model. As shown before, LRIT3 has a role in the correct localization of TRPM1 to the dendritic tips of ON-BCs, contacting both rod and cone photoreceptors. Furthermore, postsynaptic clustering of other mGluR6 cascade components such as mGluR6, GPR179 and regulatory proteins are selectively eliminated at the dendritic tips of cone ON-BCs suggesting a role for LRIT3 in the cone synapse formation [24]. This hypothesis was confirmed by electron microscopy showing a decreased number of invaginating contacts made by cone ON-BCs in the cone pedicle and a striking decrease in the number of triads [47]. Normal cone pedicles were also observed indicating that LRIT3 is not essential for the natural formation of the cone-to-cone BC synapse but plays a major role in this process [47]. Furthermore, peanut agglutinin (PNA) staining is abolished in the OPL of *Lrit3<sup>-/-</sup>* mice [24]. Similar findings were described in the LRIT3-dog model [90]. Interestingly, altered PNA staining was impaired in the affected dog retina meaning that the architecture of cones and cone-BCs is deformed and that the conformation of the synapse is distorted in these animals [90].

### C. PARANEOPLASTIC BIPOLAR CELL DYSFUNCTION (OFTEN REFERRED AS MELANOMA-ASSOCIATED RETINOPATHY OR MAR)

Similar as found in patients with CSNB, patients with paraneoplastic ON-BCs dysfunction reveal an absence of the b-wave upon ERG under scotopic conditions leading to an electronegative waveform.

## **Phenotype of melanoma-associated retinopathy patients**

Two major types of paraneoplastic retinopathies with an initial normal fundus have been reported: (1) cancer-associated retinopathy (CAR), which leads to a rapid and severe visual dysfunction with primary photoreceptor alterations and is most commonly associated with small-cell carcinomas of the lung and less frequently associated with breast, endometrial and other cancers [128, 129]; (2) melanoma-associated retinopathy (MAR), traditionally associated with metastatic melanoma [130] but now well recognized in association with other cancers such as carcinomas [131-134]. As in CSNB patients, patients affected with MAR also suffer from night blindness, and a decreased visual acuity. Constriction of the visual fields and photopsias are also key symptoms in MAR patients. Similarly to patients presenting a CSNB phenotype with normal fundi, most patients with MAR have a normal fundus (Fig.21 A and B). The ff-ERG is critical for the proper diagnosis of MAR and typically shows ON-bipolar cell dysfunction resembling the ERG abnormalities seen in cCSNB [17, 49, 61, 130]. Under dark adapted conditions, there is no detectable response to a dim flash (DA 0.01 ERG). The responses to a bright flash (DA 3.0 and 10.0 ERG) have an electronegative waveform with a normal negative a-wave, reflecting the normal hyperpolarization of photoreceptors. In contrast, the b-wave is severely reduced in keeping with ON-bipolar cell dysfunction (Fig. 21C). Light adapted responses (LA 3.0 ERG) are also abnormal, as notable by the squared shape of the a-wave, and the sharply arising b-wave resulting in a reduced b/a ratio, due to cone-ON-BCs alterations (Fig. 21C).

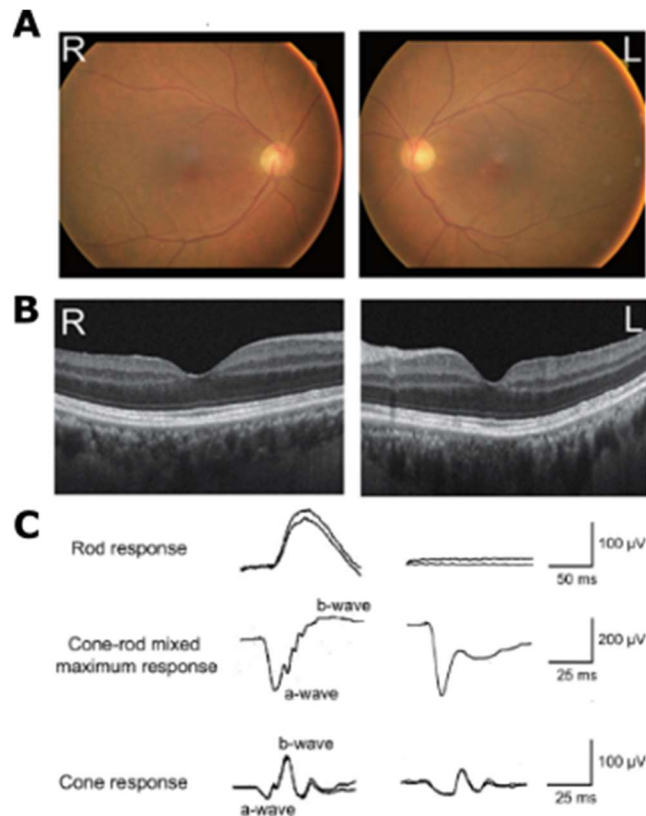


Figure 21: Usual retinal phenotype of patients affected by paraneoplastic retinopathy associated with ON-bipolar cell dysfunction. (A) Normal fundus of a CAR patient, R: right, L: left. (B) Normal SD-OCT of a CAR patient, R: right, L: left. (C) ERG findings of an unaffected individual (left) and a CAR patient (right), the b-wave is absent under scotopic condition. All figures were modified from [133].

### Anti-TRPM1 autoantibodies

The retinal phenotype of MAR patients is explained by the presence of auto-antibodies targeting retinal proteins. Interestingly, anti-TRPM1 autoantibodies have been reported in the serum of different MAR patients [133-146] and the mutated form of *TRPM1* leads to cCSNB [73-75]. To summarize, in both cases an inactivation of TRPM1 explains the absence of b-wave on the ERG in scotopic conditions and under photopic conditions either through inactivation by autoantibodies (MAR) or due to *TRPM1* mutations leading to the loss of function of the protein. TRPM1 is not only localized in retinal ON-BCs but also in melanocytes where it plays a role in pigmentation and melanocyte proliferation [147, 148], connecting melanoma and retina in MAR patients. Interestingly, no skin phenotype has yet been documented in *TRPM1*-related cCSNB [73-75].

### III. GENE THERAPY FOR INHERITED RETINAL DISORDERS (IRDs)

#### A. PRINCIPLE OF GENE THERAPY

Many ocular disorders are due to mutations in specific genes. New gene identification techniques such as next generation sequencing (NGS), whole exome sequencing (WES) or whole genomes sequencing (WGS) solved the genetic defect of many different disorders [149]. This helps to better diagnose patients but also to identify new targets to be treated by gene therapy. Indeed, several clinical trials involving gene therapy are ongoing (Fig. 22, Table 3).

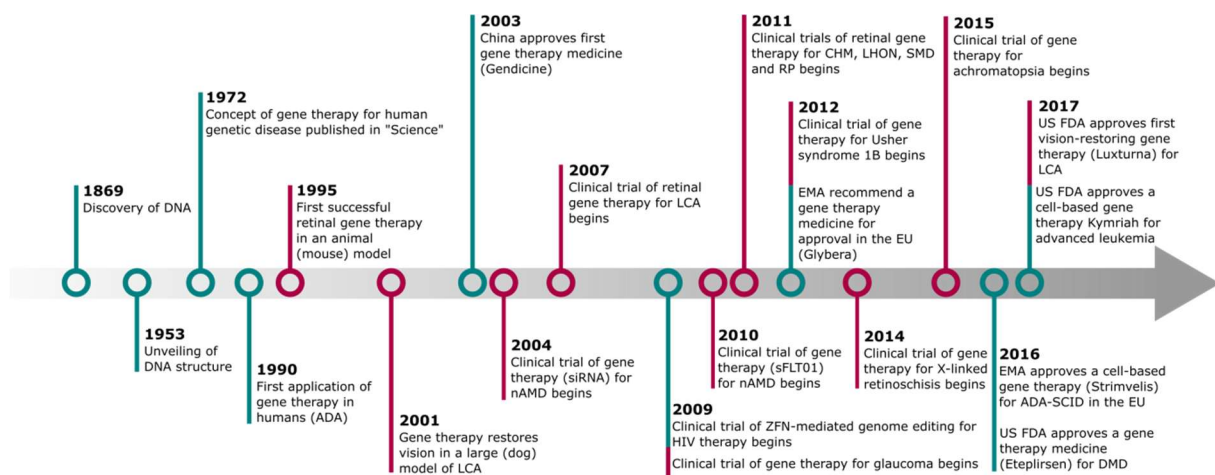


**Figure 22: Gene therapy milestones, adapted from [150].** DNA: Deoxyribonucleic acid; ADA: Adenosine deaminase deficiency; LCA: Leber Congenital Amaurosis; siRNA: small interfering ribonucleic acid; nAMD: neovascular Age-related Macular Degeneration; ZFN: Zinc Finger Nuclease; HIV: Human Immunodeficiency Virus; CHM: Choroideremia; LHON: Leber Hereditary Optic Neuropathy; SMD: Stargardt Macular Degeneration; RP: Retinitis Pigmentosa; EMA: European Medicines Agency; FDA: Food and Drug Administration; SCID: Severe Combined Immunodeficiency

Gene therapy consists in replacing, augmenting or repairing the gene defects by providing the correct DNA sequence of the gene or genetic tools to correct the causative mutation to the cell to allow it to produce the right protein and therefore restore its function. The eye has many advantages as gene therapy target organ. First, the well-known anatomy of the eye is a true asset and its limited size allows the use of relatively low doses of vector. Secondly, retinal cells do not proliferate after birth which should allow a sustained expression of the transgene [5]. Furthermore, an injection of vector into the eye will not induce a systemic release and possibly a generalized immune response as the blood-retinal barrier prevents the circulation of molecules between the retina and the blood flow. This feature makes the eye an immune-privileged tissue [151].

## Gene addition/ Gene replacement

One way to apply gene therapy is to deliver the wild-type copy of the defective gene directly into the cell that expresses it (Fig.23). This type of gene therapy can only be applied to gene defect leading to a loss of function. In diseases with gain of function mutations, as it is the case in certain autosomal dominant gene defect, delivery of the wild-type copy of the gene will not be sufficient to induce a correction of the phenotype [152]. This approach was used in the clinical trial for RPE65-related Leber Congenital Amaurosis (LCA) and is suitable for most forms of CSNB [17, 153-155].

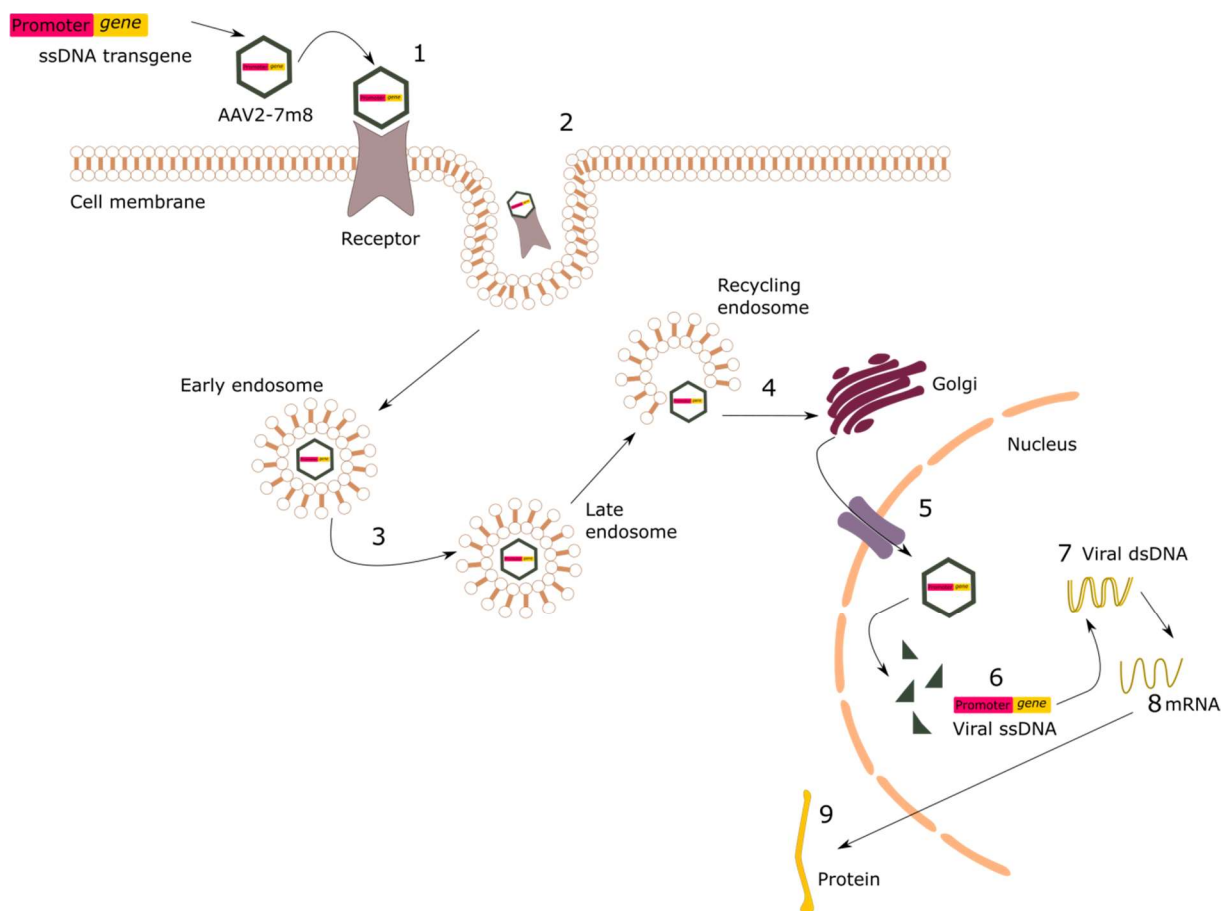
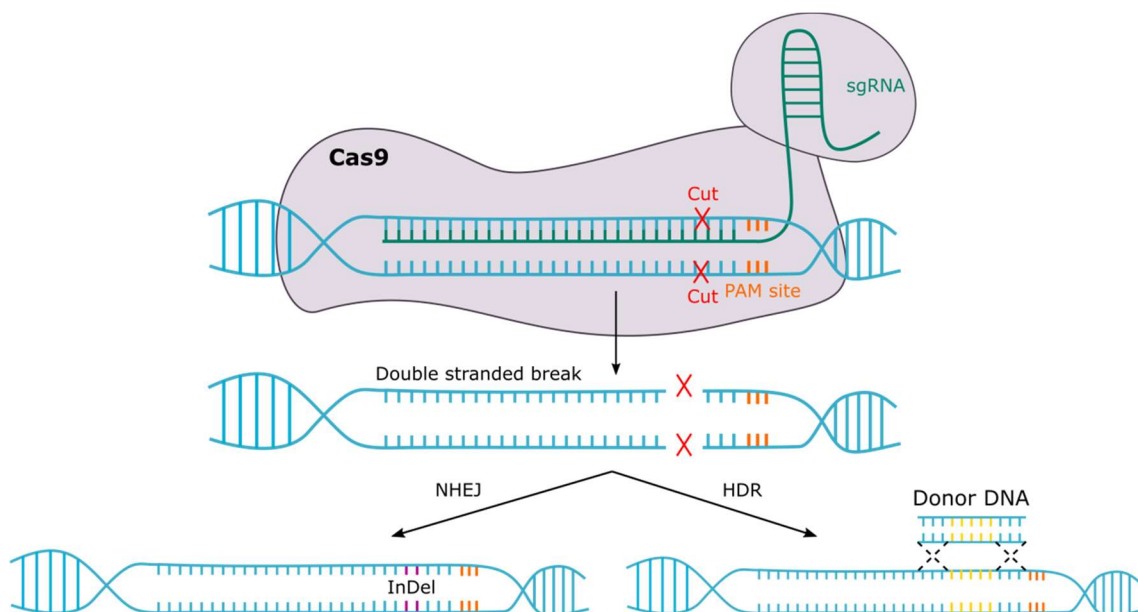


Figure 23: Schema of the gene augmentation strategy using an AAV vector. (1) The viral capsid binds its cellular receptor. (2) Endocytosis of the virus by the cell. (3) The virus is confined in endosome. (4) The virus enters the Golgi. (5) The capsid enters in the nucleus. (6) Capsid proteins are disassembled released the viral genetic information. (7) The viral DNA passes from single-stranded (ssDNA) to double-stranded (dsDNA). (8) The viral DNA is transcribed. (9) The final protein is translated in the cellular cytoplasm.

## Gene editing

In autosomal dominant cases of inherited disorders with a dominant negative effect, editing the existing copy of the mutated gene is a feasible approach to correct the phenotype. Using several techniques such as Zinc-Finger Nucleases (ZFN), TALENs or, more recently, CRISPR-Cas9, specific editing can be induced in the gene to correct the mutation [156]. For the CRISPR-Cas9 system, a localized double-stranded break is caused by the Cas9 protein. The cell can then either use a template DNA delivered in the cell to repair the double-stranded break by homology directed repair (HDR) or repair the break by non-homologous end joining (NHEJ). If the template DNA is the wild-type copy of the mutated region, the mutation will then be corrected (Fig. 24). Nevertheless, serious drawbacks as OFF-target effect, which can cause undesired cuts elsewhere in the genome, have to be considered. To date, only one clinical trial involving CRISPR-Cas9 for an inherited retinal disorder is ongoing (NCT03872479) but 16 registered clinical trials using CRISPR-Cas9 are currently running for other diseases such as cancer or beta thalassemia (clinicaltrials.gov).



**Figure 24: CRISPR-Cas9 system mechanism.** A single guide RNA (sgRNA) recognizes a genomic sequence followed by 5'-NGG-3' proto-spacer adjacent motif (PAM) site, which recruits the Cas9 DNA endonuclease. This introduces a double-stranded break that is repaired by either non-homologous end joining (NHEJ), which might result in the creation of InDels that can disrupt the gene, or by homology directed repair (HDR) in the presence of a donor DNA, used as a template to repair the break.

### **Anti-sense oligonucleotide (AON)-based therapy**

In cases of mutations altering the normal splicing of the pre-mRNA, a strategy aiming to rescue the aberrant pre-mRNA in place of addition of a normal copy of the mutated gene cDNA can be applied. AON are small and adaptable molecule that are complementary to a target mRNA and can modulate this mRNA splicing or stability. Indeed, AON have the capacity to inflect on splicing by targeting regions promoting or blocking the splicing or by masking splice sites [157]. The use of AON managed to induce exon skipping in cases of Duchenne Muscular Dystrophy, in order to restore the reading of the dystrophin mRNA [158], but can also lead to insertions of over-spliced exons. The use of AON has also been demonstrated in LCA due to mutations in CEP290, in which a recurrent intronic mutation induces the insertion of a pseudo-exon causing a premature stop-codon in 50 to 75% of transcripts. AON targeting the mutation led to the restoration of the normal splicing of *CEP290* transcripts in fibroblasts of LCA patients [159, 160]. This approach was recently tested in patients that presented no adverse effect an improved visual acuity three months after treatment [161].

### **Viral vectors**

To deliver the gene or the editing tools to the targeted cells, different vectors can be used: lentiviruses, adenoviruses, adeno-associated viruses (AAV) or non-viral vectors as liposomes for instance. The majority of clinical trials for inherited retinal disorders involve AAVs (68%) [150] (Fig.25). AAVs are the preferred vectors in gene therapy for such diseases for several reasons. They are small, non-pathogenic, single-stranded DNA viruses which can transduce non-dividing cells without integrating in the genome and exist in different serotypes [162]. In particular, the AAV2 serotype is the most frequently used (73%) [150] because it can transduce multiple retinal cell types according to the site of injection [163]. In addition, AAV capsids can be modified and selected through directed evolution to enhance the transduction of specific cells by this vector. For instance, the AAV2-7m8 serotype displays an efficient delivery of the transgene through intravitreal injection in the *rd12* mouse model of LCA, the first ocular inherited disorder to have an approved and commercially available genetic therapy [164]. Furthermore, the transgene endures a long-term expression through AAV delivery, which is a strong benefit.

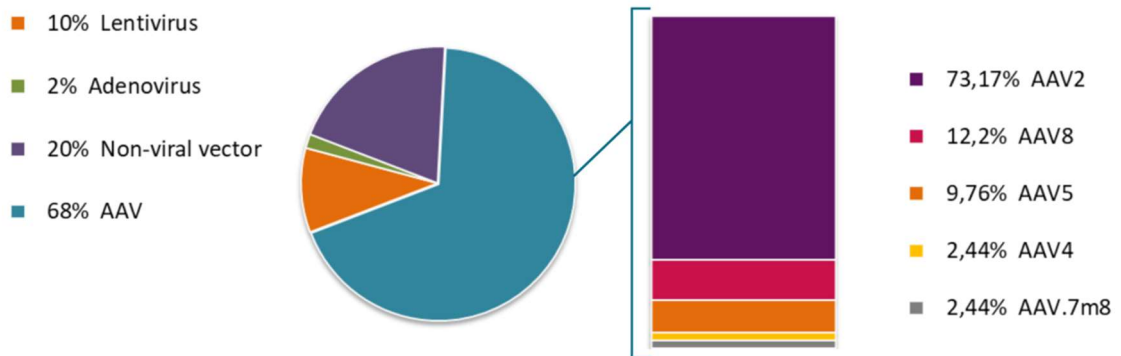


Figure 25: Proportion of types of viral vectors and the ratio of the various AAV serotypes used in ocular gene therapy, modified from [150]

### Mode of administration

Two routes of administration can be used to inject the viral vector targeting the retina in the eye. Usually, the route of administration determines which cells will be in contact with the vectors and that will most likely be the only ones targeted. Consequently, targeting photoreceptors or RPE cells generally requires an injection in the subretinal space [163, 165]. To do so, a bleb must be created beneath the retina, just between the retina and the RPE. This transitory retinal detachment will allow the delivery of the vector directly in contact with the retina. On the other hand, for an efficient transduction of RGCs or BCs, intravitreal (IVT) injections are more suitable as the vectors will be delivered in closer apposition to these cells. As its name suggests, the intravitreal injection consists on the delivery of the vectors directly in the vitreous, where it will diffuse across the INL to finally reach the retina [166] (Fig.26). However, performing subretinal injections in cases of retinal degeneration is not ideal due to the fragility of the retina, so the challenge in this case is to target photoreceptors from intravitreal injections [163].

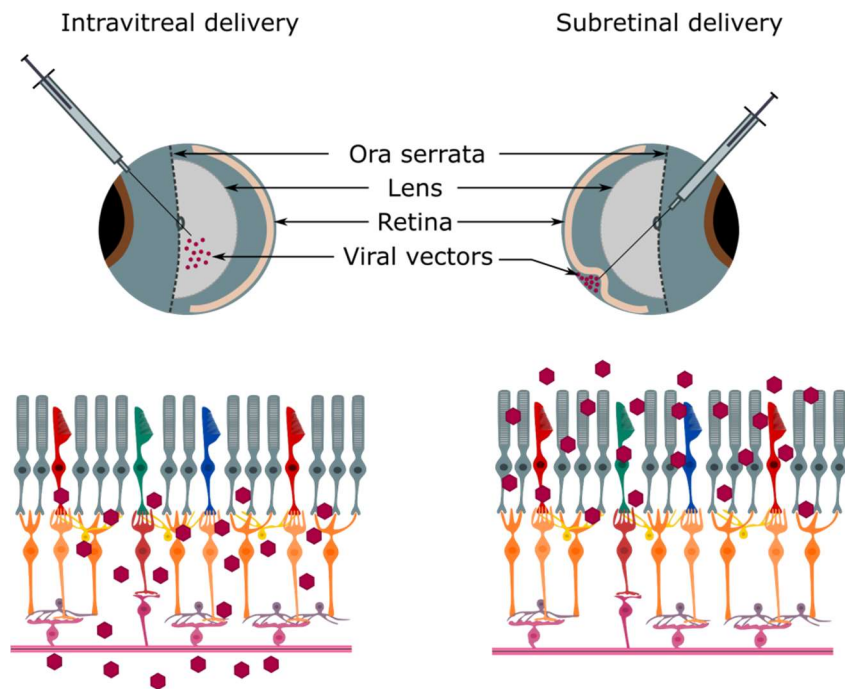


Figure 26: Schematic representation of the two modes of administration for ocular gene therapy. To perform intravitreal delivery a needle containing the vectors has to pass through the ora serrata then, the vectors are directly injected in the vitreous. It is more suitable for a transduction of RGCs or BCs. Subretinal delivery is performed through a bleb between the retina and the RPE. The vectors are then by delivered in direct contact with the retina.

## B. MAJOR GENE THERAPY AUGMENTATION TRIALS FOR IRDs

2017 marked the most important step in the field of gene therapy as it is the first time that a gene therapy treatment for a blinding disorder was approved by the USA Food and Drug Administration (FDA). However, it took about twenty years from the first attempts to this achievement.

This major break-through is the treatment of LCA due to *RPE65* mutations via gene therapy [153-155]. LCA is a form of inherited childhood blindness caused by, among others, mutations in the *RPE65* gene [167]. It is usually referred as the most severe and earliest form of IRDs which starts with severe visual impairment or complete blindness at birth followed by a slow degeneration of the photoreceptors and severely reduced or non-detectable ERG responses [168]. Restoration of the visual pigment and function in a mouse model of LCA was obtained by oral administration of retinoid [169], however, the first attempt of gene therapy for LCA was a proof-of-concept in a naturally occurring dog model of LCA, the *RPE65*<sup>-/-</sup> dog, using an AAV vector injected subretinally [170]. The researchers assessed a functional rescue by performing ERGs before and after treatment. Furthermore, the pupillary constriction was

improved in *RPE65*<sup>-/-</sup> following treatment. A long-term follow-up showed sustained restoration of the visual function in the treated dogs [171, 172]. This successful approach in a large model led to the elaboration of three clinical trials in infants affected with LCA [153-155]. A recombinant AAV2 has been injected subretinally, containing the *RPE65* coding sequence to young adults LCA patients. Treated patients showed strong visual improvements following the treatment, as improvement of visual acuity, pupillometry or better navigation between obstacles, above all in dim light conditions. The delivery of the transgene in the contralateral eye of patients has also been tested, conducting to improvements in mobility but not visual acuity up to three years [173]. The success of this gene therapy approach has several explanations: *RPE65* is a relatively small gene (2.8 kb [174]) and RPE cells are easily transduced by AAVs through subretinal injections [175].

However, in 2 clinical trials for LCA out of 3, the visual improvements were not stable, showing that the treatment did not completely abolish the degeneration course [176, 177]. Two major hypotheses are currently studied to improve this approach: the vector dose and the time-window of treatment. A higher dose might be required to ensure sustainable improvements; higher doses were actually tested and resulted in better visual sensitivity compared to patients with lower doses up to three years, however with a decline after one year of treatment [177]. Furthermore, the investigation of the photoreceptor loss in treated patients and in treated dogs was made. Treatment in patients started after the beginning of the degeneration process and did not change the natural degeneration course found in LCA [178]. However, when dogs were treated before the degeneration process was initiated, a significant rescue of the degeneration was noticed, raising the question of the treatment-window, even in slowly degenerative disorders [178].

In addition, gene therapy for other retinal disorders led to, to date, safe and efficient treatments such as for choroideremia. Indeed, it showed a high degree of safety following subretinal injections targeting the fovea and improvements of the visual acuity in patients [179, 180]. More than forty registered clinical trials are ongoing to either prove the safety or the efficacy of the treatment of various retinal disorders such as Stargardt disease or Aged-related Macular Degeneration (Table 3,[152]).

Table 3: Gene therapy clinical trials for retinal diseases using recombinant viruses, adapted from [141]

Disorder	Causative gene	Proof of concept in animal models	Viral vector used	Mode of administration	Most advanced clinical trial phase
Achromatopsia	<i>CNGB3</i>	Komaromy <i>et al.</i> , 2010 [181] <i>CNGB3<sup>m/m</sup></i> & <i>CSNB3<sup>-/-</sup></i> dog	AAV2/AAV8	Subretinal	I/II
	<i>CNGA3</i>	Alexander <i>et al.</i> , 2007 [182] <i>Cpfl3</i> mouse	AAV2		
Choroideremia	<i>REP1</i>	Seabra <i>et al.</i> , 2009 Conditional KO mouse of CHM	AAV2	Subretinal	II
LCA2	<i>RPE65</i>	Acland <i>et al.</i> , 2001 [170] <i>RPE65<sup>-/-</sup></i> dog	AAV2/AAV4/AAV5	Subretinal	III
LHON	<i>ND4</i>	Ellouze <i>et al.</i> , 2008 / rat [183]	AAV2	Intravitreal	III
Retinitis pigmentosa	<i>MERTK</i>	Smith <i>et al.</i> , 2003 / RCS rat [184]	AAV2	Subretinal	I
	<i>RLBP1</i>	Choi <i>et al.</i> , 2015 [185] <i>RLBP1<sup>-/-</sup></i> mouse	AAV8	Subretinal	I/II
	<i>PDE6B</i>	Bennett <i>et al.</i> , 1996 / <i>rd</i> mouse [186]	AAV5	Subretinal	I/II
Stargardt disease	<i>ABCA4</i>	Allocca <i>et al.</i> , 2008 [187] <i>Abca4<sup>-/-</sup></i> mouse	LV	Subretinal	I/II

Disorder	Causative gene	Proof of concept in animal models	Viral vector used	Mode of administration	Most advanced clinical trial phase
USH1B	<i>MYO7A</i>	Hashimoto <i>et al.</i> , 2007 [188] <i>Myo7a</i> <sup>-/-</sup> mouse	LV	Subretinal	I/II
X-linked RP	<i>RPGR</i>	Hong <i>et al.</i> , 2005 [189] <i>Rpgr</i> <sup>-/-</sup> mouse	AAV	Subretinal	I/II
X-linked retinoschisis	<i>RS1</i>	Zeng <i>et al.</i> , 2004 / <i>Rs1h</i> <sup>-/-</sup> mouse [190]	AAV	Intravitreal	I/II

### C. CSNB GENE THERAPY

CSNB is yet an incurable disorder. Gene therapy seems particularly suitable to treat CSNB since it represents a non-degenerative stationary disease. Since this implies that the structure of the retina is globally well preserved, patients could be in theory treated at any age. As for other retinal disorders, the eye is an easily AAV-transducible tissue. Furthermore, proof-of-concept of gene therapy for CSNB could provide further insight on the treatment of other inherited retinal disorders involving synaptic defects.

#### **Treating icCSNB**

All proteins involved in the icCSNB were found to be localized pre-synaptically in the photoreceptors [17]. *CACNA1F* is one of the genes leading to icCSNB when mutated [65] and codes for the calcium channel  $Ca_v1.4$ . It has been previously showed that  $Ca_v1.4$  plays a role in the synaptic development and maintenance since the loss of this calcium channel at the synapse provokes gross morphological abnormalities of the presynaptic terminal, like shorten ribbons [191-193]. Two strategies were studied to restore the synaptic structure in *CACNA1F* KO mice [194]. First, plasmids encoding the wild-type copy of *CACNA1F* were electroporated in P0 KO mice, which rescued rod synaptic terminal morphology and mature ribbons when studied at P21. Secondly, another plasmid with the wild-type copy of *CACNA1F* controlled by a Cre recombinase was electroporated in P0 mice, followed by tamoxifen induction of the Cre at P28. Again, it led to the restoration of rod synaptic terminal and ribbons structure. A few treated animals actually passed the vision guided water maze as it took them less time than KO animals to reach the platform. However, no conclusive ERG responses were measurable probably because of a high number of retinal detachments in the treated animals and the few likely induced electroporated cells [194]. This study suggests that rod synaptic terminals maintain a strong regenerative capacity as the treatment led to improvements even in mature rods (P28).

#### **Treating cCSNB**

##### *Nyx<sup>nob</sup>* mouse model

The first report of an attempt to rescue the cCSNB phenotype was in the *Nyx<sup>nob</sup>* mouse model by the expression of a fusion protein YFP-Nyctalopin in a transgenic *Nyx<sup>nob</sup>* mouse which led

to an expression of the protein in ON-BCs and a functional rescue [195]. Recently, a gene therapy approach using an AAV2 able to transduce most retinal cells from an intravitreal delivery [196] combined with a promoter targeting BCs [197] aimed to specifically drive the expression of *Nyx* fused with YFP in ON-BCs in P2 and P30 *Nyx<sup>hob</sup>* mice was described. Following the assessment of the production of nyctalopin in the treated retinas, ERG measurements in both scotopic and photopic conditions in mice injected at either P2 or P30 revealed partial rescue of the ERG b-wave under scotopic conditions along with an even slighter rescue under photopic conditions was noted, but only in P2 treated mice. Lack of ERG rescue was noted for the P30 injected mice. In ON-BCs expressing nyctalopin and YFP, the function of the TRPM1 channel was rescued as assessed by patch-clamp recordings. Interestingly, the expression of the transgene was higher in P30 treated animals than in P2. Fluorescence was also noted in the P30 injected retina while no functional rescue could be measured, suggesting that the hurdle to obtain an efficient rescue in P30 animals might be post-transcriptional [198].

#### *Lrit3<sup>emrgg1</sup>* mouse model

Previous studies concerning LRIT3 suggested that it localizes at the dendritic tips of ON-BCs [17, 24, 79, 116]. Interestingly, it was shown recently that after intravitreal injection of an AAV vector driving the expression of *Lrit3* by a rhodopsin promoter, therefore specifically targeting rods, TRPM1 was relocated to the dendritic tips of ON-BCs in *Lrit3<sup>emrgg1</sup>* retinas. Recordable ERG b-waves in scotopic conditions were obtained in P5 treated retinas with a milder improvement in P35 injected animals. Furthermore, this restoration of the ON-pathway was also measurable at the level of RGCs in P5 treated mice. However, no improvement was detected in photopic conditions in P5 and P35 treated retinas [126]. This study raises the question if LRIT3 is also or only expressed in photoreceptors to act trans-synaptically on the ON-BCs.

#### D. OTHER INNOVATIVE THERAPIES FOR IRDS

In cases of progressive retinal disorders which are usually characterized by a photoreceptor loss, gene therapy using gene augmentation or gene editing might not be the appropriate approach. Other innovative approaches to treat progressive inherited disorders will be

discussed below. Furthermore, these approaches are independent of the causative gene defect.

## 1. NEUROPROTECTION

In order to slow down the degeneration of photoreceptors, the intake of neurotrophic factors to the retina via AAVs has been studied. Several virally delivered neurotrophic factors have been tested in animal models such as: the ciliary neurotrophic factor (CNTF) [199], glial cells derived neurotrophic factors [200, 201], the Rod-derived Cone Viability Factor (RdCVF) [202, 203] or an X-linked inhibitor of apoptosis [204]. However, only CNTF-mediated neuroprotection has yet been tested in patients with mild benefits [205].

## 2. OPTOGENETICS

Optogenetics is a therapeutic approach for patients affected with progressive retinal disorders at later stages, when photoreceptor cells are gone. Here, gene augmentation therapies will not rescue the phenotype. The principle of optogenetics is to transform the remaining neurons of the inner retina (HCs, BCs or RGCs) photosensitive (Fig.27). Several light-sensitive microbial opsins have been identified such as the channelrhodopsin or halorhodopsin [206, 207]. By the injection of AAVs coding for the microbial opsin and targeting BCs or RGCs in animal models of retinal degeneration, light sensibility of the inner retina was obtained [46, 206-208]. However, these microbial opsins have a low light sensitivity therefore their efficient excitation demands high levels of blue-light stimuli, which can be damaging to the retina and the RPE [152]. To overcome this issue, a red-shifted version of channelrhodopsin, which has a lower risk of photochemical damage, has already been tested in mice and postmortem macaques and human retinae [209]. It led to a restoration of light responses in the mouse using orange light intensities stimuli that are not damageable for the human retina. Spike responses were also recorded in macaque and human RGCs [209].

Furthermore, the targeting of foveal cones [210], BCs or HCs [46, 208, 211] instead of RGCs might be even better as targeting RGCs bypasses the normal propagation of the light signal through the inner retina.

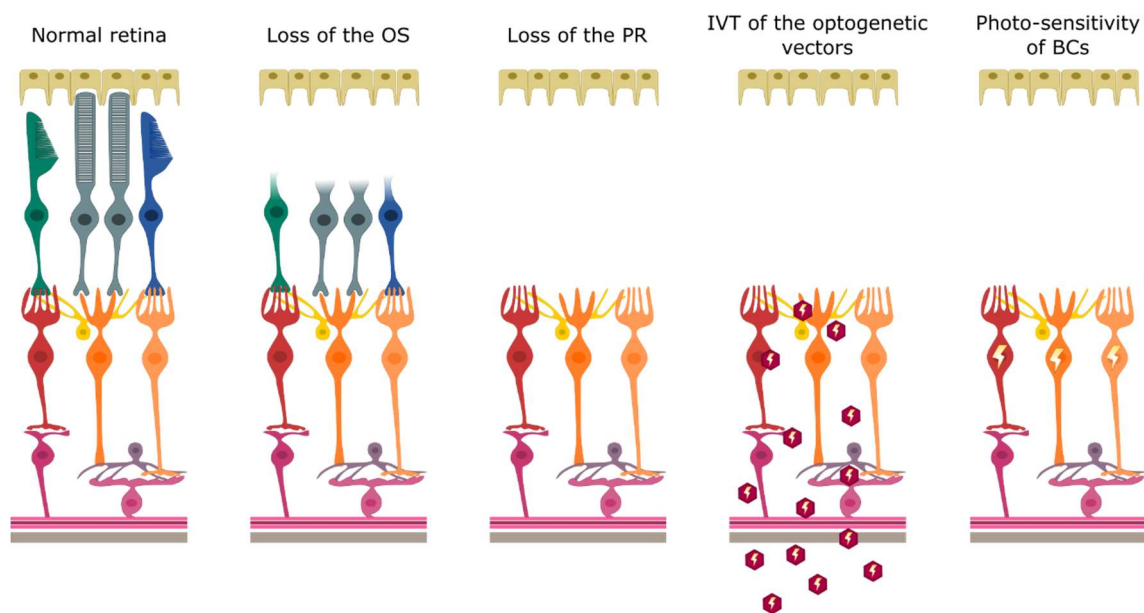


Figure 27: Schematic representation of the optogenetic principle. In cases of retinal degeneration, the outer segments (OS) of the photoreceptors are the first to degenerate followed by the nuclei. The optogenetic purpose is to transduce ON-BCs or RGCs with vectors encoding for an opsin to make these cells photosensitive.

### 3. CELL THERAPY

Another way of bypassing the progressive retinal degeneration in patients with inherited retinal disorders is through cell therapy or cell transplantation. Recent achievements in the field of stem cells led to *in vitro* production of photoreceptors, RGCs or RPE cells [212]. Bioengineering of RPE cell sheets proved its efficacy in rescuing photoreceptor loss and visual acuity in the Royal College of Surgeon (RCS) rat model, following transplantation [213]. This type of stem cell-derived RPE cell sheets transplantation has been validated in primate retina [214] and is now currently involved in a clinical trial (NCT03963154). *In vitro* production of photoreceptors from induced Pluripotent Stem (iPS) cells and their transplantation in rat retina has been studied, leading to the survival and maturation of the transplanted photoreceptors [215]. Finally, a combination of optogenetics and cell therapy has recently been investigated by the transplantation in late stage retinal degeneration mouse models of optogenetically modified photoreceptors. This pioneer approach led to a restoration of the visual function in the transplanted animals [216]. Another source of stem cells for cell therapy relies on Müller cells which have a regenerative potency and have been proved to restore vision after their differentiation in photoreceptors directly in the retina [217]. The therapies based on these stem cells whether genetically modified or not, are a valuable alternative to *in vivo* gene delivery.

# Aim of this study

---

ON-BCs dysfunction either due to cCSNB or paraneoplastic retinopathy is a disabling condition affecting diurnal and nocturnal vision. In both cases, proteins of the signaling cascade at the synapse between photoreceptors and ON-BCs are implicated. Albeit in the recent years, gene identification, *in vitro* and *in vivo* functional analyses contributed a lot to further decipher this cascade, the function of known and many other molecules remains to be understood. Indeed, one of the most recent identified genes implicated in cCSNB was *LRIT3* and TRPM1 autoantibodies were found to be responsible for the ON-BCs dysfunction in paraneoplastic retinopathy for less than a decade. By studying these two conditions, several objectives were established for this thesis project:

## Examination of three patients affected with MAR

- Study the phenotype of three new cases of MAR
- Identify the antigen recognized by the autoantibodies present in the sera of these patients
- Investigate the reactivity of these autoantibodies towards the three different isoforms of TRPM1 through immunolocalization and western blot studies

## Assessment of the feasibility of gene addition to restore the phenotype in *Grm6*<sup>-/-</sup> mice

- Examine the impact of mGluR6 on the localization of its signaling partners
- Test two strategies to recover mGluR6 localization by either targeting ON-BCs specifically or all retinal cells
- Investigate the relocalization of the proteins of the signaling cascade following treatment
- Study the functional restoration after injection

## Development of a treatment for cCSNB in the *Lrit3*<sup>-/-</sup> mouse model

- Design different constructs in order to target both sides of the photoreceptor to ON-BC synapse
- Investigate the feasibility of treatment at an adult age in this model
- Explore the restoration of the phenotype through immunolocalization studies, ERG recordings, MEA analysis and optomotor responses
- Assess the durability of the restoration through time

# Results

---

## I. IDENTIFICATION AND CHARACTERIZATION OF NOVEL TRPM1 AUTOANTIBODIES FROM SERUM OF PATIENTS WITH MELANOMA-ASSOCIATED RETINOPATHY

Anti-TRPM1 autoantibodies have previously been described in sera of patients affected by melanoma-associated retinopathy (MAR). At least three different isoforms of TRPM1 are expressed in the retina. Here, we studied three new patients with MAR and reported their ERG phenotypes. The presence of anti-TRPM1 autoantibodies in the sera of these three new MAR cases was tested by immunolocalization studies on overexpressing cells, by western blot analysis and by immunolocalization studies on *Trpm1*<sup>+/+</sup> and *Trpm1*<sup>-/-</sup> mouse retinal cryosections. In addition, their affinity towards the three isoforms of TRPM1 was investigated.

The three MAR patients studied herein presented ON-BCs dysfunction as shown by the absence of the ERG b-wave in scotopic conditions, consistent with previous reports of MAR patients displaying anti-TRPM1 autoantibodies. In addition, this work led to the identification and characterization of novel TRPM1 autoantibodies in these three MAR patients. These anti-TRPM1 autoantibodies were recognizing the three different TRPM1 isoforms with variable binding affinity. Most likely, the anti-TRPM1 autoantibodies of different patients vary in affinity and concentration. In addition, the binding of autoantibodies to TRPM1 may be conformation-dependent, with epitopes being inaccessible in some constructs (truncated polypeptides versus full-length TRPM1) or applications (western blotting versus immunohistochemistry). However, we were able to conclude that all MAR patients recognized the three isoforms of TRPM1. Therefore, the combination of multiple analyses should be done to ensure the diagnosis of anti-TRPM1 autoantibodies presence in the serum of MAR patients. These findings were published in PlosOne.

**Varin J**, Reynolds MM, Bouzidi N, Tick S, Wohlschlegel J, Becquart O, Michiels C, Dereure O, Duvoisin RM, Morgans CW, Sahel JA, Samaran Q, Guillot B, Pulido JS, Audo I, Zeitz C. Identification and characterization of novel TRPM1 autoantibodies from serum of patients with melanoma-associated retinopathy. *PLoS One*. 2020 Apr 23;15(4):e0231750.

RESEARCH ARTICLE

# Identification and characterization of novel TRPM1 autoantibodies from serum of patients with melanoma-associated retinopathy

Juliette Varin<sup>1</sup>, Margaret M. Reynolds<sup>2</sup>, Nassima Bouzidi<sup>1</sup>, Sarah Tick<sup>3</sup>, Juliette Wohlschlegel<sup>1</sup>, Ondine Becquart<sup>4</sup>, Christelle Michiels<sup>1</sup>, Olivier Dereure<sup>4</sup>, Robert M. Duvoisin<sup>5</sup>, Catherine W. Morgans<sup>5</sup>, José-Alain Sahel<sup>1,3,6,7,8</sup>, Quentin Samaran<sup>4</sup>, Bernard Guillot<sup>4</sup>, José S. Pulido<sup>9,10</sup>, Isabelle Audo<sup>1,3,11</sup>, Christina Zeitz<sup>1\*</sup>

**1** Sorbonne Université, INSERM, CNRS, Institut de la Vision, Paris, France, **2** Department of Ophthalmology, Washington University, Saint Louis, MO, United States of America, **3** CHNO des Quinze-Vingts, DHU Sight Restore, INSERM-DGOS CIC 1423, Paris, France, **4** Department of Dermatology and INSERM U1058 “Pathogenesis and control of chronic infections”, University of Montpellier, Montpellier, France, **5** Department of Chemical Physiology & Biochemistry, Oregon Health & Science University, Portland, OR, United States of America, **6** Fondation Opthalmologique Adolphe de Rothschild, Paris, France, **7** Académie des Sciences, Institut de France, Paris, France, **8** Department of Ophthalmology, The University of Pittsburgh School of Medicine, Pittsburgh, PA, United States of America, **9** Department of Ophthalmology, Mayo Clinic, Rochester, MN, United States of America, **10** Department of Molecular Medicine, Mayo Clinic, Rochester, MN, United States of America, **11** Institute of Ophthalmology, University College of London, London, United Kingdom

\* [christina.zeitz@inserm.fr](mailto:christina.zeitz@inserm.fr)

## Abstract

Melanoma-associated retinopathy (MAR) is a rare paraneoplastic retinal disorder usually occurring in the context of metastatic melanoma. Patients present with night blindness, photopsias and a constriction of the visual field. MAR is an auto-immune disorder characterized by the production of autoantibodies targeting retinal proteins, especially autoantibodies reacting to the cation channel TRPM1 produced in melanocytes and ON-bipolar cells. TRPM1 has at least three different isoforms which vary in the N-terminal region of the protein. In this study, we report the case of three new MAR patients presenting different anti-TRPM1 autoantibodies reacting to the three isoforms of TRPM1 with variable binding affinity. Two sera recognized all isoforms of TRPM1, while one recognized only the two longest isoforms upon immunolocalization studies on overexpressing cells. Similarly, the former two sera reacted with all TRPM1 isoforms on western blot, but an immunoprecipitation enrichment step was necessary to detect all isoforms with the latter serum. In contrast, all sera labelled ON-bipolar cells on *Trpm1*<sup>+/+</sup> but not on *Trpm1*<sup>-/-</sup> mouse retina as shown by co-immunolocalization. This confirms that the MAR sera specifically detect TRPM1. Most likely, the anti-TRPM1 autoantibodies of different patients vary in affinity and concentration. In addition, the binding of autoantibodies to TRPM1 may be conformation-dependent, with epitopes being inaccessible in some constructs (truncated polypeptides versus full-length TRPM1) or applications (western blotting versus immunohistochemistry). Therefore, we



## OPEN ACCESS

**Citation:** Varin J, Reynolds MM, Bouzidi N, Tick S, Wohlschlegel J, Becquart O, et al. (2020) Identification and characterization of novel TRPM1 autoantibodies from serum of patients with melanoma-associated retinopathy. PLoS ONE 15 (4): e0231750. <https://doi.org/10.1371/journal.pone.0231750>

**Editor:** Knut Stieger, Justus Liebig Universität Giessen, GERMANY

**Received:** November 6, 2019

**Accepted:** March 31, 2020

**Published:** April 23, 2020

**Copyright:** © 2020 Varin et al. This is an open access article distributed under the terms of the [Creative Commons Attribution License](https://creativecommons.org/licenses/by/4.0/), which permits unrestricted use, distribution, and reproduction in any medium, provided the original author and source are credited.

**Data Availability Statement:** All relevant data are within the manuscript and its Supporting Information files.

**Funding:** CZ:Retina France CZ:French Muscular Dystrophy Association (AFM-Téléthon) CZ: UNADEV-Aviesan call 2015 CZ:Fondation Voir et Entendre CZ:Prix Dalloz for “La recherche en ophtalmologie” CZ,IA:Ville de Paris and Region Ile de France, LABEX LIFESENSES (reference ANR-10-LABX-65) supported by French state funds,

managed by the Agence Nationale de la Recherche within the Investissements d'Avenir program (ANR-11-IDEX-0004-0) JV:Ministère de l'Enseignement Supérieur et de la Recherche.

**Competing interests:** The authors have declared that no competing interests exist.

propose that a combination of different methods should be used to test for the presence of anti-TRPM1 autoantibodies in the sera of MAR patients.

## Introduction

Paraneoplastic retinopathies are rare retinal disorders usually associated with the presence of autoantibodies against retinal proteins following the development of a primary tumor or a metastasis [1–5]. Two major types of paraneoplastic retinopathies with an initial normal fundus have been reported: (1) cancer-associated retinopathy (CAR), which leads to a rapid and severe visual dysfunction with primary photoreceptor alterations and is most commonly associated with small-cell carcinomas of the lung and less frequently associated with breast, endometrial and other cancers [6,7]; (2) melanoma-associated retinopathy (MAR), traditionally associated with metastatic melanoma [2] but now well recognized in association with other cancers such as carcinomas [8–11]. Patients presenting with MAR usually experience recent night blindness, photopsias (various perception of flickering lights), decreased vision and alterations of the visual field. The fundus examination in patients with MAR is usually normal but may show some degrees of vitritis and vasculitis [12–14]. Cases of disc pallor, vascular attenuation and pigment mottling with time [15] or small choroidal scars [16] have also been reported. The full-field electroretinogram (ff-ERG) is critical for the proper diagnosis of MAR and typically shows ON-bipolar cell dysfunction resembling the ERG abnormalities seen in a sub-group of congenital stationary night blindness (CSNB), the complete form of Schubert-Bornschein, cCSNB [2,17–19]. In this condition, while applying the International Society for Clinical Electrophysiology of Vision (ISCEV) recommended protocol [20], in MAR patients and in cCSNB patients, ff-ERG abnormalities are as follows: under dark adapted (DA, scotopic) conditions, there is no detectable response to a dim ( $0.01 \text{ cd.s.m}^{-2}$ ) flash. The responses to a bright flash ( $3.0$  and  $10.0 \text{ cd.s.m}^{-2}$ ) have an electronegative waveform with a normal negative a-wave, reflecting the normal hyperpolarization of photoreceptors, and severely reduced b-wave in keeping with ON-bipolar cell dysfunction. Light adapted (LA, photopic) responses are also abnormal due to cone-ON-bipolar alterations: a square-shaped a-wave, a sharply arising b-wave and a reduced b/a ration are recorded in response to a single  $3.0 \text{ cd.s.m}^{-2}$  flash while the 30 Hz response is delayed. Aside mutations in other genes, mutations in *TRPM1* lead to cCSNB [21–30]. The transient receptor potential cation channel subfamily M member 1 (TRPM1) is thought to mediate the depolarization of ON-bipolar cells in response to light, underlying the ERG b-wave [19,31,32]. TRPM1 is not only localized in retinal ON-bipolar cells but also in melanocytes where it plays a role in pigmentation and melanocyte proliferation [33,34]. However, no skin phenotype has been documented in *TRPM1*-related cCSNB [21–23]. Recently, autoantibodies against TRPM1 were identified in patients with MAR, as well as in a few patients with other neoplasms [10,11,35–46]. Despite the fact that anti-TRPM1 autoantibodies have been mostly reported in cases of metastatic melanoma, other groups have also reported patients with carcinoma. Interestingly those also revealed a MAR-like ON-bipolar cell dysfunction on ERG and anti-TRPM1 autoantibodies documented by western blot and immunofluorescence on monkey retina tissue [10,44]. Consequently, as patients with carcinoma can present an ON-bipolar cell dysfunction, a better classification of these two types of paraneoplastic syndromes would be paraneoplastic with photoreceptor defect (usually addressed as CAR) and paraneoplastic with ON-bipolar defect (usually addressed as MAR) [47]. Intravitreal injection of sera from patients with MAR into monkey and mouse eyes

resulted in a cCSNB-like ERG phenotype [37,38,48]. TRPM1 localization in ON-bipolar cells, and its implication in cCSNB when mutated, supports the conclusion that paraneoplastic retinopathies showing ON-bipolar cell dysfunctions are caused by autoantibodies binding TRPM1 and blocking its channel function. Whether these anti-TRPM1 antibodies cause other phenotypes such as thinning of the choroid [41] or retinal degeneration is a matter of debate [46,49]. In addition, the ocular phenotype is variable depending on the persistence or not of anti-TRPM1 autoantibodies [44,45]. Indeed, Ueno and colleagues reported clearance of autoantibodies following treatment in a patient with paraneoplastic retinopathy and ON-bipolar cell dysfunction whose ERG responses did not recover while other patients with MAR or CAR regained normal ERG responses after clearance of anti-TRPM1 antibodies [45] or following rituximab treatment [44], respectively. An interesting hypothesis to explain the occurrence of paraneoplastic retinopathy has been proposed in a case with a primary photoreceptor paraneoplastic retinopathy (referenced there as a case of CAR). Indeed, anti-recoverin antibodies have been identified as reacting to the ectopic expression of recoverin [50]. *TP53*, encoding the tumor suppressor protein P53, is located in the vicinity of recoverin. A mutation in *TP53* would give an aggressive advantage to the tumor, leading to the ectopic expression of recoverin and subsequently the development of autoantibodies cross-reacting with the retinal protein [50]. Similarly, a sequence in intron 8 of *TRPM1* encodes the tumor suppressor miR-211 which is downregulated in aggressive tumor. An alternative splicing would decrease miR-211 expression and lead to aberrant immunogenic TRPM1 promoting the development of autoantibodies [43,51–55]. While auto-antibodies against TRPM1 have been implicated in paraneoplastic ON-bipolar cell dysfunction, further studies have analyzed their specific target. Epitope mapping studies suggest that the autoantibodies target the N-terminal, intracellular domain of TRPM1 [37,43]. Besides, Oancea et al. reported three different *TRPM1* isoforms resulting from alternative splicing (i.e. 70+*TRPM1*, 92+*TRPM1* and 109+*TRPM1*), which differ in the length of their N-terminus, while the transmembrane domains and the C-terminus are conserved [33]. They demonstrated that the three different transcripts of TRPM1 were expressed in the retina using amplification by PCR on retinal cDNA. When expressed in human embryonic kidney (HEK) cells, isoforms 92+*TRPM1* and 109+*TRPM1* are expressed as full-length cation channels as suggested by western blot. However, the 92+*TRPM1* isoform was poorly expressed in the retina while the 70+*TRPM1* was well represented in the retina (no data for the 109+*TRPM1* isoform). Moreover, our group identified a mutation in the exon coding for the 92+*TRPM1* isoform [21]. Duvoisin and colleagues mapped the epitope recognized by MAR sera and defined its coding region from the exons 9 to 10 of *TRPM1* which is common to these three isoforms. To our knowledge, it is not known whether the anti-TRPM1 autoantibodies in MAR patients react differentially towards these distinct N-terminal isoforms. Therefore, in accordance with the literature, the purpose of this study was to detect and further investigate the immunoreactivity of anti-TRPM1 autoantibodies towards the three different isoforms of TRPM1, in three patients with a clinical diagnosis of MAR.

## Material and methods

### Clinical investigation and patient sera

This study was approved by the Comité de Protection des Personnes Ile-de France V and by the institutional review board of the Mayo Clinic, Rochester, MN, USA. All procedures adhered to the Tenets of Helsinki. Three patients with a clinical diagnosis of MAR, two from the Mayo Clinic in Rochester, Minnesota (referred as MAR1 and MAR2) and one from the Centre Hospitalier National d'Ophthalmologie of the Quinze-Vingts hospital, in Paris, France (referred as MAR3) underwent extensive clinical examination to confirm the diagnosis.

Testing included: assessment of best corrected visual acuity (BCVA) using the Early Treatment Diabetic Retinopathy Study (EDTRS) chart, kinetic and static perimetry. Full-field electroretinogram (ff-ERG) were performed with DTL recording electrodes and incorporated the ISCEV standard (Veris II for full-field ERG and multifocal ERG for both MAR1 and MAR2 patients while Espion<sup>2</sup> Diagnosys<sup>®</sup> was used for ff- ERG and mfERG for the MAR3 patient). Clinical assessment was completed with fundus autofluorescence imaging (FAF) and optical coherence tomography (OCT) (HRAII<sup>®</sup> and Spectralis<sup>®</sup> OCT, Heidelberg Engineering, Dossenheim, Germany) [56]. Sera from peripheral blood of the above patients were collected on dry tubes, centrifuged at 2,000 g for 10 minutes and stored at -80°C.

### Animals

Mice were maintained on a 12-hour light-dark cycle. *Trpm1*<sup>+/+</sup> and *Trpm1*<sup>-/-</sup> animals have been previously described by Morgans and colleagues [31]. All experiments were conducted in accordance with National Institutes of Health guidelines and approved by the Institutional Animal Care and Use Committees at Oregon Health & Science University.

### Immunolocalization studies in TRPM1 overexpressing mammalian cells

COS-7 cells, seeded on glass slides coated with 200µg/cm<sup>2</sup> poly-D-lysine and 1µg/cm<sup>2</sup> laminin (Sigma-Aldrich, St. Louis, MO, USA), were transfected with plasmids encoding the three different isoforms of human V5-tagged TRPM1 (70+*TRPM1*: 1603 amino acids encoded by 4812 bp, 92+*TRPM1*: 1625 amino acids encoded by 4878 bp and 109+*TRPM1*: 1642 amino acids encoded by 4929 bp; Source Bioscience ImaGenes, Berlin, Germany) using 2 M CaCl<sub>2</sub> and 2X Hepes Buffered Saline. The medium was changed 24 hours after transfection and immunofluorescent studies were performed 48 hours post-transfection. The V5-tag was present between amino acid residues 807 and 811, 832 and 833, 849 and 850 of each TRPM1 isoform, respectively, a region predicted to be localized extracellularly by *in silico* analysis (UniProtKB-Swiss-Prot). Cells were fixed (AntigenFix, Diapath, Martinengo, Italy) and permeabilized with PBST (PBS, 1% BSA, 0.1% TritonX-100), and proteins were detected with the following primary antibodies: mouse anti-V5 (1:250, Invitrogen, ThermoFisher Scientific, Waltham, MA, USA), rabbit anti-human TRPM1 (1:250, HPA014785, Sigma-Aldrich) and sera from patients (1:250). Primary antibodies were incubated for 1 hour at room temperature and after three PBS washes, slides were incubated with anti-mouse (Alexa Fluor 488), anti-rabbit (Alexa Fluor 488) or anti-human (Alexa Fluor 594) secondary antibodies (1:1000, Jackson ImmunoResearch, West Grove, PA, USA) for 30 minutes at room temperature. Cells were fixed a second time and finally washed with PBS. The slides were then cover-slipped (Vectashield, Vector Laboratories, Burlingame, USA) and air-dried overnight. Fluorescent images of transfected cells were acquired with a confocal microscope (FV1000, Olympus, Hamburg, Germany). Images brightness and contrast were adjusted for publication using the ImageJ Software (Bethesda, MD, USA).

### Preparation of retinal sections

Four *Trpm1*<sup>+/+</sup> and four *Trpm1*<sup>-/-</sup> animals [31] were sacrificed by CO<sub>2</sub> inhalation followed by cervical dislocation. Eyes were removed and dissected to keep the posterior part of the eyes which were then fixed in ice-cold 4% paraformaldehyde for 20 minutes. Subsequently, eye-cups were washed in ice-cold PBS and cryoprotected by increasing concentrations of sucrose in 0.12 M phosphate buffer (10% and 20% sucrose incubation for 1 hour each at 4°C and 30% sucrose under agitation overnight at 4°C). Subsequently, eye-cups were embedded in 7.5% gelatine—10% sucrose and the blocks frozen at -40°C in isopentane and kept at -80°C until sectioning.

Fourteen- $\mu\text{m}$  sections were prepared using a cryostat (MICROM HM 560<sup>™</sup>, ThermoFisher Scientific) and mounted on glass slides (Superfrost<sup>®</sup> Plus, ThermoFisher Scientific).

### ***Ex vivo* immunolocalization studies**

Mouse retinal sections were blocked for 1 hour at room temperature in blocking solution (PBS, 10% Donkey Serum (v/v), 0.3% Triton X-100). Primary antibodies and the dilutions used were: human MAR sera (MAR1 1:500, MAR2 1:250 and MAR3 1:250), sheep anti-TRPM1 (1:500; Cao *et al* [57]), and mouse anti-PKC $\alpha$  (1:1,000; P5704 Sigma-Aldrich, Darmstadt, Germany). The sections were incubated with primary antibodies diluted in blocking solution overnight at room temperature. After three washes with PBS, the sections were incubated with anti-human, anti-sheep and anti-mouse secondary antibodies coupled to Alexa Fluor 488, Alexa Fluor 594, or Cy3 (Jackson ImmunoResearch) along with 4',6-diamidino-2-phenylindole (DAPI), all used at 1:1000, for 1.5 hours at room temperature. Subsequently, the sections were cover-slipped with mounting medium (Mowiol, Merck Millipore, Billerica, MA, USA). Fluorescent images of retinal sections were acquired with a confocal microscope (FV1000, Olympus). Images for figures were adjusted for publication using Image J.

### **Western blot analysis**

COS-7 cells were transfected with 70+*TRPM1*, 92+*TRPM1*, 109+*TRPM1* plasmids or not transfected. After 48 hours, cells were dissociated by sonication in lysis buffer (Tris 50mM pH7.5, NaCl 150 mM, Triton X-100 1%) along with a combination of anti-protease and anti-phosphatase (Phosphatase Inhibitor Cocktail, Sigma-Aldrich) on ice for 30 minutes. Lysates were cleared by centrifugation at 13,800 x g for 10 minutes at 4°C. Protein extracts from transfected and untransfected cells were separated by SDS-Page on a 4–15% pre-cast gel (Mini-PROTEAN<sup>®</sup> TGX<sup>™</sup> Precast Protein Gels, Bio-Rad, Hercules, CA, USA) and subsequently transferred on nitrocellulose membranes (Trans-Blot<sup>®</sup> Turbo<sup>™</sup> Midi Nitrocellulose Transfer Packs, Bio-Rad). Membranes were blocked in milk for an hour and then incubated overnight at 4°C with the patients' sera (1:5,000–1:50,000) or serum from a non-MAR patient (1:50,000) and anti-V5 antibody (1:5,000, Invitrogen, ThermoFisher Scientific). The membranes were then incubated with horseradish peroxidase (HRP)-conjugated donkey anti-human or anti-mouse IgG (1:10,000, Jackson ImmunoResearch) as secondary antibody for 1 hour at room temperature. Bands were revealed using an HRP substrate for chemiluminescence (Pierce<sup>™</sup> ECL Western Blotting Substrate, ThermoFischer).

### **Immunoprecipitation**

Following protein extraction, magnetic beads (Dynabeads Protein G, ThermoFischer Scientific) were incubated with 2  $\mu\text{g}$  anti-V5 antibody (Invitrogen, ThermoFisher Scientific) for 1.5 hours at 4°C. Thereafter, tubes containing the beads covered with anti-V5 antibody were placed on a magnet and the unbound antibody containing solution was removed. The protein extract was incubated with the anti-V5-coated magnetic beads overnight at 4°C. Subsequently, beads were washed to remove the excess of protein and re-suspended in Laemmli buffer (2X SDS Urea) at 95°C for 5 minutes. The protein solution was then used for western blotting.

## **Results**

### **ON-bipolar cell dysfunction in three patients with MAR**

All patients had biopsy-proven malignant melanoma and ocular findings consistent with classic MAR. Briefly, the first patient (MAR1 patient, Fig 1) was a 63-year-old female with a stage

III metastatic malignant melanoma from an unknown primary tumor. She presented with a BCVA of 20/40 in the right eye, which decreased over 1.5 years to 20/200, while the BCVA of 20/40 in the left eye stayed stable. Visual fields showed some mild constriction of the right eye relative to the left eye. The DA 0.01 ERG response was undetectable whereas the DA 3.0 ERG revealed an electronegative response (Fig 1). Photopic responses also showed typical alterations to a single flash with a square-shaped a-wave, a delayed b-wave with however preserved amplitudes as well as a delayed 30 Hz flicker with a squared trough. The photopic ERG was unchanged at the last visit. In addition, this patient revealed also autoantibodies against carbonic anhydrase and enolase.

Ff-ERG responses to a 3.0 cd.s.m<sup>2</sup> flash under dark-adapted (DA) conditions from an unaffected subject and the three patients with a clinical diagnosis of melanoma-associated retinopathy (MAR). All three patients had a severely reduced b-wave with an electronegative response.

The second patient (MAR2 patient, Fig 1) was a 77-year-old female presenting with a metastatic cutaneous malignant melanoma of the foot with metastases to the right inguinal lymph node and left upper arm. Her BCVA was 20/20 in the right and 20/40 in the left eye. Her visual field appeared constricted bilaterally. In both eyes, the DA 0.01 ERG responses were undetectable with an electronegative response to the DA 3.0 ERG (Fig 1). This patient also displayed a square-shaped a-wave at the photopic ERG responses with a reduced b/a ratio. Multiple autoantibodies were identified in this patient's serum including anti-GAPDH and anti-enolase antibodies.

The third patient (MAR3 patient, Fig 1) was a 66-year-old female with malignant melanoma of the upper right eyelid that had been excised in 2013. BCVA was 20/160 in the right eye and 20/100 in the left. FAF and spectral domain-OCT were normal. Ff-ERG showed typical ON-bipolar cell dysfunction: there was a severely reduced b-wave to the DA 0.01 ERG responses. The DA 3.0 and DA 10.0 ERG responses showed a normal a-wave but a delayed and severely reduced b-wave leading to an electronegative ERG waveform in accordance with rod-ON bipolar cell dysfunction (Fig 1). Photopic responses were also abnormal with the LA 3.0 ERG showing a square-shaped a-wave with a sharply rising b-wave and a reduced b/a ratio typical of cone-ON bipolar defect.

### Presence of TRPM1 antibodies in all MAR sera as shown by different detection methods

In order to prove the presence of anti-TRPM1 autoantibodies in the sera of these three new cases of MAR, immunolocalization studies on overexpressing cells or mouse retinal cryosections were performed, along with western blot analysis.

### MAR1 and MAR2 sera detect all isoforms of TRPM1, while MAR3 does not react with the short isoform of TRPM1 by immunolocalization studies in overexpressing cells

Because of the previous findings that autoantibodies against TRPM1 were found in the serum of patients with MAR, the sera of the three MAR patients (MAR1-3) reported herein were tested on COS-7 cells overexpressing the different isoforms of human TRPM1 (70+TRPM1, 92+TRPM1 and 109+TRPM1). While MAR1 and MAR2 revealed typical TRPM1 staining for all three different isoforms as shown by co-staining with a commercially available antibody against TRPM1 (Fig 2A and 2B), MAR3 labelled the 92+TRPM1 and the 109+TRPM1 isoforms, but did not detect the shortest isoform of TRPM1: 70+TRPM1 (Fig 2C).

## DA 3.0 Mixed rod-cone responses

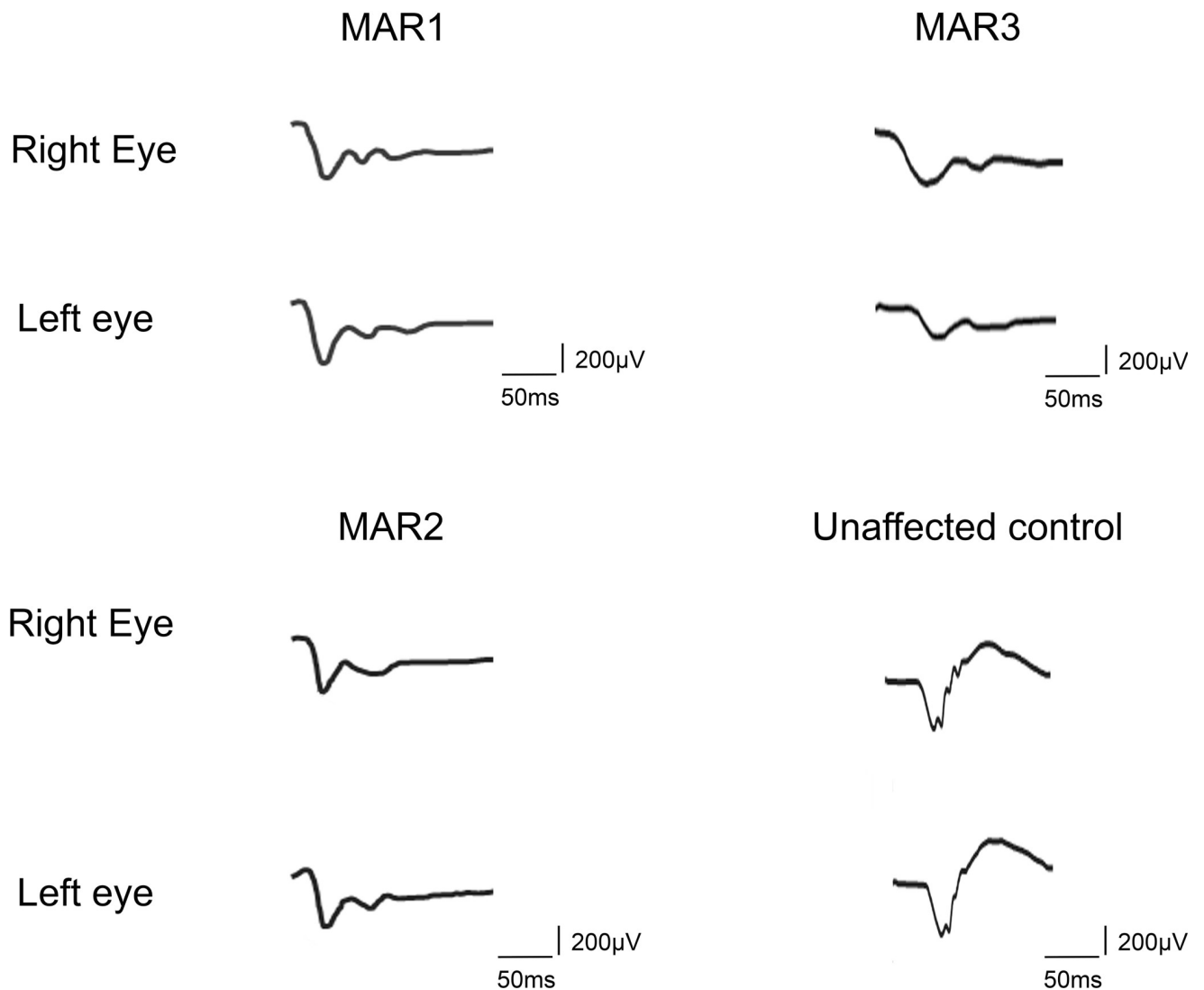


**Fig 1. Full-field ERG recordings (DA 3.0).**

<https://doi.org/10.1371/journal.pone.0231750.g001>

### MAR1, MAR2 and MAR3 sera detect all isoforms of TRPM1 by western blot analysis

MAR sera were tested for their ability to detect TRPM1 following the over-expression of the three different isoforms of V5-tagged human TRPM1 (70+TRPM1, 92+TRPM1 and 109+TRPM1) in COS-7 cells by western blot analyses. As expected, MAR1 and MAR2 sera both detected all three isoforms of TRPM1 at the expected size of about 180 kDa (Fig 3). MAR1 and MAR2 displayed comparable reactivity to 109+TRPM1 as the commercial V5 and TRPM1 antibodies, indicating that the fainter bands for this sample are due to lower expression of the longest isoform. The serum of a non-MAR patient did not lead to any staining. Under the same conditions, the MAR3 serum staining was inconclusive, as no bands were detected.

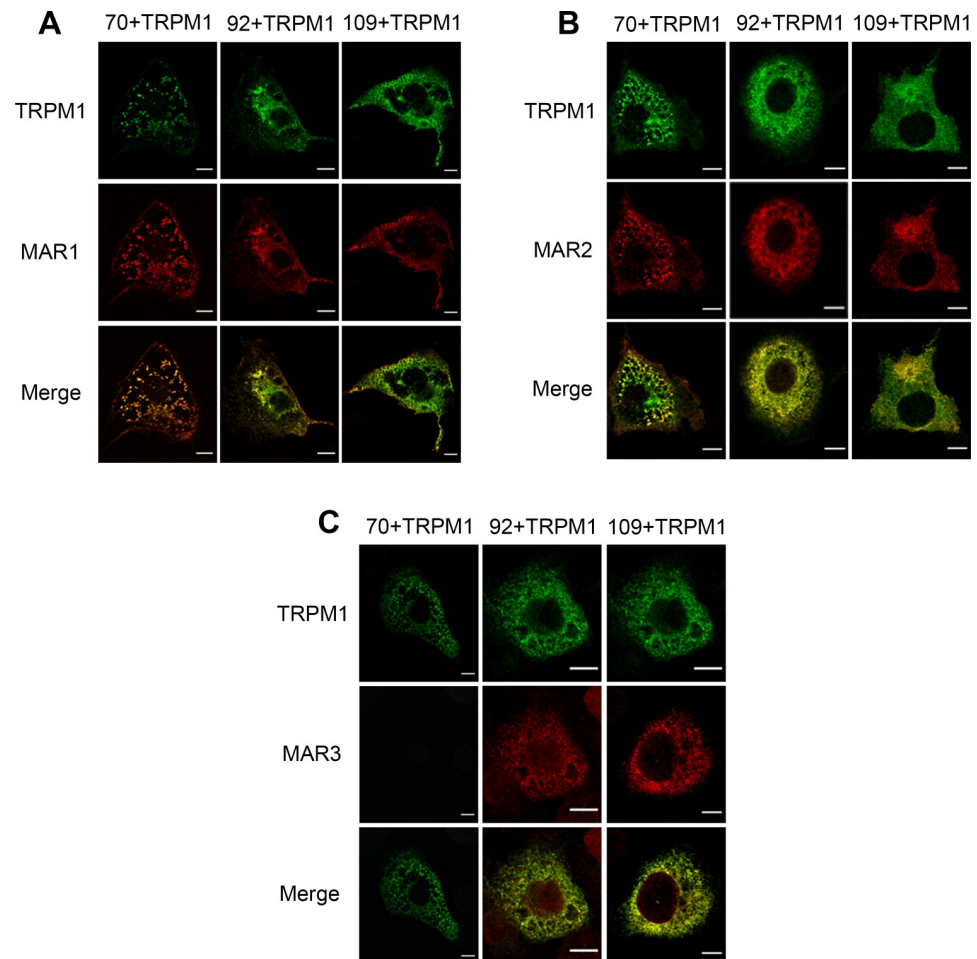


**Fig 2. Immunolocalization studies using the MAR sera and anti-TRPM1 antibody in COS-7 cells overexpressing the three isoforms of TRPM1.** (A) MAR1 (red) staining colocalized (yellow, merge) with TRPM1 (green) staining in COS-7 overexpressing all three isoforms of TRPM1. (B) MAR2 (red) staining colocalized (yellow, merge) with TRPM1 (green) staining in COS-7 overexpressing all three isoforms of TRPM1. (C) MAR3 (red) staining colocalized (yellow, merge) with TRPM1 (green) staining only in COS-7 overexpressing the 92+*TRPM1* and the 109+*TRPM1* isoform. Scale bars: 10 $\mu$ m.

<https://doi.org/10.1371/journal.pone.0231750.g002>

Thus, to obtain a specific staining, protein extracts from COS-7 cells over expressing the three TRPM1 isoforms were immunoprecipitated with the anti-V5 antibody. Subsequently, the MAR3 serum detected all three isoforms of TRPM1. Thus, by western blot analyses, the three MAR sera reacted with all three different TRPM1 isoforms.

Immuno blots of COS-7 cells transfected with the three isoforms of TRPM1 using several antibodies: an anti-TRPM1 antibody, an anti-V5 antibody, MAR1 and MAR2 sera, MAR3 sera after immunoprecipitation using an anti-V5 antibody and a control serum. All antibodies recognized the 70+*TRPM1*, 92+*TRPM1* and 109+*TRPM1* isoforms (~180-200kDa). No signal was obtained with protein extracted from untransfected cells.

### MAR1, MAR2 and MAR3 sera stain ON-bipolar cells on mouse retinal cryosections

To further confirm the results obtained *in vitro*, we tested the three sera on wild-type (*Trpm1*<sup>+/+</sup>) and knock-out *TRPM1* (*Trpm1*<sup>-/-</sup>) mouse retinal cryosections. As expected, the three sera

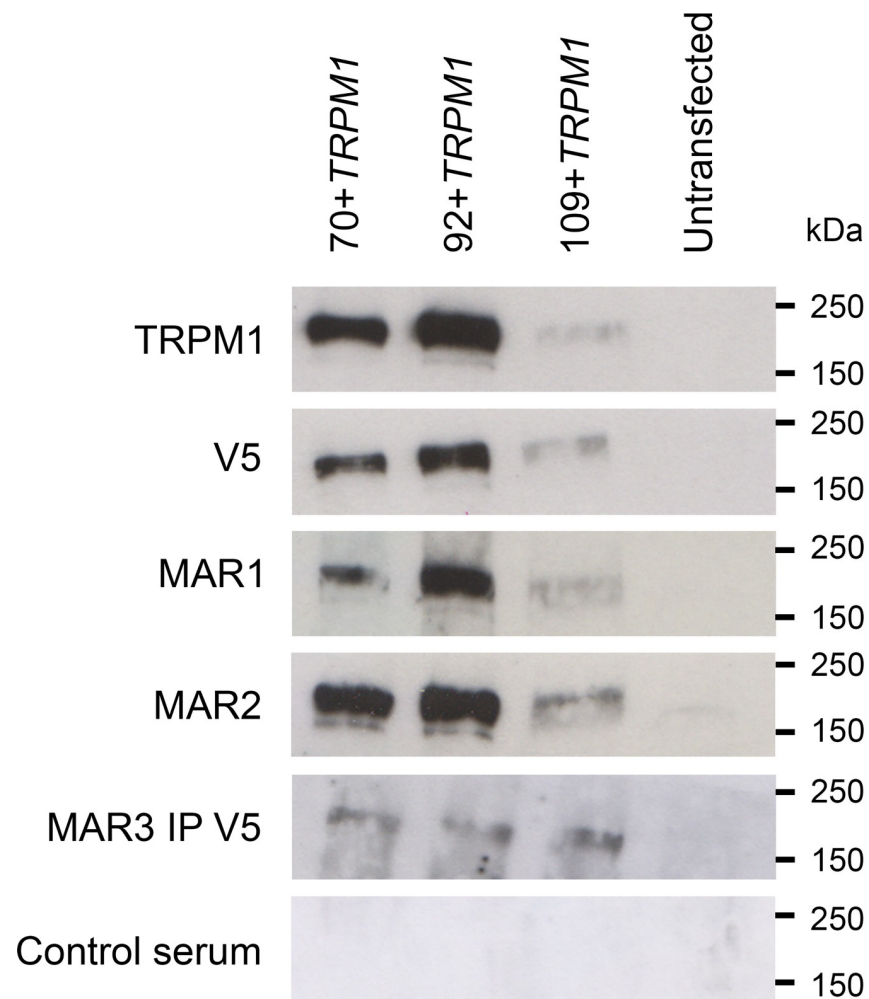


**Fig 3. Western blot analysis of TRPM1 isoforms with MAR sera.**

<https://doi.org/10.1371/journal.pone.0231750.g003>

reacted with a protein localized at the dendritic tips and around ON-bipolar cells (Fig 4A, 4B and 4C). This immunolabelling of dendritic tips and around the soma of ON-bipolar cells with all three sera was comparable to the one obtained with an anti-TRPM1 antibody, while such staining was absent using a serum from a subject with no ocular disorder (Fig 4D). This staining was absent in *Trpm1*<sup>-/-</sup> mice confirming the presence of TRPM1-dependent autoantibodies in all three sera. Immunolabelling was also observed in other retinal layers with these three sera in both wild-type and *Trpm1*<sup>-/-</sup> mice, most likely due to autoantibodies not directed towards TRPM1 (S1 Appendix).

## Discussion

In this study, we report three novel cases with MAR being in fact females. It has been suggested that MAR is more prevalent in male [8], due to melanoma being more prevalent in male patients, especially after 50 years [58,59]. However, our studied cases were all female patients. We are not aware about the presence of a higher frequency of male or female patients with MAR investigated in the respective hospitals. Interestingly it was previously shown that the average age of patients affected with paraneoplastic retinopathy is 62 [60], which is consistent with our study. Indeed, our patients were between 63 and 77 years old.

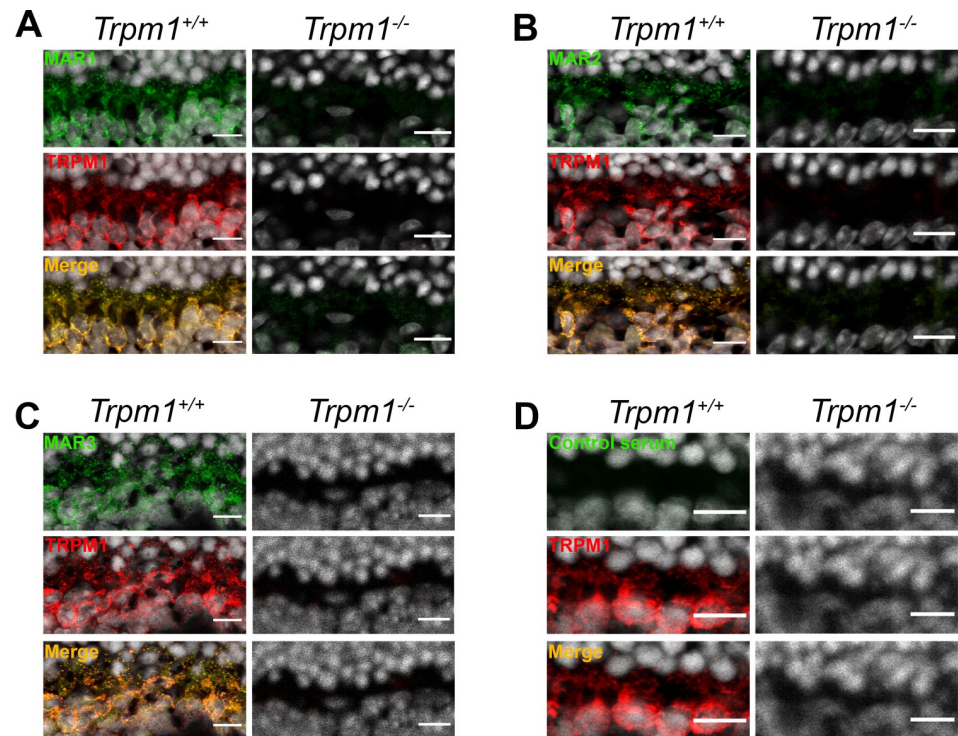


**Fig 4. Immunolocalization on *Trpm1*<sup>+/+</sup> and *Trpm1*<sup>-/-</sup> mouse retinal cryosections.** (A) TRPM1 (red) staining colocalized (yellow, merge) with MAR1 (green) in *Trpm1*<sup>+/+</sup> and both staining were absent in *Trpm1*<sup>-/-</sup> mouse. (B) TRPM1 (red) staining colocalized (yellow, merge) with MAR2 (green) in *Trpm1*<sup>+/+</sup> and both staining were absent in *Trpm1*<sup>-/-</sup> mouse. (C) TRPM1 (red) staining colocalized (yellow, merge) with MAR3 (green) in *Trpm1*<sup>+/+</sup> and both staining were absent in *Trpm1*<sup>-/-</sup> mouse. (D) No TRPM1 (red) staining was observable in *Trpm1*<sup>+/+</sup> and *Trpm1*<sup>-/-</sup> mouse and the same observation was made with a control serum. Scale bars: 10 $\mu$ m.

<https://doi.org/10.1371/journal.pone.0231750.g004>

The presence of anti-TRPM1 autoantibodies in the sera of these new cases of MAR was validated in mammalian cells overexpressing TRPM1 by immunolocalization, western blot analysis and by immunofluorescence on mouse retinal cryosections. The human TRPM1 exists in three isoforms which differ in their N-terminus [33]. Therefore, we investigated the reactivity of the anti-TRPM1 autoantibodies of our MAR patients towards all TRPM1 isoforms. All three sera contained antibodies reacting to the three isoforms of TRPM1, albeit with different apparent sensitivity. In previous reports, it has been suggested that all anti-TRPM1 autoantibodies in MAR patients recognize the same epitope located at the N-terminal, intracellular region of the protein encoded by exons 9 and 10, which is common to all three isoforms [37,43]. For our MAR patients, anti-TRPM1 autoantibodies recognized an epitope that is common to all three TRPM1 isoforms, encoded some place after exon 2, consistent with the literature, but the sensitivity to detect TRPM1 was different and was method-dependent. This was especially true for the anti-TRPM1 autoantibodies present in MAR3, which failed to label the shortest isoform of TRPM1 in the overexpressing cell system by immunofluorescence, yet detected it by western blot after enrichment, and labelled TRPM1 robustly on mouse retinal sections.

Several hypotheses can be proposed to explain this variability: the epitope recognized by the autoantibodies may vary between patients either because of the tumor type or their immune system specificities or both. In addition, the protein folding may be different depending on the TRPM1 isoforms, not allowing the anti-TRPM1 autoantibodies of the MAR3 patient to bind

to the same epitope as in MAR1 and MAR2. Variability in binding might also be explained by distinct antibody titers towards specific isoforms or differences in antibody affinity. As various results were obtained with the same serum depending on the experiment, we suggest to combine multiple tests to assess with certainty the presence of anti-TRPM1 autoantibodies even though in a study by Dalal *et al.*, immunofluorescence on tissue sections and cells were sufficient to validate the presence of anti-TRPM1 autoantibodies in a patient with MAR [39]. In our opinion, western blotting should be the first test to be performed to decipher the presence or absence of anti-TRPM1 as the denaturing conditions might promote epitope accessibility for the autoantibodies. Immunoprecipitation prior to western blotting should also be considered as the titer of the autoantibodies in the sera may vary. Finally, if the western blot analysis is inconclusive, other tests, as immunolocalization, should be performed.

In patients affected with MAR, the ERG phenotype is similar to those found in cCSNB, with a severely decreased b-wave, indicating an ON-bipolar cell dysfunction [33,34] as present in the subjects reported in this study. Other laboratories have studied the impact of intravitreal injection of sera from patients with paraneoplastic retinopathy on mouse [37,38] or monkey ERGs [48]. Ueno and colleagues [38] described a reduction of the scotopic b-wave with a relative preserved a-wave, as was also observed by Xiong *et al* [37]. Similarly, on the monkey ERG, the serum suppressed the photopic b-wave, but the effect on the a-wave was similar to the one obtained with a non-MAR serum [48]. The variable sensitivity in the three sera to detect TRPM1 herein could have also different consequences of the clinical course of the patients ERGs, as some patients recovered after diagnosis and some others deteriorated as previously described [45]. However, a follow-up of the patients studied herein is not available.

Of note, paraneoplastic syndromes can sometimes be more complex due to the occurrence of multiple autoantibodies in the same patient [16]. This may explain additional retinal alterations reported in MAR patients such as choroidal atrophy [41] and MAR patients with other clinical abnormalities [15] which may not be solely explained by anti-TRPM1 antibodies. However, as anti-TRPM1 autoantibodies are the most commonly reported autoantibodies in cases of MAR [35], the search for these other retinal autoantibodies might not have been done. The sera of our three MAR patients were found to specifically label not only the dendritic tip of ON-bipolar cells in wild-type mouse but also other retinal layers in both, wild-type and TRPM1 knock-out mouse retina, suggesting the presence of autoantibodies to multiple retinal targets. The sera of MAR1 and MAR2 patients have been tested for other autoantibodies and were positive for anti-enolase, anti-carbohydase, and anti-GAPDH antibodies. The presence of anti- $\alpha$  enolase has been associated with normal to severe cone loss [61]. It is however unclear if this autoantibody had a functional impact on the clinical presentation of our patient. Additionally, anti-carbonic anhydrase autoantibodies have been studied by Adamus *et al.*, showing their detrimental effect on a retinal cell line, leading to cell death [62]. To our knowledge, the role of anti-GAPDH autoantibodies remains unclear. Furthermore, the identification and characterization of autoantibodies responsible of the retinal phenotype of patients with paraneoplastic syndromes with either photoreceptors defect or ON-bipolar cell defect can help to establish the proper treatment for these patients. For instance, Roels and colleagues [44] reported the case of a patient with CAR and presenting anti-TRPM1 autoantibodies. Following the treatment of this patient with rituximab in order to decrease the immune response, the serology proved the clearance of the anti-TRPM1 autoantibodies. This led to a normalization of the ERG and an improvement of the symptoms in this patient.

The conclusion of our study is that it might be crucial to use different methods to determine which antigen is recognized by the autoantibodies present in MAR serum. Indeed, a combination of *in vitro* and *ex vivo* methods seems to be the most efficient way to identify

autoantibodies in the serum of MAR patients. Moreover, multiple autoantibodies can be implicated in the phenotype of patients with autoimmune retinopathy.

## Supporting information

**S1 Appendix. Immunolocalization on *Trpm1*<sup>+/+</sup> and *Trpm1*<sup>-/-</sup> mouse retinal cryosections.** Sera from MAR patients (green) stain ON-bipolar cells along with a fainter staining in the inner plexiform layer and the ganglion cell layer in both *Trpm1*<sup>+/+</sup> and *Trpm1*<sup>-/-</sup> animals. Scale bars: 10µm.

(TIF)

**S1 Raw Images.**

(PDF)

## Acknowledgments

We are grateful to patients for participation in this study, to the animal housing and imaging platform at the Institut de la Vision. We also would like to thank Profs Sean J. Pittock, MD, Svetomir Markovic MD, PhD and Kirill Martemyanov, PhD for their contribution in this study.

## Author Contributions

**Conceptualization:** Juliette Varin, Isabelle Audo, Christina Zeitz.

**Data curation:** Juliette Varin, Margaret M. Reynolds, Nassima Bouzidi, Sarah Tick.

**Investigation:** Juliette Varin, Margaret M. Reynolds, Nassima Bouzidi, Sarah Tick, Juliette Wohlschlegel, Ondine Becquart, Olivier Dereure, Quentin Samaran, Bernard Guillot, José S. Pulido, Isabelle Audo.

**Methodology:** Juliette Varin, Christelle Michiels.

**Project administration:** Christina Zeitz.

**Resources:** Robert M. Duvoisin, Catherine W. Morgans.

**Supervision:** José-Alain Sahel, José S. Pulido, Isabelle Audo, Christina Zeitz.

**Validation:** José-Alain Sahel, Isabelle Audo, Christina Zeitz.

**Writing – original draft:** Juliette Varin.

**Writing – review & editing:** Margaret M. Reynolds, Robert M. Duvoisin, Catherine W. Morgans, José-Alain Sahel, José S. Pulido, Isabelle Audo, Christina Zeitz.

## References

1. Boeck K, Hofmann S, Klopfer M, Ian U, Schmidt T, et al. (1997) Melanoma-associated paraneoplastic retinopathy: case report and review of the literature. *Br J Dermatol* 137: 457–460. PMID: [9349350](https://pubmed.ncbi.nlm.nih.gov/9349350/)
2. Berson EL, Lessell S (1988) Paraneoplastic night blindness with malignant melanoma. *Am J Ophthalmol* 106: 307–311. [https://doi.org/10.1016/0002-9394\(88\)90366-2](https://doi.org/10.1016/0002-9394(88)90366-2) PMID: [2971322](https://pubmed.ncbi.nlm.nih.gov/2971322/)
3. Lu Y, Jia L, He S, Hurley MC, Leys MJ, et al. (2009) Melanoma-associated retinopathy: a paraneoplastic autoimmune complication. *Arch Ophthalmol* 127: 1572–1580. <https://doi.org/10.1001/archophthalmol.2009.311> PMID: [20008709](https://pubmed.ncbi.nlm.nih.gov/20008709/)
4. Rahimy E, Sarraf D (2013) Paraneoplastic and non-paraneoplastic retinopathy and optic neuropathy: evaluation and management. *Surv Ophthalmol* 58: 430–458. <https://doi.org/10.1016/j.survophthal.2012.09.001> PMID: [23969019](https://pubmed.ncbi.nlm.nih.gov/23969019/)

5. Chan JW (2003) Paraneoplastic retinopathies and optic neuropathies. *Surv Ophthalmol* 48: 12–38. [https://doi.org/10.1016/s0039-6257\(02\)00416-2](https://doi.org/10.1016/s0039-6257(02)00416-2) PMID: [12559325](#)
6. Thirkill CE, FitzGerald P, Sergott RC, Roth AM, Tyler NK, et al. (1989) Cancer-associated retinopathy (CAR syndrome) with antibodies reacting with retinal, optic-nerve, and cancer cells. *N Engl J Med* 321: 1589–1594. <https://doi.org/10.1056/NEJM198912073212307> PMID: [2555714](#)
7. Thirkill CE, Roth AM, Keltner JL (1987) Cancer-associated retinopathy. *Arch Ophthalmol* 105: 372–375. <https://doi.org/10.1001/archophth.1987.01060030092033> PMID: [2950846](#)
8. Canamary AM Jr., Takahashi WY, Sallum JMF (2018) Autoimmune retinopathy: A Review. *Int J Retina Vitreous* 4: 1. <https://doi.org/10.1186/s40942-017-0104-9> PMID: [29340169](#)
9. Alexander KR, Fishman GA, Peachey NS, Marchese AL, Tso MO (1992) 'On' response defect in paraneoplastic night blindness with cutaneous malignant melanoma. *Invest Ophthalmol Vis Sci* 33: 477–483. PMID: [1544774](#)
10. Kondo M, Sanuki R, Ueno S, Nishizawa Y, Hashimoto N, et al. (2011) Identification of autoantibodies against TRPM1 in patients with paraneoplastic retinopathy associated with ON bipolar cell dysfunction. *PLoS One* 6: e19911. <https://doi.org/10.1371/journal.pone.0019911> PMID: [21611200](#)
11. Goetgebuer G, Kestelyn-Stevens AM, De Laey JJ, Kestelyn P, Leroy BP (2008) Cancer-associated retinopathy (CAR) with electronegative ERG: a case report. *Doc Ophthalmol* 116: 49–55. <https://doi.org/10.1007/s10633-007-9074-9> PMID: [17721792](#)
12. Anastasakis A, Dick AD, Damato EM, Spry PG, Majid MA (2011) Cancer-associated retinopathy presenting as retinal vasculitis with a negative ERG suggestive of on-bipolar cell pathway dysfunction. *Doc Ophthalmol* 123: 59–63. <https://doi.org/10.1007/s10633-011-9277-y> PMID: [21674222](#)
13. Remulla JF, Pineda R, Gaudio AR, Milam AH (1995) Cutaneous melanoma-associated retinopathy with retinal periphlebitis. *Arch Ophthalmol* 113: 854–855. <https://doi.org/10.1001/archophth.1995.011100070024015> PMID: [7605271](#)
14. Murayama K, Takita H, Kiyohara Y, Shimizu Y, Tsuchida T, et al. (2006) [Melanoma-associated retinopathy with unknown primary site in a Japanese woman]. *Nippon Ganka Gakkai Zasshi* 110: 211–217. PMID: [16562510](#)
15. Keltner JL, Thirkill CE, Yip PT (2001) Clinical and immunologic characteristics of melanoma-associated retinopathy syndrome: eleven new cases and a review of 51 previously published cases. *J Neuroophthalmol* 21: 173–187. <https://doi.org/10.1097/00041327-200109000-00004> PMID: [11725182](#)
16. Roberts P, Fishman GA, Joshi K, Jampol LM (2016) Chorioretinal Lesions in a Case of Melanoma-Associated Retinopathy Treated With Pembrolizumab. *JAMA Ophthalmol* 134: 1184–1188. <https://doi.org/10.1001/jamaophthalmol.2016.2944> PMID: [27540851](#)
17. Schubert G, Bornschein H (1952) Analysis of the human electroretinogram. *Ophthalmologica* 123: 396–413. <https://doi.org/10.1159/000301211> PMID: [14957416](#)
18. Miyake Y, Yagasaki K, Horiguchi M, Kawase Y, Kanda T (1986) Congenital stationary night blindness with negative electroretinogram. A new classification. *Arch Ophthalmol* 104: 1013–1020. <https://doi.org/10.1001/archophth.1986.01050190071042> PMID: [3488053](#)
19. Zeitz C, Robson AG, Audo I (2015) Congenital stationary night blindness: an analysis and update of genotype-phenotype correlations and pathogenic mechanisms. *Prog Retin Eye Res* 45: 58–110. <https://doi.org/10.1016/j.preteyeres.2014.09.001> PMID: [25307992](#)
20. McCulloch DL, Marmor MF, Brigell MG, Hamilton R, Holder GE, et al. (2015) ISCEV Standard for full-field clinical electroretinography (2015 update). *Doc Ophthalmol* 130: 1–12.
21. Audo I, Kohl S, Leroy BP, Munier FL, Guillonnet X, et al. (2009) TRPM1 is mutated in patients with autosomal-recessive complete congenital stationary night blindness. *Am J Hum Genet* 85: 720–729. <https://doi.org/10.1016/j.ajhg.2009.10.013> PMID: [19896113](#)
22. Li Z, Sergouniotis PI, Michaelides M, Mackay DS, Wright GA, et al. (2009) Recessive mutations of the gene TRPM1 abrogate ON bipolar cell function and cause complete congenital stationary night blindness in humans. *Am J Hum Genet* 85: 711–719. <https://doi.org/10.1016/j.ajhg.2009.10.003> PMID: [19878917](#)
23. van Genderen MM, Bijveld MM, Claassen YB, Florijn RJ, Pearing JN, et al. (2009) Mutations in TRPM1 are a common cause of complete congenital stationary night blindness. *Am J Hum Genet* 85: 730–736. <https://doi.org/10.1016/j.ajhg.2009.10.012> PMID: [19896109](#)
24. Dryja TP, McGee TL, Berson EL, Fishman GA, Sandberg MA, et al. (2005) Night blindness and abnormal cone electroretinogram ON responses in patients with mutations in the GRM6 gene encoding mGluR6. *Proc Natl Acad Sci U S A* 102: 4884–4889. <https://doi.org/10.1073/pnas.0501233102> PMID: [15781871](#)
25. Zeitz C, van Genderen M, Neidhardt J, Luhmann UF, Hoeber F, et al. (2005) Mutations in GRM6 cause autosomal recessive congenital stationary night blindness with a distinctive scotopic 15-Hz flicker

- electroretinogram. *Invest Ophthalmol Vis Sci* 46: 4328–4335. <https://doi.org/10.1167/iovs.05-0526> PMID: [16249515](https://pubmed.ncbi.nlm.nih.gov/16249515/)
26. Audo I, Bujakowska K, Orhan E, Poloschek CM, Defoort-Dhellemmes S, et al. (2012) Whole-exome sequencing identifies mutations in GPR179 leading to autosomal-recessive complete congenital stationary night blindness. *Am J Hum Genet* 90: 321–330. <https://doi.org/10.1016/j.ajhg.2011.12.007> PMID: [22325361](https://pubmed.ncbi.nlm.nih.gov/22325361/)
  27. Peachey NS, Ray TA, Florijn R, Rowe LB, Sjoerdsma T, et al. (2012) GPR179 is required for depolarizing bipolar cell function and is mutated in autosomal-recessive complete congenital stationary night blindness. *Am J Hum Genet* 90: 331–339. <https://doi.org/10.1016/j.ajhg.2011.12.006> PMID: [22325362](https://pubmed.ncbi.nlm.nih.gov/22325362/)
  28. Zeitz C, Jacobson SG, Hamel CP, Bujakowska K, Neuille M, et al. (2013) Whole-exome sequencing identifies LRIT3 mutations as a cause of autosomal-recessive complete congenital stationary night blindness. *Am J Hum Genet* 92: 67–75. <https://doi.org/10.1016/j.ajhg.2012.10.023> PMID: [23246293](https://pubmed.ncbi.nlm.nih.gov/23246293/)
  29. Pusch CM, Zeitz C, Brandau O, Pesch K, Achatz H, et al. (2000) The complete form of X-linked congenital stationary night blindness is caused by mutations in a gene encoding a leucine-rich repeat protein. *Nat Genet* 26: 324–327. <https://doi.org/10.1038/81627> PMID: [11062472](https://pubmed.ncbi.nlm.nih.gov/11062472/)
  30. Bech-Hansen NT, Naylor MJ, Maybaum TA, Sparkes RL, Koop B, et al. (2000) Mutations in NYX, encoding the leucine-rich proteoglycan nyctalopin, cause X-linked complete congenital stationary night blindness. *Nat Genet* 26: 319–323. <https://doi.org/10.1038/81619> PMID: [11062471](https://pubmed.ncbi.nlm.nih.gov/11062471/)
  31. Morgans CW, Zhang J, Jeffrey BG, Nelson SM, Burke NS, et al. (2009) TRPM1 is required for the depolarizing light response in retinal ON-bipolar cells. *Proc Natl Acad Sci U S A* 106: 19174–19178. <https://doi.org/10.1073/pnas.0908711106> PMID: [19861548](https://pubmed.ncbi.nlm.nih.gov/19861548/)
  32. Koike C, Numata T, Ueda H, Mori Y, Furukawa T (2010) TRPM1: a vertebrate TRP channel responsible for retinal ON bipolar function. *Cell Calcium* 48: 95–101. <https://doi.org/10.1016/j.ceca.2010.08.004> PMID: [20846719](https://pubmed.ncbi.nlm.nih.gov/20846719/)
  33. Oancea E, Vriens J, Brauchi S, Jun J, Splawski I, et al. (2009) TRPM1 forms ion channels associated with melanin content in melanocytes. *Sci Signal* 2: ra21. <https://doi.org/10.1126/scisignal.2000146> PMID: [19436059](https://pubmed.ncbi.nlm.nih.gov/19436059/)
  34. Devi S, Kedlaya R, Maddodi N, Bhat KM, Weber CS, et al. (2009) Calcium homeostasis in human melanocytes: role of transient receptor potential melastatin 1 (TRPM1) and its regulation by ultraviolet light. *Am J Physiol Cell Physiol* 297: C679–687. <https://doi.org/10.1152/ajpcell.00092.2009> PMID: [19587221](https://pubmed.ncbi.nlm.nih.gov/19587221/)
  35. Dhingra A, Fina ME, Neinstein A, Ramsey DJ, Xu Y, et al. (2011) Autoantibodies in melanoma-associated retinopathy target TRPM1 cation channels of retinal ON bipolar cells. *J Neurosci* 31: 3962–3967. <https://doi.org/10.1523/JNEUROSCI.6007-10.2011> PMID: [21411639](https://pubmed.ncbi.nlm.nih.gov/21411639/)
  36. Wang Y, Abu-Asab MS, Li W, Aronow ME, Singh AD, et al. (2012) Autoantibody against transient receptor potential M1 cation channels of retinal ON bipolar cells in paraneoplastic vitelliform retinopathy. *BMC Ophthalmol* 12: 56. <https://doi.org/10.1186/1471-2415-12-56> PMID: [23148706](https://pubmed.ncbi.nlm.nih.gov/23148706/)
  37. Xiong WH, Duvoisin RM, Adamus G, Jeffrey BG, Gellman C, et al. (2013) Serum TRPM1 autoantibodies from melanoma associated retinopathy patients enter retinal on-bipolar cells and attenuate the electroretinogram in mice. *PLoS One* 8: e69506. <https://doi.org/10.1371/journal.pone.0069506> PMID: [23936334](https://pubmed.ncbi.nlm.nih.gov/23936334/)
  38. Ueno S, Nishiguchi KM, Tanioka H, Enomoto A, Yamanouchi T, et al. (2013) Degeneration of retinal on bipolar cells induced by serum including autoantibody against TRPM1 in mouse model of paraneoplastic retinopathy. *PLoS One* 8: e81507. <https://doi.org/10.1371/journal.pone.0081507> PMID: [24282602](https://pubmed.ncbi.nlm.nih.gov/24282602/)
  39. Dalal MD, Morgans CW, Duvoisin RM, Gamboa EA, Jeffrey BG, et al. (2013) Diagnosis of occult melanoma using transient receptor potential melastatin 1 (TRPM1) autoantibody testing: a novel approach. *Ophthalmology* 120: 2560–2564. <https://doi.org/10.1016/j.ophtha.2013.07.037> PMID: [24053997](https://pubmed.ncbi.nlm.nih.gov/24053997/)
  40. Morita Y, Kimura K, Fujitsu Y, Enomoto A, Ueno S, et al. (2014) Autoantibodies to transient receptor potential cation channel, subfamily M, member 1 in a Japanese patient with melanoma-associated retinopathy. *Jpn J Ophthalmol* 58: 166–171. <https://doi.org/10.1007/s10384-013-0300-6> PMID: [24468869](https://pubmed.ncbi.nlm.nih.gov/24468869/)
  41. Ueno S, Ito Y, Maruko R, Kondo M, Terasaki H (2014) Choroidal atrophy in a patient with paraneoplastic retinopathy and anti-TRPM1 antibody. *Clin Ophthalmol* 8: 369–373. <https://doi.org/10.2147/OPTH.S55124> PMID: [24523577](https://pubmed.ncbi.nlm.nih.gov/24523577/)
  42. Ueno S, Nakanishi A, Nishi K, Suzuki S, Terasaki H (2015) Case of paraneoplastic retinopathy with retinal ON-bipolar cell dysfunction and subsequent resolution of ERGs. *Doc Ophthalmol* 130: 71–76. <https://doi.org/10.1007/s10633-014-9470-x> PMID: [25391361](https://pubmed.ncbi.nlm.nih.gov/25391361/)
  43. Duvoisin RM, Haley TL, Ren G, Strycharska-Orczyk I, Bonaparte JP, et al. (2017) Autoantibodies in Melanoma-Associated Retinopathy Recognize an Epitope Conserved Between TRPM1 and TRPM3. *Invest Ophthalmol Vis Sci* 58: 2732–2738. <https://doi.org/10.1167/iovs.17-21443> PMID: [28549093](https://pubmed.ncbi.nlm.nih.gov/28549093/)

44. Roels D, Ueno S, Talianu CD, Draganova D, Kondo M, et al. (2017) Unilateral cancer-associated retinopathy: diagnosis, serology and treatment. *Doc Ophthalmol* 135: 233–240. <https://doi.org/10.1007/s10633-017-9605-y> PMID: 28815346
45. Ueno S, Inooka D, Nakanishi A, Okado S, Yasuda S, et al. (2018) Clinical Course of Paraneoplastic Retinopathy with Anti-Trpm1 Autoantibody in Japanese Cohort. *Retina*.
46. Duvoisin RM, Ren G, Haley TL, Taylor MH, Morgans CW (2019) TRPM1 Autoantibodies in Melanoma Patients Without Self-Reported Visual Symptoms. *Invest Ophthalmol Vis Sci* 60: 2330–2335. <https://doi.org/10.1167/iov.19-26775> PMID: 31117125
47. Touhami S, Audo I, Terrada C, Gaudric A, LeHoang P, et al. (2019) Neoplasia and intraocular inflammation: From masquerade syndromes to immunotherapy-induced uveitis. *Prog Retin Eye Res* 72: 100761. <https://doi.org/10.1016/j.preteyeres.2019.05.002> PMID: 31091471
48. Lei B, Bush RA, Milam AH, Sieving PA (2000) Human melanoma-associated retinopathy (MAR) antibodies alter the retinal ON-response of the monkey ERG in vivo. *Invest Ophthalmol Vis Sci* 41: 262–266. PMID: 10634629
49. Nishiguchi KM, Fujita K, Inoue T, Nakazawa T (2018) Anti-TRPM1 antibodies in patients with retinal degeneration. *Clin Exp Ophthalmol* 46: 1087–1089. <https://doi.org/10.1111/ceo.13341> PMID: 29927037
50. Polans AS, Witkowska D, Haley TL, Amundson D, Baizer L, et al. (1995) Recoverin, a photoreceptor-specific calcium-binding protein, is expressed by the tumor of a patient with cancer-associated retinopathy. *Proc Natl Acad Sci U S A* 92: 9176–9180. <https://doi.org/10.1073/pnas.92.20.9176> PMID: 7568096
51. Mazar J, DeYoung K, Khaitan D, Meister E, Almodovar A, et al. (2010) The regulation of miRNA-211 expression and its role in melanoma cell invasiveness. *PLoS One* 5: e13779. <https://doi.org/10.1371/journal.pone.0013779> PMID: 21072171
52. Levy C, Khaled M, Iliopoulos D, Janas MM, Schubert S, et al. (2010) Intronic miR-211 assumes the tumor suppressive function of its host gene in melanoma. *Mol Cell* 40: 841–849. <https://doi.org/10.1016/j.molcel.2010.11.020> PMID: 21109473
53. Boyle GM, Woods SL, Bonazzi VF, Stark MS, Hacker E, et al. (2011) Melanoma cell invasiveness is regulated by miR-211 suppression of the BRN2 transcription factor. *Pigment Cell Melanoma Res* 24: 525–537. <https://doi.org/10.1111/j.1755-148X.2011.00849.x> PMID: 21435193
54. Zhiqi S, Soltani MH, Bhat KM, Sangha N, Fang D, et al. (2004) Human melastatin 1 (TRPM1) is regulated by MITF and produces multiple polypeptide isoforms in melanocytes and melanoma. *Melanoma Res* 14: 509–516. <https://doi.org/10.1097/00008390-200412000-00011> PMID: 15577322
55. Fang D, Setaluri V (2000) Expression and Up-regulation of alternatively spliced transcripts of melastatin, a melanoma metastasis-related gene, in human melanoma cells. *Biochem Biophys Res Commun* 279: 53–61. <https://doi.org/10.1006/bbrc.2000.3894> PMID: 11112417
56. Audo I, Friedrich A, Mohand-Said S, Lancelot ME, Antonio A, et al. (2010) An unusual retinal phenotype associated with a novel mutation in RHO. *Arch Ophthalmol* 128: 1036–1045. <https://doi.org/10.1001/archophthalmol.2010.162> PMID: 20697005
57. Cao Y, Posokhova E, Martemyanov KA (2011) TRPM1 forms complexes with nyctalopin in vivo and accumulates in postsynaptic compartment of ON-bipolar neurons in mGluR6-dependent manner. *J Neurosci* 31: 11521–11526. <https://doi.org/10.1523/JNEUROSCI.1682-11.2011> PMID: 21832182
58. Enninga EAL, Moser JC, Weaver AL, Markovic SN, Brewer JD, et al. (2017) Survival of cutaneous melanoma based on sex, age, and stage in the United States, 1992–2011. *Cancer Med* 6: 2203–2212. <https://doi.org/10.1002/cam4.1152> PMID: 28879661
59. Robsahm TE, Bergva G, Hestvik UE, Moller B (2013) Sex differences in rising trends of cutaneous malignant melanoma in Norway, 1954–2008. *Melanoma Res* 23: 70–78. <https://doi.org/10.1097/CMR.0b013e32835c7e48> PMID: 23222548
60. Adamus G, Ren G, Weleber RG (2004) Autoantibodies against retinal proteins in paraneoplastic and autoimmune retinopathy. *BMC Ophthalmol* 4: 5. <https://doi.org/10.1186/1471-2415-4-5> PMID: 15180904
61. Grewal DS, Fishman GA, Jampol LM (2014) Autoimmune retinopathy and antiretinal antibodies: a review. *Retina* 34: 827–845. <https://doi.org/10.1097/IAE.000000000000119> PMID: 24646664
62. Adamus G, Karren L (2009) Autoimmunity against carbonic anhydrase II affects retinal cell functions in autoimmune retinopathy. *J Autoimmun* 32: 133–139. <https://doi.org/10.1016/j.jaut.2009.02.001> PMID: 19269136

CORRECTION

# Correction: Identification and characterization of novel TRPM1 autoantibodies from serum of patients with melanoma-associated retinopathy

The PLOS ONE Staff

The following information is missing from the Funding statement: JV, NB, JW, CZ, IA, JAS: IHU FOReSIGHT (ANR-18-IAHU-0001) supported by French state funds managed by the Agence Nationale de la Recherche within the Investissements d’Avenir program.

The legends for Figs 1 and 3 mistakenly appear in the body of the article. There is an error in the legend for panel B of Fig 4. Please see the complete, correct legends for Figs 1, 3 and 4 here.

### DA 3.0 Mixed rod-cone responses

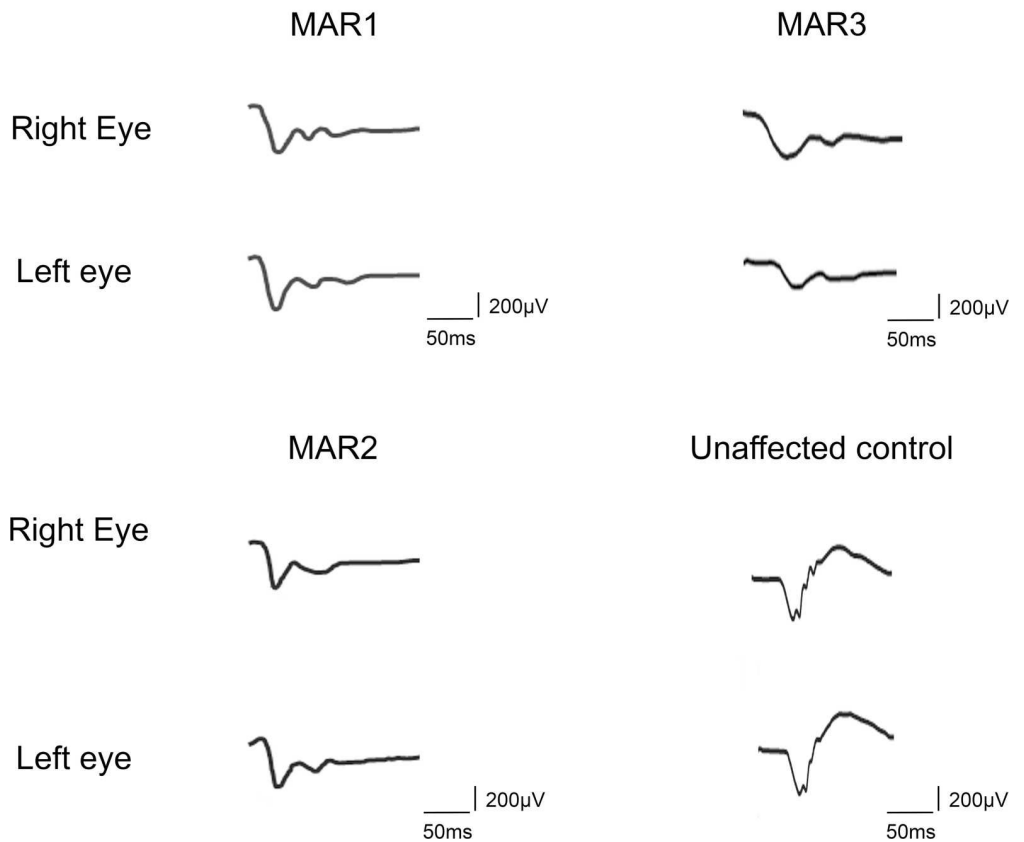


**Fig 1. Full-field ERG recordings (DA 3.0).** Ff-ERG responses to a 3.0 cd.s.m<sup>2</sup> flash under dark-adapted (DA) conditions from an unaffected subject and the three patients with a clinical diagnosis of melanoma-associated retinopathy (MAR). All three patients had a severely reduced b-wave with an electronegative response.

<https://doi.org/10.1371/journal.pone.0233424.g001>



**OPEN ACCESS**

**Citation:** The PLOS ONE Staff (2020) Correction: Identification and characterization of novel TRPM1 autoantibodies from serum of patients with melanoma-associated retinopathy. PLoS ONE 15 (5): e0233424. <https://doi.org/10.1371/journal.pone.0233424>

**Published:** May 13, 2020

**Copyright:** © 2020 The PLOS ONE Staff. This is an open access article distributed under the terms of the [Creative Commons Attribution License](https://creativecommons.org/licenses/by/4.0/), which permits unrestricted use, distribution, and reproduction in any medium, provided the original author and source are credited.

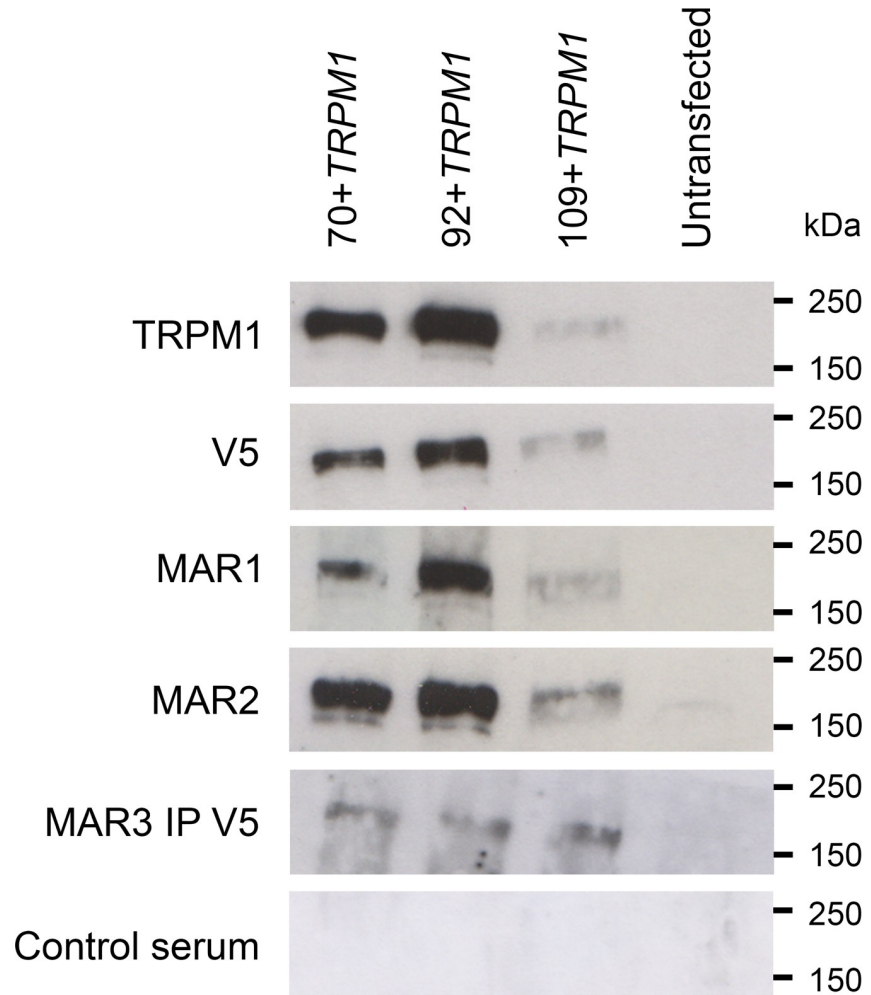


**Fig 3. Western blot analysis of TRPM1 isoforms with MAR sera.** Immuno blots of COS-7 cells transfected with the three isoforms of TRPM1 using several antibodies: an anti-TRPM1 antibody, an anti-V5 antibody, MAR1 and MAR2 sera, MAR3 sera after immunoprecipitation using an anti-V5 antibody and a control serum. All antibodies recognized the 70+TRPM1, 92+TRPM1 and 109+TRPM1 isoforms (~180-200kDa). No signal was obtained with protein extracted from untransfected cells.

<https://doi.org/10.1371/journal.pone.0233424.g002>

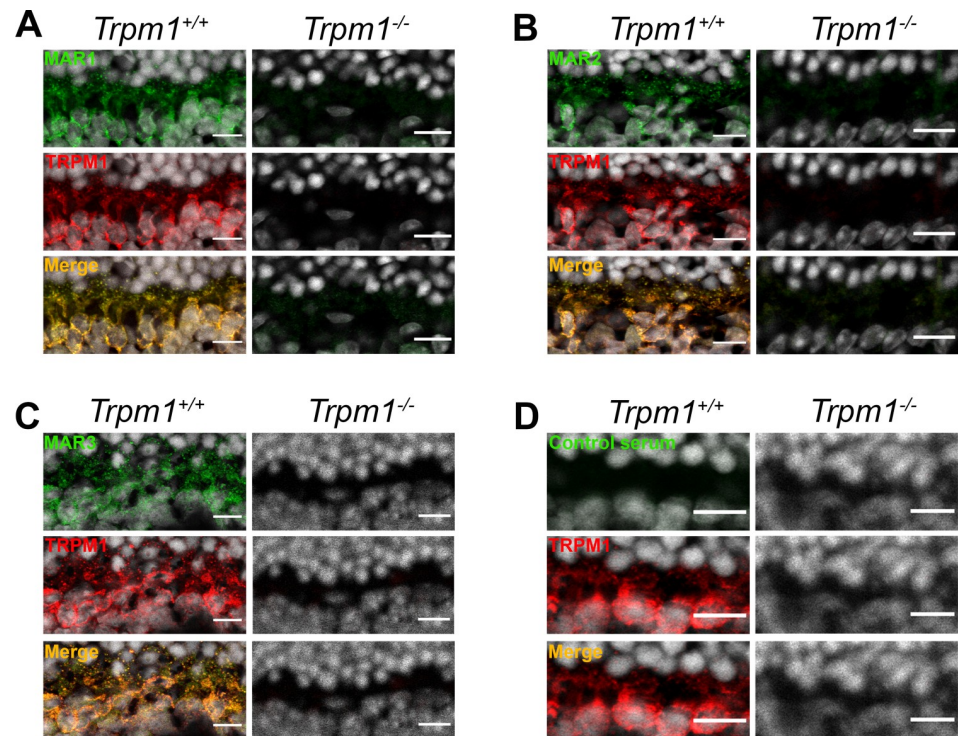


**Fig 4. Immunolocalization on *Trpm1*<sup>+/+</sup> and *Trpm1*<sup>-/-</sup> mouse retinal cryosections.** (A) TRPM1 (red) staining colocalized (yellow, merge) with MAR1 (green) in *Trpm1*<sup>+/+</sup> and both staining were absent in *Trpm1*<sup>-/-</sup> mouse. (B) TRPM1 (red) staining colocalized (yellow, merge) with MAR2 (green) in *Trpm1*<sup>+/+</sup> and both staining were absent in *Trpm1*<sup>-/-</sup> mouse. (C) TRPM1 (red) staining colocalized (yellow, merge) with MAR3 (green) in *Trpm1*<sup>+/+</sup> and both staining were absent in *Trpm1*<sup>-/-</sup> mouse. (D) TRPM1 (red) staining was present in *Trpm1*<sup>+/+</sup> and absent in *Trpm1*<sup>-/-</sup> mice. Control serum did not reveal any staining. Scale bars: 10μm.

<https://doi.org/10.1371/journal.pone.0233424.g003>

The citation for reference 20 is incomplete. The complete reference is: McCulloch DL, Marmor MF, Brigell MG, Hamilton R, Holder GE, et al. (2015) ISCEV Standard for full-field clinical electroretinography (2015 update). *Doc Ophthalmol* 130: 1–12. pmid: 25502644

The publisher apologize for the errors.

## Reference

1. Varin J, Reynolds MM, Bouzidi N, Tick S, Wohlschlegel J, Becquart O, et al. (2020) Identification and characterization of novel TRPM1 autoantibodies from serum of patients with melanoma-associated retinopathy. *PLoS ONE* 15(4): e0231750. <https://doi.org/10.1371/journal.pone.0231750> PMID: 32324760

# Results

---

## II. RESTORATION OF mGLUR6 LOCALIZATION FOLLOWING AAV-MEDIATED DELIVERY IN A MOUSE MODEL OF CONGENITAL STATIONARY NIGHT BLINDNESS

To date, treatment for cCSNB is unavailable. Gene replacement strategy might be a suitable approach to treat cCSNB since it represents a stationary non-degenerative disorder and the genetics of this disorder is well characterized. Mutations in *GRM6* are the third most prevalent cause of cCSNB. The *Grm6<sup>tm1Nak</sup>* (referred as *Grm6<sup>-/-</sup>*) mouse model mimics the phenotype observed in patients and has been studied to understand the ON-BCs signaling cascade. The aim of this study was to restore protein localization and function in *Grm6<sup>-/-</sup>* mice using an AAV-based approach with two different promoters, either targeting specifically ON-BCs (GRM6) or the entire retina (CAG).

Following treatment, mGluR6 was relocalized at the dendritic tips of ON-BCs using both constructs. The efficiency of mGluR6-transduced retinas in the OPL was 2.5% versus 11% when the GRM6-*Grm6* and CAG-*Grm6* were used, respectively. Relocalization of TRPM1, GPR179 and Gβ5 was also noted using both constructs. However, the restoration of the localization of RGS7 and RGS11 was more evident in GRM6-*Grm6* than in CAG-*Grm6* treated retinas. Functional rescue after treatment as measured by ERG failed to appear. These findings give hope that by improving the vector-constructions the efficiency of transduction will be improved and cCSNB due to mutations in *GRM6* could be treated.

These findings will be submitted to the journal of Investigative Ophthalmology and Visual Science (IOVS)

**Varin J**, Bouzidi N, Dias MS, Pugliese T, Michiels C, Robert C, Desrosiers M, Sahel JA, Audo I, Dalkara D, Zeitz C. Restoration of mGluR6 localization following AAV-mediated delivery in a mouse model of congenital stationary night blindness. **IOVS** (to be submitted)

## **Restauration of mGluR6 localization following AAV-mediated delivery in a mouse model of Congenital Stationary Night Blindness**

Juliette Varin<sup>1</sup>, Nassima Bouzidi<sup>1</sup>, Miguel Miranda De Sousa Dias<sup>1</sup>, Thomas Pugliese<sup>1</sup>,  
Christelle Michiels, Camille Robert, Melissa Desrosiers<sup>1</sup>, José-Alain Sahel<sup>1,2,3,4,5</sup>, Isabelle  
Audo<sup>1,2,6</sup>, Deniz Dalkara<sup>1</sup>, Christina Zeitz<sup>1</sup>

<sup>1</sup>Sorbonne Université, INSERM, CNRS, Institut de la Vision, Paris, France.

<sup>2</sup>CHNO des Quinze-Vingts, DHU Sight Restore, INSERM-DGOS CIC 1423, Paris, France.

<sup>3</sup>Fondation Ophtalmologique Adolphe de Rothschild, Paris, France

<sup>4</sup>Academie des Sciences, Institut de France, Paris, France

<sup>5</sup>Department of Ophthalmology, The University of Pittsburgh School of Medicine, Pittsburgh,  
PA 15213, United States

<sup>6</sup>Institute of Ophthalmology, University College of London, London, United Kingdom

This study was carried out in Paris, France

Corresponding author:

Christina Zeitz PhD, DR2

INSERM, UMR\_S968

CNRS, UMR\_7210

Sorbonne University

Institut de la Vision

Department of Genetics

17, rue Moreau

75012 Paris

France

Tel.: +33 1 53 46 25 40

## **Abstract (250 words)**

Purpose: Complete congenital stationary night blindness (cCSNB) is an incurable inherited retinal disorder characterized by an ON-bipolar cell (ON-BC) defect. *GRM6* mutations are the third most prevalent cause of cCSNB. The *Grm6*<sup>-/-</sup> mouse model mimics the human phenotype showing no ON-BC responses upon electroretinogram (ERG), loss of mGluR6 and other proteins of the same cascade at the outer plexiform layer (OPL). Our aim was to restore protein localization and function in *Grm6*<sup>-/-</sup> mice.

Methods: Adeno-associated virus-constructs using two different promoters (*GRM6-Grm6* and *CAG-Grm6*) were injected intravitreally in P15 *Grm6*<sup>-/-</sup> mice. ERG recordings at 2 and 4 months were performed in *Grm6*<sup>+/+</sup> *Grm6*<sup>-/-</sup> and *Grm6*<sup>-/-</sup> treated mice. Similarly, immunolocalization studies were performed on retinal slices before or/and after treatment using antibodies against mGluR6, TRPM1, GPR179, RGS7, RGS11 and Gβ5.

Results: Following treatment, mGluR6 was relocalized at the dendritic tips of ON-BCs using both constructs. The efficiency of mGluR6-transduced retinas in the OPL was 2.5% versus 11% when the *GRM6-Grm6* and *CAG-Grm6* were used, respectively. Relocalization of TRPM1, GPR179 and Gβ5 was also noted using both constructs. However, the restoration of the localization of RGS7 and RGS11 was more evident in *GRM6-Grm6* than in *CAG-Grm6* treated retinas. Functional rescue after treatment as measured by ERG failed to appear.

Conclusions: Our findings show the potential of treating cCSNB with *GRM6*-mutations. However, to restore visual function the transduction rate of both constructs needs to be improved.

## Introduction

Congenital stationary night blindness (CSNB) is a non-progressive retinal disorder <sup>1</sup>. Patients suffering from this disease often present an impairment of night vision, delayed dark-to-light adaptation and difficulties to sense contrasts properly in dim-light conditions. It is also often associated with high myopia, strabismus and nystagmus<sup>2</sup>. Considering the retinal response on the electroretinogram (ERG), CSNB has been divided in two groups: the Riggs-type <sup>3</sup> of CSNB, associated with a rod-photoreceptor defect and the Schubert-Bornschein type <sup>1</sup> of CSNB in which the underlying defect relies in the signal transmission from photoreceptors to bipolar cells <sup>4</sup>. The Schubert-Bornschein type of CSNB can be classified in the incomplete CSNB (icCSNB) and the complete CSNB (cCSNB) <sup>4</sup>. We will focus on the latter one in this study. Patients with cCSNB show an electronegative ERG, representing normal a-wave amplitudes with severely or absent b-waves under scotopic conditions, hence the denomination complete. Photopic responses are less altered<sup>2</sup>. More specifically, ON-responses are affected, while OFF- responses remain globally normal<sup>2</sup>. This ERG profile is consistent with a transmission defect between photoreceptors and ON-bipolar cells (ON-BCs). cCSNB is due to mutations in *NYX*<sup>5, 6</sup>, *TRPM1*<sup>7-9</sup>, *GRM6*<sup>10, 11</sup>, *GPR179*<sup>12, 13</sup> and *LRIT3*<sup>14</sup>. All code for proteins involved in the signaling cascade at the photoreceptor to ON-BC synapse. Mutations in *GRM6* are the third most prevalent cause of cCSNB<sup>2</sup>. *GRM6* codes for a metabotropic receptor that mediates glutamate synaptic transmission between photoreceptors and ON-BCs<sup>15</sup>. In the retina, mGluR6 is exclusively localized in ON-BCs<sup>16</sup>. In absence of light, glutamate released at the synaptic cleft activates mGluR6, which initiates the ON-BC signaling cascade <sup>17</sup> leading to the closure of the cation channel TRPM1<sup>18</sup>. In contrast, in response to light, less glutamate binds to mGluR6 leading to the opening of the TRPM1 channel<sup>19</sup>. Thus, ON-BCs are depolarized leading to the b-wave, which is severely

reduced or absent in cCSNB. Five mouse models with a *Grm6* defect have been described: *Grm6<sup>tm1Nak</sup>* (will be further referred as *Grm6<sup>-/-</sup>*), *nob3*, *nob4*, *nob7* and *nob8*<sup>20-24</sup>. Of those, four including *Grm6<sup>-/-</sup>* show a similar ERG-phenotype as patients with cCSNB under scotopic conditions, namely an absent b-wave, while the a-wave appears normal. Furthermore, in these four models, mGluR6 is abolished. It has been also described that mGluR6 is important for the proper localization of other proteins of the cascade such as regulatory of G protein signaling (RGS) proteins (RGS7, RGS11, Gβ5 and R9AP)<sup>25, 26</sup>, and TRPM1<sup>25</sup> at the dendritic tips of ON-BCs. The absence of TRPM1 at the dendritic tips of ON-BCs renders this channel non-functional<sup>25</sup>. The interdependence of GPR179 on mGluR6, important for the targeting and/or maintaining of the RGS proteins<sup>27</sup> has found to be model and condition-dependent<sup>28,29</sup>. Albeit the gross morphology of the retina in patients and mice lacking mGluR6 is not affected, detailed clinical examinations and morphological studies detected differences compared to unaffected retinas. Indeed, three patients harboring mutations in *GRM6* exhibited reduced retinal thickness in the extrafoveal region as revealed by SD-OCT measurements<sup>30</sup>. Furthermore, in mice lacking *Grm6*, invaginating dendrites of rod-bipolar-cells (RBCs) are larger and often contain ectopic ribbons while the number of invaginating dendrites of cone ON-BCs and ribbons decrease at the cone pedicles in the *Grm6<sup>-/-</sup>* mouse model<sup>31</sup>. Tummala and colleagues<sup>32</sup> showed that mGluR6 has also a role pre-synaptically as several presynaptic matrix-associated proteins are reduced at the rod-to-rod bipolar cell synapse in the same *Grm6<sup>-/-</sup>* model. To date, no treatment is available for cCSNB. Gene replacement strategy might be a suitable approach to treat cCSNB since it represents a stationary non-degenerative disorder and the genetics of this disorder is well characterized<sup>2</sup>. Two different approaches targeting two genes involved in cCSNB, *Nyx* and *Lrit3*, reported a partial restoration of the function upon protein relocalization in mouse models<sup>33, 34</sup>.

However, this partial rescue was mainly obtained at a very young age (P2 or P5) and only under scotopic condition. These two strategies aiming to treat cCSNB show the challenge to obtain a functional rescue in adult cCSNB mice. Our study aimed to restore the protein localization, along with its missing partners, and ERG phenotype, by treating P15 *Grm6*<sup>-/-</sup> <sup>20</sup> mice with an AAV-mediated intravitreal delivery of the transgene. In order to compare their efficacy, two different promoters were used: a *Grm6*-200bp/SV40 promoter, specifically targeting ON-BCs and a CAG promoter driving ubiquitous expression of the transgene. Transgene expression, protein localization and functional rescue were investigated.

## **Material and methods**

### Ethical statement

All animal procedures were performed according to the Council Directive 2010/63EU of the European Parliament and the Council of September 22, 2010, on the protection of animals used for scientific purposes, with the National Institutes of Health guidelines and with the ARVO Statement for the Use of Animals in Ophthalmic and Vision Research. They were approved by the French Minister of National Education, Superior Education and Research (authorization delivered on January 21, 2019).

### Intravitreal injections

Mice were anesthetized by isoflurane inhalation (5% in oxygen for induction and 2% for maintenance). Intravitreal injections were performed at 15 (P15) days of age. Pupils were dilated (0.5% mydriaticum) and a 33-gauge needle was passed through the sclera at the ora serrata level. 1  $\mu\text{L}$  of a viral stock solution at a concentration of  $1.6 \cdot 10^{13}$  vg/ml (CAG-*Grm6* construct) and  $5.8 \cdot 10^{13}$  vg/ml (GRM6-*Grm6*) maximum was injected directly in the vitreous cavity of eight *Grm6*<sup>-/-</sup> mice for each promoter. Viral vectors were produced as described in Macé *et al.*, 2015<sup>35</sup>.

### Immunolocalization studies

Animals were sacrificed by CO<sub>2</sub> inhalation followed by cervical dislocation. Eyes were removed and dissected to keep the posterior part of the eyes which were then fixed in ice-cold 4% paraformaldehyde for 20 minutes. Subsequently, eye-cups were washed in ice-cold PBS and cryoprotected by increasing concentrations of sucrose (ranging from 10% to 30%) in water and 0.24 M phosphate buffer for 1 hour at 4°C for 10% sucrose and 20% sucrose solutions and overnight at 4°C under agitation for the 30% sucrose solution. The eye-cups were then embedded in 7.5% gelatin - 10% sucrose and the blocks frozen at -40°C in

isopentane and kept at  $-80^{\circ}\text{C}$  until cutting. Sections of  $12\ \mu\text{m}$  were generated using a cryostat (MICROM HM 560™, ThermoFisher Scientific, Waltham, MA, USA) and mounted on glass slides (Superfrost® Plus, ThermoFisher Scientific). Mouse retina sections were blocked for 1 hour at room temperature in PBS1X 10% Donkey Serum (v/v), 0.1% Triton X-100. Primary antibodies and the dilutions used were: sheep anti-TRPM1 (1:500, Cao et al <sup>36</sup>), guinea pig anti-mGluR6 (1:15000; AP20134SU-N, Acris, Herford, Germany), rabbit anti-Gβ5 (1:500, C16068, Antibodies Online), goat anti-RGS11 (1:300, sc-9725, Santa-Cruz, Dallas, USA), rabbit anti-RGS7 (1:100, Cao et al, <sup>37</sup>) or mouse anti-GPR179 (1:200, AB0887-YOM, Primm, Cambridge, MA, USA). The sections were incubated with primary antibodies diluted in PBS1X 2% Donkey Serum, 0.1% Triton X-100 for 1 hour at room temperature. After washes with PBS1X, 0.1% Triton X-100, the sections were incubated with anti-human, anti-guinea pig, anti-goat, anti-rabbit or anti-mouse secondary antibodies or peanut agglutinin (PNA-488, L21409, Waltham, MA, USA) coupled with Alexa Fluor 488, 594 or Cy3 (Jackson ImmunoResearch) along with 4',6-diamidino-2-phenylindole (DAPI), all used at 1:1000, for 0.5 hours at room temperature. Subsequently, the sections were cover-slipped with mounting medium (Mowiol, Merck Millipore, Billerica, MA, USA). Fluorescence images retinal sections were acquired with a confocal microscope (FV1000, Olympus). Images for figures were handled with the Image J software (ImageJ Software).

### ERG recordings

ERG recordings were performed in accordance with the description in Neullé *et al.*, 2014 <sup>38</sup>. All scotopic ERG were made first using six increasing light-intensity of flashes ranging from 0.003 to 30.0  $\text{cd}\cdot\text{s}/\text{m}^2$ . To ensure a saturation of rod photoreceptors and the recording of cone-driven responses, a 10-minutes light-adaptation step at  $20\text{cd}/\text{m}^2$  was done. All data were analyzed with GraphPad Prism v.6 (GraphPad Software, La Jolla, CA, USA).

## Results

Herein, to rescue the phenotype in the *Grm6*<sup>-/-</sup> mouse model, two different constructs were designed using two different promoters. To drive expression of the transgene specifically to ON-bipolar cells, the *Grm6* promoter was used<sup>35</sup>. To drive ubiquitous expression of the transgene throughout the retina the CAG promoter was used<sup>39</sup>. These two constructs were encapsidated in the AAV2-7m8 serotype<sup>39</sup> and will be referred as GRM6-*Grm6* or CAG-*Grm6*.

### mGluR6 relocates at the dendritic tips of ON-BCs following treatment

In *Grm6*<sup>-/-</sup> mice, mGluR6 production is completely abolished in the OPL<sup>20</sup> (Figure 1A). Its localization at the dendritic tips of ON-BCs is essential to ensure a proper transmission of the visual information between photoreceptors and ON-BCs. The relocation of mGluR6 at the dendritic tips of ON-BCs five months following treatment was investigated through immunolocalization studies. *Grm6*<sup>-/-</sup>-GRM6-*Grm6* retinas treated at P15 displayed areas where mGluR6 was present in the OPL which was absent in untreated *Grm6*<sup>-/-</sup> retinas (Figure 1A, n=8). We also noticed that ON-BCs bodies were sometimes stained (Figure 1B, stars). However, mGluR6 staining was only present in small areas of the retina (~2.5% of the OPL presented an mGluR6 staining, Figure 2C, red arrows). Similarly, *Grm6*<sup>-/-</sup>-CAG-*Grm6* retinas treated at P15 displayed mGluR6 staining in the OPL (Figure 1A), which seemed to be stronger and more homogeneously distributed (Figures 1B and 1C) compared to *Grm6*<sup>-/-</sup>-GRM6-*Grm6* treated retinas (~11% of the OPL presented an mGluR6 staining, Figure 1C, red arrows). In addition, for the latter construct a staining was also noted in some areas in the inner plexiform layer (IPL) (Figure 1B). Furthermore, this mGluR6 staining seemed more diffuse in several areas (Figure 1B). Using either CAG-*Grm6* or GRM6-*Grm6* constructs, mGluR6 staining was absent at the dendritic tips of cone ON-BCs.

### Signaling partners of mGluR6 are relocalized at the dendritic tips of ON-BCs

It was previously described that several molecules involved in the signaling cascade of ON-BCs were impacted by the absence of mGluR6<sup>2</sup>. This is consistent with our finding, showing reduced or abolished staining of molecules of the same cascade including TRPM1, RGS7, RGS11 and Gβ5 (Figure 2 and 3, second column). Although different observation of the dependence of GPR179 on mGluR6<sup>28, 29</sup> were described, herein we observed a severe decrease in the localization of GPR179 at the dendritic tips of ON-BCs in *Grm6*<sup>-/-</sup> mice (Figure 3). *Grm6*<sup>-/-</sup>-GRM6-*Grm6* and *Grm6*<sup>-/-</sup>-CAG-*Grm6* retinas revealed restoration of TRPM1, Gβ5 and GPR179 localization at the dendritic tips of ON-BCs after treatment (Figure 2 and 3). In addition, a restoration of the localization of RGS7 and RGS11 was noted, which was more evident in GRM6-*Grm6* than in CAG-*Grm6* treated retinas (Figure 3).

### mGluR6 protein restoration does not induce a functional rescue

Due to the disruption of the signal transmission between photoreceptors and ON-BCs in the *Grm6*<sup>-/-</sup> mouse model, the b-wave is abolished in both scotopic and photopic conditions (Figure 4). In order to study the functional restoration of the phenotype ERG-measurements were performed on P15-treated mice at two time-points: two- and four-months post-injection (n= 8). At both time points, none of the treated animals revealed restoration of the b-wave neither at scotopic nor photopic conditions using intravitreal injections of either, CAG-*Grm6* and or GRM6-*Grm6* treated mice (Figure 4).

## Discussion

GRM6 is the first element of the signaling cascade at the dendritic tips of ON-BCs, responsible for the transmission of the signal from photoreceptors to ON-BCs. When *GRM6* is mutated it leads to cCSNB. Patients displaying cCSNB have night blindness, high myopia, nystagmus and sometimes strabismus, which influence the quality of life during day and night-time. The disease can be correctly diagnosed by measuring the electroretinogram (ERG). Patients as well as mice with this gene defect show loss of mGluR6 function and reveal an electronegative ERG in which the a-wave is preserved while the b-wave is absent<sup>20, 40</sup>. In addition, mice lacking *Grm6* are characterized through the absence of the respective protein, and several other proteins of the same cascade being mislocalized, abolished or reduced at the dendritic tips of ON-BCs: GPR179 and TRPM1 are reduced along with the RGS proteins (Gβ5, RGS7 and RGS11) being abolished<sup>26</sup>. We investigated the localization of these proteins in *Grm6*<sup>-/-</sup> mice and compared our findings, with reported studies. Herein we showed that, in *Grm6*<sup>-/-</sup> mice GPR179 localization at the dendritic tips of ON-BCs is dramatically reduced but still present. Ray and co-workers reported no difference in GPR179 localization in *Grm6*<sup>-/-</sup> mice upon immunolocalization studies but using western blot analysis estimated a decrease in GPR179 of ~50% in *Grm6*<sup>-/-</sup> retinas<sup>29</sup>. In contrast, Orlandi and co-workers reported similar than us a dramatic reduction of GPR179 at the dendritic tips of ON-BCs in a mouse model lacking *Grm6* (*nob3*). Indeed, in contrast to Ray and co-workers the group by Orlandi and us used the same antibody. Further investigations need to be performed to explain these different observations. However, since GPR179 is only reduced but not completely abolished at the dendritic tips of ON-BCs in *Grm6*<sup>-/-</sup> mice, it indicates that mGluR6 plays a major role in the proper localization of GPR179 at the dendritic tips but is not essential to this process.

To date, for most IRDs, treatment is unavailable. However, a gene addition approach mediated by AAV for Leber Congenital Amaurosis (LCA) was validated by the Food and Drug Administration in the US three years ago, paving the way of treatment of IRDs by gene therapy<sup>41-44</sup>. CSNB is a rare heterogenous group of retinal disorders and yet incurable<sup>2</sup>. Two gene therapy approaches for cCSNB have been reported so far, one targeting *Nyx*<sup>33</sup> and the other one *Lrit3*<sup>34</sup>. In both strategies, the wild-type copy of the gene was delivered in newborn (P2 or P5) and adult (P30 or P35) CSNB mice. A partial rescue of the scotopic ERG was obtained mainly in treated newborn mice, under scotopic conditions<sup>33, 34</sup>. To our knowledge, a gene therapy approach to rescue the phenotype due to the *GRM6*-gene defect is unavailable. Mutations in *GRM6* were found to be the third most prevalent gene defect causing cCSNB<sup>2</sup>. To restore the phenotype of mice lacking mGluR6, a combination of the AAV2.7m8 capsid along with either the *GRM6*-200bp/SV40 promoter to drive the expression of *Grm6*<sup>35</sup> (referred as *GRM6-Grm6*) or a CAG promoter<sup>39</sup> (*CAG-Grm6*) were chosen. Although the functional restoration stayed out, intravitreal injections of adult mice revealed relocalization of mGluR6 and its signaling partners. Furthermore, the specificity of the *GRM6-Grm6* construct was higher than the *CAG-Grm6* combination, with however a milder transduction rate.

Studying the expression of the transgene by RNA *in situ* hybridization would explain whether the low production of *GRM6* in the treated mice is due to a mild transduction or a problem of the ON-BCs in producing the protein from the transgene. The lack of functional rescue and relatively low transduction efficiency of our approach may be due to the size and structure of mGluR6. Substantial limitation of AAV vectors is their small packaging capacity that is generally considered to be <5 kb<sup>45</sup>. Our constructs were 3.5 kb and 3.8 kb in size for the *GRM6-Grm6* and for the *CAG-Grm6* constructs, respectively of which the coding sequence of

*Grm6* is 2.6 kb. Together, these constructs are in the range <5 kb so the encapsidation of those should not pose any problem. Successful gene therapies with partial functional restoration for nyctalopin<sup>33</sup> and LRIT3<sup>34</sup> (Varin et al., submitted) using similar vectors focused on even smaller genes (1.4 and 2 kb respectively) encoding small and structurally simpler proteins than mGluR6. Perhaps, it is still more complicating to produce slightly larger proteins, like mGluR6 composed of seven transmembrane domains, than smaller molecules. In addition, the constructs used may need to be improved. Of course, using the full promoter and intronic regions enhancing and controlling the expression and protein production would most likely improve the efficacy of the treatment<sup>46</sup>. However, the size of such a transgene is too large to be encapsidated by our used approach. Oversized AAV-vectors encapsidating up to 9 kb of transgene were shown to be not validated for clinical use since gene fragmentation occurs. As an alternative to the oversized AAV approach, different research groups have tested the use of dual and triple AAV vector systems showing, however here as well very low levels of protein expression<sup>47</sup>. Recently, Lu and co-workers tested different modulations of the *Grm6* promoter in order to increase its efficiency and finally described two promoters with a high specificity and a higher expression of the transgene than our used GRM6-200bp/SV40 promoter<sup>48</sup> by using the endogenous promoter of *Grm6*. The added sequence is only ~300 bp larger compared to our GRM6-*Grm6* construct and thus could be easily used for a gene therapy approach to restore the mGluR6 phenotype. Compared with the construct used by us, the fluorescence intensity of mCherry under the control of this new promoter was ~5 times higher<sup>48</sup>. However, the number of transduced cells was not significantly improved with this promoter compared to ours. It remains questionable if this new promoter would be enough to increase the transduction efficiency to obtain a homogeneous protein immunolocalization and functional rescue. This shows that efficient

transduction of ON-BCs with no off-target is still difficult to obtain. In order to overcome this issue, other improved AAV-promoter combinations could be tested.

To test the efficiency of those different promoters, fluorescent proteins such as GFP or mCherry are often used<sup>35, 48</sup>. However, these promoters used in combination with these genes will localize the respective protein in ON-BCs but not specifically at the dendritic tips of ON-BCs where mGluR6 should be localized<sup>35, 48</sup>. Thus, the obtained transduction efficiency of those vectors may not indicate if trafficking to the dendritic tips of ON-BCs can be achieved. It has been previously reported that the targeting of transmembrane proteins to neuronal dendrites was myosin-dependent<sup>49</sup>. Therefore, we tried to improve this trafficking to the dendritic tips by adding a myosin-binding domain (MBD) to *Grm6*. However, this did not result on further improvement concerning the transduction efficiency nor restoration of the phenotype (data not shown). We also decided to wait several months after injection to record ERGs and perform immunolocalization studies since it has been shown that the peak of transgene expression is at 6-to-8 weeks after injection<sup>50</sup>. However, even four months after treatment, the phenotype of treated animals could not be restored.

As previously described, proteins involved in cCSNB also have a role in synapse formation and/or maintenance. Indeed, in *Lrit3*<sup>-/-</sup> mice, a decreased number of invaginating contacts made by cone ON-BCs in the cone pedicle and a striking decrease in the number of triads<sup>51</sup> was observed. Normal cone pedicles were also noted indicating that LRIT3 is not essential for the natural formation of the cone-to-cone BC synapse but plays a major role in this process<sup>51</sup>. The same observation was made in *Gβ5*<sup>-/-</sup> mice where there is a significant reduction of the number of triads in the OPL of these mice<sup>52</sup>. Finally, it was also described that mGluR6 seems to play a role at the photoreceptor to bipolar cell synapse. Indeed,

invaginating dendrites of RBCs are larger and often contain ectopic ribbons while the number of invaginating dendrites of cone ON-BCs and ribbons decrease at the cone pedicles in the *Grm6*<sup>-/-</sup> mouse model<sup>31, 53</sup>. In conclusion, there are strong indications that proteins at the synapse between photoreceptors and ON-BCs also have a structural role. Similar, structural alterations were noted in patients<sup>30</sup>. This could explain the lack of functional rescue in our *Grm6*<sup>-/-</sup> treated mice, as applying such treatment in adult mice, when the synapse is fully formed, might not restore the signal transmission between photoreceptors and ON-BCs if the synapse is constitutively diminished. In addition, it has been pointed out that mGluR6 was detectable in the rat retina 6-to-8 days post-natal, dispersely distributed in the somata and dendrites of the INL cells<sup>54</sup>. It might be essential to provide *Grm6* as early as P6 to ensure a correct synaptogenesis and later a functional restoration.

Finally, regulatory proteins that are abolished at the dendritic tips of ON-BCs (RGS7, RGS11 and Gβ5) when mGluR6 is absent were back at the dendritic tips when mGluR6 was observable at the OPL when the retina was treated with GRM6-*Grm6* construct but it was less evident using the CAG-*Grm6* construct. This might partially explain why even if the transduction rate was increased by using a CAG promoter, still no functional rescue was observed in these treated mice as RGS11 and RGS7 are involved in the sensitivity and time-course of light-evoked responses<sup>37</sup>.

We showed here for the first time restoration of mGluR6 localization at the dendritic tips of ON-BCs following a gene addition strategy in P15-treated *Grm6*<sup>-/-</sup> mice. This restoration led to the relocalization of other partners of the cascade such as TRPM1, GPR179, RGS7, RGS11 and Gβ5. However, functional rescue after treatment as measured by ERG failed to appear. These findings give hope that by improving the vector-promoter combination the efficiency

of ON-BCs transduction will be improved and cCSNB due to mutations in *GRM6* could be treated.

## **Acknowledgments**

The authors are grateful to the platform of animal housing and imaging at the Institut de la Vision and more specifically Julie Degradin, Manuel Simonutti, Quenol Cesar, Marie-Laure Niepon, Stéphane Fouquet. We thank Kirill Martemyanov, Yan Cao and Anna Verschueren for the fruitful discussions. This work was supported by Retina France (CZ), by the French Muscular Dystrophy Association (AFM-Téléthon) (CZ), by UNADEV-Aviesan call 2015 (CZ), Fondation Voir et Entendre (CZ), Prix Dalloz for “la recherche en ophtalmologie” (CZ), Fondation pour la Recherche Médicale (FRM DVS20131228918) in partnership with Fondation Roland Bailly (CZ), Fédération des Aveugles et Amblyopes de France (MN), Ville de Paris and Région Ile de France, LABEX LIFESENSES (reference ANR-10-LABX-65) supported by French state funds managed by the Agence Nationale de la Recherche within the Investissements d’Avenir programme (ANR11-IDEX-0004-0), with the support of the Programme Investissements d’Avenir IHU FOReSIGHT (ANR-18-IAHU-01) and the Ministère de l’enseignement supérieur et de la recherche (JV). The funders had no role in study design, data collection, analysis and interpretation, decision to publish, or preparation of the manuscript. DD is an inventor on a patent of adeno-associated virus virions with variant capsid and methods of use thereof with royalties paid to Avalanche Biotech (WO2012145601 A2).

## Figure legends

### Figure 1: GRM6 localization after treatment

A) Representative confocal images of cross-sections centered on the OPL of *Grm6<sup>+/+</sup>*, *Grm6<sup>-/-</sup>*, *Grm6<sup>-/-</sup>-GRM6-Grm6* and *Grm6<sup>-/-</sup>-CAG-Grm6* retinas stained with an antibody against GRM6 (red). Scale bar, 10  $\mu$ m. B) Specific features of *Grm6<sup>-/-</sup>-GRM6-Grm6* (top row, asterisks represent putative somas of ON-BCs) and *Grm6<sup>-/-</sup>-CAG-Grm6* (bottom row, diffuse staining) retinas. ONL: outer nuclear layer, OPL: outer plexiform layer, INL: inner nuclear layer, IPL: inner plexiform layer, GCL: ganglion cell layer. Scale bar, 10 $\mu$ m. C) Representative confocal images of cross-sections of the entire retina of *Grm6<sup>-/-</sup>-GRM6-Grm6* and *Grm6<sup>-/-</sup>-CAG-Grm6* treated mice. Red arrows point GRM6 staining. Scale bar, 100 $\mu$ m.

### Figure 2: Localization of TRPM1 after treatment

Representative confocal images of cross-sections centered on the OPL of *Grm6<sup>+/+</sup>*, *Grm6<sup>-/-</sup>*, *Grm6<sup>-/-</sup>-GRM6-Grm6* and *Grm6<sup>-/-</sup>-CAG-Grm6* retinas co-stained (yellow, merge) with an antibody against GRM6 (red) and TRPM1 (green). Scale bar, 10  $\mu$ m.

### Figure 3: Localization of proteins of the ON-BCs signaling cascade after treatment

Representative confocal images of cross-sections centered on the OPL of *Grm6<sup>+/+</sup>*, *Grm6<sup>-/-</sup>*, *Grm6<sup>-/-</sup>-GRM6-Grm6* and *Grm6<sup>-/-</sup>-CAG-Grm6* retinas co-stained (yellow, merge) with an antibody against GRM6 (red) and either GPR179, RGS11, RGS7 or G $\beta$ 5 (green). Scale bar, 10  $\mu$ m.

### Figure 4: ERG recordings

A) Representative scotopic ERG traces at 2 months post-injection for *Grm6<sup>+/+</sup>* (green line), *Grm6<sup>-/-</sup>* (red line), *Grm6<sup>-/-</sup>-GRM6-Grm6* (black line) and *Grm6<sup>-/-</sup>-CAG-Grm6* (blue line) at a

flash intensity of 0.03 cd.s/m<sup>2</sup> under scotopic conditions (left) and of 3.0 cd.s/m<sup>2</sup> under photopic conditions (right). B) Representative scotopic ERG traces at 4 months post-injection for a flash intensity of 0.03 cd.s/m<sup>2</sup> (left) and photopic ERG traces for a flash intensity of 3.0 cd.s/m<sup>2</sup> (right).

## Bibliography

1. Schubert, G, and Bornschein, H (1952). Analysis of the human electroretinogram. *Ophthalmologica* **123**: 396-413.
2. Zeitz, C, Robson, AG, and Audo, I (2015). Congenital stationary night blindness: an analysis and update of genotype-phenotype correlations and pathogenic mechanisms. *Progress in retinal and eye research* **45**: 58-110.
3. Riggs, LA (1954). Electroretinography in cases of night blindness. *American journal of ophthalmology* **38**: 70-78.
4. Miyake, Y, Yagasaki, K, Horiguchi, M, Kawase, Y, and Kanda, T (1986). Congenital stationary night blindness with negative electroretinogram. A new classification. *Archives of ophthalmology* **104**: 1013-1020.
5. Pusch, CM, Zeitz, C, Brandau, O, Pesch, K, Achatz, H, Feil, S, *et al.* (2000). The complete form of X-linked congenital stationary night blindness is caused by mutations in a gene encoding a leucine-rich repeat protein. *Nature genetics* **26**: 324-327.
6. Bech-Hansen, NT, Naylor, MJ, Maybaum, TA, Sparkes, RL, Koop, B, Birch, DG, *et al.* (2000). Mutations in NYX, encoding the leucine-rich proteoglycan nyctalopin, cause X-linked complete congenital stationary night blindness. *Nature genetics* **26**: 319-323.
7. Audo, I, Kohl, S, Leroy, BP, Munier, FL, Guillonneau, X, Mohand-Said, S, *et al.* (2009). TRPM1 is mutated in patients with autosomal-recessive complete congenital stationary night blindness. *American journal of human genetics* **85**: 720-729.
8. van Genderen, MM, Bijveld, MM, Claassen, YB, Florijn, RJ, Pearing, JN, Meire, FM, *et al.* (2009). Mutations in TRPM1 are a common cause of complete congenital stationary night blindness. *American journal of human genetics* **85**: 730-736.
9. Li, Z, Sergouniotis, PI, Michaelides, M, Mackay, DS, Wright, GA, Devery, S, *et al.* (2009). Recessive mutations of the gene TRPM1 abrogate ON bipolar cell function and cause complete congenital stationary night blindness in humans. *American journal of human genetics* **85**: 711-719.
10. Zeitz, C, van Genderen, M, Neidhardt, J, Luhmann, UF, Hoeben, F, Forster, U, *et al.* (2005). Mutations in GRM6 cause autosomal recessive congenital stationary night blindness with a distinctive scotopic 15-Hz flicker electroretinogram. *Investigative ophthalmology & visual science* **46**: 4328-4335.
11. Dryja, TP, McGee, TL, Berson, EL, Fishman, GA, Sandberg, MA, Alexander, KR, *et al.* (2005). Night blindness and abnormal cone electroretinogram ON responses in patients with mutations in the GRM6 gene encoding mGluR6. *Proceedings of the National Academy of Sciences of the United States of America* **102**: 4884-4889.
12. Audo, I, Bujakowska, K, Orhan, E, Poloschek, CM, Defoort-Dhellemmes, S, Drumare, I, *et al.* (2012). Whole-exome sequencing identifies mutations in GPR179 leading to autosomal-recessive complete congenital stationary night blindness. *American journal of human genetics* **90**: 321-330.
13. Peachey, NS, Ray, TA, Florijn, R, Rowe, LB, Sjoerdsma, T, Contreras-Alcantara, S, *et al.* (2012). GPR179 is required for depolarizing bipolar cell function and is mutated in autosomal-recessive complete congenital stationary night blindness. *American journal of human genetics* **90**: 331-339.
14. Zeitz, C, Jacobson, SG, Hamel, CP, Bujakowska, K, Neuville, M, Orhan, E, *et al.* (2013). Whole-exome sequencing identifies LRIT3 mutations as a cause of autosomal-recessive complete congenital stationary night blindness. *American journal of human genetics* **92**: 67-75.
15. Nakajima, K, Saito, T, Tamura, A, Suzuki, M, Nakano, T, Adachi, M, *et al.* (1993). Cholesterol in remnant-like lipoproteins in human serum using monoclonal anti apo B-100 and anti apo A-I immunoaffinity mixed gels. *Clinica chimica acta; international journal of clinical chemistry* **223**: 53-71.

16. Nakajima, Y, Iwakabe, H, Akazawa, C, Nawa, H, Shigemoto, R, Mizuno, N, *et al.* (1993). Molecular characterization of a novel retinal metabotropic glutamate receptor mGluR6 with a high agonist selectivity for L-2-amino-4-phosphonobutyrate. *The Journal of biological chemistry* **268**: 11868-11873.
17. Nawy, S (1999). The metabotropic receptor mGluR6 may signal through G(o), but not phosphodiesterase, in retinal bipolar cells. *The Journal of neuroscience : the official journal of the Society for Neuroscience* **19**: 2938-2944.
18. Morgans, CW, Brown, RL, and Duvoisin, RM (2010). TRPM1: the endpoint of the mGluR6 signal transduction cascade in retinal ON-bipolar cells. *BioEssays : news and reviews in molecular, cellular and developmental biology* **32**: 609-614.
19. Morgans, CW, Zhang, J, Jeffrey, BG, Nelson, SM, Burke, NS, Duvoisin, RM, *et al.* (2009). TRPM1 is required for the depolarizing light response in retinal ON-bipolar cells. *Proceedings of the National Academy of Sciences of the United States of America* **106**: 19174-19178.
20. Masu, M, Iwakabe, H, Tagawa, Y, Miyoshi, T, Yamashita, M, Fukuda, Y, *et al.* (1995). Specific deficit of the ON response in visual transmission by targeted disruption of the mGluR6 gene. *Cell* **80**: 757-765.
21. Maddox, DM, Vessey, KA, Yarbrough, GL, Invergo, BM, Cantrell, DR, Inayat, S, *et al.* (2008). Allelic variance between GRM6 mutants, Grm6nob3 and Grm6nob4 results in differences in retinal ganglion cell visual responses. *The Journal of physiology* **586**: 4409-4424.
22. Pinto, LH, Vitaterna, MH, Shimomura, K, Siepka, SM, Balannik, V, McDearmon, EL, *et al.* (2007). Generation, identification and functional characterization of the nob4 mutation of Grm6 in the mouse. *Visual neuroscience* **24**: 111-123.
23. Qian, H, Ji, R, Gregg, RG, and Peachey, NS (2015). Identification of a new mutant allele, Grm6(nob7), for complete congenital stationary night blindness. *Visual neuroscience* **32**: E004.
24. Peachey, NS, Hasan, N, FitzMaurice, B, Burrill, S, Pangeni, G, Karst, SY, *et al.* (2017). A missense mutation in Grm6 reduces but does not eliminate mGluR6 expression or rod depolarizing bipolar cell function. *Journal of neurophysiology* **118**: 845-854.
25. Xu, Y, Dhingra, A, Fina, ME, Koike, C, Furukawa, T, and Vardi, N (2012). mGluR6 deletion renders the TRPM1 channel in retina inactive. *Journal of neurophysiology* **107**: 948-957.
26. Gregg, RGR, T. A.; Hasan, N.; McCall, M. A.; Peachey N. S. (2014). Interdependence Among Members of the mGluR6 G-protein Mediated Signalplex of Retinal Depolarizing Bipolar Cells. In: Springer (ed). *G Protein Signaling Mechanisms in the Retina*. pp 67-79.
27. Orlandi, C, Posokhova, E, Masuho, I, Ray, TA, Hasan, N, Gregg, RG, *et al.* (2012). GPR158/179 regulate G protein signaling by controlling localization and activity of the RGS7 complexes. *The Journal of cell biology* **197**: 711-719.
28. Orlandi, C, Cao, Y, and Martemyanov, KA (2013). Orphan receptor GPR179 forms macromolecular complexes with components of metabotropic signaling cascade in retina ON-bipolar neurons. *Investigative ophthalmology & visual science* **54**: 7153-7161.
29. Ray, TA, Heath, KM, Hasan, N, Noel, JM, Samuels, IS, Martemyanov, KA, *et al.* (2014). GPR179 is required for high sensitivity of the mGluR6 signaling cascade in depolarizing bipolar cells. *The Journal of neuroscience : the official journal of the Society for Neuroscience* **34**: 6334-6343.
30. Godara, P, Cooper, RF, Sergouniotis, PI, Diederichs, MA, Streb, MR, Genead, MA, *et al.* (2012). Assessing retinal structure in complete congenital stationary night blindness and Oguchi disease. *American journal of ophthalmology* **154**: 987-1001 e1001.
31. Tsukamoto, Y, and Omi, N (2014). Effects of mGluR6-deficiency on photoreceptor ribbon synapse formation: comparison of electron microscopic analysis of serial sections with random sections. *Visual neuroscience* **31**: 39-46.
32. Tummala, SR, Dhingra, A, Fina, ME, Li, JJ, Ramakrishnan, H, and Vardi, N (2016). Lack of mGluR6-related cascade elements leads to retrograde trans-synaptic effects on rod

- photoreceptor synapses via matrix-associated proteins. *The European journal of neuroscience* **43**: 1509-1522.
33. Scalabrino, ML, Boye, SL, Fransen, KM, Noel, JM, Dyka, FM, Min, SH, *et al.* (2015). Intravitreal delivery of a novel AAV vector targets ON bipolar cells and restores visual function in a mouse model of complete congenital stationary night blindness. *Human molecular genetics* **24**: 6229-6239.
  34. Hasan, N, Pangeni, G, Cobb, CA, Ray, TA, Nettesheim, ER, Ertel, KJ, *et al.* (2019). Presynaptic Expression of LRIT3 Transsynaptically Organizes the Postsynaptic Glutamate Signaling Complex Containing TRPM1. *Cell reports* **27**: 3107-3116 e3103.
  35. Mace, E, Caplette, R, Marre, O, Sengupta, A, Chaffiol, A, Barbe, P, *et al.* (2015). Targeting channelrhodopsin-2 to ON-bipolar cells with vitreally administered AAV Restores ON and OFF visual responses in blind mice. *Molecular therapy : the journal of the American Society of Gene Therapy* **23**: 7-16.
  36. Cao, Y, Posokhova, E, and Martemyanov, KA (2011). TRPM1 forms complexes with nyctalopin in vivo and accumulates in postsynaptic compartment of ON-bipolar neurons in mGluR6-dependent manner. *The Journal of neuroscience : the official journal of the Society for Neuroscience* **31**: 11521-11526.
  37. Cao, Y, Pahlberg, J, Sarria, I, Kamasawa, N, Sampath, AP, and Martemyanov, KA (2012). Regulators of G protein signaling RGS7 and RGS11 determine the onset of the light response in ON bipolar neurons. *Proceedings of the National Academy of Sciences of the United States of America* **109**: 7905-7910.
  38. Neuille, M, El Shamieh, S, Orhan, E, Michiels, C, Antonio, A, Lancelot, ME, *et al.* (2014). Lrit3 deficient mouse (nob6): a novel model of complete congenital stationary night blindness (cCSNB). *PLoS one* **9**: e90342.
  39. Dalkara, D, Byrne, LC, Klimczak, RR, Visel, M, Yin, L, Merigan, WH, *et al.* (2013). In vivo-directed evolution of a new adeno-associated virus for therapeutic outer retinal gene delivery from the vitreous. *Science translational medicine* **5**: 189ra176.
  40. Zeitz, C, Forster, U, Neidhardt, J, Feil, S, Kalin, S, Leifert, D, *et al.* (2007). Night blindness-associated mutations in the ligand-binding, cysteine-rich, and intracellular domains of the metabotropic glutamate receptor 6 abolish protein trafficking. *Human mutation* **28**: 771-780.
  41. Leber, T (1869). Uber retinitis pigmentosa und angeborene amaurose. *Graefe's archive for clinical and experimental ophthalmology = Albrecht von Graefes Archiv fur klinische und experimentelle Ophthalmologie* **15**: 1-25.
  42. Bainbridge, JW, Smith, AJ, Barker, SS, Robbie, S, Henderson, R, Balaggan, K, *et al.* (2008). Effect of gene therapy on visual function in Leber's congenital amaurosis. *The New England journal of medicine* **358**: 2231-2239.
  43. Maguire, AM, Simonelli, F, Pierce, EA, Pugh, EN, Jr., Mingozzi, F, Bennicelli, J, *et al.* (2008). Safety and efficacy of gene transfer for Leber's congenital amaurosis. *The New England journal of medicine* **358**: 2240-2248.
  44. Cideciyan, AV, Aleman, TS, Boye, SL, Schwartz, SB, Kaushal, S, Roman, AJ, *et al.* (2008). Human gene therapy for RPE65 isomerase deficiency activates the retinoid cycle of vision but with slow rod kinetics. *Proceedings of the National Academy of Sciences of the United States of America* **105**: 15112-15117.
  45. Wu, Z, Yang, H, and Colosi, P (2010). Effect of genome size on AAV vector packaging. *Molecular therapy : the journal of the American Society of Gene Therapy* **18**: 80-86.
  46. Powell, SK, Rivera-Soto, R, and Gray, SJ (2015). Viral expression cassette elements to enhance transgene target specificity and expression in gene therapy. *Discov Med* **19**: 49-57.
  47. French, LSM, C. B.; Chen F.K.; Carvalho L. S. (2020). A Review of Gene, Drug and Cell-Based Therapies for Usher Syndrome. *Front Cell Neurosci* **14**.
  48. Lu, Q, Ganjawala, TH, Ivanova, E, Cheng, JG, Troilo, D, and Pan, ZH (2016). AAV-mediated transduction and targeting of retinal bipolar cells with improved mGluR6 promoters in rodents and primates. *Gene therapy* **23**: 680-689.

49. Lewis, TL, Jr., Mao, T, Svoboda, K, and Arnold, DB (2009). Myosin-dependent targeting of transmembrane proteins to neuronal dendrites. *Nature neuroscience* **12**: 568-576.
50. Natkunarajah, M, Trittibach, P, McIntosh, J, Duran, Y, Barker, SE, Smith, AJ, *et al.* (2008). Assessment of ocular transduction using single-stranded and self-complementary recombinant adeno-associated virus serotype 2/8. *Gene therapy* **15**: 463-467.
51. Neuille, M, Cao, Y, Caplette, R, Guerrero-Given, D, Thomas, C, Kamasawa, N, *et al.* (2017). LRIT3 Differentially Affects Connectivity and Synaptic Transmission of Cones to ON- and OFF-Bipolar Cells. *Investigative ophthalmology & visual science* **58**: 1768-1778.
52. Rao, A, Dallman, R, Henderson, S, and Chen, CK (2007). Gbeta5 is required for normal light responses and morphology of retinal ON-bipolar cells. *The Journal of neuroscience : the official journal of the Society for Neuroscience* **27**: 14199-14204.
53. Ishii, M, Morigiwa, K, Takao, M, Nakanishi, S, Fukuda, Y, Mimura, O, *et al.* (2009). Ectopic synaptic ribbons in dendrites of mouse retinal ON- and OFF-bipolar cells. *Cell and tissue research* **338**: 355-375.
54. Nomura, A, Shigemoto, R, Nakamura, Y, Okamoto, N, Mizuno, N, and Nakanishi, S (1994). Developmentally regulated postsynaptic localization of a metabotropic glutamate receptor in rat rod bipolar cells. *Cell* **77**: 361-369.

**Figure 1**

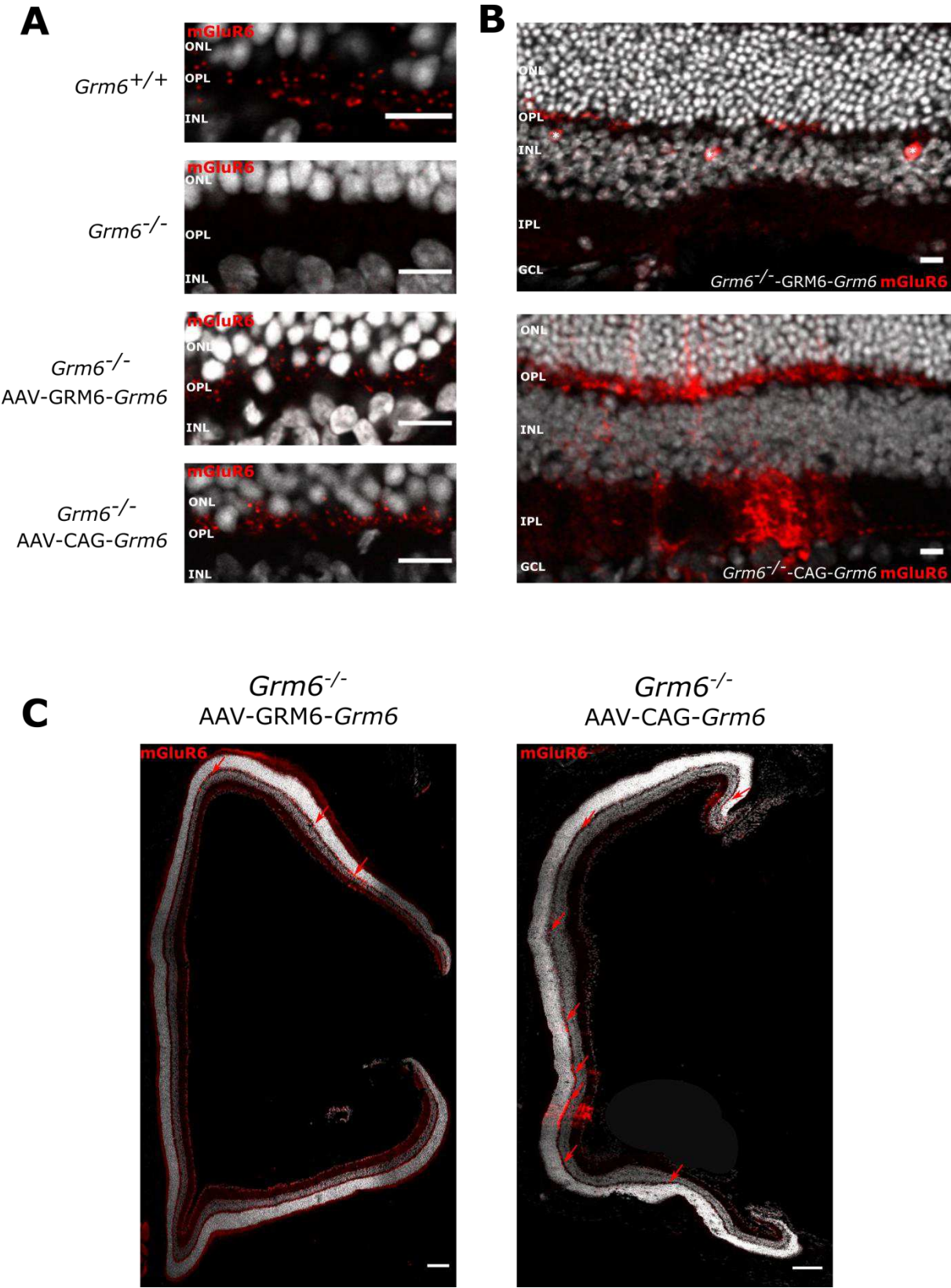
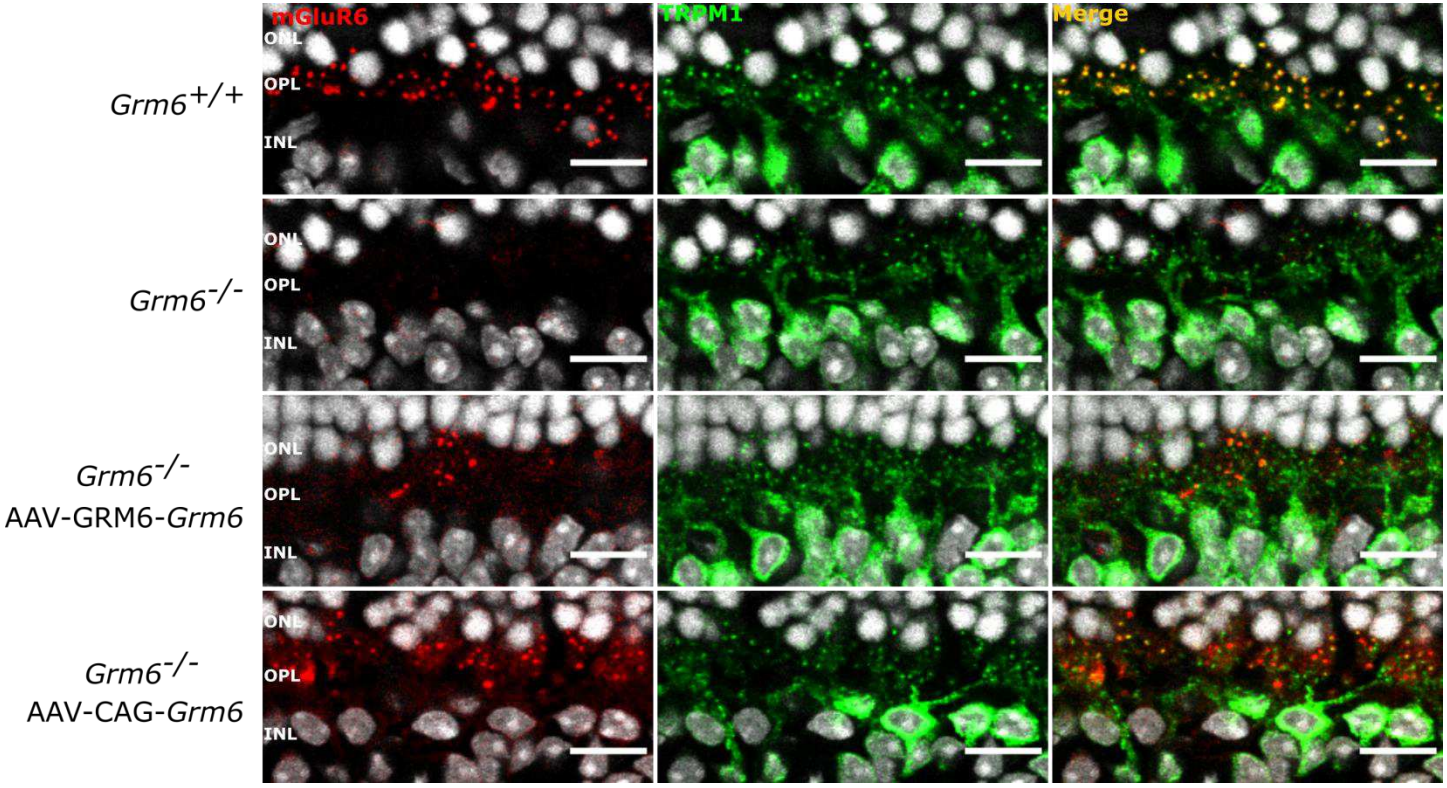


Figure 2



**Figure 3**

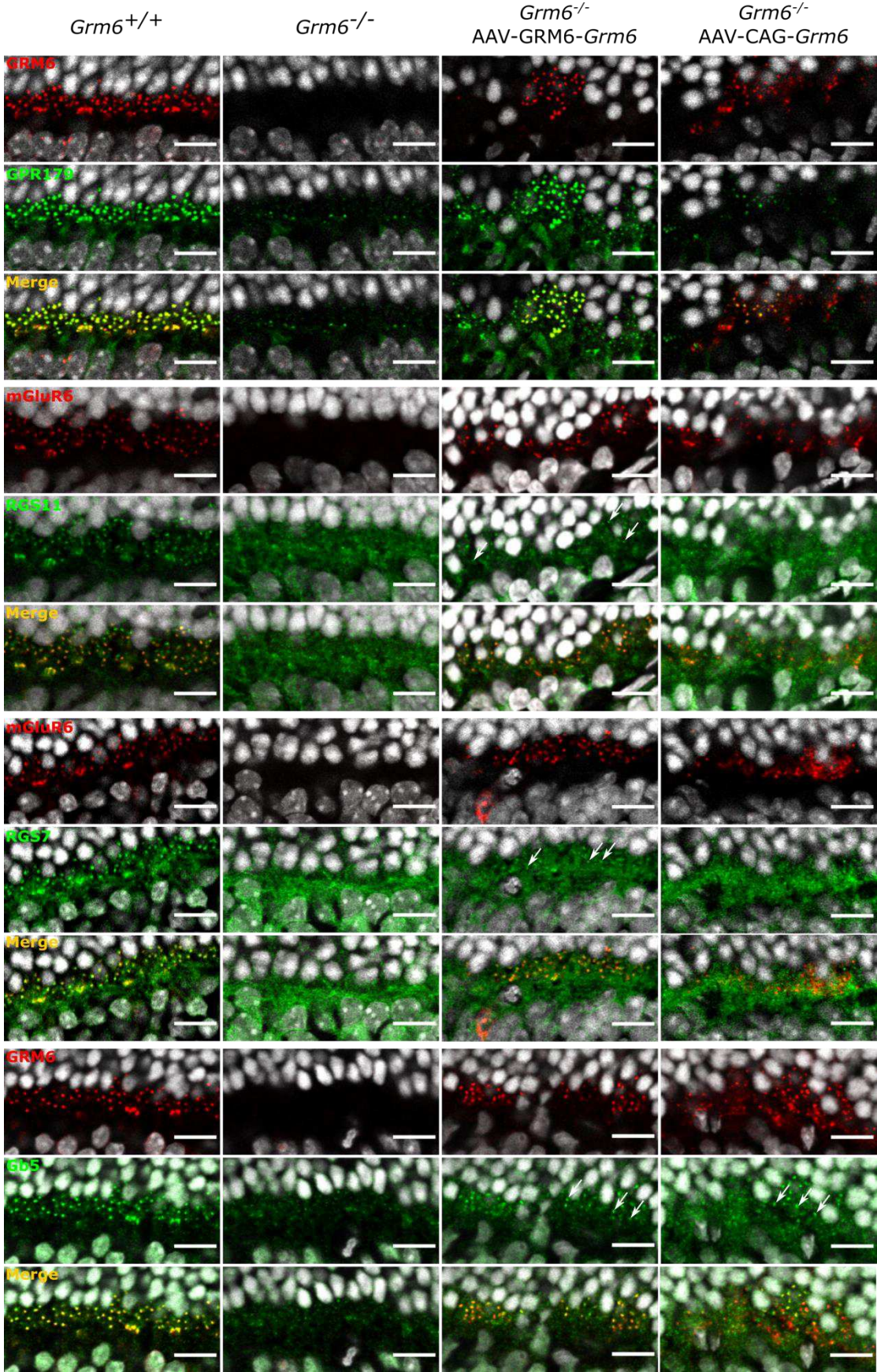
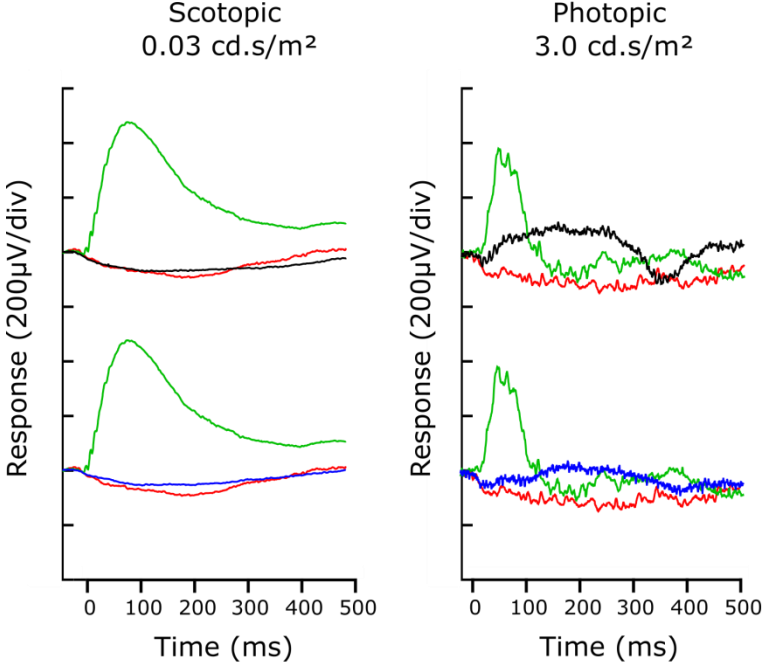


Figure 4

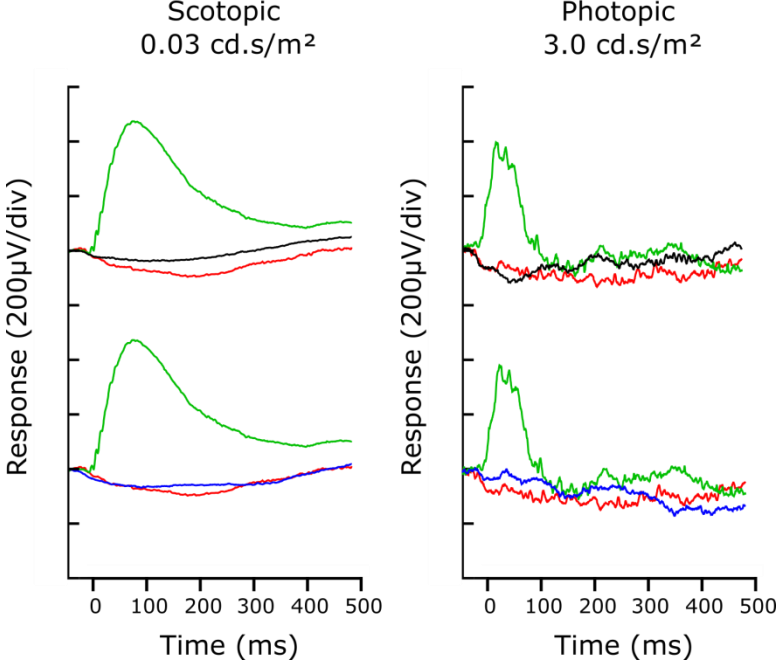
**A**

**2 months post-injection**



**B**

**4 months post-injection**



# Results

---

### III. RESTORATION OF NIGHT VISION IN ADULT MICE WITH CONGENITAL STATIONARY NIGHT BLINDNESS

As mentioned before, cCSNB is yet incurable. A suitable approach to treat cCSNB might be gene addition. Recently, two reports documented on a partial restoration of the phenotype using a gene therapy approach in cCSNB mice lacking nyctalopin and LRIT3. Despite the stationary course of the disease, in both reports, a functional rescue was mainly found in newborn or very young mice (P2 or P5) while no or a milder rescue was obtained in adult mice (P30 or P35). Here, we studied the possibility to induce a functional rescue in adult mice lacking *Lrit3*, and displaying cCSNB, by using three different approaches targeting either ON-BC, photoreceptors or both.

For all three constructs, LRIT3 was produced and well localized in the OPL and this restoration allowed the proper relocalization of the channel TRPM1 at the dendritic tips of ON-BCs. Protein localization of LRIT3 and TRPM1 at the dendritic tips of ON-BCs, functional rescue under scotopic conditions and ON-responses at the ganglion cell level was achieved in a limited number of mice when ON-BCs were targeted. Similarly, a few treated adult *Lrit3*<sup>-/-</sup> mice revealed partial functional restoration when both, ON-BC and photoreceptors were targeted. More importantly, significant number of treated adult *Lrit3*<sup>-/-</sup> mice revealed high ERG b-wave recovery under scotopic conditions, improved optomotor responses and on-time ON-responses at the ganglion cell level when photoreceptors were targeted. Functional rescue was maintained four-month after treatment.

These findings will be submitted to the journal *Molecular Therapy*

**Varin J**, Bouzidi N, Gauvain G\*, Joffrois C\*, Desrosiers M, Robert C, Dias MS, Neuillé M, Michiels C, Nassisi M, Sahel JA, Audo I, Dalkara D, Zeitz C. Restoration of night blindness in adult mice with congenital stationary night blindness. **Molecular Therapy** (to be submitted)

## **Restoration of night vision in adult mice with congenital stationary night blindness**

### **Short title: Recovery of night vision in adult mice with CSNB**

Juliette Varin<sup>1</sup>, Nassima Bouzidi<sup>1</sup>, Gregory Gauvain<sup>1\*</sup>, Corentin Joffrois<sup>1\*</sup>, Melissa Desrosiers<sup>1</sup>,  
Camille Robert<sup>1</sup>, Miguel Miranda De Sousa Dias<sup>1</sup>, Marion Neuillé<sup>1</sup>, Christelle Michiels<sup>1</sup>, Marco  
Nassisi<sup>1</sup>, José-Alain Sahel<sup>1,2,3,4,5</sup>, Serge Picaud<sup>1</sup>, Isabelle Audo<sup>1,2,6</sup>, Deniz Dalkara<sup>1</sup>, Christina  
Zeitzi<sup>1</sup>

<sup>1</sup>Sorbonne Université, INSERM, CNRS, Institut de la Vision, Paris, France.

<sup>2</sup>CHNO des Quinze-Vingts, DHU Sight Restore, INSERM-DGOS CIC 1423, Paris, France.

<sup>3</sup>Fondation Ophtalmologique Adolphe de Rothschild, Paris, France

<sup>4</sup>Académie des Sciences, Institut de France, Paris, France

<sup>5</sup>Department of Ophthalmology, The University of Pittsburgh School of Medicine, Pittsburgh,  
PA 15213, United States

<sup>6</sup>Institute of Ophthalmology, University College of London, London, United Kingdom

\*These authors contributed equally to the study

This study was carried out in Paris, France

Corresponding author:

Christina Zeitzi PhD, DR2

INSERM, UMR\_S968

CNRS, UMR\_7210

Sorbonne University

Institut de la Vision

Department of Genetics

17, rue Moreau

75012 Paris, France

Tel.: +33 1 53 46 25 40

## **Abstract**

Complete congenital stationary night blindness (cCSNB) due to mutations in *TRPM1*, *GRM6*, *GPR179*, *NYX* or *LRIT3* is an incurable inherited retinal disorder characterized by an ON-bipolar cell (ON-BC) defect. Since the disease is non-degenerative and stable, treatment could be administrated at any time making it an attractive target for gene therapy. However, until now AAV-mediated therapies lead to functional improvements only in newborn cCSNB mice. Here we aimed to restore protein localization and function in adult *Lrit3*<sup>-/-</sup> mice. LRIT3 resides in the outer plexiform layer, is crucial for TRPM1 localization at the dendritic tips of ON-BCs and the electroretinogram (ERG)-b-wave. AAV2-7m8-*Lrit3* intravitreal injections were performed targeting either ON-BCs, photoreceptors (PRs) or both by co-injection. Protein localization of LRIT3 and TRPM1 at the dendritic tips of ON-BCs, functional rescue of scotopic responses and ON-responses at the ganglion cell level were achieved in a limited number of mice when ON-BCs or both PRs and ON-BCs, were targeted. More importantly, a significant number of treated adult *Lrit3*<sup>-/-</sup> mice revealed an ERG b-wave recovery under scotopic conditions, improved optomotor responses and on-time ON-responses at the ganglion cell level when PRs were targeted. Functional rescue was maintained for at least four-months after treatment.

## Introduction

Congenital stationary night blindness (CSNB) is a heterogeneous group of non-progressive rare inherited retinal disorders (IRD)<sup>1</sup>. The most frequent type of CSNB is the Schubert-Bornschein-type, which is due to a disruption of the signal transmission between photoreceptors (PR) and ON-bipolar cells (ON-BCs)<sup>1,2</sup>. It can be further subdivided in two forms: incomplete CSNB (icCSNB) and complete CSNB (cCSNB)<sup>3</sup>. Here we focus on the latter one. cCSNB-affected subjects are mainly characterized by impairment of night vision, decreased visual acuity, severe myopia, nystagmus and sometimes strabismus. cCSNB is a largely non-degenerative disease with normal fundus. Clinically, it can be diagnosed by full-field electroretinogram (ERG) recording showing an isolated ON-BC defect<sup>4</sup>. At low light intensities in dark-adapted (DA, scotopic) conditions, the b-wave is absent. With a brighter flash, the a-wave is normal, representing normal rod and cone function, while the b-wave is absent in keeping with a transmission defect between PRs and ON-BCs. In light-adapted (LA, photopic) conditions, the responses to a single flash reveal a sharply arising b-wave with no oscillatory potentials and variable but often decreased b/a ratio indicating cone ON-BC dysfunction<sup>2</sup>. This is in accordance with the expression of the genes mutated in patients with cCSNB including *NYX*<sup>5,6</sup>, *TRPM1*<sup>7-9</sup>, *GRM6*<sup>10,11</sup>, *GPR179*<sup>12,13</sup> and *LRIT3*<sup>14</sup>. Indeed, these genes code for proteins localized in the outer plexiform layer (OPL) affecting signal transmission between PR and ON-BCs<sup>2</sup>. Several animal models of cCSNB have been described, including *Appaloosa* horses with a *TRPM1* defect, beagle dogs with an *LRIT3* defect and different mouse models lacking genes implicated in cCSNB<sup>2,15-17</sup>. All display an ERG in scotopic conditions, similar to those of patients: while the a-wave is preserved, the b-wave is absent. Under photopic conditions *Appaloosa* horses with the *TRPM1* defect and beagle dogs with the *LRIT3* defect, resemble also the cCSNB phenotype observed in patients

showing an altered but present b-wave. In contrast, all mouse models for cCSNB show a significantly different phenotype than patients showing also a complete absence of the b-wave under photopic conditions. Herein, we focus on cCSNB due to mutations in *LRIT3* that codes for the Leucine-rich Repeat Immunoglobulin-like Transmembrane Domain 3 (LRIT3) protein and the respective mouse model (*nob6* also called *Lrit3*<sup>-/-</sup>)<sup>14, 18</sup>. *Lrit3*<sup>-/-</sup> mice are characterized by the absence of LRIT3 in the OPL, a lack of the ERG b-wave under both scotopic and photopic conditions, altered optomotor responses under scotopic conditions and abolished ON-responses at the retinal ganglion cell level<sup>18, 19</sup>. Albeit the role of LRIT3 has not been completely elucidated, we showed that LRIT3 is crucial for the correct localization of TRPM1 at the dendritic tips of all ON-BCs<sup>20</sup> and that it is a key actor of the cone synapse formation/maintenance<sup>21</sup>. Recently it was suggested that LRIT3 is essential for the localization of nyctalopin, encoded by *NYX*, and that the loss of TRPM1 in mice lacking LRIT3 was due to the loss of nyctalopin<sup>22</sup>. Several gene therapies for IRDs have been developed over the years<sup>23</sup>. However, treatment for CSNB patients is yet unavailable. The most suitable treatment for cCSNB appears to be gene replacement therapy. Indeed, cCSNB represents a non-progressive disorder, in which retinal morphology is well preserved<sup>18</sup>, genes underlying this disorder have been identified and specific targeting of ON-bipolar cells in primate retinas with AAV-vectors has been demonstrated<sup>24</sup>. Due to this stable non-degenerative condition, treatment could be in theory administered at any time. However, recent findings revealed functional restoration mainly in very young mice<sup>25, 26</sup>. Indeed, a partial functional rescue of the b-wave under scotopic conditions using an intravitreal AAV-mediated gene replacement approach has been obtained in mice lacking *Nyx*, when treating mice at P2 and targeting only the bipolar cells<sup>25</sup>. Similar observations were made in mice lacking *Lrit3*, when mice were injected at P5 or P35 and targeting rod PRs, with more

significant restoration at P5<sup>25</sup>. In addition, restoration of the respective proteins, TRPM1 was also relocalized<sup>25, 26</sup>. However, restoration of the b-wave under photopic conditions could not be obtained<sup>18, 25, 26</sup>. The aim of our study was to restore the production and function of LRIT3 in the adult *nob6* mouse model.

## Results

Immunolocalization studies in human and mouse retinas showed LRIT3 protein in the outer plexiform layer (OPL)<sup>14, 20, 26</sup>. It is a matter of debate whether this correlates with post-synaptic localization at the dendritic tips of ON-BCs or/and a presynaptic localization at the synapse of PRs. Herein, to rescue the phenotype in the *nob6* mouse model (referred later as *Lrit3*<sup>-/-</sup>), two different constructs were designed using two different promoters: the 200 bp enhancer of the mouse *Grm6* gene fused to the SV40 promoter (referred as *GRM6* promoter) that has been shown to drive expression of the transgene specifically to ON-BCs<sup>24</sup> and the *hGRK* promoter which promotes expression in both, rod and cone PRs<sup>27</sup>. These two constructs were encapsidated in the AAV2-7m8 serotype<sup>28</sup> and either injected alone or mixed at a ratio of 1:1. Mice injected with the *Grm6* promoter construct will be noted as *Lrit3*<sup>-/-</sup>-BC-*Lrit3*, mice treated with the *GRK* promoter construct will be referred as *Lrit3*<sup>-/-</sup>-PR-*Lrit3* and mice injected with both constructs will be named *Lrit3*<sup>-/-</sup>-OPL-*Lrit3* (Figure 1).

### Transgene expression rescues LRIT3 localization at the dendritic tips of ON-BCs

In the *Lrit3*<sup>-/-</sup> mice, LRIT3 production is abolished in the OPL in both rod-to-rod BC and cone-to-cone BC synapses<sup>20</sup>. The restoration and proper localization of LRIT3 following treatment was investigated through immunolocalization studies. All treated retinas, *Lrit3*<sup>-/-</sup>-BC-*Lrit3*, *Lrit3*<sup>-/-</sup>-OPL-*Lrit3* and *Lrit3*<sup>-/-</sup>-PR-*Lrit3*, injected at P30, displayed LRIT3 immunostaining in the OPL which is absent in untreated *Lrit3*<sup>-/-</sup> retinas. The majority of LRIT3 staining appeared at rod-to-rod ON-BC synapses (arrow, Figure 2, LRIT3 left), with fewer LRIT3 staining at cone-to-cone ON-BC synapses (arrow-head, Figure 2, LRIT3 left) in *Lrit3*<sup>-/-</sup>-PR-*Lrit3* retinas (Figure 2, Supplementary Figure 1).

### TRPM1 relocates to the dendritic tips of rod ON-BCs following treatment

To ensure correct ON-BC signal transmission, the correct localization of TRPM1 at the dendritic tips of ON-BCs is essential. In the *Lrit3*<sup>-/-</sup> mouse model, albeit TRPM1 is still present in the cell bodies of ON-BCs, the dendritic tip staining at the ON-BCs is abolished in these mice<sup>20</sup> (Figure 2, TRPM1, right). The relocation of TRPM1 following treatment in either PRs or ON-BCs was investigated through immunolocalization studies. In all treated retinas, *Lrit3*<sup>-/-</sup>-BC-*Lrit3*, *Lrit3*<sup>-/-</sup>-OPL-*Lrit3* and *Lrit3*<sup>-/-</sup>-PR-*Lrit3*, TRPM1 was relocated at the dendritic tips of rod ON-BCs (arrow, Figure 2, TRPM1, right) after treatment: TRPM1 staining at the dendritic tips of cone ON-BCs was undetectable. These results indicate that restoration of the signaling cascade was selective for the rod-to-rod ON-BC synapse.

### AAV-mediated LRIT3 expression in the OPL restores the ERG b-wave up to four months

In *Lrit3*<sup>-/-</sup> animals, the transmission of the visual signal between PRs and ON-BCs is disrupted as shown by the absence of the b-wave on the ERG under scotopic and photopic conditions<sup>18</sup> (Figure 3). ERG recordings performed two months after treatment on *Lrit3*<sup>-/-</sup>-BC-*Lrit3* mice injected at P30 revealed a partial rescue of the b-wave under scotopic conditions (Figure 3A, left) with the highest restoration at the lowest flash intensity. The amplitude of the b-wave corresponded to a rescue of 45% compared to the b-wave amplitudes of *Lrit3*<sup>+/+</sup> mice (Figure 3C). No improvement of the photopic b-wave was recorded in the *Lrit3*<sup>-/-</sup> treated mice (Figure 3B). However, these results were obtained in a non-significant number of *Lrit3*<sup>-/-</sup>-BC-*Lrit3* mice. Similarly, ERG recordings in *Lrit3*<sup>-/-</sup>-OPL-*Lrit3* mice treated at P30 also presented a b-wave (Figure 3A, middle) which amplitude corresponded to 45% of *Lrit3*<sup>+/+</sup> mice at the lowest light intensity (Figure 3C). As *Lrit3*<sup>-/-</sup>-BC-*Lrit3* mice, the scotopic b-wave was the highest at low flash-intensities and the restoration was only observed under scotopic conditions (Figure 3A, 3B and 3C). Only a few treated mice revealed this functional

restoration. Strikingly, partial restoration was obtained in *Lrit3*<sup>-/-</sup>-PR-*Lrit3* animals (N = 4) treated at P30 under scotopic conditions (Figure 3A, right). The amplitude of the b-wave was rescued at 58% compared to the b-wave amplitude of *Lrit3*<sup>+/+</sup> mice (Figure 3C), but again only under scotopic conditions (Figure 3B). To monitor the supposedly sustained partial rescue, a follow-up ERG recording was made up to four months post-injection. In all animals presenting a b-wave, independently of the construct used, the b-wave was still recordable, and of sustained amplitude, four months after treatment (Figure 3D).

#### ON-BCs signaling pathway restoration recovers ON-responses in RGCs

As previously described, in *Lrit3*<sup>-/-</sup> mice ON-responses are also abolished at the level of retinal ganglion cells (RGCs)<sup>19</sup> (Figure 4). LRIT3 proper localization is mandatory for TRPM1 localization and function and therefore for the further propagation of the visual signal towards ON-ganglion cells. To confirm the functional rescue following treatment, we used 256 channel multi-electrode array (MEA-256) to record light-evoked responses in isolated retinas from *Lrit3*<sup>+/+</sup>, *Lrit3*<sup>-/-</sup>, *Lrit3*<sup>-/-</sup>-BC-*Lrit3*, *Lrit3*<sup>-/-</sup>-OPL-*Lrit3* and *Lrit3*<sup>-/-</sup>-PR-*Lrit3* retinas to measure the potential ON-responses rescue on ganglion cell level. In contrast with *Lrit3*<sup>+/+</sup> retinas, in untreated *Lrit3*<sup>-/-</sup> retinas we observed ON responses with small amplitude and high temporal variability (Figure 4A and B). Indeed, in untreated *Lrit3*<sup>-/-</sup> retinas only ~5% of recorded electrodes displayed ON responses (ON + ON-OFF: 86/1663 responsive electrodes, figure 4C). In comparison, RGCs from *Lrit3*<sup>-/-</sup>-BC-*Lrit3* retinas displayed ~40% of ON-responses: (ON + ON-OFF: 33/85 responsive electrode), but all ON-responses recorded were delayed, with an average peak firing rate at 674 ms after light onset. Strikingly, in *Lrit3*<sup>-/-</sup>-OPL-*Lrit3* and *Lrit3*<sup>-/-</sup>-PR-*Lrit3* retinas, peak firing rate for ON-responses were significantly closer to the stimulus onset (*Lrit3*<sup>-/-</sup>-OPL-*Lrit3* = 454 ms, n= 206, *Lrit3*<sup>-/-</sup>-PR-*Lrit3* = 350 ms, n= 261, compared to *Lrit3*<sup>-/-</sup>-BC-*Lrit3*, p<0.0001). Concerning the number of responsive

electrodes displaying ON-responses, both *Lrit3*<sup>-/-</sup>-OPL-*Lrit3* and *Lrit3*<sup>-/-</sup>-PR-*Lrit3* retinas showed an increase in the proportion of ON-responses in the overall RGCs population recorded (*Lrit3*<sup>-/-</sup>-OPL-*Lrit3*: ~22%, 206/903 and *Lrit3*<sup>-/-</sup>-PR-*Lrit3*: ~32%, 261/801). To establish if the rescued ON-responses observed here are due to the restoration of the mGluR6 signaling, we performed experiments with bath application of the mGluR6 agonist (L-AP4) on our different conditions (Supplementary Figure 2). Surprisingly, if L-AP4 blocked the ON-responses observed in *Lrit3*<sup>-/-</sup>-OPL-*Lrit3* and *Lrit3*<sup>-/-</sup>-PR-*Lrit3* retinas, with reduced firing rate and fewer electrodes recording ON-responses, it does not seem to affect the ON-responses recorded in *Lrit3*<sup>-/-</sup>-BC-*Lrit3* retinas.

#### LRIT3 partial rescue improved optomotor responses in treated mice

It has been shown that the transmission defect between PRs and ON-BCs in the *Lrit3*<sup>-/-</sup> mouse had an impact on the visual perception of these mice<sup>18</sup>. Thus, treated animals with a partial functional rescue observed by ERG recordings and MEA were investigated by measurements of optomotor responses. For the two types of treated mice, *Lrit3*<sup>-/-</sup>-BC-*Lrit3* and *Lrit3*<sup>-/-</sup>-OPL-*Lrit3*, optomotor reflexes seemed to be improved compared to untreated *Lrit3*<sup>-/-</sup> mice, however as specified above only few animals were tested. Strikingly, the *Lrit3*<sup>-/-</sup>-PR-*Lrit3* mice revealed a significant improvement of the optomotor responses, compared to untreated *Lrit3*<sup>-/-</sup> mice (n=8), for the two lowest spatial frequencies under scotopic conditions (n=4, p=0.006 for the first optometer and p=0.03 for the second, Figure 5). Under photopic conditions, *Lrit3*<sup>-/-</sup> mice presented diminished optomotor responses compared to *Lrit3*<sup>+/+</sup> mice (p=0.001). Under photopic conditions, there was no statistically significant improvement of optomotor responses in *Lrit3*<sup>-/-</sup>-PR-*Lrit3* mice compared to untreated *Lrit3*<sup>-/-</sup> mice (Figure 5).

## Discussion

Over 2 million people worldwide are affected by IRDs, yet no treatment is available for most cases. A FDA approved gene therapy product has been put on the market for three years to treat one of the most severe IRD, Leber Congenital Amaurosis (Luxturna, Spark Therapeutics), due to mutations in *RPE65* opening the way for the development of new gene therapies for other well characterized IRDs<sup>29-33</sup>. Today, it is still challenging to treat retinal disorders involving PR loss, since the therapeutic window is small as the degeneration of PRs is taking place<sup>34</sup>. Thus, to ensure proper targeting of PRs and to increase efficient and ongoing treatment, patients need to be treated at early stages of the disease before PR degeneration has advanced<sup>23,34</sup>. In addition, albeit the structure and function of most genes in animals are homologous to those in humans and can thus serve as good models to test therapeutic approaches, their physiology is often different<sup>35</sup>. Although dogs lacking functional RPE65 and treated with a RPE65-gene replacement therapy revealed partial restoration of the ERG phenotype, no ERG improvements were recorded in LCA patients treated with the same construct<sup>31,36</sup>. Here we aimed to restore the cCSNB phenotype, another IRD. As the name implicates, cCSNB is present since birth, does not evolve over time and represents a signal transmission defect between PRs and ON-BCs<sup>2</sup>. In addition, the retinal structure is preserved, e.g. the morphology of PR and BCs are largely normal; hence, treatment should be applicable at adult ages<sup>2</sup>. In contrast, two previously reported gene therapy approaches for cCSNB described partial functional rescue mainly in newborn mice (P2 or P5 vs. P30)<sup>25,26</sup>. It was suggested that supplementation of an ON BC-specific transgene is most effective when delivered while bipolar cells are still differentiating explaining the lack of efficient rescue in adult mice<sup>25,37,38</sup>. The lack of efficient therapy in adult nob mice, lacking *Nyx* was thought to be post-transcriptional. Although efficient transgene transcript

was produced, the protein could not be produced to restore the phenotype in adult mice<sup>25</sup>. Lower treatment efficacy in adult mice, lacking *Lrit3* was thought to be also due to the function of LRIT3 itself, being most likely important for the development of synapses<sup>19</sup>. Indeed, at P35 synapses are already formed and the therapy would not be as effective as in retinas where this process is not completed yet. In addition, AAVs are thought to favor immature retinas to mature ones, in keeping with more efficient treatment at P5 than P35 old mice<sup>26</sup>. In addition, the strength of the promoter and the specificity of the vectors used may influence the efficiency to transfect bipolar cells at different ages. Since a gene therapy approach in newborn patients is less applicable than in adults and keeping in mind the non-degenerative nature of the cCSNB disease course, we aimed to restore the cCSNB phenotype in adult *Lrit3*<sup>-/-</sup> mice (P30). Our study shows for the first time that it is indeed possible to obtain a partial rescue of the phenotype, at the protein level and at the functional level, in adult CSNB mice, most likely due to the use of a highly specific AAV capsid (AAV2-7m8) which has already been shown to efficiently transduce all retinal layers<sup>28</sup>.

Previously, LRIT3 was thought to be localized post-synaptically at the dendritic tips of ON-BCs in the OPL due to the isolated ON-BC defect observed in cCSNB patients<sup>14</sup> and other proteins involved in cCSNB, localizing at the ON-BCs dendritic tips<sup>2</sup>. However, expression data<sup>39</sup> and recent findings<sup>26</sup> suggest PR expression of *Lrit3* and presynaptic localization. Hence, the pre- or post-synaptic localization of LRIT3 is still not clearly elucidated, but it is certainly present in the OPL in human and mouse retina<sup>14, 21, 22, 26</sup>. Thus, different vector-promoter combinations were applied to drive efficient OPL-LRIT3 localization in the *Lrit3*<sup>-/-</sup> mice. Our findings using the different approaches clearly revealed partial restoration of the cCSNB phenotype, but the question of the exact *Lrit3* expression in one or the other retinal cell type and if LRIT3 is localized pre- or/and postsynaptically remains unresolved. Indeed,

partial restoration was obtained when ON-BCs, both ON-BCs and PRs and solely PRs, were targeted. However, this rescue could be only shown in a significant number of animals when PR cells were targeted. These findings indicate that LRIT3 either targeted to the ON-BCs or PR cells can partially restore the localization of LRIT3 and TRPM1 and the visual function, but the exact cellular expression and localization is yet not solved. Thus, it seems to be more important that LRIT3 can be targeted efficiently to the OPL, than targeting a specific cell type. Different reasons may account for the fact that restoration was only obtained in a significant number of animals when PR cells were targeted. This might be indeed due to the predominant expression of *Lrit3* in PRs and thus targeting PRs re-establishes the normal pathway. However, our studies showed as well a partial restoration when ON-BCs were targeted, although only in few animals. This might be due the fact that BCs are more difficult to target than PRs<sup>40</sup>. In case of co-injection to target both ON-BC and PRs, a stronger effectiveness was expected since both sides of the synaptic cleft were targeted; however, this was not the case. The effect of each construct might have been decreased by the co-injection, since each vector was diluted at 50% to have the same injection volume, compared to injection of only one construct. One way to circumvent this issue might be to have in the same construction *Lrit3* under the control of both promoters, hGRK1 and GRM6.

Interestingly, ERG rescue and improved optomotor responses were only obtained under scotopic conditions, indicating that solely night vision was partially restored. In the study from Scalabrino and colleagues<sup>25</sup> partial restoration of the scotopic b-wave was obtained while the restoration of the photopic response was less evident, although the authors concluded that the photopic ERGs “included components that resemble WT, including a waveform ‘deflection’ (oscillatory potential)”. Recently, *Lrit3* knock-out mice intravitreally injected with an AAV-vector targeting rod-PRs using a rhodopsin promoter revealed partial

restoration under scotopic but not photopic conditions<sup>26</sup>. The authors argued that this might be due to the fact that only rod but not cone PRs were targeted<sup>26</sup>. However, our study using a GRK promoter, targeting both, rod and cone PRs still did not restore the function under photopic conditions as shown by ERG and behavioral tests. Previously it was shown that cone synapses of *Lrit3*<sup>-/-</sup> mice have significantly less invaginating cone ON-BC dendrites compared to wild-type animals, indicating a role for LRIT3 in the development and or maintenance of the cone synapse<sup>19</sup>. A hypothesis explaining the lack of photopic restoration might be that applying such treatment in adult mice, when the synapse is fully formed, will not restore the cone-mediated pathway as the transmission between cones and cone ON-BCs is constitutively diminished. Cone initiate ribbon synapse formation between P4 and P5 in mice<sup>41</sup>, and the cone synaptogenesis is completed by P14 to P15<sup>41, 42</sup>. Indeed, although our studies revealed LRIT3 relocalization in treated animals, the staining was more present in the OPL close to rods than cones. In addition, it did not seem that TRPM1 localization at the dendritic tips of cone ON-BCs was restored conversely to rod BCs. This implication of CSNB proteins in synaptic development was also noticed in the *Grm6*<sup>tm1Nak</sup> mouse, in which invaginating dendrites of rod-BC are larger and often contain ectopic ribbons while the number of invaginating dendrites of cone ON-BCs and ribbons decrease at the cone pedicle<sup>43</sup>, as observed in the *Lrit3*<sup>-/-</sup> mouse model<sup>19</sup>. Other molecules, implicated in the development of the ribbon synapse might be influenced at an early developmental stage by the absence of LRIT3 and thus will not be restored when treatment occurs at an adult stage. Treatment at a younger age using a promoter targeting cone PRs and delivery of other molecules influenced by the absence of LRIT3 might rescue the photopic phenotype in *Lrit3*<sup>-/-</sup> mice. However, in general the photopic phenotype of cCSNB mice models is more severe than the one of patients or larger animal models: no b-wave is observed in photopic conditions in any of the cCSNB

mouse models <sup>2</sup> while cone-driven responses are comparable between CNSB dogs, horses and patients e.g. mildly reduced <sup>2, 15, 16, 44</sup>; scotopic ERG responses are similar in all models <sup>2</sup>. This difference of the cone ERG b-wave might be explained by the different cellular contribution that was noted between rodents and primates. For example, in the latter, OFF-BCs contribute to a large proportion to the cone ERG b-wave responses <sup>45</sup> while in the mouse cone ERG, only a small contribution of the OFF-BCs was noted <sup>46</sup>. Therefore, different pathways may be implicated in cCSNB mouse model, explaining the absence of functional restoration under photopic conditions. Consequently, using a mouse model of CSNB displaying a more severe photopic phenotype than patients might therefore not be the ideal way to assess cone-driven pathway restoration following treatment. The gene therapy approach described in this study should be further tested on larger animal models such as the CSNB beagle dog affected by *LRIT3* mutations <sup>47</sup> in order to more precisely evaluate the photopic phenotype. To conclude, this study reports a restoration of night vision in adult mice displaying congenital stationary night blindness as assessed by immunolocalization studies, ERG recordings, MEA analysis and optomotor responses measurements.

## **Material & Methods**

### Ethical statement

All animal procedures were performed according to the Council Directive 2010/63EU of the European Parliament and the Council of September 22, 2010, on the protection of animals used for scientific purposes, with the National Institutes of Health guidelines and with the ARVO Statement for the Use of Animals in Ophthalmic and Vision Research. They were approved by the French Minister of National Education, Superior Education and Research (authorization delivered on January 21, 2019).

### AAV production

The production of recombinant AAVs was made by following the plasmid cotransfection method<sup>48</sup>. Lysates were then purified using iodixanol gradient ultracentrifugation as previously described: 40% iodixanol fraction was concentrated and buffer exchanged using Amicon Ultra-15 Centrifugal Filter Units (Merck Millipore, Billerica, MA, USA). Real-time PCR was used to titer the vector stocks for DNase-resistant vector genomes relatively to a standard<sup>49</sup>.

### Intravitreal injections

Mice were anesthetized by isoflurane inhalation (5% in oxygen for induction and 2% for maintenance). Intravitreal injections were performed at 2 (P2) or 30 (P30) days of age. Pupils were dilated (0.5% mydriaticum) and a 33-gauge needle was passed through the sclera at the ora serrata level. 1  $\mu$ l of a viral stock solution at a concentration of  $1.73 \times 10^{14}$  vg/ml maximum was injected directly in the vitreous cavity.

### Electroretinogram

Mice were dark-adapted overnight before performing the ERG recordings. They were anesthetized by ketamine (80mg/kg) and xylazine (8mg/kg) and eye drops were used to dilate their pupils (0.5% mydriaticum 5% neosynephrine) and anesthetize the cornea (0.4% oxybuprocaine chlorohydrate). Mice corporal temperature was maintained through a heating pad along the test. Upper and lower eyelids were retracted to keep the eyes opened and bulging. Corneal lenses (Mayo Corporation, Japan) were applied on corneal surface to record the ERG. A reference electrode was placed on the nose while the ground electrode was placed above the tail. Recordings from both eyes were made in parallel. All scotopic ERG were made first using six increasing light intensity of flashes ranging from 0.003 to 30.0 cd.s/m<sup>2</sup>. Each trace corresponding to one light-intensity results from the average of five traces originating from five flashes. To ensure a saturation of rod PRs and the recording of cone-driven responses, a 10-minutes light-adaptation step at 20 cd/m<sup>2</sup> was done. Following this light-adaptation step, photopic ERGs were recorded first at 3.0 cd.s/m<sup>2</sup> and at the same intensity; 5 Hz and 10 Hz flickers were also checked. All data were analyzed with GraphPad Prism v.6 (GraphPad Software, La Jolla, CA, USA)

### Optomotor test

Optomotor test was performed as described previously<sup>18</sup>. Mice were dark-adapted overnight before the optomotor test. Ten wild-type animals and ten knock-out animals of each lineage were studied along with the treated animals. Mice were placed on a grid platform (11.5 cm diameter, 19 cm above the bottom of the drum) at the center of a motorized drum (29 cm diameter) covered by vertical black and white stripes of a defined spatial frequency (0.063, 0.125, 0.25, 0.5 and 0.75 cycles per degree). A five minutes break

was made before the test so the animal gets used to its new environment. The stripes were rotated for 1 minute clockwise and 1 minute counter-clockwise at a speed of 2 rotations per minute. An interval of 10 sec was made after the first minute. Each test was recorded with a digital infrared camera to count head movements of the mice. Tests were firstly performed under scotopic conditions then in photopic condition after 5 minutes of light adaptation (two lamps of 60 Watts). Head movements in both directions were considered to obtain the number of head movements per minute.

### MEA

After overnight dark adaptation, mice were sacrificed by CO<sub>2</sub> inhalation followed by cervical dislocation. Retinas were carefully dissected under dim-red light and conserved in Ames medium (Sigma-Aldrich, St. Louis, MO, USA) oxygenated with 95% oxygen and 5% CO<sub>2</sub>. Retinas were placed on a Spectra/Por membrane (Spectrum Laboratories, Rancho Dominguez, CA, USA) previously coated with poly-D-lysine and gently pressed against an MEA (MEA256 100/30 iR-ITO; Multi Channel Systems MCS, Reutlingen, Germany) using a micromanipulator, RGCs facing the electrodes. Retinas were continuously perfused with bubbled Ames medium at 34°C at a rate of 1 to 2 ml/min and let to rest for 45 minutes before the recording session. Under dark conditions, 10 repeated full-field light stimuli at a 450 nm wavelength were applied to the samples at 10<sup>14</sup> photons/cm<sup>2</sup>/s for 2 seconds with 10-second interval by using a Polychrome V monochromator (Olympus, Hamburg, Germany) driven by an STG2008 stimulus generator (MCS). Raw RGC activity recorded by MEA was amplified (gain 1000–1200) and sampled at 20 kHz by using MCRack software (MCS). Resulting data were stored and filtered with a 200-Hz high-pass filter. Raster plots were obtained by using a combination of threshold detection, template matching, and cluster grouping based on principal component analysis using Spike2 v.7 software (CED Co.,

Cambridge, UK). Peristimulus time histograms were plotted with a bin size of 50 ms by using a custom-made script in MATLAB v.R2014b (MathWorks, Inc., Natick, MA, USA). Only RGCs with a mean spontaneous firing frequency superior to 1 Hz were considered. We subsequently determined for each sorted RGC the maximum firing frequency in an interval of 2 seconds after light onset (for ON-responses) and in an interval of 2 seconds after light offset (for OFF-responses). These values were normalized to the mean spontaneous firing frequency of the corresponding RGC. Considering that significant responses have a maximum firing frequency that is superior to the mean spontaneous firing frequency  $\pm 5$  SD, we determined the time at which these significant frequencies were reached after the light onset for ON-responses and after the light offset for OFF-responses. The histograms were traced with GraphPad Prism v.6 (GraphPad Software, La Jolla, CA, USA).

#### Immunolocalization studies

Animals were sacrificed by CO<sub>2</sub> inhalation followed by cervical dislocation. Eyes were removed and dissected to keep the posterior part of the eyes which were then fixed in ice-cold 4% paraformaldehyde for 20 minutes. Subsequently, the eye cups were washed in ice-cold PBS and cryoprotected by increasing concentrations of sucrose (ranging from 10% to 30%) in water and 0.24 M phosphate buffer for 1 hour at 4°C for 10% sucrose and 20% sucrose solutions and overnight at 4°C under agitation for the 30% sucrose solution. The eye-cups were then embedded in 7.5% gelatin - 10% sucrose and the blocks frozen at -40°C in isopentane and kept at -80°C until cutting. Sections of 12  $\mu$ m were generated using a cryostat (MICROM HM 560™, ThermoFisher Scientific, Waltham, MA, USA) and mounted on glass slides (Superfrost® Plus, ThermoFisher Scientific). Mouse retina sections were treated to decrease background noise (Antigen Retrieval Reagent, Biotechne, Minneapolis, MN, USA) for 4 minutes at 92°C and subsequently blocked for 1 hour at room temperature in PBS1X

10% Donkey Serum (v/v), 0.1% Triton X-100. Primary antibodies and the dilutions used were: rabbit anti-LRIT3 (1:200, Neuillé et al., 2015) and sheep anti-TRPM1 (1:500; Cao *et al*). The sections were incubated with primary antibodies diluted in PBS1X 2% Donkey Serum (v/v), 0.1% Triton X-100 for 1 hour at room temperature. After washes with PBS1X 0.1% Triton-X100, the sections were incubated with anti-rabbit and anti-sheep secondary antibodies coupled with Alexa Fluor 488, or Cy3 (Jackson ImmunoResearch) along with 4',6-diamidino-2-phenylindole (DAPI), all used at 1:1000, for 0.5 hours at room temperature. Subsequently, the sections were cover-slipped with mounting medium (Mowiol, Merck Millipore, Billerica, MA, USA). Fluorescence images retinal sections were acquired with a confocal microscope (FV1000, Olympus). Images for figures were handled with the Image J software (ImageJ Software).

## Figure legends

### Figure 1: Schematic representation of the cellular targets of the three constructs.

PR-*Lrit3* construct targeting both, rod (grey) and cone (blue, green and red) PRs, the BC-*Lrit3* construct targeting both, rod (dark orange) and cone ON-BCs (light orange) and the OPL-*Lrit3* construct targeting both, rod and cone PRs and ON-BCs by co-injection of the PR-*Lrit3* and BC-*Lrit3* constructs.

### Figure 2: Localization of LRIT3 and TRPM1

Representative confocal images of cross-sections centered on the OPL of *Lrit3*<sup>+/+</sup>, *Lrit3*<sup>-/-</sup>, *Lrit3*<sup>-/-</sup>-BC-*Lrit3*, *Lrit3*<sup>-/-</sup>-OPL-*Lrit3* and *Lrit3*<sup>-/-</sup>-PR-*Lrit3* retinas stained with an antibody against LRIT3 (green) and TRPM1 (red). Scale bar, 10 μm.

### Figure 3: ERG recordings.

A) Representative scotopic ERG traces at 2 months post-injection for *Lrit3*<sup>+/+</sup> (green line), *Lrit3*<sup>-/-</sup> (red line), *Lrit3*<sup>-/-</sup>-BC-*Lrit3* (blue line), *Lrit3*<sup>-/-</sup>-OPL-*Lrit3* (purple line) and *Lrit3*<sup>-/-</sup>-PR-*Lrit3* (black line) mice, values on the right of the row of waveforms specify the flash intensity in log cd.s/m<sup>2</sup>. B) Representative photopic ERG traces at 2 months post-injection for a flash intensity of 3.0 cd.s/m<sup>2</sup>. C) Average amplitude of the scotopic ERG b-wave at 2 months post-injection. D) Comparison between the average amplitude of the scotopic ERG b-wave at 2 months (filled) and 4 months (hatched) post-injection for *Lrit3*<sup>-/-</sup>-BC-*Lrit3* (blue), *Lrit3*<sup>-/-</sup>-OPL-*Lrit3* (purple) and *Lrit3*<sup>-/-</sup>-PR-*Lrit3* (black) mice, no statistically significant difference between 2 and 4 months for the *Lrit3*<sup>-/-</sup>-PR-*Lrit3* mice (Wilcoxon statistical test, p=0.8).

### Figure 4: ON responses in treated retinas using MEA-256 recordings.

A) Spike density function for all responsive electrodes displaying an ON component (ON only and ON-OFF) recorded on all treated retina (1 *Lrit3*<sup>-/-</sup>-BC-*Lrit3* (85 responsive electrodes), 1 *Lrit3*<sup>-/-</sup>-OPL-*Lrit3* retina, 4 *Lrit3*<sup>-/-</sup>-PR-*Lrit3* retina, 7 *Lrit3*<sup>-/-</sup> retina and 6 *Lrit3*<sup>+/+</sup> retina). Light stimuli is indicated as a black bar and light grey area, responses recorded at individual electrode are displayed as grey line (average of 10 repetitions), the peak firing rate amplitude and latency is overlaid with the traces as colored open circle. *Lrit3*<sup>+/+</sup> recording have a different scaling (upper left) than all other conditions (middle). B) ON peak firing rate (up) and ON peak latency (bottom) for all responsive electrodes in the different conditions. Horizontal black bar represent the average value, and vertical black bar the mean +/- SD. C) Fraction of the electrode population displaying ON, ON-OFF or OFF profile of response. Unresponsive electrodes are electrodes where spontaneous activity is recorded without light-evoked spiking.

#### Figure 5: Optomotor responses under both scotopic and photopic conditions

The number of head movements per minute was obtained under both scotopic and photopic conditions with spatial frequencies of 0.063 and 0.125 cycles/degree (scotopic) or 0.063 alone (photopic) for *Lrit3*<sup>-/-</sup>-BC-*Lrit3* (blue), *Lrit3*<sup>-/-</sup>-OPL-*Lrit3* (purple) and *Lrit3*<sup>-/-</sup>-PR-*Lrit3* (black) mice and compared using Mann-Whitney statistical test with representative *Lrit3*<sup>+/+</sup> (green) and *Lrit3*<sup>-/-</sup> (red) mice. The star indicates a significant test (p<0.05).

#### Figure S1: Localization of LRIT3

Representative confocal images of cross-sections of *Lrit3*<sup>-/-</sup>-BC-*Lrit3*, *Lrit3*<sup>-/-</sup>-OPL-*Lrit3* and *Lrit3*<sup>-/-</sup>-PR-*Lrit3* retinas stained with an antibody against LRIT3 (green). Scale bar, 10  $\mu$ m.

Figure S2: L-AP4 treatment reduce restored ON responses.

A- Spike density function for all recorded electrodes with ON responses (grey), before (control), during (L-AP4), and after (Washout) perfusion of L-AP4. Peak indicated on individual traces during the light stimulation (light grey area). B- Peak firing rate for the different condition during the pharmacological experiment. C- Evolution of the number of electrodes with a ON response with the addition and removal of L-AP4 in the solution.

## **Acknowledgments**

The authors are grateful to the platform of animal housing, vectorology and imaging at the Institut de la Vision and more specifically Julie Degradin, Manuel Simonutti, Quenol Cesar, Camille Robert, Mélissa Desrosiers, Marie-Laure Niepon and Stephan Fouquet. We thank Kirill Martemyanov Yan Cao; Xavier Guillonneau and Florian Sennlaub for fruitful discussion. This work was supported by Retina France (CZ), by the French Muscular Dystrophy Association (AFM-Téléthon) (CZ), by UNADEV-Aviesan call 2015 (CZ), Fondation Voir et Entendre (CZ), Prix Dalloz for "la recherche en ophtalmologie" (CZ), Fondation pour la Recherche Médicale (FRM DVS20131228918) in partnership with Fondation Roland Bailly (CZ), Fédération des Aveugles et Amblyopes de France (MN), Ville de Paris and Région Ile de France, LABEX LIFESENSES (reference ANR-10-LABX-65) supported by French state funds managed by the Agence Nationale de la Recherche within the Investissements d'Avenir programme (ANR11-IDEX-0004-0), with the support of the Programme Investissements d'Avenir IHU FOReSIGHT (ANR-18-IAHU-01) and the Ministère de l'enseignement supérieur et de la recherche (JV). The funders had no role in study design, data collection, analysis and interpretation, decision to publish, or preparation of the manuscript. JV, DD, SP, JAS and CZ are inventors on pending patent application on "Treatment of congenital stationary night blindness using gene therapy" (SL0160 [CLBEnaco-F2478 36WO]). DD is an inventor on a patent of adeno-associated virus virions with variant capsid and methods of use thereof with royalties paid to Avalanche Biotech (WO2012145601 A2)

## References

1. Schubert, G, and Bornschein, H (1952). Analysis of the human electroretinogram. *Ophthalmologica* **123**: 396-413.
2. Zeitz, C, Robson, AG, and Audo, I (2015). Congenital stationary night blindness: an analysis and update of genotype-phenotype correlations and pathogenic mechanisms. *Progress in retinal and eye research* **45**: 58-110.
3. Miyake, Y, Yagasaki, K, Horiguchi, M, Kawase, Y, and Kanda, T (1986). Congenital stationary night blindness with negative electroretinogram. A new classification. *Archives of ophthalmology* **104**: 1013-1020.
4. Miyake, Y, Yagasaki, K, Horiguchi, M, and Kawase, Y (1987). On- and off-responses in photopic electroretinogram in complete and incomplete types of congenital stationary night blindness. *Japanese journal of ophthalmology* **31**: 81-87.
5. Pusch, CM, Zeitz, C, Brandau, O, Pesch, K, Achatz, H, Feil, S, *et al.* (2000). The complete form of X-linked congenital stationary night blindness is caused by mutations in a gene encoding a leucine-rich repeat protein. *Nature genetics* **26**: 324-327.
6. Bech-Hansen, NT, Naylor, MJ, Maybaum, TA, Sparkes, RL, Koop, B, Birch, DG, *et al.* (2000). Mutations in NYX, encoding the leucine-rich proteoglycan nyctalopin, cause X-linked complete congenital stationary night blindness. *Nature genetics* **26**: 319-323.
7. Audo, I, Kohl, S, Leroy, BP, Munier, FL, Guillonneau, X, Mohand-Said, S, *et al.* (2009). TRPM1 is mutated in patients with autosomal-recessive complete congenital stationary night blindness. *American journal of human genetics* **85**: 720-729.
8. Li, Z, Sergouniotis, PI, Michaelides, M, Mackay, DS, Wright, GA, Devery, S, *et al.* (2009). Recessive mutations of the gene TRPM1 abrogate ON bipolar cell function and cause complete congenital stationary night blindness in humans. *American journal of human genetics* **85**: 711-719.
9. van Genderen, MM, Bijveld, MM, Claassen, YB, Florijn, RJ, Pearing, JN, Meire, FM, *et al.* (2009). Mutations in TRPM1 are a common cause of complete congenital stationary night blindness. *American journal of human genetics* **85**: 730-736.
10. Zeitz, C, van Genderen, M, Neidhardt, J, Luhmann, UF, Hoeben, F, Forster, U, *et al.* (2005). Mutations in GRM6 cause autosomal recessive congenital stationary night blindness with a distinctive scotopic 15-Hz flicker electroretinogram. *Investigative ophthalmology & visual science* **46**: 4328-4335.
11. Dryja, TP, McGee, TL, Berson, EL, Fishman, GA, Sandberg, MA, Alexander, KR, *et al.* (2005). Night blindness and abnormal cone electroretinogram ON responses in patients with mutations in the GRM6 gene encoding mGluR6. *Proceedings of the National Academy of Sciences of the United States of America* **102**: 4884-4889.
12. Audo, I, Bujakowska, K, Orhan, E, Poloschek, CM, Defoort-Dhellemmes, S, Drumare, I, *et al.* (2012). Whole-exome sequencing identifies mutations in GPR179 leading to autosomal-recessive complete congenital stationary night blindness. *American journal of human genetics* **90**: 321-330.
13. Peachey, NS, Ray, TA, Florijn, R, Rowe, LB, Sjoerdsma, T, Contreras-Alcantara, S, *et al.* (2012). GPR179 is required for depolarizing bipolar cell function and is mutated in autosomal-recessive complete congenital stationary night blindness. *American journal of human genetics* **90**: 331-339.
14. Zeitz, C, Jacobson, SG, Hamel, CP, Bujakowska, K, Neuille, M, Orhan, E, *et al.* (2013). Whole-exome sequencing identifies LRIT3 mutations as a cause of autosomal-recessive complete congenital stationary night blindness. *Am J Hum Genet* **92**: 67-75.
15. Sandmeyer, LS, Breaux, CB, Archer, S, and Grahn, BH (2007). Clinical and electroretinographic characteristics of congenital stationary night blindness in the Appaloosa and the association with the leopard complex. *Veterinary ophthalmology* **10**: 368-375.

16. Kondo, M, Das, G, Imai, R, Santana, E, Nakashita, T, Imawaka, M, *et al.* (2015). A Naturally Occurring Canine Model of Autosomal Recessive Congenital Stationary Night Blindness. *PLoS one* **10**: e0137072.
17. Pardue, MT, and Peachey, NS (2014). Mouse b-wave mutants. *Documenta ophthalmologica Advances in ophthalmology* **128**: 77-89.
18. Neuille, M, El Shamieh, S, Orhan, E, Michiels, C, Antonio, A, Lancelot, ME, *et al.* (2014). Lrit3 deficient mouse (nob6): a novel model of complete congenital stationary night blindness (cCSNB). *PLoS one* **9**: e90342.
19. Neuille, M, Cao, Y, Caplette, R, Guerrero-Given, D, Thomas, C, Kamasawa, N, *et al.* (2017). LRIT3 Differentially Affects Connectivity and Synaptic Transmission of Cones to ON- and OFF-Bipolar Cells. *Investigative ophthalmology & visual science* **58**: 1768-1778.
20. Neuille, M, Morgans, CW, Cao, Y, Orhan, E, Michiels, C, Sahel, JA, *et al.* (2015). LRIT3 is essential to localize TRPM1 to the dendritic tips of depolarizing bipolar cells and may play a role in cone synapse formation. *Invest Ophthalmol Vis Sci*: ARVO E-Abstract 2612.
21. Neuille, M, Morgans, CW, Cao, Y, Orhan, E, Michiels, C, Sahel, JA, *et al.* (2015). LRIT3 is essential to localize TRPM1 to the dendritic tips of depolarizing bipolar cells and may play a role in cone synapse formation. *The European journal of neuroscience* **42**: 1966-1975.
22. Hasan, N, Pangeni, G, Ray, TA, Fransen, KM, Noel, J, Borghuis, BG, *et al.* (2020). LRIT3 is required for Nyctalopin expression and normal ON and OFF pathway signaling in the retina. *eNeuro*.
23. Trapani, I, and Auricchio, A (2018). Seeing the Light after 25 Years of Retinal Gene Therapy. *Trends in molecular medicine* **24**: 669-681.
24. Mace, E, Caplette, R, Marre, O, Sengupta, A, Chaffiol, A, Barbe, P, *et al.* (2015). Targeting channelrhodopsin-2 to ON-bipolar cells with vitreally administered AAV Restores ON and OFF visual responses in blind mice. *Molecular therapy : the journal of the American Society of Gene Therapy* **23**: 7-16.
25. Scalabrino, ML, Boye, SL, Fransen, KM, Noel, JM, Dyka, FM, Min, SH, *et al.* (2015). Intravitreal delivery of a novel AAV vector targets ON bipolar cells and restores visual function in a mouse model of complete congenital stationary night blindness. *Human molecular genetics* **24**: 6229-6239.
26. Hasan, N, Pangeni, G, Cobb, CA, Ray, TA, Nettesheim, ER, Ertel, KJ, *et al.* (2019). Presynaptic Expression of LRIT3 Transsynaptically Organizes the Postsynaptic Glutamate Signaling Complex Containing TRPM1. *Cell reports* **27**: 3107-3116 e3103.
27. Khani, SC, Pawlyk, BS, Bulgakov, OV, Kasperek, E, Young, JE, Adamian, M, *et al.* (2007). AAV-mediated expression targeting of rod and cone photoreceptors with a human rhodopsin kinase promoter. *Investigative ophthalmology & visual science* **48**: 3954-3961.
28. Dalkara, D, Byrne, LC, Klimczak, RR, Visel, M, Yin, L, Merigan, WH, *et al.* (2013). In vivo-directed evolution of a new adeno-associated virus for therapeutic outer retinal gene delivery from the vitreous. *Science translational medicine* **5**: 189ra176.
29. Leber, T (1869). Uber retinitis pigmentosa und angeborene amaurose. *Graefe's archive for clinical and experimental ophthalmology = Albrecht von Graefes Archiv fur klinische und experimentelle Ophthalmologie* **15**: 1-25.
30. Marlhens, F, Bareil, C, Griffoin, JM, Zrenner, E, Amalric, P, Eliaou, C, *et al.* (1997). Mutations in RPE65 cause Leber's congenital amaurosis. *Nature genetics* **17**: 139-141.
31. Bainbridge, JW, Smith, AJ, Barker, SS, Robbie, S, Henderson, R, Balaggan, K, *et al.* (2008). Effect of gene therapy on visual function in Leber's congenital amaurosis. *The New England journal of medicine* **358**: 2231-2239.
32. Cideciyan, AV, Aleman, TS, Boye, SL, Schwartz, SB, Kaushal, S, Roman, AJ, *et al.* (2008). Human gene therapy for RPE65 isomerase deficiency activates the retinoid cycle of vision but with slow rod kinetics. *Proceedings of the National Academy of Sciences of the United States of America* **105**: 15112-15117.

33. Maguire, AM, Simonelli, F, Pierce, EA, Pugh, EN, Jr., Mingozzi, F, Bennicelli, J, *et al.* (2008). Safety and efficacy of gene transfer for Leber's congenital amaurosis. *The New England journal of medicine* **358**: 2240-2248.
34. Cideciyan, AV, Jacobson, SG, Beltran, WA, Sumaroka, A, Swider, M, Iwabe, S, *et al.* (2013). Human retinal gene therapy for Leber congenital amaurosis shows advancing retinal degeneration despite enduring visual improvement. *Proceedings of the National Academy of Sciences of the United States of America* **110**: E517-525.
35. Wolfe, JH (2009). Gene therapy in large animal models of human genetic diseases. Introduction. *ILAR journal* **50**: 107-111.
36. Le Meur, G, Stieger, K, Smith, AJ, Weber, M, Deschamps, JY, Nivard, D, *et al.* (2007). Restoration of vision in RPE65-deficient Briard dogs using an AAV serotype 4 vector that specifically targets the retinal pigmented epithelium. *Gene therapy* **14**: 292-303.
37. Cepko, C (2014). Intrinsically different retinal progenitor cells produce specific types of progeny. *Nature reviews Neuroscience* **15**: 615-627.
38. Rapaport, DH, Wong, LL, Wood, ED, Yasumura, D, and LaVail, MM (2004). Timing and topography of cell genesis in the rat retina. *The Journal of comparative neurology* **474**: 304-324.
39. Shekhar, K, Lapan, SW, Whitney, IE, Tran, NM, Macosko, EZ, Kowalczyk, M, *et al.* (2016). Comprehensive Classification of Retinal Bipolar Neurons by Single-Cell Transcriptomics. *Cell* **166**: 1308-1323 e1330.
40. van Wyk, M, Hulliger, EC, Girod, L, Ebner, A, and Kleinlogel, S (2017). Present Molecular Limitations of ON-Bipolar Cell Targeted Gene Therapy. *Frontiers in neuroscience* **11**: 161.
41. Sherry, DM, Wang, MM, Bates, J, and Frishman, LJ (2003). Expression of vesicular glutamate transporter 1 in the mouse retina reveals temporal ordering in development of rod vs. cone and ON vs. OFF circuits. *The Journal of comparative neurology* **465**: 480-498.
42. Rich, KA, Zhan, Y, and Blanks, JC (1997). Migration and synaptogenesis of cone photoreceptors in the developing mouse retina. *The Journal of comparative neurology* **388**: 47-63.
43. Tsukamoto, Y, and Omi, N (2014). Effects of mGluR6-deficiency on photoreceptor ribbon synapse formation: comparison of electron microscopic analysis of serial sections with random sections. *Visual neuroscience* **31**: 39-46.
44. Witzel, DA, Smith, EL, Wilson, RD, and Aguirre, GD (1978). Congenital stationary night blindness: an animal model. *Investigative ophthalmology & visual science* **17**: 788-795.
45. Sieving, PA, Murayama, K, and Naarendorp, F (1994). Push-pull model of the primate photopic electroretinogram: a role for hyperpolarizing neurons in shaping the b-wave. *Visual neuroscience* **11**: 519-532.
46. Sharma, S, Ball, SL, and Peachey, NS (2005). Pharmacological studies of the mouse cone electroretinogram. *Visual neuroscience* **22**: 631-636.
47. Das, RG, Becker, D, Jagannathan, V, Goldstein, O, Santana, E, Carlin, K, *et al.* (2019). Genome-wide association study and whole-genome sequencing identify a deletion in LRIT3 associated with canine congenital stationary night blindness. *Scientific reports* **9**: 14166.
48. Choi, VW, Asokan, A, Haberman, RA, and Samulski, RJ (2007). Production of recombinant adeno-associated viral vectors for in vitro and in vivo use. *Current protocols in molecular biology* **Chapter 16**: Unit 16 25.
49. Aurnhammer, C, Haase, M, Muether, N, Hausl, M, Rauschhuber, C, Huber, I, *et al.* (2012). Universal real-time PCR for the detection and quantification of adeno-associated virus serotype 2-derived inverted terminal repeat sequences. *Human gene therapy methods* **23**: 18-28.

Figure 1

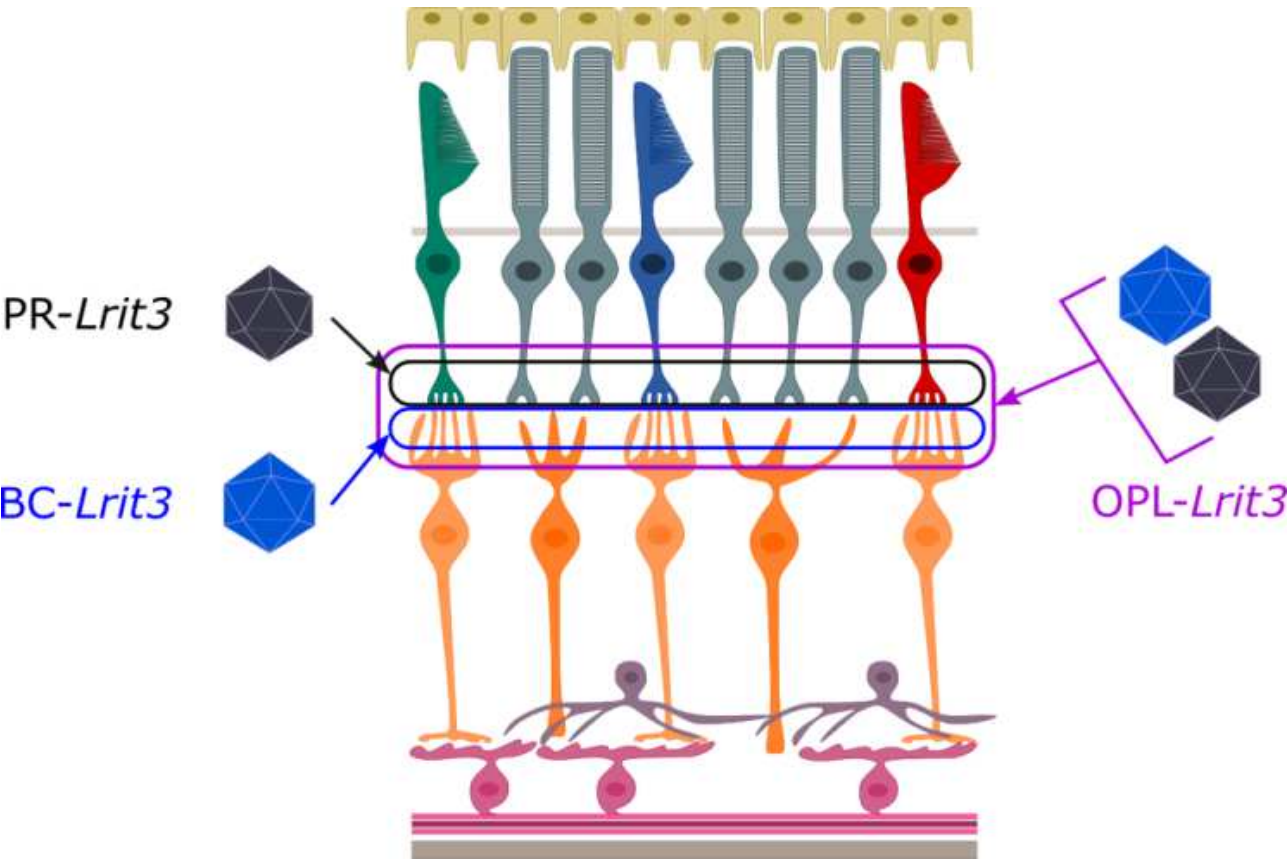
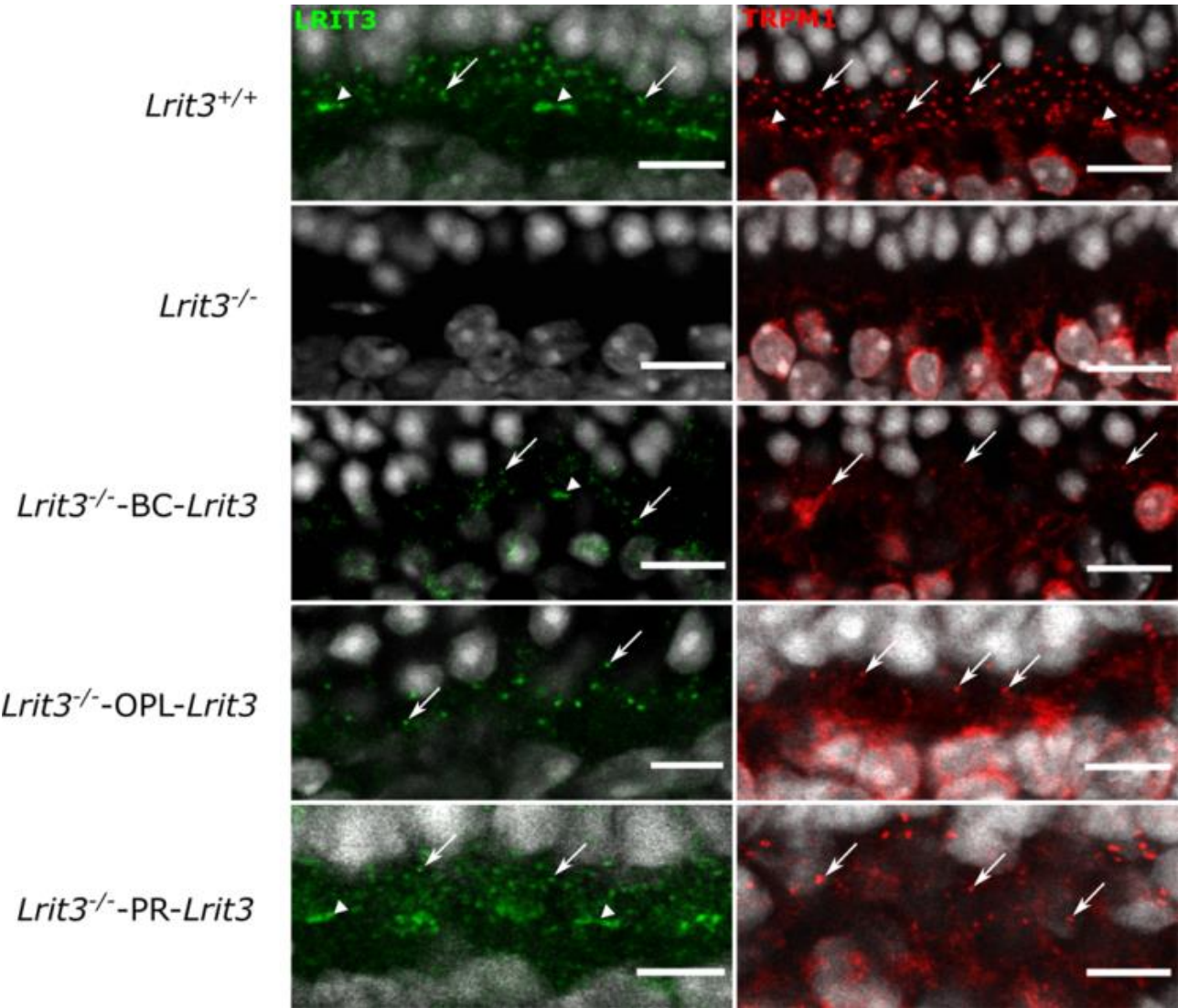
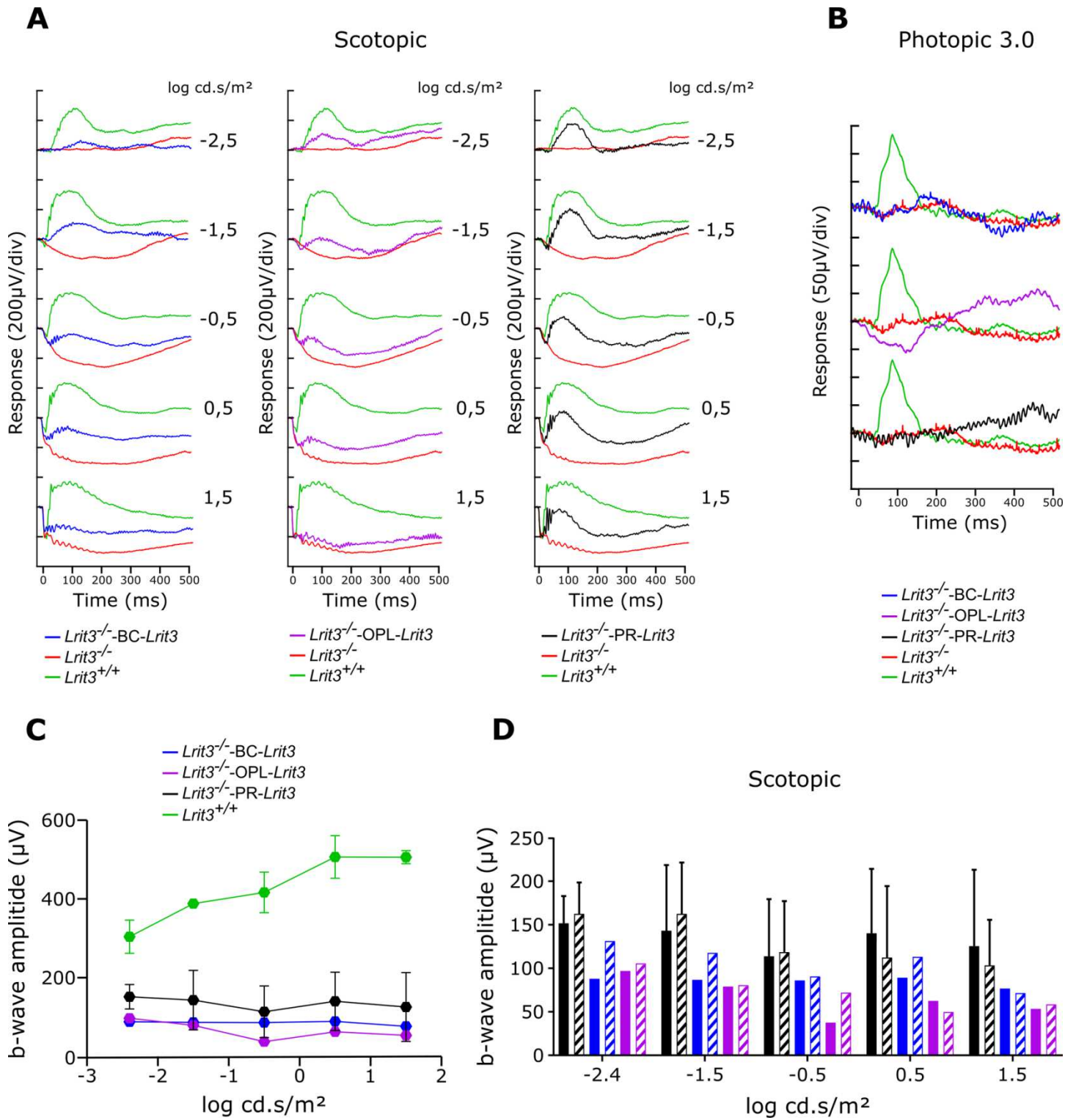


Figure 2



**Figure 3**



**Figure 4**

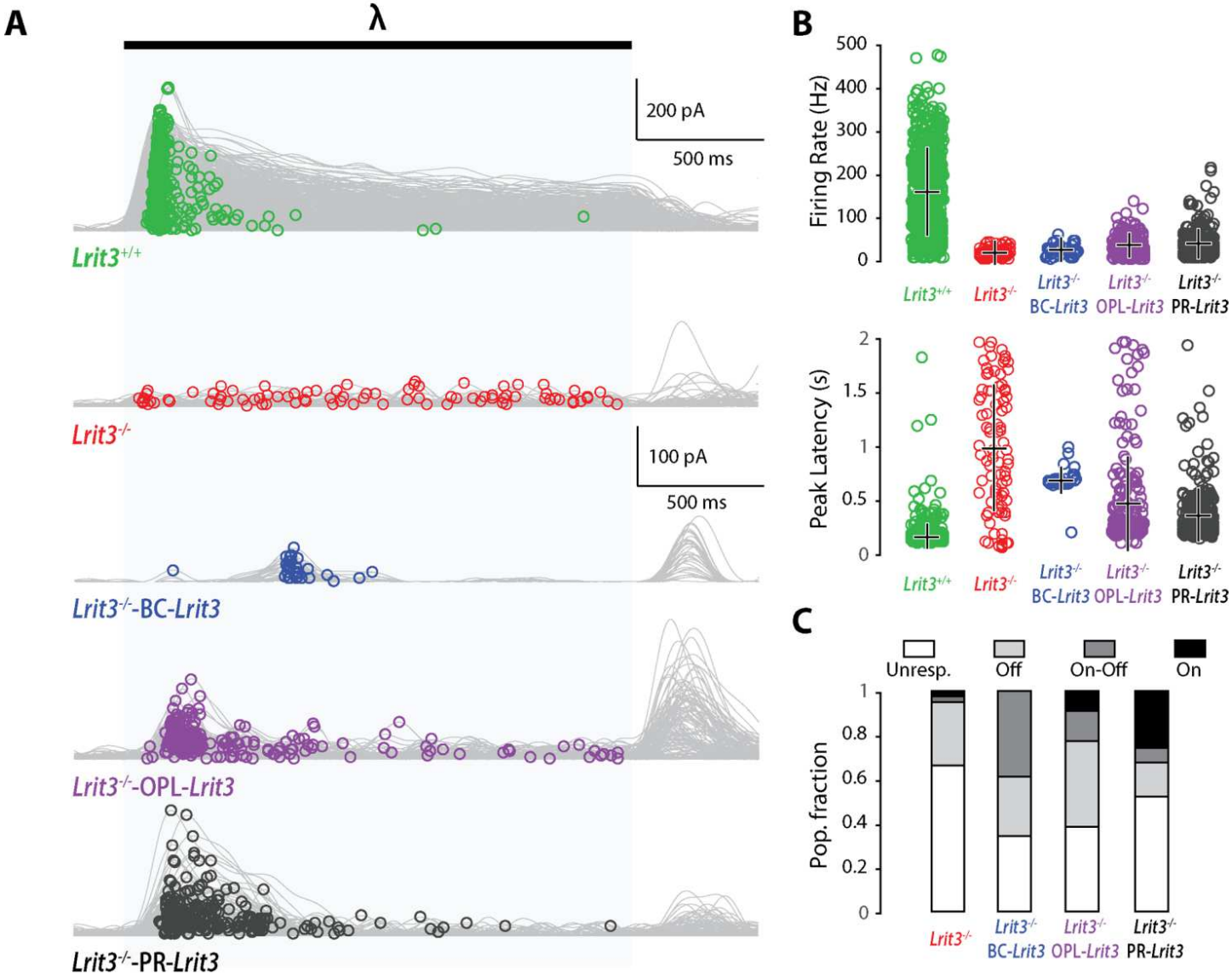
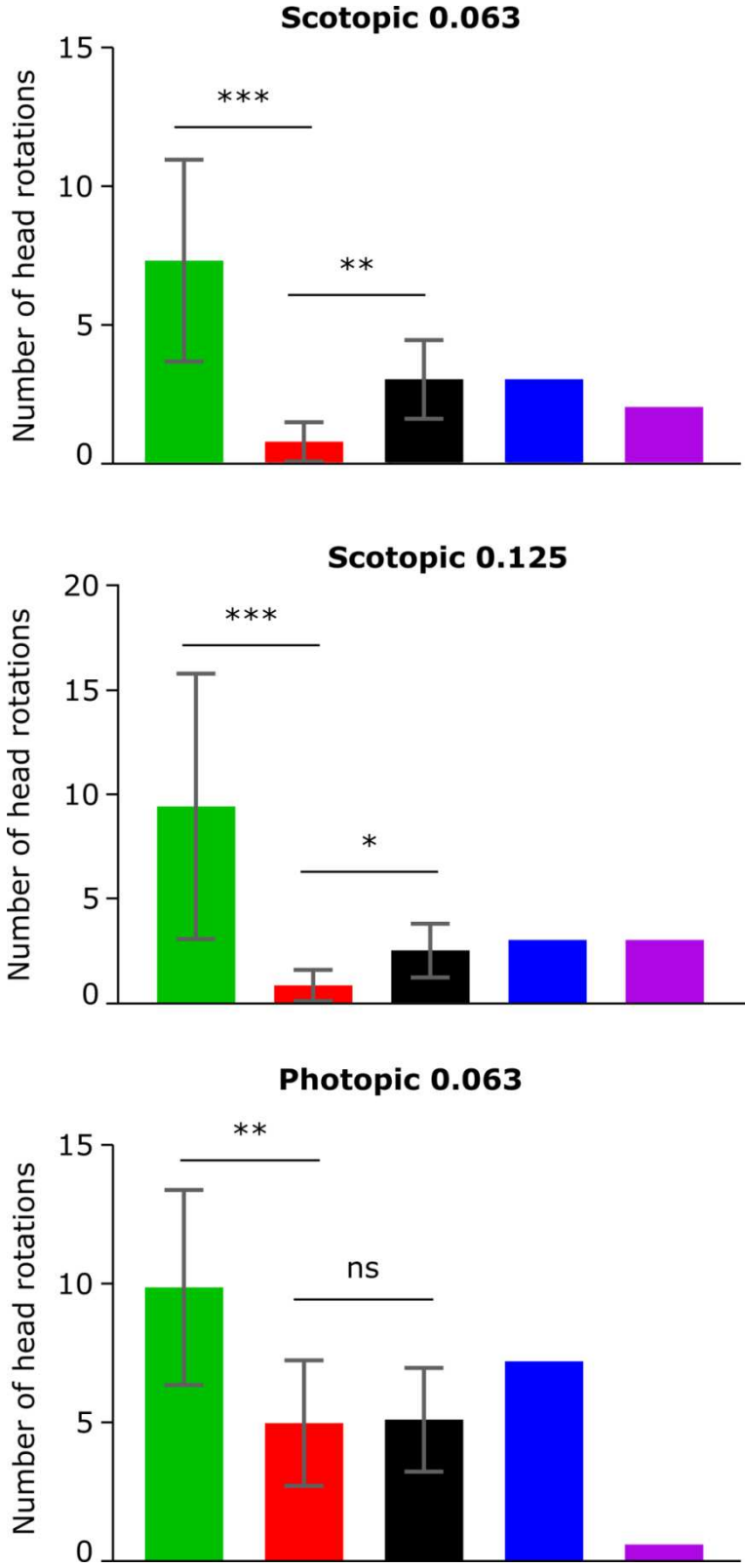
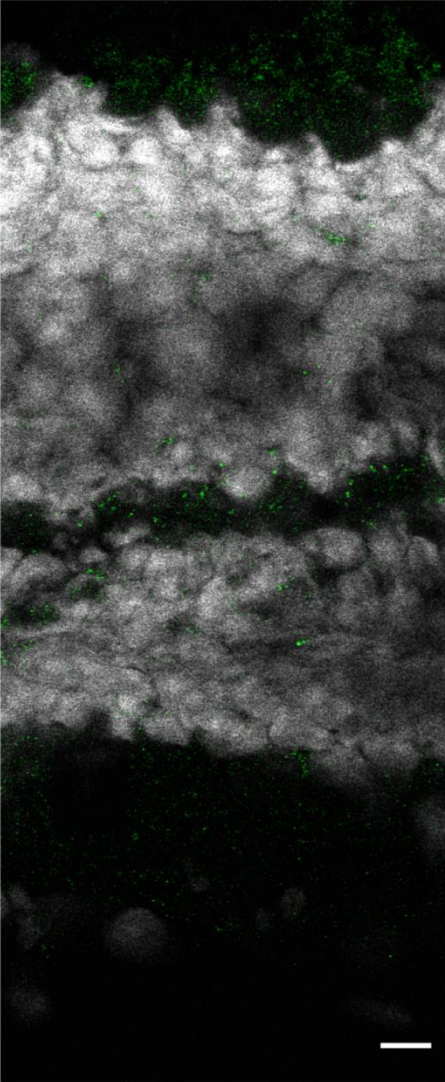


Figure 5

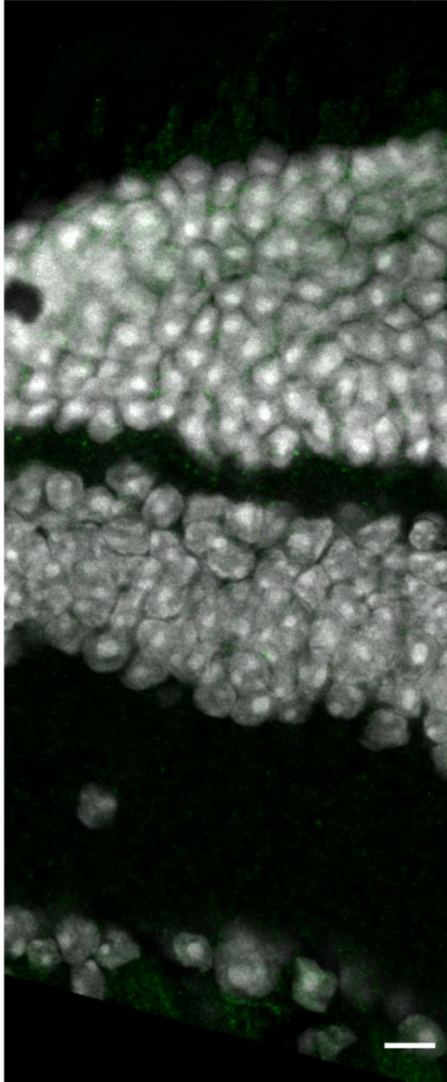


Supplementary figure 1

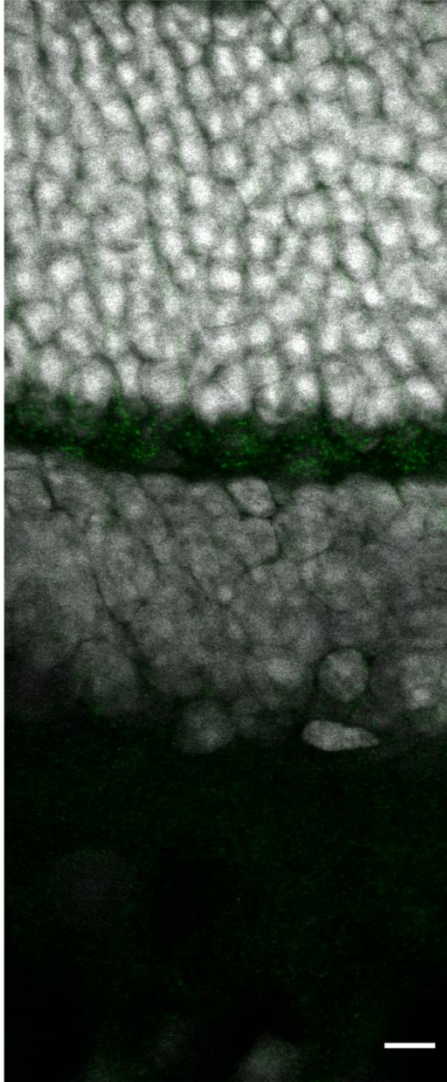
*Lrit3*<sup>-/-</sup>  
BC-*Lrit3*



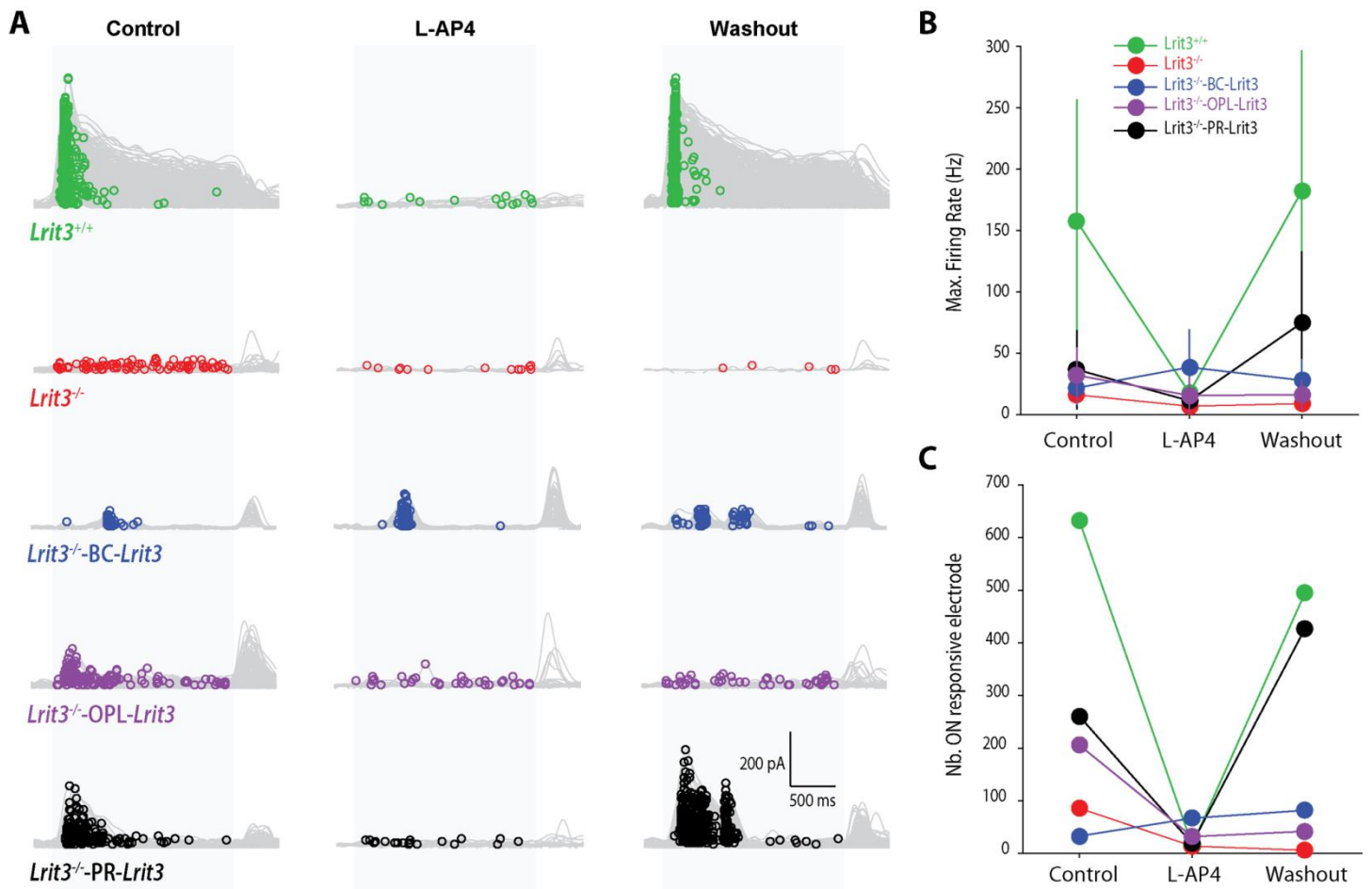
*Lrit3*<sup>-/-</sup>  
OPL-*Lrit3*



*Lrit3*<sup>-/-</sup>  
PR-*Lrit3*



## Supplementary figure 2



# Discussion & Perspectives

---

Congenital stationary night blindness (CSNB) is a clinically and genetically heterogeneous inherited retinal disorder [17]. My PhD thesis mainly concentrated on the complete form of CSNB (cCSNB). This form is the only retinal disorder which solely affects the function of ON-BCs. However, ON-BC defects have already been associated with other clinical features as in Duchenne Muscular Dystrophy [218] and more importantly for this work, in paraneoplastic retinopathy (PR) and frequently in melanoma associated retinopathy (MAR) [219]. Interestingly, both, mutations in *TRPM1* or abolishment of *TRPM1* due to anti-*TRPM1* autoantibodies present in patients with PR lead to this ON-BC defect. In this thesis, we focused on both conditions affecting the ON-BC function.

## I. IDENTIFICATION OF AUTOANTIBODIES INVOLVED IN PARANEOPLASTIC RETINOPATHY ASSOCIATED WITH ON-BCS DYSFUNCTION: FUNDAMENTAL AND THERAPEUTIC INTEREST

As mentioned before, mutations in *TRPM1* is one cause of cCSNB [71-80] and was identified by a candidate gene approach by comparing the ON-BC defect observed in *Appaloosa* horses with patients with cCSNB. Indeed, *TRPM1*, also known as Melastatin (*MLSN1*) was significantly down-regulated in the retina and the skin in affected animals [86]. Thus it was proposed that *TRPM1* is responsible for altering BC signaling but also melanocyte function causing both CSNB and the coat color phenotype in those horses [220]. The insertion of 1kb in the first exon of *TRPM1* causing CSNB and LSC in *Appaloosa* horses leads to the disruption of the transcription by premature poly-adenylation[86]. In *TRPM1*-related cCSNB in patients, no skin phenotype has been documented [73-75]. However, my host laboratory recognized in some patients with *TRPM1* mutations [73] specific skin features (unpublished data, Table 4). In other families either no data about the skin pigmentation was available or patients did not show any striking differences or this phenotype did not co-segregate with the mutation. A more systematic study is needed to evaluate if *TRPM1* mutations are indeed associated with pigmentation in humans.

**Table 4: Patients harboring mutations in TRPM1 leading to cCSNB and which presented unusual skin features**

Reference number of the patients	Nucleotide exchange	Allele state	Protein effect	Ocular phenotype	Skin features
4497 Tuebingen, Germany	c.31C>T c.296T>C	het het	p.Gln11Stop p.Leu99Pro	cCSNB nystagmus myopia	mild vitiligo
8214 Tuebingen, Germany	c.1197G>A c.3491delA	het het	c.Pro399Pro/splice defect? p.Gln1164ArgfsX31	cCSNB myopia strabismus	psoriasis
CIC00612 Paris, France	c.215A>G c.3094G>T	het het	p.Tyr72Cys p.Glu1032Stop	cCSNB myopia nystagmus strabismus	freckles in 1 het and 1 homo for normal alleles
D0704708 Ghent, Belgium /27533 Zurich, Switzerland	c.1-27C>T (70+TRPM1) alternatively: c.40C>T (92+TRPM1)	homo	5'UTR  p.Arg14Trp	cCSNB strabismus hypermetropia	2 of 4 het have pale skin with freckles

The goal of my work was to identify autoantibodies in three females affected with cutaneous melanoma which presented an ON-BC defect upon ERG. Using immunolocalization studies, western blot analysis and immunofluorescence on wild-type and *Trpm1*<sup>-/-</sup> mice retinal cryosections, we validated the presence of anti-TRPM1 autoantibodies in the sera of these new cases of MAR. Furthermore, as the human TRPM1 exists in three isoforms which differ in their N-terminus [147], we investigated the reactivity of these autoantibodies towards all TRPM1 isoforms. All three sera contained antibodies reacting to the three isoforms of TRPM1, albeit with different apparent sensitivity. They presumably recognized an epitope that is common to all three TRPM1 isoforms, encoded some place after exon 2, consistent with the literature [143]. The sensitivity to detect the different isoforms of TRPM1 was different and

was method-dependent. This was especially true for the anti-TRPM1 autoantibodies present in MAR3, which failed to label the shortest isoform of TRPM1 in the overexpressing cell system by immunofluorescence, yet detected it by western blot after enrichment, and labelled TRPM1 robustly on mouse retinal sections.

Paraneoplastic syndromes can sometimes be more complex due to the occurrence of multiple autoantibodies in the same patient [221] or autoantibodies targeting different retinal proteins in different patients [219]. Indeed, reports mentioned autoantibodies against TRPM1 but also Bestrophin, aldolase A and C or interphotoreceptor retinoid-binding protein in patients with MAR. Studying the reactivity of the autoantibodies of patients with paraneoplastic retinopathy associated ON-BC dysfunction could reveal new proteins involved in the signaling cascade of ON-BCs. This identification and characterization of the causing autoantibodies can help to establish the proper treatment for these patients. For instance, Roels and colleagues [144] reported the case of a patient with CAR and presenting anti-TRPM1 autoantibodies. Following the treatment of this patient with rituximab in order to decrease the immune response, the serology proved the clearance of the anti-TRPM1 autoantibodies. This led to a normalization of the ERG and an improvement of the symptoms in this patient [144].

Following this identification of autoantibodies in the sera of three new MAR cases and the subsequent publication [222], we became a reference center to analyze the sera of patients displaying an ON-BC defect associated with different types of cancer.

## II. TREATING CSNB THROUGH GENE THERAPY

In this thesis we developed two gene therapy strategies to treat cCSNB either due to mutations in *LRIT3* or *GRM6*. In both we succeeded to relocalize mGluR6 or LRIT3 at the OPL while they were absent in *Grm6*<sup>-/-</sup> and *Lrit3*<sup>-/-</sup> mice, respectively. However, we managed to obtain a functional rescue only for the LRIT3 approach and under scotopic conditions.

### **Efficient ON-BCs targeting**

For both project we used the AAV2.7m8 serotype combined with different promoters: the *Grm6*-200bp/SV40 promoter [46] to target ON-BCs, the CAG promoter [164] to induce a wide expression of mGluR6 in the retina and the hGRK1 promoter to target photoreceptors in the LRIT3 gene therapy. These choices were made in collaboration with Dr. Deniz Dalkara. Indeed,

the AAV2.7m8\_Grm6-200bp/SV40 combination used by Macé and colleagues, led to an expression of GFP in about 52 to 74% of ON-BCs in 4- to 8-weeks-old *rd1* mice [46]. These proportions were of interest for our project since we wanted to test a gene therapy approach for cCSNB in adult mice. However, only a few mice injected with the construct targeting ON-BCs responded to the treatment in the LRIT3 approach while only ~2.5% of the OPL presented an mGluR6 staining in treated *Grm6*<sup>-/-</sup> mice vs. ~11% with a CAG promoter. Therefore, it appears that the transduction of ON-BCs was a limitation in both projects.

The two reports of AAV-mediated gene therapy for CSNB used different AAV serotypes and promoters than the ones used in this thesis (Table 5, grey lines). However, Scalabrino and colleagues aimed also to target ON-BCs to relocalize nyctalopin at the dendritic tips of ON-BCs. They reported a production of the protein in about 21% of ON-BCs and a much lower percentage in P30 injected mice [198]. Functional rescue was investigated and scotopic ERG responses showed a partial rescue of the b-wave and photopic responses had “components that resembled the one found in wild-type” but in P30 injected mice no improvement was observed [198]. The low percentage of ON-BCs expressing the protein might be one reason explaining the mild functional rescue in these cCSNB mice, as in our mGluR6 approach.

Over the years, different AAV\_promoter combinations have been identified and modified in order to increase the transduction efficiency of the retina [152]. Table 5 summarizes the different AAV serotypes and promoters described to target ON-BCs through intravitreal or subretinal injections. During this thesis, new promoters targeting ON-BCs were reported as inducing an increase in ON-BCs targeting compared to the AAV2.7m8\_Grm6-200bp/SV40. The AAV2.7m8-Y444F\_In4s-In3-200En-mGluR500P combination was described as inducing increasing transduction efficiency compared to AAV2.7m8\_Grm6-200bp/SV40, however, with an expression predominantly in RBCs [223] and the AAV2.7m8\_770En\_454P(hGRM6) displayed a 70.6% ± 5% specificity towards ON-BCs in 12-weeks-old wild-type mice [224]. Using these constructs to try to increase the production of mGluR6 in *Grm6*<sup>-/-</sup> mice and restore a functional rescue should be investigated.

Table 5: AAV serotypes and promoters used to target ON-BCs in the retina

AAV serotype	Promoter	Targeted cells	Route of administration	<i>In vivo</i> validation	First publication
AAV2.7m8	GRM6-200bp/SV40	ON-BCs	IVT	Mouse	Macé et al 2015
	770En_454P(hGRM6)	ON-BCs	IVT	Mouse	Hulliger 2020
AAV2 (Y252,272,444,500, 700,730F)	GRM6/svV40	ON-BCs	Subretinal and IVT	Mouse	Van Wyck 2015[225]
AAV2/2-Y444F	mGluR500P	Mostly RBCs	IVT	Mouse	Lu 2016
	200En-SV40	Mostly RBCs	IVT	Mouse	Lu 2016
	In4s-In3-200En-mGluR500P	ON-BCs	IVT	Mouse and marmoset	Lu 2016
AAV2.7m8-Y444F	In4s-In3-200En-mGluR500P	ON-BCs	IVT	Mouse and marmoset	Lu 2016
AAV2/8BP2	4xGRM6-SV40	ON-BCs	Subretinal and IVT	Mouse	Cronin 2014[226]
AAV2(quadY-F+T-V)	Ple155	BCs	IVT	Mouse	Scalabrino 2015
AAV2/2[ <i>MAX</i> ]	RHO	Rods	IVT	Mouse	Hasan 2019

## Timing of treatment

cCSNB is congenital and stationary and yet no treatment is available. Gene therapy seems the best approach and should be, in theory, applicable at any age.

The first attempt to restore the cCSNB phenotype was done in the *nob* model, lacking *Nyx*. Gregg and colleagues generated transgenic mice through pronuclear injection of a transgene consisting of a promoter fragment of the GABA<sub>A</sub>ρ1 gene, to drive the expression of the gene in BCs, and the cDNA of the murine *Nyx* gene fused to EYFP. These animals were bred with *Nyx<sup>nob/nob</sup>* mice leading to heterozygous mice producing the EYFP-*Nyx* protein, and called “*nob* rescued”. EYFP-*Nyx* was localized to the dendritic tips of ON-BCs in these *nob*-rescued mice, along with ERG responses under both scotopic and photopic conditions and RGCs ON-responses [195]. This study showed that a wild-type copy of nyctalopin expressed in BCs was sufficient to restore the cCSNB phenotype in *nob* mice, when introduced prior to birth.

In the first LRIT3 gene therapy proof-of-concept, a stronger functional rescue was obtained in P5 injected mice (about 45% of the b-wave amplitude found in wild-type) compared to P35 injected mice (about 20%). Similarly, no functional rescue was obtained for the *Nyx* gene therapy approach in P30 treated animals while a partial rescue of the scotopic b-wave was observed in P2 treated animals [198]. In parallel, we decided to try to restore LRIT3 expression in P30 *Lrit3<sup>-/-</sup>* mice. When targeting photoreceptors, we managed to partially restore the ERG b-wave under scotopic conditions in adult *Lrit3<sup>-/-</sup>* mice in an even better proportion than in P5 animals as described by Hasan and coworkers [126]. In regard to these three studies, the choice of the AAV/promoter is decisive to ensure an efficient transduction of the adult retina.

However, in the *Nyx* approach, photopic responses rescue was mild and was described as having “components that resembled the one found in wild-type”. In the study by Hasan and colleagues, at both ages, no photopic ERG responses were recorded, probably due to the use of the rhodopsin promoter which is supposed to drive the expression of the transgene in rod photoreceptors [126]. In our LRIT3 approach, no photopic restoration was noted even in mice that presented a strong rescue under scotopic conditions. These gene therapy approaches for cCSNB point out the fact that photopic restoration is harder to achieve than scotopic rescue.

## Photopic rescue

It has been shown that proteins involved in either icCSNB or cCSNB also have a role in synapse formation and/or maintenance. Indeed, in *Lrit3*<sup>-/-</sup> mice, a decreased number of invaginating contacts made by CBCs in the cone pedicle and a striking decrease in the number of triads [47]. Normal cone pedicles were also observed indicating that LRIT3 is not essential for the natural formation of the cone-to-cone BC synapse but plays a major role in this process [47]. Furthermore, peanut agglutinin (PNA) staining is abolished in the OPL of *Lrit3*<sup>-/-</sup> mice [24] and LRIT3 mutated dogs [90], meaning that conformation of the synapse is distorted in these animals [90]. It was also described that mGluR6 seems to play a role at the photoreceptor to BC synapse. Indeed, invaginating dendrites of RBCs are larger and often contain ectopic ribbons while the number of invaginating dendrites of cone ON-BCs and ribbons decrease at the cone pedicles in the *Grm6*<sup>tm1Nak</sup> mouse model [121, 122]. The same observation was made in *Gβ5*<sup>-/-</sup> mice where there is a significant reduction of the number of triads in the OPL of these mice [227]. Finally, it has been previously shown that Ca<sub>v</sub>1.4, encoded by CACNA1F which mutations induce icCSNB, plays a role in the synaptic development and maintenance since the loss of this calcium channel at the synapse provokes gross morphological abnormalities of the presynaptic terminal, like shortened ribbons [191-193]. In conclusion, there are strong indicators that proteins at the synapse between photoreceptors and ON-BCs also have a structural role. This would explain the lack of photopic rescue in our *Lrit3*<sup>-/-</sup> treated mice, as applying such treatment in adult mice, when the synapse is fully formed, might not restore the cone-mediated pathway as the transmission between cones and cone ON-BCs is constitutively diminished. Cone initiate ribbon synapse formation between P4 and P5 in mice [228], and the cone synaptogenesis is completed by P14 to P15 [228, 229]. It would also clarify why P2 animals in the NYX gene therapy better responded to the treatment than P30 mice, and consistent with normal photopic responses noted in “nob rescued” animals [195]. Expression studies of the different proteins of the ON-BCs signaling cascade throughout the development of the retina would be interesting to perform. It also cannot be excluded that these proteins are important for synaptogenesis in mice but might not be in humans. Therefore, for the LRIT3 project, it would be interesting to perform injections with our construct targeting both rods and cones in younger mice, to decipher if the lack of photopic rescue is solely due to the timing of treatment.

However, in general the photopic phenotype of cCSNB mice models is more severe than the one of patients or larger animal models: no b-wave is observed in photopic conditions in any of the cCSNB mice models [17] while cone-driven responses are comparable between CSNB dogs, horses and patients e.g. mildly reduced [17, 82, 87, 88]; scotopic ERG responses are similar in all models [17]. Different cellular contribution in the origin of the photopic b-wave noted between rodents and primates might explain this difference of the cone ERG b-wave. For example, in the mouse cone ERG, only a small contribution of the OFF-BCs to the photopic b-wave was noted [230] while OFF-BCs contribute to a large proportion to the cone ERG b-wave responses in primates [231]. Therefore, different pathways may be implicated in cCSNB mouse model, explaining the absence of functional restoration under photopic conditions. Consequently, using a mouse model of CSNB displaying a more severe photopic phenotype than patients might therefore not be the ideal way to assess cone-driven pathway restoration following treatment. Recently a CSNB beagle dog affected by *LRIT3* mutations was described [88, 90] and the testing of the gene therapy approach described in this thesis on this large animal model would probably evaluate more precisely the photopic phenotype restoration after treatment.

### III. WHAT IS LEFT TO DECIPHER

Following the testing of two different promoters to drive the expression of *Lrit3* either in ON-BCs or in photoreceptors as described in this thesis, the exact localization of LRIT3 is still puzzling. Previously, LRIT3 was thought to be localized post-synaptically at the dendritic tips of ON-BCs in the OPL due to the isolated ON-BC defect observed in cCSNB patients [79] and other proteins involved in cCSNB localize at the ON-BCs dendritic tips [17]. However, expression data [127] and recent findings [126] suggest photoreceptor expression of *Lrit3* and presynaptic localization. Hence, the pre- or post-synaptic localization of LRIT3 is still not clearly elucidated, but it is certainly present in the OPL in human and mouse retina [79, 116, 125, 126]. We also obtained a restoration of the functional phenotype when targeting ON-BCs, PRs or both. One way to decipher the exact localization of LRIT3 would be through expansion microscopy [232]. This technique allows much a higher-resolution than regular light microscopy. Following staining of LRIT3, this technique would allow observing the synapse between photoreceptors and ON-BCs in a much precise way and concluding on the localization of LRIT3.

TRPM1 is the second most prevalent gene causing cCSNB, is expressed by both melanocytes and ON-BCs and is crucial for the proper signal transmission between photoreceptors and ON-BCS [147]. Yet, TRPM1 gene therapy has not been tested. Indeed, its relatively big size (5.4 kb) prevents its encapsidation in AAVs. This issue, encountered in several other IRDs like Stargardt's disease (STGD1) or Usher Syndrome type 1B (USH1B), could in theory be overcome by the use of the dual AAV technique or lentiviral vectors. Dual AAVs can be used to each one encapsidate one part of the gene that will, once injected, reconstitute the gene by splicing, homologous recombination or a combination of both. This technique has already been validated in mice models of STGD1 or USH1B after subretinal injection [233]. However, the studies published about dual AAVs so far did not describe expression levels that matched the ones obtained with a single AAV vector [234-236]. Lentiviral vectors (LV) are less efficient in photoreceptor transduction than AAVs [237]. However, the EIAV LV subtype of LV showed photoreceptors transduction in the macaque retina after subretinal injection [238]. To date, none of these approaches have been tested using intravitreal injection to target ON-BCs.

# References

---

1. Kolb H, Fernandez E, Nelson R. Simple anatomy of the retina. *Webvision : The organization of the Retina and the Visual System*. 2005. PubMed PMID: 17428984.
2. Treuting PM. *Special Sense: Eye*. Academic Press. 2012; *Comparative Anatomy and Histology*:395-418. doi: <https://doi.org/10.1016/B978-0-12-381361-9.00021-4>.
3. Bassett EA, Wallace VA. Cell fate determination in the vertebrate retina. *Trends in neurosciences*. 2012;35(9):565-73. doi: 10.1016/j.tins.2012.05.004. PubMed PMID: 22704732.
4. Mann I. *The Development of the Human Eye*, 3rd Edition. Grune and Stratton, Inc. 1964.
5. Lu Y. Single-cell analysis of human retina identifies evolutionarily conserved and species-specific mechanisms controlling development. *BioRxiv*. 2019. doi: <https://doi.org/10.1101/779694>
6. Nathans J. In the eye of the beholder: visual pigments and inherited variation in human vision. *Cell*. 1994;78(3):357-60. doi: 10.1016/0092-8674(94)90414-6. PubMed PMID: 8062382.
7. Jacobs GH, Neitz J, Deegan JF, 2nd. Retinal receptors in rodents maximally sensitive to ultraviolet light. *Nature*. 1991;353(6345):655-6. doi: 10.1038/353655a0. PubMed PMID: 1922382.
8. Curcio CA, Sloan KR, Kalina RE, Hendrickson AE. Human photoreceptor topography. *The Journal of comparative neurology*. 1990;292(4):497-523. doi: 10.1002/cne.902920402. PubMed PMID: 2324310.
9. Volland S, Esteve-Rudd J, Hoo J, Yee C, Williams DS. A comparison of some organizational characteristics of the mouse central retina and the human macula. *PloS one*. 2015;10(4):e0125631. doi: 10.1371/journal.pone.0125631. PubMed PMID: 25923208; PubMed Central PMCID: PMC4414478.
10. Carter-Dawson LD, LaVail MM. Rods and cones in the mouse retina. I. Structural analysis using light and electron microscopy. *The Journal of comparative neurology*. 1979;188(2):245-62. doi: 10.1002/cne.901880204. PubMed PMID: 500858.
11. Zeitz C. Molecular genetics and protein function involved in nocturnal vision. *Expert Rev Ophthalmol*. 2007;2:19.
12. Ahnelt P, Keri C, Kolb H. Identification of pedicles of putative blue-sensitive cones in the human retina. *The Journal of comparative neurology*. 1990;293(1):39-53. doi: 10.1002/cne.902930104. PubMed PMID: 2312791.
13. Haverkamp S, Grunert U, Wassle H. The cone pedicle, a complex synapse in the retina. *Neuron*. 2000;27(1):85-95. doi: 10.1016/s0896-6273(00)00011-8. PubMed PMID: 10939333.
14. Wassle H. Parallel processing in the mammalian retina. *Nature reviews Neuroscience*. 2004;5(10):747-57. doi: 10.1038/nrn1497. PubMed PMID: 15378035.
15. Catterall WA. Structure and regulation of voltage-gated Ca<sup>2+</sup> channels. *Annual review of cell and developmental biology*. 2000;16:521-55. doi: 10.1146/annurev.cellbio.16.1.521. PubMed PMID: 11031246.
16. Arikath J, Campbell KP. Auxiliary subunits: essential components of the voltage-gated calcium channel complex. *Current opinion in neurobiology*. 2003;13(3):298-307. doi: 10.1016/s0959-4388(03)00066-7. PubMed PMID: 12850214.

17. Zeitz C, Robson AG, Audo I. Congenital stationary night blindness: an analysis and update of genotype-phenotype correlations and pathogenic mechanisms. *Prog Retin Eye Res.* 2015;45:58-110. doi: 10.1016/j.preteyeres.2014.09.001. PubMed PMID: 25307992.
18. Nakajima Y, Iwakabe H, Akazawa C, Nawa H, Shigemoto R, Mizuno N, et al. Molecular characterization of a novel retinal metabotropic glutamate receptor mGluR6 with a high agonist selectivity for L-2-amino-4-phosphonobutyrate. *J Biol Chem.* 1993;268(16):11868-73. PubMed PMID: 8389366.
19. Nomura A, Shigemoto R, Nakamura Y, Okamoto N, Mizuno N, Nakanishi S. Developmentally regulated postsynaptic localization of a metabotropic glutamate receptor in rat rod bipolar cells. *Cell.* 1994;77(3):361-9. doi: 10.1016/0092-8674(94)90151-1. PubMed PMID: 8181056.
20. Nawy S. The metabotropic receptor mGluR6 may signal through G(o), but not phosphodiesterase, in retinal bipolar cells. *J Neurosci.* 1999;19(8):2938-44. PubMed PMID: 10191311.
21. Morgans CW, Zhang J, Jeffrey BG, Nelson SM, Burke NS, Duvoisin RM, et al. TRPM1 is required for the depolarizing light response in retinal ON-bipolar cells. *Proceedings of the National Academy of Sciences of the United States of America.* 2009;106(45):19174-8. doi: 10.1073/pnas.0908711106. PubMed PMID: 19861548; PubMed Central PMCID: PMC2776419.
22. Ray TA, Heath KM, Hasan N, Noel JM, Samuels IS, Martemyanov KA, et al. GPR179 is required for high sensitivity of the mGluR6 signaling cascade in depolarizing bipolar cells. *The Journal of neuroscience : the official journal of the Society for Neuroscience.* 2014;34(18):6334-43. doi: 10.1523/JNEUROSCI.4044-13.2014. PubMed PMID: 24790204; PubMed Central PMCID: PMC4004817.
23. Pearring JN, Bojang P, Jr., Shen Y, Koike C, Furukawa T, Nawy S, et al. A role for nyctalopin, a small leucine-rich repeat protein, in localizing the TRP melastatin 1 channel to retinal depolarizing bipolar cell dendrites. *The Journal of neuroscience : the official journal of the Society for Neuroscience.* 2011;31(27):10060-6. doi: 10.1523/JNEUROSCI.1014-11.2011. PubMed PMID: 21734298; PubMed Central PMCID: PMC3139999.
24. Neuille M, Morgans CW, Cao Y, Orhan E, Michiels C, Sahel JA, et al. LRIT3 is essential to localize TRPM1 to the dendritic tips of depolarizing bipolar cells and may play a role in cone synapse formation. *Invest Ophthalmol Vis Sci.* 2015:ARVO E-Abstract 2612.
25. DeVries SH, Baylor DA. An alternative pathway for signal flow from rod photoreceptors to ganglion cells in mammalian retina. *Proceedings of the National Academy of Sciences of the United States of America.* 1995;92(23):10658-62. doi: 10.1073/pnas.92.23.10658. PubMed PMID: 7479860; PubMed Central PMCID: PMC40671.
26. Schneiderman H. The Fundusoscopic Examination. In: rd, Walker HK, Hall WD, Hurst JW, editors. *Clinical Methods: The History, Physical, and Laboratory Examinations.* Boston1990.
27. Marmor MF. Long-term follow-up of the physiologic abnormalities and fundus changes in fundus albipunctatus. *Ophthalmology.* 1990;97(3):380-4. doi: 10.1016/s0161-6420(90)32577-0. PubMed PMID: 2336278.
28. Sorsby A, Franceschetti A, Joseph R, Davey JB. Choroideremia; clinical and genetic aspects. *The British journal of ophthalmology.* 1952;36(10):547-81. doi: 10.1136/bjo.36.10.547. PubMed PMID: 12978235; PubMed Central PMCID: PMC1323990.
29. Hartong DT, Berson EL, Dryja TP. Retinitis pigmentosa. *Lancet.* 2006;368(9549):1795-809. doi: 10.1016/S0140-6736(06)69740-7. PubMed PMID: 17113430.

30. Mitamura Y, Mitamura-Aizawa S, Nagasawa T, Katome T, Eguchi H, Naito T. Diagnostic imaging in patients with retinitis pigmentosa. *The journal of medical investigation : JMI*. 2012;59(1-2):1-11. doi: 10.2152/jmi.59.1. PubMed PMID: 22449988.
31. Berger A, Cavallero S, Dominguez E, Barbe P, Simonutti M, Sahel JA, et al. Spectral-domain optical coherence tomography of the rodent eye: highlighting layers of the outer retina using signal averaging and comparison with histology. *PloS one*. 2014;9(5):e96494. doi: 10.1371/journal.pone.0096494. PubMed PMID: 24788712; PubMed Central PMCID: PMC4008571.
32. Luu MKaC. Visual Acuity. *Webvision : The organization of the Retina and the Visual System*.
33. Cline D, Hofstetter HW., Griffin JR. *Dictionary of visual science*. Butterworth-Heinemann. 1997.
34. Group ETDRSR. Early Treatment Diabetic Retinopathy Study Design and Baseline Patient Characteristics: ETDRS Report Number 7. *Ophthalmology*. 1991.
35. Ferris FL, 3rd, Freidlin V, Kassoff A, Green SB, Milton RC. Relative letter and position difficulty on visual acuity charts from the Early Treatment Diabetic Retinopathy Study. *American journal of ophthalmology*. 1993;116(6):735-40. doi: 10.1016/s0002-9394(14)73474-9. PubMed PMID: 8250077.
36. Kniestedt C, Stamper RL. Visual acuity and its measurement. *Ophthalmology clinics of North America*. 2003;16(2):155-70, v. doi: 10.1016/s0896-1549(03)00013-0. PubMed PMID: 12809155.
37. Braddick O. Where is the naso-temporal asymmetry? Motion processing. *Current biology : CB*. 1996;6(3):250-3. doi: 10.1016/s0960-9822(02)00470-0. PubMed PMID: 8805231.
38. Abdeljalil J, Hamid M, Abdel-Mouttalib O, Stephane R, Raymond R, Johan A, et al. The optomotor response: a robust first-line visual screening method for mice. *Vision research*. 2005;45(11):1439-46. doi: 10.1016/j.visres.2004.12.015. PubMed PMID: 15743613.
39. Dawson WW, Trick GL, Litzkow CA. Improved electrode for electroretinography. *Investigative ophthalmology & visual science*. 1979;18(9):988-91. PubMed PMID: 478786.
40. McCulloch DL, Marmor MF, Brigell MG, Hamilton R, Holder GE, Tzekov R, et al. ISCEV Standard for full-field clinical electroretinography (2015 update). *Documenta ophthalmologica Advances in ophthalmology*. 2015;130(1):1-12. doi: 10.1007/s10633-014-9473-7. PubMed PMID: 25502644.
41. Heynen H, Wachtmeister L, van Norren D. Origin of the oscillatory potentials in the primate retina. *Vision research*. 1985;25(10):1365-73. doi: 10.1016/0042-6989(85)90214-7. PubMed PMID: 4090272.
42. Miyake Y. Macular oscillatory potentials in humans. Macular OPs. *Documenta ophthalmologica Advances in ophthalmology*. 1990;75(2):111-24. doi: 10.1007/bf00146547. PubMed PMID: 2276312.
43. Noell WK. The origin of the electroretinogram. *American journal of ophthalmology*. 1954;38(1:2):78-90. doi: 10.1016/0002-9394(54)90012-4. PubMed PMID: 13180621.
44. Steinberg RH, Schmidt R, Brown KT. Intracellular responses to light from cat pigment epithelium: origin of the electroretinogram c-wave. *Nature*. 1970;227(5259):728-30. doi: 10.1038/227728a0. PubMed PMID: 5432076.
45. Xu X, Karwoski C. Current source density analysis of the electroretinographic d wave of frog retina. *Journal of neurophysiology*. 1995;73(6):2459-69. doi: 10.1152/jn.1995.73.6.2459. PubMed PMID: 7666152.

46. Mace E, Caplette R, Marre O, Sengupta A, Chaffiol A, Barbe P, et al. Targeting channelrhodopsin-2 to ON-bipolar cells with vitreally administered AAV Restores ON and OFF visual responses in blind mice. *Molecular therapy : the journal of the American Society of Gene Therapy*. 2015;23(1):7-16. doi: 10.1038/mt.2014.154. PubMed PMID: 25095892; PubMed Central PMCID: PMC4270733.
47. Neuille M, Cao Y, Caplette R, Guerrero-Given D, Thomas C, Kamasawa N, et al. LRIT3 Differentially Affects Connectivity and Synaptic Transmission of Cones to ON- and OFF-Bipolar Cells. *Investigative ophthalmology & visual science*. 2017;58(3):1768-78. doi: 10.1167/iovs.16-20745. PubMed PMID: 28334377; PubMed Central PMCID: PMC5374884.
48. Riggs LA. Electroretinography in cases of night blindness. *American journal of ophthalmology*. 1954;38(1:2):70-8. PubMed PMID: 13180620.
49. Schubert G, Bornschein H. Analysis of the human electroretinogram. *Ophthalmologica*. 1952;123(7):396-413. PubMed PMID: 26203955.
50. Dryja TP, Berson EL, Rao VR, Oprian DD. Heterozygous missense mutation in the rhodopsin gene as a cause of congenital stationary night blindness. *Nature genetics*. 1993;4(3):280-3. doi: 10.1038/ng0793-280. PubMed PMID: 8358437.
51. Gal A, Orth U, Baehr W, Schwinger E, Rosenberg T. Heterozygous missense mutation in the rod cGMP phosphodiesterase beta-subunit gene in autosomal dominant stationary night blindness. *Nature genetics*. 1994;7(1):64-8. doi: 10.1038/ng0594-64. PubMed PMID: 8075643.
52. Gal A, Xu S, Piczenik Y, Eiberg H, Duvigneau C, Schwinger E, et al. Gene for autosomal dominant congenital stationary night blindness maps to the same region as the gene for the beta-subunit of the rod photoreceptor cGMP phosphodiesterase (PDEB) in chromosome 4p16.3. *Human molecular genetics*. 1994;3(2):323-5. doi: 10.1093/hmg/3.2.323. PubMed PMID: 8004102.
53. Dryja TP, Hahn LB, Reboul T, Arnaud B. Missense mutation in the gene encoding the alpha subunit of rod transducin in the Nougaret form of congenital stationary night blindness. *Nature genetics*. 1996;13(3):358-60. doi: 10.1038/ng0796-358. PubMed PMID: 8673138.
54. Riazuddin SA, Shahzadi A, Zeitz C, Ahmed ZM, Ayyagari R, Chavali VR, et al. A mutation in SLC24A1 implicated in autosomal-recessive congenital stationary night blindness. *American journal of human genetics*. 2010;87(4):523-31. doi: 10.1016/j.ajhg.2010.08.013. PubMed PMID: 20850105; PubMed Central PMCID: PMC2948789.
55. Neuille M, Malaichamy S, Vadala M, Michiels C, Condroyer C, Sachidanandam R, et al. Next-generation sequencing confirms the implication of SLC24A1 in autosomal-recessive congenital stationary night blindness. *Clin Genet*. 2016;89(6):690-9. doi: 10.1111/cge.12746. PubMed PMID: 26822852.
56. Yamamoto H, Simon A, Eriksson U, Harris E, Berson EL, Dryja TP. Mutations in the gene encoding 11-cis retinol dehydrogenase cause delayed dark adaptation and fundus albipunctatus. *Nature genetics*. 1999;22(2):188-91. doi: 10.1038/9707. PubMed PMID: 10369264.
57. Dryja TP. Molecular genetics of Oguchi disease, fundus albipunctatus, and other forms of stationary night blindness: LVII Edward Jackson Memorial Lecture. *American journal of ophthalmology*. 2000;130(5):547-63. doi: 10.1016/s0002-9394(00)00737-6. PubMed PMID: 11078833.
58. Oguchi C. Uber eine Abart von Hemeralopie. *Acta Soc Ophthalmol Jpn*. 1907;11:123-34.

59. Mizuo B. On a new discovery in the dark adaptation of Oguchi's disease. *Acta Soc Ophthalmol Jpn.* 1913;17:1854-9.
60. Mizuo G, Nakamura, B. . On new discovery in dark adaptation in Oguchi's disease. *Acta Soc Ophthalmol Jpn.* 1914;18:73-127.
61. Miyake Y, Yagasaki K, Horiguchi M, Kawase Y, Kanda T. Congenital stationary night blindness with negative electroretinogram. A new classification. *Archives of ophthalmology.* 1986;104(7):1013-20. PubMed PMID: 3488053.
62. Bijveld MM, van Genderen MM, Hoeben FP, Katzin AA, van Nispen RM, Riemsdag FC, et al. Assessment of night vision problems in patients with congenital stationary night blindness. *PLoS one.* 2013;8(5):e62927. doi: 10.1371/journal.pone.0062927. PubMed PMID: 23658786; PubMed Central PMCID: PMC3643903.
63. Bijveld MM, Florijn RJ, Bergen AA, van den Born LI, Kamermans M, Prick L, et al. Genotype and phenotype of 101 dutch patients with congenital stationary night blindness. *Ophthalmology.* 2013;120(10):2072-81. PubMed PMID: 23714322.
64. Sustar M, Holder GE, Kremers J, Barnes CS, Lei B, Khan NW, et al. ISCEV extended protocol for the photopic On-Off ERG. *Documenta ophthalmologica Advances in ophthalmology.* 2018;136(3):199-206. doi: 10.1007/s10633-018-9645-y. PubMed PMID: 29934802; PubMed Central PMCID: PMC6061123.
65. Bech-Hansen NT, Naylor MJ, Maybaum TA, Pearce WG, Koop B, Fishman GA, et al. Loss-of-function mutations in a calcium-channel alpha1-subunit gene in Xp11.23 cause incomplete X-linked congenital stationary night blindness. *Nat Genet.* 1998;19(3):264-7. PubMed PMID: 9662400.
66. Strom TM, Nyakatura G, Apfelstedt-Sylla E, Hellebrand H, Lorenz B, Weber BH, et al. An L-type calcium-channel gene mutated in incomplete X-linked congenital stationary night blindness. *Nature genetics.* 1998;19(3):260-3. doi: 10.1038/940. PubMed PMID: 9662399.
67. Zeitz C, Kloeckener-Gruissem B, Forster U, Kohl S, Magyar I, Wissinger B, et al. Mutations in CABP4, the gene encoding the Ca<sup>2+</sup>-binding protein 4, cause autosomal recessive night blindness. *American journal of human genetics.* 2006;79(4):657-67. doi: 10.1086/508067. PubMed PMID: 16960802; PubMed Central PMCID: PMC1592568.
68. Wycisk KA, Zeitz C, Feil S, Wittmer M, Forster U, Neidhardt J, et al. Mutation in the auxiliary calcium-channel subunit CACNA2D4 causes autosomal recessive cone dystrophy. *American journal of human genetics.* 2006;79(5):973-7. doi: 10.1086/508944. PubMed PMID: 17033974; PubMed Central PMCID: PMC1698577.
69. Ba-Abbad R, Arno G, Carss K, Stirrups K, Penkett CJ, Moore AT, et al. Mutations in CACNA2D4 Cause Distinctive Retinal Dysfunction in Humans. *Ophthalmology.* 2016;123(3):668-71 e2. doi: 10.1016/j.optha.2015.09.045. PubMed PMID: 26560832.
70. Zeitz C, Varin J., Audo I. Congenital Stationary Night Blindness (CSNB). In: Hartnett, editor. *Genetics and Developmental Disorders in Pediatric Retina. III: Wolters Kluwer, Inc; 2020.*
71. Bech-Hansen NT, Naylor MJ, Maybaum TA, Sparkes RL, Koop B, Birch DG, et al. Mutations in NYX, encoding the leucine-rich proteoglycan nyctalopin, cause X-linked complete congenital stationary night blindness. *Nature genetics.* 2000;26(3):319-23. doi: 10.1038/81619. PubMed PMID: 11062471.
72. Pusch CM, Zeitz C, Brandau O, Pesch K, Achatz H, Feil S, et al. The complete form of X-linked congenital stationary night blindness is caused by mutations in a gene encoding a leucine-rich repeat protein. *Nature genetics.* 2000;26(3):324-7. doi: 10.1038/81627. PubMed PMID: 11062472.

73. Audo I, Kohl S, Leroy BP, Munier FL, Guillonneau X, Mohand-Said S, et al. TRPM1 is mutated in patients with autosomal-recessive complete congenital stationary night blindness. *American journal of human genetics*. 2009;85(5):720-9. doi: 10.1016/j.ajhg.2009.10.013. PubMed PMID: 19896113; PubMed Central PMCID: PMC2775830.
74. Li Z, Sergouniotis PI, Michaelides M, Mackay DS, Wright GA, Devery S, et al. Recessive mutations of the gene TRPM1 abrogate ON bipolar cell function and cause complete congenital stationary night blindness in humans. *American journal of human genetics*. 2009;85(5):711-9. doi: 10.1016/j.ajhg.2009.10.003. PubMed PMID: 19878917; PubMed Central PMCID: PMC2775833.
75. van Genderen MM, Bijveld MM, Claassen YB, Florijn RJ, Pearring JN, Meire FM, et al. Mutations in TRPM1 are a common cause of complete congenital stationary night blindness. *American journal of human genetics*. 2009;85(5):730-6. doi: 10.1016/j.ajhg.2009.10.012. PubMed PMID: 19896109; PubMed Central PMCID: PMC2775826.
76. Dryja TP, McGee TL, Berson EL, Fishman GA, Sandberg MA, Alexander KR, et al. Night blindness and abnormal cone electroretinogram ON responses in patients with mutations in the GRM6 gene encoding mGluR6. *Proceedings of the National Academy of Sciences of the United States of America*. 2005;102(13):4884-9. doi: 10.1073/pnas.0501233102. PubMed PMID: 15781871; PubMed Central PMCID: PMC555731.
77. Zeitz C, van Genderen M, Neidhardt J, Luhmann UF, Hoeben F, Forster U, et al. Mutations in GRM6 cause autosomal recessive congenital stationary night blindness with a distinctive scotopic 15-Hz flicker electroretinogram. *Investigative ophthalmology & visual science*. 2005;46(11):4328-35. doi: 10.1167/iovs.05-0526. PubMed PMID: 16249515.
78. Audo I, Bujakowska K, Orhan E, Poloschek CM, Defoort-Dhellemmes S, Drumare I, et al. Whole-exome sequencing identifies mutations in GPR179 leading to autosomal-recessive complete congenital stationary night blindness. *American journal of human genetics*. 2012;90(2):321-30. doi: 10.1016/j.ajhg.2011.12.007. PubMed PMID: 22325361; PubMed Central PMCID: PMC3276675.
79. Zeitz C, Jacobson SG, Hamel CP, Bujakowska K, Neuville M, Orhan E, et al. Whole-exome sequencing identifies LRIT3 mutations as a cause of autosomal-recessive complete congenital stationary night blindness. *American journal of human genetics*. 2013;92(1):67-75. doi: 10.1016/j.ajhg.2012.10.023. PubMed PMID: 23246293; PubMed Central PMCID: PMC3542465.
80. Peachey NS, Ray TA, Florijn R, Rowe LB, Sjoerdsma T, Contreras-Alcantara S, et al. GPR179 is required for depolarizing bipolar cell function and is mutated in autosomal-recessive complete congenital stationary night blindness. *American journal of human genetics*. 2012;90(2):331-9. doi: 10.1016/j.ajhg.2011.12.006. PubMed PMID: 22325362; PubMed Central PMCID: PMC3276656.
81. Dan H, Song X, Li J, Xing Y, Li T. Mutation screening of the LRIT3, CABP4, and GPR179 genes in Chinese patients with Schubert-Bornschein congenital stationary night blindness. *Ophthalmic genetics*. 2017;38(3):206-10. doi: 10.1080/13816810.2016.1193876. PubMed PMID: 27428514.
82. Witzel DA, Smith EL, Wilson RD, Aguirre GD. Congenital stationary night blindness: an animal model. *Invest Ophthalmol Vis Sci*. 1978;17(8):788-95. PubMed PMID: 308060.
83. Sandmeyer LS, Bellone RR, Archer S, Bauer BS, Nelson J, Forsyth G, et al. Congenital stationary night blindness is associated with the leopard complex in the Miniature Horse. *Veterinary ophthalmology*. 2012;15(1):18-22. doi: 10.1111/j.1463-5224.2011.00903.x. PubMed PMID: 22051042.

84. Hack YL, Crabtree EE, Avila F, Sutton RB, Grahn RA, Oh A, et al. Whole genome sequencing identifies missense mutation in GRM6 as the likely cause of congenital stationary night blindness in a Tennessee Walking Horse. *Equine veterinary journal*. 2020. doi: 10.1111/evj.13318. PubMed PMID: 32654228.
85. Bellone RR, Forsyth G, Leeb T, Archer S, Sigurdsson S, Imsland F, et al. Fine-mapping and mutation analysis of TRPM1: a candidate gene for leopard complex (LP) spotting and congenital stationary night blindness in horses. *Brief Funct Genomics*. 2010;9(3):193-207. doi: 10.1093/bfgp/elq002. PubMed PMID: 20353955.
86. Bellone RR, Holl H, Setaluri V, Devi S, Maddodi N, Archer S, et al. Evidence for a retroviral insertion in TRPM1 as the cause of congenital stationary night blindness and leopard complex spotting in the horse. *PloS one*. 2013;8(10):e78280. doi: 10.1371/journal.pone.0078280. PubMed PMID: 24167615; PubMed Central PMCID: PMC3805535.
87. Sandmeyer LS, Breaux CB, Archer S, Grahn BH. Clinical and electroretinographic characteristics of congenital stationary night blindness in the Appaloosa and the association with the leopard complex. *Vet Ophthalmol*. 2007;10(6):368-75. PubMed PMID: 17970998.
88. Kondo M, Das G, Imai R, Santana E, Nakashita T, Imawaka M, et al. A Naturally Occurring Canine Model of Autosomal Recessive Congenital Stationary Night Blindness. *PloS one*. 2015;10(9):e0137072. doi: 10.1371/journal.pone.0137072. PubMed PMID: 26368928; PubMed Central PMCID: PMC4569341.
89. Oh A, Loew ER, Foster ML, Davidson MG, English RV, Gervais KJ, et al. Phenotypic characterization of complete CSNB in the inbred research beagle: how common is CSNB in research and companion dogs? *Documenta ophthalmologica Advances in ophthalmology*. 2018;137(2):87-101. doi: 10.1007/s10633-018-9653-y. PubMed PMID: 30051304.
90. Das RG, Becker D, Jagannathan V, Goldstein O, Santana E, Carlin K, et al. Genome-wide association study and whole-genome sequencing identify a deletion in LRIT3 associated with canine congenital stationary night blindness. *Scientific reports*. 2019;9(1):14166. doi: 10.1038/s41598-019-50573-7. PubMed PMID: 31578364; PubMed Central PMCID: PMC6775105.
91. Bahadori R, Biehlmaier O, Zeitz C, Labhart T, Makhankov YV, Forster U, et al. Nyctalopin is essential for synaptic transmission in the cone dominated zebrafish retina. *The European journal of neuroscience*. 2006;24(6):1664-74. doi: 10.1111/j.1460-9568.2006.05053.x. PubMed PMID: 17004930.
92. Huang YY, Haug MF, Gesemann M, Neuhaus SC. Novel expression patterns of metabotropic glutamate receptor 6 in the zebrafish nervous system. *PloS one*. 2012;7(4):e35256. doi: 10.1371/journal.pone.0035256. PubMed PMID: 22523578; PubMed Central PMCID: PMC3327648.
93. Pardue MT, McCall MA, LaVail MM, Gregg RG, Peachey NS. A naturally occurring mouse model of X-linked congenital stationary night blindness. *Investigative ophthalmology & visual science*. 1998;39(12):2443-9. PubMed PMID: 9804152.
94. Gregg RGR, T. A.; Hasan, N.; McCall, M. A.; Peachey N. S. Interdependence Among Members of the mGluR6 G-protein Mediated Signalplex of Retinal Depolarizing Bipolar Cells. In: Springer, editor. *G Protein Signaling Mechanisms in the Retina* 2014. p. 67-79.
95. Gregg RG, Mukhopadhyay S, Candille SI, Ball SL, Pardue MT, McCall MA, et al. Identification of the gene and the mutation responsible for the mouse nob phenotype. *Investigative ophthalmology & visual science*. 2003;44(1):378-84. doi: 10.1167/iovs.02-0501. PubMed PMID: 12506099.

96. Koike C, Obara T, Uriu Y, Numata T, Sanuki R, Miyata K, et al. TRPM1 is a component of the retinal ON bipolar cell transduction channel in the mGluR6 cascade. *Proceedings of the National Academy of Sciences of the United States of America*. 2010;107(1):332-7. doi: 10.1073/pnas.0912730107. PubMed PMID: 19966281; PubMed Central PMCID: PMC2806705.
97. Cao Y, Sarria I, Fehlhauer KE, Kamasawa N, Orlandi C, James KN, et al. Mechanism for Selective Synaptic Wiring of Rod Photoreceptors into the Retinal Circuitry and Its Role in Vision. *Neuron*. 2015;87(6):1248-60. doi: 10.1016/j.neuron.2015.09.002. PubMed PMID: 26402607; PubMed Central PMCID: PMC4583715.
98. Shen Y, Heimel JA, Kamermans M, Peachey NS, Gregg RG, Nawy S. A transient receptor potential-like channel mediates synaptic transmission in rod bipolar cells. *The Journal of neuroscience : the official journal of the Society for Neuroscience*. 2009;29(19):6088-93. doi: 10.1523/JNEUROSCI.0132-09.2009. PubMed PMID: 19439586; PubMed Central PMCID: PMC2752970.
99. Peachey NS, Pearing JN, Bojang P, Jr., Hirschtritt ME, Sturgill-Short G, Ray TA, et al. Depolarizing bipolar cell dysfunction due to a Trpm1 point mutation. *Journal of neurophysiology*. 2012;108(9):2442-51. doi: 10.1152/jn.00137.2012. PubMed PMID: 22896717; PubMed Central PMCID: PMC3545183.
100. Masu M, Iwakabe H, Tagawa Y, Miyoshi T, Yamashita M, Fukuda Y, et al. Specific deficit of the ON response in visual transmission by targeted disruption of the mGluR6 gene. *Cell*. 1995;80(5):757-65. PubMed PMID: 7889569.
101. Xu Y, Dhingra A, Fina ME, Koike C, Furukawa T, Vardi N. mGluR6 deletion renders the TRPM1 channel in retina inactive. *J Neurophysiol*. 2012;107(3):948-57. PubMed PMID: 22131384.
102. Tagawa Y, Sawai H, Ueda Y, Tauchi M, Nakanishi S. Immunohistological studies of metabotropic glutamate receptor subtype 6-deficient mice show no abnormality of retinal cell organization and ganglion cell maturation. *J Neurosci*. 1999;19(7):2568-79. PubMed PMID: 10087070; PubMed Central PMCID: PMC6786083.
103. Maddox DM, Vessey KA, Yarbrough GL, Invergo BM, Cantrell DR, Inayat S, et al. Allelic variance between GRM6 mutants, Grm6nob3 and Grm6nob4 results in differences in retinal ganglion cell visual responses. *The Journal of physiology*. 2008;586(18):4409-24. doi: 10.1113/jphysiol.2008.157289. PubMed PMID: 18687716; PubMed Central PMCID: PMC2614010.
104. Orlandi C, Cao Y, Martemyanov KA. Orphan receptor GPR179 forms macromolecular complexes with components of metabotropic signaling cascade in retina ON-bipolar neurons. *Investigative ophthalmology & visual science*. 2013;54(10):7153-61. doi: 10.1167/iovs.13-12907. PubMed PMID: 24114537; PubMed Central PMCID: PMC3813323.
105. Cao Y, Posokhova E, Martemyanov KA. TRPM1 forms complexes with nyctalopin in vivo and accumulates in postsynaptic compartment of ON-bipolar neurons in mGluR6-dependent manner. *The Journal of neuroscience : the official journal of the Society for Neuroscience*. 2011;31(32):11521-6. doi: 10.1523/JNEUROSCI.1682-11.2011. PubMed PMID: 21832182; PubMed Central PMCID: PMC3164511.
106. Morgans CW, Weiwei L, Wensel TG, Brown RL, Perez-Leon JA, Bearnot B, et al. Gbeta5-RGS complexes co-localize with mGluR6 in retinal ON-bipolar cells. *The European journal of neuroscience*. 2007;26(10):2899-905. doi: 10.1111/j.1460-9568.2007.05867.x. PubMed PMID: 18001285; PubMed Central PMCID: PMC435197.
107. Pinto LH, Vitaterna MH, Shimomura K, Siepka SM, Balannik V, McDearmon EL, et al. Generation, identification and functional characterization of the nob4 mutation of Grm6 in

- the mouse. *Visual neuroscience*. 2007;24(1):111-23. doi: 10.1017/S0952523807070149. PubMed PMID: 17430614; PubMed Central PMCID: PMC3770726.
108. Cao Y, Masuho I, Okawa H, Xie K, Asami J, Kammermeier PJ, et al. Retina-specific GTPase accelerator RGS11/G beta 5S/R9AP is a constitutive heterotrimer selectively targeted to mGluR6 in ON-bipolar neurons. *The Journal of neuroscience : the official journal of the Society for Neuroscience*. 2009;29(29):9301-13. doi: 10.1523/JNEUROSCI.1367-09.2009. PubMed PMID: 19625520; PubMed Central PMCID: PMC3770726.
109. Qian H, Ji R, Gregg RG, Peachey NS. Identification of a new mutant allele, *Grm6(nob7)*, for complete congenital stationary night blindness. *Visual neuroscience*. 2015;32:E004. doi: 10.1017/S0952523815000012. PubMed PMID: 26241901; PubMed Central PMCID: PMC4648616.
110. Peachey NS, Hasan N, FitzMaurice B, Burrill S, Pangen G, Karst SY, et al. A missense mutation in *Grm6* reduces but does not eliminate mGluR6 expression or rod depolarizing bipolar cell function. *Journal of neurophysiology*. 2017;118(2):845-54. doi: 10.1152/jn.00888.2016. PubMed PMID: 28490646; PubMed Central PMCID: PMC5539458.
111. Orlandi C, Posokhova E, Masuho I, Ray TA, Hasan N, Gregg RG, et al. GPR158/179 regulate G protein signaling by controlling localization and activity of the RGS7 complexes. *The Journal of cell biology*. 2012;197(6):711-9. doi: 10.1083/jcb.201202123. PubMed PMID: 22689652; PubMed Central PMCID: PMC3373406.
112. Sarria I, Orlandi C, McCall MA, Gregg RG, Martemyanov KA. Intermolecular Interaction between Anchoring Subunits Specify Subcellular Targeting and Function of RGS Proteins in Retina ON-Bipolar Neurons. *The Journal of neuroscience : the official journal of the Society for Neuroscience*. 2016;36(10):2915-25. doi: 10.1523/JNEUROSCI.3833-15.2016. PubMed PMID: 26961947; PubMed Central PMCID: PMC4783495.
113. Balmer J, Ji R, Ray TA, Selber F, Gassmann M, Peachey NS, et al. Presence of the *Gpr179(nob5)* allele in a C3H-derived transgenic mouse. *Molecular vision*. 2013;19:2615-25. PubMed PMID: 24415894; PubMed Central PMCID: PMC3883591.
114. Neuille M, El Shamieh S, Orhan E, Michiels C, Antonio A, Lancelot ME, et al. *Lrit3* deficient mouse (*nob6*): a novel model of complete congenital stationary night blindness (cCSNB). *PloS one*. 2014;9(3):e90342. doi: 10.1371/journal.pone.0090342. PubMed PMID: 24598786; PubMed Central PMCID: PMC3943948.
115. Charette JR, Samuels IS, Yu M, Stone L, Hicks W, Shi LY, et al. A Chemical Mutagenesis Screen Identifies Mouse Models with ERG Defects. *Advances in experimental medicine and biology*. 2016;854:177-83. doi: 10.1007/978-3-319-17121-0\_24. PubMed PMID: 26427409.
116. Hasan N, Pangen G, Ray TA, Fransen KM, Noel J, Borghuis BG, et al. *LRIT3* is required for Nyctalopin expression and normal ON and OFF pathway signaling in the retina. *eNeuro*. 2020. doi: 10.1523/ENEURO.0002-20.2020. PubMed PMID: 31959619.
117. Nakamura M, Sanuki R, Yasuma TR, Onishi A, Nishiguchi KM, Koike C, et al. *TRPM1* mutations are associated with the complete form of congenital stationary night blindness. *Molecular vision*. 2010;16:425-37. PubMed PMID: 20300565; PubMed Central PMCID: PMC2838739.
118. Zeitz C, Forster U, Neidhardt J, Feil S, Kalin S, Leifert D, et al. Night blindness-associated mutations in the ligand-binding, cysteine-rich, and intracellular domains of the metabotropic glutamate receptor 6 abolish protein trafficking. *Human mutation*. 2007;28(8):771-80. doi: 10.1002/humu.20499. PubMed PMID: 17405131.

119. Dong JY, Fan PD, Frizzell RA. Quantitative analysis of the packaging capacity of recombinant adeno-associated virus. *Human gene therapy*. 1996;7(17):2101-12. doi: 10.1089/hum.1996.7.17-2101. PubMed PMID: 8934224.
120. Hashimoto T, Inazawa J, Okamoto N, Tagawa Y, Bessho Y, Honda Y, et al. The whole nucleotide sequence and chromosomal localization of the gene for human metabotropic glutamate receptor subtype 6. *The European journal of neuroscience*. 1997;9(6):1226-35. PubMed PMID: 9215706.
121. Ishii M, Morigiwa K, Takao M, Nakanishi S, Fukuda Y, Mimura O, et al. Ectopic synaptic ribbons in dendrites of mouse retinal ON- and OFF-bipolar cells. *Cell and tissue research*. 2009;338(3):355-75. doi: 10.1007/s00441-009-0880-0. PubMed PMID: 19859741; PubMed Central PMCID: PMC2779389.
122. Tsukamoto Y, Omi N. Effects of mGluR6-deficiency on photoreceptor ribbon synapse formation: comparison of electron microscopic analysis of serial sections with random sections. *Visual neuroscience*. 2014;31(1):39-46. doi: 10.1017/S0952523813000473. PubMed PMID: 24801622.
123. Tummala SR, Dhingra A, Fina ME, Li JJ, Ramakrishnan H, Vardi N. Lack of mGluR6-related cascade elements leads to retrograde trans-synaptic effects on rod photoreceptor synapses via matrix-associated proteins. *The European journal of neuroscience*. 2016;43(11):1509-22. doi: 10.1111/ejn.13243. PubMed PMID: 27037829; PubMed Central PMCID: PMC4899192.
124. Kim SD, Liu JL, Roscioli T, Buckley MF, Yagnik G, Boyadjiev SA, et al. Leucine-rich repeat, immunoglobulin-like and transmembrane domain 3 (LRIT3) is a modulator of FGFR1. *FEBS letters*. 2012;586(10):1516-21. doi: 10.1016/j.febslet.2012.04.010. PubMed PMID: 22673519; PubMed Central PMCID: PMC3372856.
125. Neuille M, Morgans CW, Cao Y, Orhan E, Michiels C, Sahel JA, et al. LRIT3 is essential to localize TRPM1 to the dendritic tips of depolarizing bipolar cells and may play a role in cone synapse formation. *The European journal of neuroscience*. 2015;42(3):1966-75. doi: 10.1111/ejn.12959. PubMed PMID: 25997951.
126. Hasan N, Pangeni G, Cobb CA, Ray TA, Nettesheim ER, Ertel KJ, et al. Presynaptic Expression of LRIT3 Transsynaptically Organizes the Postsynaptic Glutamate Signaling Complex Containing TRPM1. *Cell reports*. 2019;27(11):3107-16 e3. doi: 10.1016/j.celrep.2019.05.056. PubMed PMID: 31189098; PubMed Central PMCID: PMC6628893.
127. Shekhar K, Lapan SW, Whitney IE, Tran NM, Macosko EZ, Kowalczyk M, et al. Comprehensive Classification of Retinal Bipolar Neurons by Single-Cell Transcriptomics. *Cell*. 2016;166(5):1308-23 e30. doi: 10.1016/j.cell.2016.07.054. PubMed PMID: 27565351; PubMed Central PMCID: PMC5003425.
128. Thirkill CE, FitzGerald P, Sergott RC, Roth AM, Tyler NK, Keltner JL. Cancer-associated retinopathy (CAR syndrome) with antibodies reacting with retinal, optic-nerve, and cancer cells. *The New England journal of medicine*. 1989;321(23):1589-94. doi: 10.1056/NEJM198912073212307. PubMed PMID: 2555714.
129. Thirkill CE, Roth AM, Keltner JL. Cancer-associated retinopathy. *Arch Ophthalmol*. 1987;105(3):372-5. PubMed PMID: 2950846.
130. Berson EL, Lessell S. Paraneoplastic night blindness with malignant melanoma. *Am J Ophthalmol*. 1988;106(3):307-11. PubMed PMID: 2971322.

131. Canamary AM, Jr., Takahashi WY, Sallum JMF. Autoimmune retinopathy: A Review. *International journal of retina and vitreous*. 2018;4:1. doi: 10.1186/s40942-017-0104-9. PubMed PMID: 29340169; PubMed Central PMCID: PMC5759752.
132. Alexander KR, Fishman GA, Peachey NS, Marchese AL, Tso MO. 'On' response defect in paraneoplastic night blindness with cutaneous malignant melanoma. *Investigative ophthalmology & visual science*. 1992;33(3):477-83. PubMed PMID: 1544774.
133. Kondo M, Sanuki R, Ueno S, Nishizawa Y, Hashimoto N, Ohguro H, et al. Identification of autoantibodies against TRPM1 in patients with paraneoplastic retinopathy associated with ON bipolar cell dysfunction. *PLoS ONE*. 2011;6(5):e19911. doi: 10.1371/journal.pone.0019911. PubMed PMID: 21611200; PubMed Central PMCID: PMC3096646.
134. Goetgebuer G, Kestelyn-Stevens AM, De Laey JJ, Kestelyn P, Leroy BP. Cancer-associated retinopathy (CAR) with electronegative ERG: a case report. *Documenta ophthalmologica Advances in ophthalmology*. 2008;116(1):49-55. doi: 10.1007/s10633-007-9074-9. PubMed PMID: 17721792.
135. Dhingra A, Fina ME, Neinstein A, Ramsey DJ, Xu Y, Fishman GA, et al. Autoantibodies in melanoma-associated retinopathy target TRPM1 cation channels of retinal ON bipolar cells. *The Journal of neuroscience : the official journal of the Society for Neuroscience*. 2011;31(11):3962-7. doi: 10.1523/JNEUROSCI.6007-10.2011. PubMed PMID: 21411639; PubMed Central PMCID: PMC3073846.
136. Wang Y, Abu-Asab MS, Li W, Aronow ME, Singh AD, Chan CC. Autoantibody against transient receptor potential M1 cation channels of retinal ON bipolar cells in paraneoplastic vitelliform retinopathy. *BMC ophthalmology*. 2012;12:56. doi: 10.1186/1471-2415-12-56. PubMed PMID: 23148706; PubMed Central PMCID: PMC3514129.
137. Xiong WH, Duvoisin RM, Adamus G, Jeffrey BG, Gellman C, Morgans CW. Serum TRPM1 autoantibodies from melanoma associated retinopathy patients enter retinal on-bipolar cells and attenuate the electroretinogram in mice. *PloS one*. 2013;8(8):e69506. doi: 10.1371/journal.pone.0069506. PubMed PMID: 23936334; PubMed Central PMCID: PMC3731326.
138. Ueno S, Nishiguchi KM, Tanioka H, Enomoto A, Yamanouchi T, Kondo M, et al. Degeneration of retinal on bipolar cells induced by serum including autoantibody against TRPM1 in mouse model of paraneoplastic retinopathy. *PloS one*. 2013;8(11):e81507. doi: 10.1371/journal.pone.0081507. PubMed PMID: 24282602; PubMed Central PMCID: PMC3840061.
139. Dalal MD, Morgans CW, Duvoisin RM, Gamboa EA, Jeffrey BG, Garg SJ, et al. Diagnosis of occult melanoma using transient receptor potential melastatin 1 (TRPM1) autoantibody testing: a novel approach. *Ophthalmology*. 2013;120(12):2560-4. doi: 10.1016/j.ophtha.2013.07.037. PubMed PMID: 24053997; PubMed Central PMCID: PMC4928578.
140. Morita Y, Kimura K, Fujitsu Y, Enomoto A, Ueno S, Kondo M, et al. Autoantibodies to transient receptor potential cation channel, subfamily M, member 1 in a Japanese patient with melanoma-associated retinopathy. *Jpn J Ophthalmol*. 2014;58(2):166-71. doi: 10.1007/s10384-013-0300-6. PubMed PMID: 24468869.
141. Ueno S, Ito Y, Maruko R, Kondo M, Terasaki H. Choroidal atrophy in a patient with paraneoplastic retinopathy and anti-TRPM1 antibody. *Clinical ophthalmology*. 2014;8:369-73. doi: 10.2147/OPHTH.S55124. PubMed PMID: 24523577; PubMed Central PMCID: PMC3921079.

142. Ueno S, Nakanishi A, Nishi K, Suzuki S, Terasaki H. Case of paraneoplastic retinopathy with retinal ON-bipolar cell dysfunction and subsequent resolution of ERGs. *Documenta ophthalmologica Advances in ophthalmology*. 2015;130(1):71-6. doi: 10.1007/s10633-014-9470-x. PubMed PMID: 25391361.
143. Duvoisin RM, Haley TL, Ren G, Strycharska-Orczyk I, Bonaparte JP, Morgans CW. Autoantibodies in Melanoma-Associated Retinopathy Recognize an Epitope Conserved Between TRPM1 and TRPM3. *Investigative ophthalmology & visual science*. 2017;58(5):2732-8. doi: 10.1167/iovs.17-21443. PubMed PMID: 28549093; PubMed Central PMCID: PMC5455167.
144. Roels D, Ueno S, Talianu CD, Draganova D, Kondo M, Leroy BP. Unilateral cancer-associated retinopathy: diagnosis, serology and treatment. *Documenta ophthalmologica Advances in ophthalmology*. 2017;135(3):233-40. doi: 10.1007/s10633-017-9605-y. PubMed PMID: 28815346.
145. Ueno S, Inooka D, Nakanishi A, Okado S, Yasuda S, Kominami T, et al. Clinical Course of Paraneoplastic Retinopathy with Anti-Trpm1 Autoantibody in Japanese Cohort. *Retina*. 2018. doi: 10.1097/IAE.0000000000002329. PubMed PMID: 30260920.
146. Duvoisin RM, Ren G, Haley TL, Taylor MH, Morgans CW. TRPM1 Autoantibodies in Melanoma Patients Without Self-Reported Visual Symptoms. *Investigative ophthalmology & visual science*. 2019;60(6):2330-5. doi: 10.1167/iovs.19-26775. PubMed PMID: 31117125; PubMed Central PMCID: PMC6532695.
147. Oancea E, Vriens J, Brauchi S, Jun J, Splawski I, Clapham DE. TRPM1 forms ion channels associated with melanin content in melanocytes. *Science signaling*. 2009;2(70):ra21. doi: 10.1126/scisignal.2000146. PubMed PMID: 19436059; PubMed Central PMCID: PMC4086358.
148. Devi S, Kedlaya R, Maddodi N, Bhat KM, Weber CS, Valdivia H, et al. Calcium homeostasis in human melanocytes: role of transient receptor potential melastatin 1 (TRPM1) and its regulation by ultraviolet light. *American journal of physiology Cell physiology*. 2009;297(3):C679-87. doi: 10.1152/ajpcell.00092.2009. PubMed PMID: 19587221; PubMed Central PMCID: PMC2740396.
149. Broadgate S, Yu J, Downes SM, Halford S. Unravelling the genetics of inherited retinal dystrophies: Past, present and future. *Progress in retinal and eye research*. 2017;59:53-96. doi: 10.1016/j.preteyeres.2017.03.003. PubMed PMID: 28363849.
150. Lee JH, Wang JH, Chen J, Li F, Edwards TL, Hewitt AW, et al. Gene therapy for visual loss: Opportunities and concerns. *Progress in retinal and eye research*. 2019;68:31-53. doi: 10.1016/j.preteyeres.2018.08.003. PubMed PMID: 30170104.
151. Willett K, Bennett J. Immunology of AAV-Mediated Gene Transfer in the Eye. *Frontiers in immunology*. 2013;4:261. doi: 10.3389/fimmu.2013.00261. PubMed PMID: 24009613; PubMed Central PMCID: PMC3757345.
152. Trapani I, Auricchio A. Seeing the Light after 25 Years of Retinal Gene Therapy. *Trends in molecular medicine*. 2018;24(8):669-81. doi: 10.1016/j.molmed.2018.06.006. PubMed PMID: 29983335.
153. Cideciyan AV, Aleman TS, Boye SL, Schwartz SB, Kaushal S, Roman AJ, et al. Human gene therapy for RPE65 isomerase deficiency activates the retinoid cycle of vision but with slow rod kinetics. *Proceedings of the National Academy of Sciences of the United States of America*. 2008;105(39):15112-7. doi: 10.1073/pnas.0807027105. PubMed PMID: 18809924; PubMed Central PMCID: PMC2567501.

154. Bainbridge JW, Smith AJ, Barker SS, Robbie S, Henderson R, Balaggan K, et al. Effect of gene therapy on visual function in Leber's congenital amaurosis. *The New England journal of medicine*. 2008;358(21):2231-9. doi: 10.1056/NEJMoa0802268. PubMed PMID: 18441371.
155. Maguire AM, Simonelli F, Pierce EA, Pugh EN, Jr., Mingozzi F, Bennicelli J, et al. Safety and efficacy of gene transfer for Leber's congenital amaurosis. *The New England journal of medicine*. 2008;358(21):2240-8. doi: 10.1056/NEJMoa0802315. PubMed PMID: 18441370; PubMed Central PMCID: PMC2829748.
156. LaFontaine JS, Fathe K, Smyth HD. Delivery and therapeutic applications of gene editing technologies ZFNs, TALENs, and CRISPR/Cas9. *International journal of pharmaceutics*. 2015;494(1):180-94. doi: 10.1016/j.ijpharm.2015.08.029. PubMed PMID: 26278489.
157. Hammond SM, Wood MJ. Genetic therapies for RNA mis-splicing diseases. *Trends in genetics : TIG*. 2011;27(5):196-205. doi: 10.1016/j.tig.2011.02.004. PubMed PMID: 21497936.
158. Kole R, Krieg AM. Exon skipping therapy for Duchenne muscular dystrophy. *Advanced drug delivery reviews*. 2015;87:104-7. doi: 10.1016/j.addr.2015.05.008. PubMed PMID: 25980936.
159. Gerard X, Perrault I, Hanein S, Silva E, Bigot K, Defoort-Delhemmes S, et al. AON-mediated Exon Skipping Restores Ciliation in Fibroblasts Harboring the Common Leber Congenital Amaurosis CEP290 Mutation. *Molecular therapy Nucleic acids*. 2012;1:e29. doi: 10.1038/mtna.2012.21. PubMed PMID: 23344081; PubMed Central PMCID: PMC3390222.
160. Collin RW, den Hollander AI, van der Velde-Visser SD, Bennicelli J, Bennett J, Cremers FP. Antisense Oligonucleotide (AON)-based Therapy for Leber Congenital Amaurosis Caused by a Frequent Mutation in CEP290. *Molecular therapy Nucleic acids*. 2012;1:e14. doi: 10.1038/mtna.2012.3. PubMed PMID: 23343883; PubMed Central PMCID: PMC3381589.
161. Cideciyan AV, Jacobson SG, Drack AV, Ho AC, Charng J, Garafalo AV, et al. Effect of an intravitreal antisense oligonucleotide on vision in Leber congenital amaurosis due to a photoreceptor cilium defect. *Nature medicine*. 2019;25(2):225-8. doi: 10.1038/s41591-018-0295-0. PubMed PMID: 30559420.
162. Warrington KH, Jr., Herzog RW. Treatment of human disease by adeno-associated viral gene transfer. *Human genetics*. 2006;119(6):571-603. doi: 10.1007/s00439-006-0165-6. PubMed PMID: 16612615.
163. Petrs-Silva H, Dinculescu A, Li Q, Min SH, Chiodo V, Pang JJ, et al. High-efficiency transduction of the mouse retina by tyrosine-mutant AAV serotype vectors. *Molecular therapy : the journal of the American Society of Gene Therapy*. 2009;17(3):463-71. doi: 10.1038/mt.2008.269. PubMed PMID: 19066593; PubMed Central PMCID: PMC2835095.
164. Dalkara D, Byrne LC, Klimczak RR, Visel M, Yin L, Merigan WH, et al. In vivo-directed evolution of a new adeno-associated virus for therapeutic outer retinal gene delivery from the vitreous. *Science translational medicine*. 2013;5(189):189ra76. doi: 10.1126/scitranslmed.3005708. PubMed PMID: 23761039.
165. Surace EM, Auricchio A. Versatility of AAV vectors for retinal gene transfer. *Vision research*. 2008;48(3):353-9. doi: 10.1016/j.visres.2007.07.027. PubMed PMID: 17923143.
166. Khabou H, Dalkara D. [Developments in gene delivery vectors for ocular gene therapy]. *Medecine sciences : M/S*. 2015;31(5):529-37. doi: 10.1051/medsci/20153105015. PubMed PMID: 26059304.
167. Marlhens F, Bareil C, Griffoin JM, Zrenner E, Amalric P, Eliaou C, et al. Mutations in RPE65 cause Leber's congenital amaurosis. *Nature genetics*. 1997;17(2):139-41. doi: 10.1038/ng1097-139. PubMed PMID: 9326927.

168. Leber T. Uber retinitis pigmentosa und angeborene amaurose. Graefe's archive for clinical and experimental ophthalmology = Albrecht von Graefes Archiv fur klinische und experimentelle Ophthalmologie. 1869;15:1–25.
169. Van Hooser JP, Aleman TS, He YG, Cideciyan AV, Kuksa V, Pittler SJ, et al. Rapid restoration of visual pigment and function with oral retinoid in a mouse model of childhood blindness. *Proceedings of the National Academy of Sciences of the United States of America*. 2000;97(15):8623-8. doi: 10.1073/pnas.150236297. PubMed PMID: 10869443; PubMed Central PMCID: PMC26998.
170. Acland GM, Aguirre GD, Ray J, Zhang Q, Aleman TS, Cideciyan AV, et al. Gene therapy restores vision in a canine model of childhood blindness. *Nature genetics*. 2001;28(1):92-5. doi: 10.1038/ng0501-92. PubMed PMID: 11326284.
171. Bennicelli J, Wright JF, Komaromy A, Jacobs JB, Hauck B, Zeleniaia O, et al. Reversal of blindness in animal models of leber congenital amaurosis using optimized AAV2-mediated gene transfer. *Molecular therapy : the journal of the American Society of Gene Therapy*. 2008;16(3):458-65. doi: 10.1038/sj.mt.6300389. PubMed PMID: 18209734; PubMed Central PMCID: PMC2842085.
172. Acland GM, Aguirre GD, Bennett J, Aleman TS, Cideciyan AV, Bennicelli J, et al. Long-term restoration of rod and cone vision by single dose rAAV-mediated gene transfer to the retina in a canine model of childhood blindness. *Molecular therapy : the journal of the American Society of Gene Therapy*. 2005;12(6):1072-82. doi: 10.1016/j.ymthe.2005.08.008. PubMed PMID: 16226919; PubMed Central PMCID: PMC3647373.
173. Bennett J, Wellman J, Marshall KA, McCague S, Ashtari M, DiStefano-Pappas J, et al. Safety and durability of effect of contralateral-eye administration of AAV2 gene therapy in patients with childhood-onset blindness caused by RPE65 mutations: a follow-on phase 1 trial. *Lancet*. 2016;388(10045):661-72. doi: 10.1016/S0140-6736(16)30371-3. PubMed PMID: 27375040; PubMed Central PMCID: PMC5351775.
174. Nicoletti A, Wong DJ, Kawase K, Gibson LH, Yang-Feng TL, Richards JE, et al. Molecular characterization of the human gene encoding an abundant 61 kDa protein specific to the retinal pigment epithelium. *Human molecular genetics*. 1995;4(4):641-9. doi: 10.1093/hmg/4.4.641. PubMed PMID: 7633413.
175. Ali RR, Reichel MB, Thrasher AJ, Levinsky RJ, Kinnon C, Kanuga N, et al. Gene transfer into the mouse retina mediated by an adeno-associated viral vector. *Human molecular genetics*. 1996;5(5):591-4. doi: 10.1093/hmg/5.5.591. PubMed PMID: 8733124.
176. Jacobson SG, Cideciyan AV, Aguirre GD, Roman AJ, Sumaroka A, Hauswirth WW, et al. Improvement in vision: a new goal for treatment of hereditary retinal degenerations. *Expert opinion on orphan drugs*. 2015;3(5):563-75. doi: 10.1517/21678707.2015.1030393. PubMed PMID: 26246977; PubMed Central PMCID: PMC4487613.
177. Bainbridge JW, Mehat MS, Sundaram V, Robbie SJ, Barker SE, Ripamonti C, et al. Long-term effect of gene therapy on Leber's congenital amaurosis. *The New England journal of medicine*. 2015;372(20):1887-97. doi: 10.1056/NEJMoa1414221. PubMed PMID: 25938638; PubMed Central PMCID: PMC4497809.
178. Cideciyan AV, Jacobson SG, Beltran WA, Sumaroka A, Swider M, Iwabe S, et al. Human retinal gene therapy for Leber congenital amaurosis shows advancing retinal degeneration despite enduring visual improvement. *Proceedings of the National Academy of Sciences of the United States of America*. 2013;110(6):E517-25. doi: 10.1073/pnas.1218933110. PubMed PMID: 23341635; PubMed Central PMCID: PMC3568385.

179. MacLaren RE, Groppe M, Barnard AR, Cottrill CL, Tolmachova T, Seymour L, et al. Retinal gene therapy in patients with choroideremia: initial findings from a phase 1/2 clinical trial. *Lancet*. 2014;383(9923):1129-37. doi: 10.1016/S0140-6736(13)62117-0. PubMed PMID: 24439297; PubMed Central PMCID: PMC4171740.
180. Edwards TL, Jolly JK, Groppe M, Barnard AR, Cottrill CL, Tolmachova T, et al. Visual Acuity after Retinal Gene Therapy for Choroideremia. *The New England journal of medicine*. 2016;374(20):1996-8. doi: 10.1056/NEJMc1509501. PubMed PMID: 27120491; PubMed Central PMCID: PMC4996318.
181. Komaromy AM, Alexander JJ, Rowlan JS, Garcia MM, Chiodo VA, Kaya A, et al. Gene therapy rescues cone function in congenital achromatopsia. *Human molecular genetics*. 2010;19(13):2581-93. doi: 10.1093/hmg/ddq136. PubMed PMID: 20378608; PubMed Central PMCID: PMC2883338.
182. Alexander JJ, Umino Y, Everhart D, Chang B, Min SH, Li Q, et al. Restoration of cone vision in a mouse model of achromatopsia. *Nature medicine*. 2007;13(6):685-7. doi: 10.1038/nm1596. PubMed PMID: 17515894; PubMed Central PMCID: PMC3985124.
183. Ellouze S, Augustin S, Bouaita A, Bonnet C, Simonutti M, Forster V, et al. Optimized allotopic expression of the human mitochondrial ND4 prevents blindness in a rat model of mitochondrial dysfunction. *American journal of human genetics*. 2008;83(3):373-87. doi: 10.1016/j.ajhg.2008.08.013. PubMed PMID: 18771762; PubMed Central PMCID: PMC2556433.
184. Smith AJ, Schlichtenbrede FC, Tschernutter M, Bainbridge JW, Thrasher AJ, Ali RR. AAV-Mediated gene transfer slows photoreceptor loss in the RCS rat model of retinitis pigmentosa. *Molecular therapy : the journal of the American Society of Gene Therapy*. 2003;8(2):188-95. doi: 10.1016/s1525-0016(03)00144-8. PubMed PMID: 12907141.
185. Choi VW, Bigelow CE, McGee TL, Gujar AN, Li H, Hanks SM, et al. AAV-mediated RLBP1 gene therapy improves the rate of dark adaptation in Rlbp1 knockout mice. *Molecular therapy Methods & clinical development*. 2015;2:15022. doi: 10.1038/mtm.2015.22. PubMed PMID: 26199951; PubMed Central PMCID: PMC4495722.
186. Bennett J, Tanabe T, Sun D, Zeng Y, Kjeldbye H, Gouras P, et al. Photoreceptor cell rescue in retinal degeneration (rd) mice by in vivo gene therapy. *Nature medicine*. 1996;2(6):649-54. doi: 10.1038/nm0696-649. PubMed PMID: 8640555.
187. Allocca M, Doria M, Petrillo M, Colella P, Garcia-Hoyos M, Gibbs D, et al. Serotype-dependent packaging of large genes in adeno-associated viral vectors results in effective gene delivery in mice. *The Journal of clinical investigation*. 2008;118(5):1955-64. doi: 10.1172/JCI34316. PubMed PMID: 18414684; PubMed Central PMCID: PMC2298836.
188. Hashimoto T, Gibbs D, Lillo C, Azarian SM, Legacki E, Zhang XM, et al. Lentiviral gene replacement therapy of retinas in a mouse model for Usher syndrome type 1B. *Gene therapy*. 2007;14(7):584-94. doi: 10.1038/sj.gt.3302897. PubMed PMID: 17268537.
189. Hong DH, Pawlyk BS, Adamian M, Sandberg MA, Li T. A single, abbreviated RPGR-ORF15 variant reconstitutes RPGR function in vivo. *Investigative ophthalmology & visual science*. 2005;46(2):435-41. doi: 10.1167/iovs.04-1065. PubMed PMID: 15671266.
190. Zeng Y, Takada Y, Kjellstrom S, Hiriyanna K, Tanikawa A, Wawrousek E, et al. RS-1 Gene Delivery to an Adult Rs1h Knockout Mouse Model Restores ERG b-Wave with Reversal of the Electronegative Waveform of X-Linked Retinoschisis. *Investigative ophthalmology & visual science*. 2004;45(9):3279-85. doi: 10.1167/iovs.04-0576. PubMed PMID: 15326152.
191. Mansergh F, Orton NC, Vessey JP, Lalonde MR, Stell WK, Tremblay F, et al. Mutation of the calcium channel gene *Cacna1f* disrupts calcium signaling, synaptic transmission and

- cellular organization in mouse retina. *Human molecular genetics*. 2005;14(20):3035-46. doi: 10.1093/hmg/ddi336. PubMed PMID: 16155113.
192. Liu X, Kerov V, Haeseleer F, Majumder A, Artemyev N, Baker SA, et al. Dysregulation of Ca(v)1.4 channels disrupts the maturation of photoreceptor synaptic ribbons in congenital stationary night blindness type 2. *Channels*. 2013;7(6):514-23. doi: 10.4161/chan.26376. PubMed PMID: 24064553; PubMed Central PMCID: PMC4042486.
193. Zabouri N, Haverkamp S. Calcium channel-dependent molecular maturation of photoreceptor synapses. *PLoS ONE*. 2013;8(5):e63853. doi: 10.1371/journal.pone.0063853. PubMed PMID: 23675510; PubMed Central PMCID: PMC3652833.
194. Laird JG, Gardner SH, Kopel AJ, Kerov V, Lee A, Baker SA. Rescue of Rod Synapses by Induction of Cav Alpha 1F in the Mature Cav1.4 Knock-Out Mouse Retina. *Investigative ophthalmology & visual science*. 2019;60(8):3150-61. doi: 10.1167/iovs.19-27226. PubMed PMID: 31335952; PubMed Central PMCID: PMC6656410.
195. Gregg RG, Kamermans M, Klooster J, Lukasiewicz PD, Peachey NS, Vessey KA, et al. Nyctalopin expression in retinal bipolar cells restores visual function in a mouse model of complete X-linked congenital stationary night blindness. *Journal of neurophysiology*. 2007;98(5):3023-33. doi: 10.1152/jn.00608.2007. PubMed PMID: 17881478; PubMed Central PMCID: PMC2933657.
196. Kay CN, Ryals RC, Aslanidi GV, Min SH, Ruan Q, Sun J, et al. Targeting photoreceptors via intravitreal delivery using novel, capsid-mutated AAV vectors. *PloS one*. 2013;8(4):e62097. doi: 10.1371/journal.pone.0062097. PubMed PMID: 23637972; PubMed Central PMCID: PMC3637363.
197. de Leeuw CN, Dyka FM, Boye SL, Laprise S, Zhou M, Chou AY, et al. Targeted CNS Delivery Using Human MiniPromoters and Demonstrated Compatibility with Adeno-Associated Viral Vectors. *Molecular therapy Methods & clinical development*. 2014;1:5. doi: 10.1038/mtm.2013.5. PubMed PMID: 24761428; PubMed Central PMCID: PMC3992516.
198. Scalabrino ML, Boye SL, Fransen KM, Noel JM, Dyka FM, Min SH, et al. Intravitreal delivery of a novel AAV vector targets ON bipolar cells and restores visual function in a mouse model of complete congenital stationary night blindness. *Human molecular genetics*. 2015;24(21):6229-39. doi: 10.1093/hmg/ddv341. PubMed PMID: 26310623; PubMed Central PMCID: PMC4612567.
199. Liang FQ, Aleman TS, Dejneka NS, Dudas L, Fisher KJ, Maguire AM, et al. Long-term protection of retinal structure but not function using RAAV.CNTF in animal models of retinitis pigmentosa. *Molecular therapy : the journal of the American Society of Gene Therapy*. 2001;4(5):461-72. doi: 10.1006/mthe.2001.0473. PubMed PMID: 11708883.
200. McGee Sanftner LH, Abel H, Hauswirth WW, Flannery JG. Glial cell line derived neurotrophic factor delays photoreceptor degeneration in a transgenic rat model of retinitis pigmentosa. *Molecular therapy : the journal of the American Society of Gene Therapy*. 2001;4(6):622-9. doi: 10.1006/mthe.2001.0498. PubMed PMID: 11735347.
201. Buch PK, MacLaren RE, Duran Y, Balaggan KS, MacNeil A, Schlichtenbrede FC, et al. In contrast to AAV-mediated Cntf expression, AAV-mediated Gdnf expression enhances gene replacement therapy in rodent models of retinal degeneration. *Molecular therapy : the journal of the American Society of Gene Therapy*. 2006;14(5):700-9. doi: 10.1016/j.ymthe.2006.05.019. PubMed PMID: 16872907.
202. Byrne LC, Dalkara D, Luna G, Fisher SK, Clerin E, Sahel JA, et al. Viral-mediated RdCVF and RdCVFL expression protects cone and rod photoreceptors in retinal degeneration. *The*

- Journal of clinical investigation. 2015;125(1):105-16. doi: 10.1172/JCI65654. PubMed PMID: 25415434; PubMed Central PMCID: PMC4382269.
203. Leveillard T, Mohand-Said S, Lorentz O, Hicks D, Fintz AC, Clerin E, et al. Identification and characterization of rod-derived cone viability factor. *Nature genetics*. 2004;36(7):755-9. doi: 10.1038/ng1386. PubMed PMID: 15220920.
204. Yao J, Feathers KL, Khanna H, Thompson D, Tsilfidis C, Hauswirth WW, et al. XIAP therapy increases survival of transplanted rod precursors in a degenerating host retina. *Investigative ophthalmology & visual science*. 2011;52(3):1567-72. doi: 10.1167/iovs.10-5998. PubMed PMID: 20926819; PubMed Central PMCID: PMC3101692.
205. Birch DG, Bennett LD, Duncan JL, Weleber RG, Pennesi ME. Long-term Follow-up of Patients With Retinitis Pigmentosa Receiving Intraocular Ciliary Neurotrophic Factor Implants. *American journal of ophthalmology*. 2016;170:10-4. doi: 10.1016/j.ajo.2016.07.013. PubMed PMID: 27457255; PubMed Central PMCID: PMC5056139.
206. Bi A, Cui J, Ma YP, Olshevskaya E, Pu M, Dizhoor AM, et al. Ectopic expression of a microbial-type rhodopsin restores visual responses in mice with photoreceptor degeneration. *Neuron*. 2006;50(1):23-33. doi: 10.1016/j.neuron.2006.02.026. PubMed PMID: 16600853; PubMed Central PMCID: PMC1459045.
207. Tomita H, Sugano E, Yawo H, Ishizuka T, Isago H, Narikawa S, et al. Restoration of visual response in aged dystrophic RCS rats using AAV-mediated channelopsin-2 gene transfer. *Investigative ophthalmology & visual science*. 2007;48(8):3821-6. doi: 10.1167/iovs.06-1501. PubMed PMID: 17652757.
208. Lagali PS, Balya D, Awatramani GB, Munch TA, Kim DS, Busskamp V, et al. Light-activated channels targeted to ON bipolar cells restore visual function in retinal degeneration. *Nature neuroscience*. 2008;11(6):667-75. doi: 10.1038/nn.2117. PubMed PMID: 18432197.
209. Sengupta A, Chaffiol A, Mace E, Caplette R, Desrosiers M, Lampic M, et al. Red-shifted channelrhodopsin stimulation restores light responses in blind mice, macaque retina, and human retina. *EMBO molecular medicine*. 2016;8(11):1248-64. doi: 10.15252/emmm.201505699. PubMed PMID: 27679671; PubMed Central PMCID: PMC5090658.
210. Khabou H, Garita-Hernandez M, Chaffiol A, Reichman S, Jaillard C, Brazhnikova E, et al. Noninvasive gene delivery to foveal cones for vision restoration. *JCI insight*. 2018;3(2). doi: 10.1172/jci.insight.96029. PubMed PMID: 29367457; PubMed Central PMCID: PMC5821199.
211. De Silva SR, Barnard AR, Hughes S, Tam SKE, Martin C, Singh MS, et al. Long-term restoration of visual function in end-stage retinal degeneration using subretinal human melanopsin gene therapy. *Proceedings of the National Academy of Sciences of the United States of America*. 2017;114(42):11211-6. doi: 10.1073/pnas.1701589114. PubMed PMID: 28973921; PubMed Central PMCID: PMC5651734.
212. Hiramami Y, Osakada F, Takahashi K, Okita K, Yamanaka S, Ikeda H, et al. Generation of retinal cells from mouse and human induced pluripotent stem cells. *Neuroscience letters*. 2009;458(3):126-31. doi: 10.1016/j.neulet.2009.04.035. PubMed PMID: 19379795.
213. Ben M'Barek K, Habeler W, Plancheron A, Jarraya M, Regent F, Terray A, et al. Human ESC-derived retinal epithelial cell sheets potentiate rescue of photoreceptor cell loss in rats with retinal degeneration. *Science translational medicine*. 2017;9(421). doi: 10.1126/scitranslmed.aai7471. PubMed PMID: 29263231.
214. Ben M'Barek K, Bertin S, Brazhnikova E, Jaillard C, Habeler W, Plancheron A, et al. Clinical-grade production and safe delivery of human ESC derived RPE sheets in primates and

- rodents. *Biomaterials*. 2020;230:119603. doi: 10.1016/j.biomaterials.2019.119603. PubMed PMID: 31732225.
215. Gagliardi G, Ben M'Barek K, Chaffiol A, Slembrouck-Brec A, Conart JB, Nanteau C, et al. Characterization and Transplantation of CD73-Positive Photoreceptors Isolated from Human iPSC-Derived Retinal Organoids. *Stem cell reports*. 2018;11(3):665-80. doi: 10.1016/j.stemcr.2018.07.005. PubMed PMID: 30100409; PubMed Central PMCID: PMC6135113.
216. Garita-Hernandez M, Lampic M, Chaffiol A, Guibbal L, Routet F, Santos-Ferreira T, et al. Restoration of visual function by transplantation of optogenetically engineered photoreceptors. *Nature communications*. 2019;10(1):4524. doi: 10.1038/s41467-019-12330-2. PubMed PMID: 31586094; PubMed Central PMCID: PMC6778196.
217. Yao K, Qiu S, Wang YV, Park SJH, Mohns EJ, Mehta B, et al. Restoration of vision after de novo genesis of rod photoreceptors in mammalian retinas. *Nature*. 2018;560(7719):484-8. doi: 10.1038/s41586-018-0425-3. PubMed PMID: 30111842; PubMed Central PMCID: PMC6107416.
218. Fitzgerald KM, Cibis GW, Giambrone SA, Harris DJ. Retinal signal transmission in Duchenne muscular dystrophy: evidence for dysfunction in the photoreceptor/depolarizing bipolar cell pathway. *The Journal of clinical investigation*. 1994;93(6):2425-30. doi: 10.1172/JCI117250. PubMed PMID: 8200977; PubMed Central PMCID: PMC6778196.
219. Grewal DS, Fishman GA, Jampol LM. Autoimmune retinopathy and antiretinal antibodies: a review. *Retina*. 2014;34(5):827-45. doi: 10.1097/IAE.000000000000119. PubMed PMID: 24646664.
220. Bellone RR, Brooks SA, Sandmeyer L, Murphy BA, Forsyth G, Archer S, et al. Differential gene expression of TRPM1, the potential cause of congenital stationary night blindness and coat spotting patterns (LP) in the Appaloosa horse (*Equus caballus*). *Genetics*. 2008;179(4):1861-70. doi: 10.1534/genetics.108.088807. PubMed PMID: 18660533; PubMed Central PMCID: PMC2516064.
221. Roberts P, Fishman GA, Joshi K, Jampol LM. Chorioretinal Lesions in a Case of Melanoma-Associated Retinopathy Treated With Pembrolizumab. *JAMA ophthalmology*. 2016;134(10):1184-8. doi: 10.1001/jamaophthalmol.2016.2944. PubMed PMID: 27540851.
222. Varin J, Reynolds MM, Bouzidi N, Tick S, Wohlschlegel J, Becquart O, et al. Identification and characterization of novel TRPM1 autoantibodies from serum of patients with melanoma-associated retinopathy. *PloS one*. 2020;15(4):e0231750. doi: 10.1371/journal.pone.0231750. PubMed PMID: 32324760; PubMed Central PMCID: PMC6778196.
223. Lu Q, Ganjawala TH, Ivanova E, Cheng JG, Troilo D, Pan ZH. AAV-mediated transduction and targeting of retinal bipolar cells with improved mGluR6 promoters in rodents and primates. *Gene therapy*. 2016;23(8-9):680-9. doi: 10.1038/gt.2016.42. PubMed PMID: 27115727; PubMed Central PMCID: PMC6778196.
224. Hulliger EC, Hostettler SM, Kleinlogel S. Empowering Retinal Gene Therapy with a Specific Promoter for Human Rod and Cone ON-Bipolar Cells. *Molecular therapy Methods & clinical development*. 2020;17:505-19. doi: 10.1016/j.omtm.2020.03.003. PubMed PMID: 32258214; PubMed Central PMCID: PMC6778196.
225. van Wyk M, Pielecka-Fortuna J, Lowel S, Kleinlogel S. Restoring the ON Switch in Blind Retinas: Opto-mGluR6, a Next-Generation, Cell-Tailored Optogenetic Tool. *PLoS biology*. 2015;13(5):e1002143. doi: 10.1371/journal.pbio.1002143. PubMed PMID: 25950461; PubMed Central PMCID: PMC6778196.

226. Cronin T, Vandenberghe LH, Hantz P, Juttner J, Reimann A, Kacso AE, et al. Efficient transduction and optogenetic stimulation of retinal bipolar cells by a synthetic adeno-associated virus capsid and promoter. *EMBO molecular medicine*. 2014;6(9):1175-90. doi: 10.15252/emmm.201404077. PubMed PMID: 25092770; PubMed Central PMCID: PMC4197864.
227. Rao A, Dallman R, Henderson S, Chen CK. Gbeta5 is required for normal light responses and morphology of retinal ON-bipolar cells. *The Journal of neuroscience : the official journal of the Society for Neuroscience*. 2007;27(51):14199-204. doi: 10.1523/JNEUROSCI.4934-07.2007. PubMed PMID: 18094259; PubMed Central PMCID: PMC46673526.
228. Sherry DM, Wang MM, Bates J, Frishman LJ. Expression of vesicular glutamate transporter 1 in the mouse retina reveals temporal ordering in development of rod vs. cone and ON vs. OFF circuits. *The Journal of comparative neurology*. 2003;465(4):480-98. doi: 10.1002/cne.10838. PubMed PMID: 12975811.
229. Rich KA, Zhan Y, Blanks JC. Migration and synaptogenesis of cone photoreceptors in the developing mouse retina. *The Journal of comparative neurology*. 1997;388(1):47-63. PubMed PMID: 9364238.
230. Sharma S, Ball SL, Peachey NS. Pharmacological studies of the mouse cone electroretinogram. *Visual neuroscience*. 2005;22(5):631-6. doi: 10.1017/S0952523805225129. PubMed PMID: 16332274.
231. Sieving PA, Murayama K, Naarendorp F. Push-pull model of the primate photopic electroretinogram: a role for hyperpolarizing neurons in shaping the b-wave. *Vis Neurosci*. 1994;11(3):519-32. PubMed PMID: 8038126.
232. Chen F, Tillberg PW, Boyden ES. Optical imaging. Expansion microscopy. *Science*. 2015;347(6221):543-8. doi: 10.1126/science.1260088. PubMed PMID: 25592419; PubMed Central PMCID: PMC4312537.
233. Trapani I, Colella P, Sommella A, Iodice C, Cesi G, de Simone S, et al. Effective delivery of large genes to the retina by dual AAV vectors. *EMBO molecular medicine*. 2014;6(2):194-211. doi: 10.1002/emmm.201302948. PubMed PMID: 24150896; PubMed Central PMCID: PMC3927955.
234. Trapani I, Auricchio A. Has retinal gene therapy come of age? From bench to bedside and back to bench. *Human molecular genetics*. 2019;28(R1):R108-R18. doi: 10.1093/hmg/ddz130. PubMed PMID: 31238338; PubMed Central PMCID: PMC6797000.
235. Colella P, Trapani I, Cesi G, Sommella A, Manfredi A, Puppo A, et al. Efficient gene delivery to the cone-enriched pig retina by dual AAV vectors. *Gene therapy*. 2014;21(4):450-6. doi: 10.1038/gt.2014.8. PubMed PMID: 24572793.
236. Carvalho LS, Turunen HT, Wassmer SJ, Luna-Velez MV, Xiao R, Bennett J, et al. Evaluating Efficiencies of Dual AAV Approaches for Retinal Targeting. *Frontiers in neuroscience*. 2017;11:503. doi: 10.3389/fnins.2017.00503. PubMed PMID: 28943836; PubMed Central PMCID: PMC5596095.
237. Miyoshi H, Takahashi M, Gage FH, Verma IM. Stable and efficient gene transfer into the retina using an HIV-based lentiviral vector. *Proceedings of the National Academy of Sciences of the United States of America*. 1997;94(19):10319-23. doi: 10.1073/pnas.94.19.10319. PubMed PMID: 9294208; PubMed Central PMCID: PMC23360.
238. Binley K, Widdowson P, Loader J, Kelleher M, Iqbal S, Ferrige G, et al. Transduction of photoreceptors with equine infectious anemia virus lentiviral vectors: safety and biodistribution of StarGen for Stargardt disease. *Investigative ophthalmology & visual science*.

2013;54(6):4061-71. doi: 10.1167/iops.13-11871. PubMed PMID: 23620430; PubMed Central PMCID: PMC3681475.